



University
of Glasgow

Hueber, Axel Johannes (2011) *The role of the cytokines IL-17A and IL-33 in inflammatory arthritis and psoriasis.*
PhD thesis.

<http://theses.gla.ac.uk/2629/>

Copyright and moral rights for this thesis are retained by the author

A copy can be downloaded for personal non-commercial research or study, without prior permission or charge

This thesis cannot be reproduced or quoted extensively from without first obtaining permission in writing from the Author

The content must not be changed in any way or sold commercially in any format or medium without the formal permission of the Author

When referring to this work, full bibliographic details including the author, title, awarding institution and date of the thesis must be given

**The role of the cytokines IL-17A and IL-33
in inflammatory arthritis and psoriasis**

by

Axel Johannes Hueber

MD

Submitted in fulfillment of the requirements for the degree of Doctor of
Philosophy

Division of Immunology, Infection & Inflammation
Faculty of Medicine
University of Glasgow

Abstract

The inflammatory autoimmune diseases rheumatoid arthritis, psoriatic arthritis and psoriasis have seen a break through in therapy by targeting cytokines in the last decade. Interleukin-17A, a potential new target, is considered as a crucial player in rheumatoid arthritis, and has been suggested to be produced by CD4⁺ T cells (Th17 cells). I explored the cellular sources of IL-17A in human established RA synovium. Surprisingly, only a small proportion of IL-17 positive cells were T cells without expression of a Th17 marker CCR6. Unexpectedly, the majority of IL-17A expression colocalized within mast cells. These data do not contradict a crucial role for IL-17A in RA pathogenesis, however, suggest that in addition to Th17 cells, cells of the innate immune system, particularly mast cells, may be an important component of the effector IL-17A response.

Psoriasis is a common chronic autoimmune disease of the skin characterized by hyperplasia of epidermal keratinocytes with associated inflammation. IL-33 is a new member of the IL-1 superfamily that signals through the ST2 receptor and was originally defined as an inducer of T helper 2 (Th2) cytokines. Recently broader immune potential has been discovered for IL-33 particularly via mast cell activation. With its expression at body barrier surfaces it is assumed to act as an alarmin. In this thesis I demonstrate that IL-33 expression is up-regulated in the epidermis of psoriatic lesions, compared to healthy skin, thus indicating that IL-33 may be a mediator regulating crosstalk between keratinocytes and infiltrating immune cells in psoriatic plaques. In a phorbol ester-induced model of skin inflammation ST2^{-/-} mice exhibited reduced cutaneous inflammatory responses compared to WT mice. Furthermore, consecutive injections of IL-33 into the ears of mice induced a psoriasis-like inflammatory lesion. This was partially mast cell dependent and cellular analysis demonstrated recruitment of neutrophils to the ear. This concludes that IL-33, via activation of mast cells and recruitment of neutrophils, may play a role in psoriasis plaque inflammation.

In the last part of the thesis I tested if nanoparticles can be utilized to image cytokine driven inflammation. Bio-linkages with protein-nanoparticles have been established and in vivo detection of nanoparticles performed. This final interdisciplinary outlook demonstrates a still to be established/finalized method with great potential.

Table of Contents

Abstract	2
Table of Contents.....	3
List of Tables	6
List of Figures	7
List of Figures	7
Acknowledgement.....	9
Author's declaration	10
Abbreviations.....	11
1 Introduction	15
1.1 Autoimmune inflammation - rheumatoid arthritis, psoriatic arthritis and psoriasis.....	17
1.1.1 The spectrum of clinical presentation of inflammatory arthropathies and psoriasis.....	17
1.1.2 Pathogenesis of rheumatoid arthritis	28
1.1.3 Pathogenesis of psoriatic arthritis and psoriasis	31
1.1.4 Pathogenic immune cells in inflammatory arthritis.....	32
1.1.5 Cytokines in synovitis and dermatitis	34
1.1.6 Mouse models of inflammatory skin disease	40
1.2 Th17 cells and their role in rheumatoid arthritis/psoriasis	42
1.3 The role of the cytokine Interleukin 33 in health and disease.....	51
1.3.1 IL-33 in the context of its IL-1 receptor / Toll like receptor family members	51
1.3.2 Structure of IL-33	56
1.3.3 Tissue localisation and cellular expression of IL-33.....	61
1.3.4 Release of IL-33	61
1.3.5 IL-33 receptor signalling via ST2 and IL1RacP	63
1.3.6 Cellular biological functions of IL-33.....	67
1.3.7 Regulation of IL-33.....	68
1.3.8 IL-33 in disease.....	68
1.4 Nanoparticles in inflammation.....	72
1.4.1 What are nanoparticles?	73
1.4.2 Magnetofluorescent nanoparticles	76
1.4.3 Fluorescent nanoparticles	80
1.4.4 Surface-enhanced Raman spectroscopy (SERS).....	81
1.5 Aims of this thesis	82
2 Material and Methods.....	83
2.1 General reagents & buffers	83
2.1.1 Materials and reagents	83
2.1.2 Buffers and culture media.....	83
2.2 Patients	83
2.3 Skin biopsy.....	84
2.4 Tissue preparation.....	84
2.4.1 Paraffin embedded tissue.....	85
2.4.2 Frozen tissue.....	85
2.5 ImmunHistoChemistry (IHC) of paraffin embedded sections.....	85
2.5.1 Single staining for light microscopy	85
2.5.2 Double staining for light microscopy.....	87
2.5.3 Double staining for fluorescent microscopy.....	87
2.5.4 Quantification of fluorescent IHC	89

2.5.5	Mast cell staining using Toluidine blue	89
2.6	ELISA.....	89
2.7	Luminex cytokine analysis.....	89
2.8	Cell culture	89
2.8.1	Culture of adherent cells	89
2.8.2	Culture of suspension cells	90
2.8.3	Purification of monocytes	90
2.8.4	Splenocyte harvest.....	91
2.9	FACS analysis	91
2.10	Animals.....	92
2.11	IL-33 related mouse experiments	94
2.11.1	TPA skin inflammation model	94
2.11.2	Cytokine ear injection model.....	96
2.11.3	Wound healing biopsy model	98
2.11.4	Analysis of mouse embryos	101
2.12	Production of a K14-IL-33 construct	101
2.12.1	Cloning of K14-IL-33	101
2.12.2	Transfection of K14-IL-33 in HaCaT	102
2.13	Nanoparticle methods.....	103
2.13.1	Protein linked SERRS active nanoparticles	103
2.13.2	Western blot of protein-linked NP	104
2.13.3	ETA-NP binding capacity	105
2.13.4	HeLa cell activation with TNF- α and blockade with ETA-NP.....	106
2.13.5	Nanoparticles in vivo	106
2.13.6	Carrageenan foot paw injection model	108
2.14	Statistical analysis.....	108
3	Interleukin-23 and Interleukin-17 in inflammatory arthropathies ...	109
3.1	Aim and Introduction.....	110
3.2	IL-23 expression in inflammatory arthropathies	112
3.2.1	Synovial expression of IL-23p19.....	112
3.2.2	Expression of IL-23 in synovial fluid.....	113
3.3	The source of IL-17 in rheumatoid arthritis.....	116
3.3.1	IL-17 is expressed in RA synovium but only scarce in OA synovium .	116
3.3.2	IL-17 is rarely expressed by Th17 cells in RA synovium	118
3.3.3	IL-17 is produced by innate immune cells mainly mast cells	126
3.4	Discussion & conclusion.....	129
4	Analysis of Interleukin-33 as an alarmin in psoriasis	133
4.1	Aim and Introduction.....	134
4.2	IL-33 and ST2 is expressed in inflammatory tissue such as psoriasis...	136
4.2.1	Expression of IL-33 and ST2 in autoimmune diseases.....	136
4.2.2	Interaction of IL-33 with mast cells	150
4.3	The role of IL-33 in skin inflammation mouse models.....	152
4.3.1	TPA induced skin inflammation	152
4.3.2	IL-33 intradermal ear injections - a model of skin inflammation	157
4.4	Addendum - Miscellaneous biologic questions surrounding IL-33	169
4.4.1	IL-33 in wound healing	170
4.4.2	IL-33 expressed under the K14 promotor.....	172
4.4.3	Embryonic function of IL-33	175
4.5	Discussion	178
5	The use of nanoparticles to image inflammation	184
5.1	Aim and Introduction.....	185
5.2	Size and form of nanoparticles	187
5.3	Linking proteins to nanoparticles	189

5.3.1	Testing quantities of ETA on linked nanoparticles	191
5.3.2	Biological binding properties of ETA linked nanoparticles to TNF- α	193
5.3.3	Biological function of ETA linked nanoparticles in HeLa cells.....	197
5.4	The detection of nanoparticles in vivo	201
5.4.1	SERRS profile of NP (Strathclyde)	201
5.4.2	Detection of NPs in tissue	203
5.4.3	The detection of NPs in inflammation	205
5.4.4	Switch of detection laser and Nanoparticles to Nanotags	209
5.4.5	SERRS profile of nanotags (NT)	209
5.4.6	Detection of i.v. administered NT440 in vivo.....	211
5.4.7	Ex vivo SERRS mapping analysis of spleen.....	213
5.4.8	Multiplexing of NT in vivo and ex vivo	215
5.5	Conclusion and Discussion	217
6	Discussion & conclusion	220
7	References.....	224
8	Publications.....	251

List of Tables

Table 1.1 criteria 1987 Criteria for the classification of rheumatoid arthritis (1)	19
Table 1.2 The 2010 American College of Rheumatology/European League Against Rheumatism classification criteria for rheumatoid arthritis (adapted from (2)).	19
Table 1.3 CASPAR criteria for classification of PsA (adapted from (8)).	20
Table 1.4 Comparison of rheumatoid arthritis, psoriatic arthritis, ankylosing spondylitis and osteoarthritis.	24
Table 1.5 Susceptibility genes in arthritis.	29
Table 1.6 Selected cytokines implicated in pathogenesis of RA, PsA and psoriasis	38
Table 1.7 IL-1 family - members and nomenclature	53
Table 2.1 Antibodies for IHC	88
Table 2.2 ELISA cytokines and companies	88
Table 2.3 Mouse strains used in experiments	93
Table 3.1 Percentage of double positive cells compared to IL-17+ cells.	128

List of Figures

Figure 1.1 Cytokine receptor interaction	27
Figure 1.2 Picture of synovial joint inflammation	30
Figure 1.3 T helper cell differentiation (overview).	43
Figure 1.4 Th17 cell differentiation in mice.....	46
Figure 1.5 Th17 polarisation in humans.	46
Figure 1.6 IL-18 receptor complex.	55
Figure 1.7 Structure of IL-33 HTH like motif	58
Figure 1.8 IL-33 structural components and cleavage sites.	60
Figure 1.9 IL-33 binding to ST2 and IL1RacP signals via MyD88.....	66
Figure 1.10 Nanoparticle - size comparison	74
Figure 2.1 Overview of the timeline - TPA skin inflammation model.....	95
Figure 2.2 IL-33 intradermal ear injection.....	97
Figure 2.3 Wound healing model.....	100
Figure 2.4 SERRS imaging ex vivo.	107
Figure 3.1 Synovial expression of IL-23 in inflammatory arthropathies.	114
Figure 3.2 Detection of IL-23 in synovial fluid.	115
Figure 3.3 IL-17A expression in RA/OA synovium.	117
Figure 3.4 Establishing staining for CCR6 in RA	119
Figure 3.5 Doublestaining IL-17 and CCR6 by light IHC	120
Figure 3.6 Back to back staining CD3/CCR6 and IL-17	122
Figure 3.7 Doublestaining of Th17 cell markers and IL-17A.	124
Figure 3.8 Doublestaining of Th17 marker CCR6 with IL-17A.	125
Figure 3.9 Doublestaining of IL-17 pos. cells with CD68	127
Figure 3.10 Mast cells express IL-17A in RA synovium.	127
Figure 3.11 RORC dependent IL-17A production by CD34+ derived mast cells. .	132
Figure 4.1 Hypothesis for the role of IL-33 in psoriasis	135
Figure 4.2 IL-33 in tonsil - work up of IHC staining.....	137
Figure 4.3 IL-33 expression in healthy skin	137
Figure 4.4 IL-33 in psoriasis.....	138
Figure 4.5 IL-33 is not expressed by basal keratinocyte stem cells.....	140
Figure 4.6 ST2 expression in healthy skin.....	142
Figure 4.7 ST2 expression in psoriatic skin.	143
Figure 4.8 IL-33 expression in rheumatoid arthritis	145
Figure 4.9 ST2 and IL-33 expression in rheumatoid arthritis.....	146
Figure 4.10 IL-33 expression in synovial fibroblasts	147
Figure 4.11 sST2 expression in PsA and healthy control serum and PsA and OA synovial fluid	149
Figure 4.12 Expression of ST2 in HMC-1 and HaCaTs	151
Figure 4.13 Stimulation of HMC-1 with IL-33	151
Figure 4.14 TPA induced skin inflammation - Role of IL-33/ST2	153
Figure 4.15 TPA induced skin inflammation - Ki67 proliferation analysis.	154
Figure 4.16 TPA induced skin inflammation ST2 dependency resolved after 3 days.....	156
Figure 4.17 TPA induced skin inflammation in mast cell deficient mice - no difference after 3 days.	156
Figure 4.18 Validation of the biological function of recombinant IL-33.....	158
Figure 4.19 Model of injection and <i>in vivo</i> biological activity of IL-33	158
Figure 4.20 IL-33 induces ear swelling in an ear injection model.....	160
Figure 4.21 IL-33 injection- histological readout (H&E)	160

Figure 4.22 IL-33 ear injection -infiltration of mast cells and eosinophils.....	162
Figure 4.23 IL-33 ear inflammation is ST2 dependent	164
Figure 4.24 IL-33 initial effect in ear inflammation is partial dependent on mast cells	166
Figure 4.25 Cellular recruitment by IL-33	168
Figure 4.26 ST2 deficiency does not influence wound healing	171
Figure 4.27 Construct and design of the K14 IL-33 plasmid.	173
Figure 4.28 Transfection of HaCaTs with K14 IL-33	174
Figure 4.29 Embryo preparation day D9.5	176
Figure 4.30 IL-33 is not expressed in the dorsal aorta day 9.5 or 10.5	177
Figure 4.31 Splice variants of IL-33.	183
Figure 5.1 SEM on nanoparticles (nanotags).....	188
Figure 5.2 Schematic linking of proteins to NPs.	190
Figure 5.3 Total protein on ETA linked nanoparticles	192
Figure 5.4 Competition ELISA to test TNF- α binding to NPs.....	195
Figure 5.5 Biological binding properties of ETA-NPs.	195
Figure 5.6 Biological binding properties of ETA-NT440.	196
Figure 5.7 Establishing TNF stimulation of Hela cells with ETA blockade.....	198
Figure 5.8 IL-6 production by TNF stimulated HeLa cells blocked with Au-ETA.	198
Figure 5.9 Nanoparticles aggregate over time.	200
Figure 5.10 Linkage and bioactivity of ETA-NP (Au) with BSA.	200
Figure 5.11 SERRS profile of NIR-Au-NP.	202
Figure 5.12 Detection of Nanoparticles in tissue	204
Figure 5.13 Detection of NPs in the carragean footpad injection model.....	206
Figure 5.14 Tracking of Nanoparticles to the site of inflammation.	208
Figure 5.15 SERRS profile of NT440 and NT420	210
Figure 5.16 SERRS signal of NT440 in tissue.	212
Figure 5.17 SERRS image of a spleen section.....	214
Figure 5.18 SERRS signals of liver and spleen in NT injected mice.	216

Acknowledgement

I would like to thank Professor Iain McInnes for his great support during the 3 ½ years in Glasgow. Professor McInnes has been an inspiring clinical and scientific mentor and has always tried to help developing my career in the best possible ways throughout this period and beyond.

This thesis would not have been possible without the help and support from my laboratory and clinical colleagues. I am particularly grateful to Dr Ashley Miller and Dr Darren Asquith for their guidance throughout these years. Day to day technical and scientific supervision with a strong support of activities made the time flying by. This was great supported by Lucy Ballantine.

In the CRD lab group I would also like to express my gratitude to Jim “IHC warlock” Reilly and Shauna Kerr (“IHC witch”). Taking myself as the worst apprentice on board to teach what real “bucket” science is like, was very kind and I appreciate the knowledge and insights I have learnt. Also I want to thank Ashley Gilmour and Alastair Fraser for all their help.

I would like to thank Mr Neal Millar who gave me the opportunity to see how real doctors work and for a successful orthopaedic/rheumatology collaboration.

I would also like to thank Professor Sturrock, Dr Max Field, Dr David McCarey and especially Dr Hilary Wilson but also the nurses for providing me with patient samples. In addition I would like to thank the patients from the rheumatology clinic who donated samples for this project.

Thanks to Dr Derek Gilchrist for helping me with the IL-33 biology work and Dr Ross Stevenson for insights and collaboration regarding nanoparticle science.

Special thanks also to my wife and family (Ralf for 3 Glasgow visits including for the surprise visit while I was taking a shower...). My wife, especially, has sacrificed a lot to allow me to have an enjoyable life and successful career and for that I will always be extremely thankful.

The German Research Foundation (DFG) funded three years of this project.

Author's declaration

The work described in this thesis represents original work which has been generated through my own efforts and does not consist of work forming part of a thesis to be submitted elsewhere. Furthermore, no data has been given to me by anybody else to be submitted as part of my thesis. Where practical support has been provided by others appropriate acknowledgements have been made.

Abbreviations

ACPA	Anti-Citrullinate Protein Antibodies
ACR	American College of Rheumatology
APO	Apolipoprotein
AS	Ankylosing Spondylitis
Au	Aurum=gold
Au-ETA	Etanercept linked to gold nanoparticle
Au-IgG	IgG linked to gold nanoparticle
CBM	Chromatin binding motif
CIA	Collagen-Induced Arthritis
CRP	C-Reactive Protein
CTLA-4	Cytotoxic T Lymphocyte Associated Antigen 4
CVD	Cardiovascular Disease
DAMP	Danger-associated molecular pattern
DMARD	Disease modifying anti rheumatic drug
EAE	Experimental Autoimmune Encephalomyelitis
ELISA	Enzyme linked immunosorbent assay
ER	Endoplasmic Reticulum
ETA	Etanercept

FCS	Foetal calf serum
FLS	fibroblast like synoviocytes
GM-CSF	Granulocyte Macrophage Colony Stimulating Factor
HaCaT	Human keratinocyte cell line
HeLa	stromal tumor cell line derived from the patient Henrietta Largs
HLA	Human leukocyte antigen
HTH	helix turn helix
IgG	Immunglobulin G
IL	Interleukin
LPS	Lipopolysaccharide
MCSF	Macrophage colony stimulating factor
MHA	1-mercaptoundec-11-yl)hexa(ethylene glycol)
MMP	Matrix Metalloproteinase
MNP	Magnetic nanoparticles
MRI	Magnetic resonance imaging
MTX	methotrexate
NIR	Near infrared
NLS	nucleus localisation site
NP	Nanoparticle

NT	Nanotag
OA	Osteoarthritis
PAMP	Pathogen-associated molecular pattern
PBMCs	Peripheral Blood Mononuclear Cells
PET	Positron emission tomography
PsA	Psoriatic Arthritis
RA	Rheumatoid Arthritis
RANK	Receptor Activator of NF- κ B
RANKL	Receptor Activator of NF- κ B Ligand
RF	Rheumatoid Factor
SEM	Scanning electron microscope OR standard error mean
SERRS	Surface enhanced resonance Raman scattering
SERS	Surface enhanced Raman spectroscopy
SNP	Single Nucleotide Polymorphism
TcKs	Cytokine Activated T cells
TLR4	Toll Like Receptor 4
TNF α	Tumour Necrosis Factor
TNFi	Tumour Necrosis Factor inhibitors
TMB	3,3',5,5'-tetramethylbenzidine

TPA Phorbol ester, 12-O-tetradecanoylphorbol-13-acetate

1 Introduction

Content of this chapter has been published in the following manuscripts:

- **Hueber AJ** and **McInnes IB**
Immune regulation in psoriasis and psoriatic arthritis - recent developments.
Immunol Lett. 2007 Dec 15;114(2):59-65. Review.
- **Hueber AJ**, **Asquith DL**, **McInnes IB**, **Miller AM**
Embracing novel cytokines in RA - Complexity grows as does opportunity!
Best Pract Res Clin Rheumatol. 2010 Aug;24(4):479-87. Review.
- **Hueber AJ** and **McInnes IB**
Pathogenesis in RA - Cytokines.
Rheumatoid Arthritis, Hochberg, et al. 11 Dec 2008, Mosby, 0323054757. Book chapter
- **Hueber AJ**, **Stevenson R**, **Stokes RJ**, **Graham D**, **Garside P**, **McInnes IB**
Imaging inflammation in real time - future use of nanoparticles.
Autoimmunity. 2009 May;42(4):368-72. Review
- **Kurowska-Stolarska M**, **Hueber AJ**, **Stolarski B** and **McInnes IB**.
IL-33 - a novel mediator with a role in distinct disease pathologies.
J Intern Med 2011 Jan;269(1):29-35. Review.

Autoimmunity is a process in which the immune system reacts against self structures. Thus potent immune cells are implicated in a vicious circle leading to damage to self organs. This loss in tolerance against self is a chronic process and often only ends after complete destruction of the target. The clinical challenge in autoimmunity is to break through this vicious circle, and either reset, re-programme and/or retrain the immune system. Thus damage can be prevented and long term impairment avoided.

This challenge to stop tissue destruction, deformity and disability but also to prevent comorbidities (reduction of cardiovascular risk) is exemplified best in rheumatoid arthritis and psoriatic arthritis. Currently these autoimmune diseases are chronic diseases with no cure. Over the last decades more and more insights have been gained in regard to the delicate network of the immune system and its interactions. Obviously the future goal would be to detect prone individuals before failure of the immune system occurs. More insights into epigenetics but also metabolomics in autoimmune diseases will lead to future improvements in therapeutics.

Here, I shall give an overview of these autoimmune diseases, describing the success of cytokine targeted therapies and will allude to new targets that are evolving. Finally, I will provide an outlook as to how future technologies such as Nanometrology can help in detecting inflammation earlier with more sensitive approaches.

1.1 Autoimmune inflammation – rheumatoid arthritis, psoriatic arthritis and psoriasis

I shall first introduce the autoimmune diseases (rheumatoid arthritis, psoriatic arthritis and psoriasis) studied in this thesis. Thereafter I shall introduce the relevant cytokine biology focussing mainly on the cytokine TNF- α as a core example for a successful targeted therapy in autoimmune arthritis.

1.1.1 The spectrum of clinical presentation of inflammatory arthropathies and psoriasis

Inflammatory arthropathies have multiple causes; but they all share one defining feature: namely arthritis predicated on the presence of inflammatory infiltration of the synovial membrane and attendant structural damage. On clinical presentation patients usually offer the following hallmarks of inflammation: calor (heat), rubor (redness), dolor (pain) and tumor (swelling) as described by Celsus Aulus (Aurelius) Cornelius (30 B.C. to 45 A.D.). Functio laese (loss of function) is another hallmark of arthropathies which has been later added by Claudius Galenus (AD 129–ca. 200). However, arthritis does not always present itself as described above. I will therefore summarize the clinical commonalities and differences across the autoimmune arthropathies “rheumatoid arthritis” (RA) and “psoriatic arthritis” (PsA). Further, the connection to autoimmune skin diseases will be discussed.

Clinical diagnosis - Rheumatoid arthritis vs. psoriatic arthritis

Rheumatoid arthritis (RA) is a chronic systemic autoimmune disease of unknown aetiology primarily affecting joints. Arthritis occurs symmetrically, and if untreated will lead to tissue destruction, deformity and disability. Prevalence of RA is about 1% in Caucasians with women being affected 2-3 times more often than men. Clinical features of RA are used as tools for diagnosis and serve within every classification criteria set thus far prepared. These include arthritis of small and large joints, rheumatoid nodules, morning stiffness, erosions on X-Rays and changes in serum markers such as rheumatoid factor. Table 1.1 summarizes the hallmarks used in the American College of Rheumatology (ACR) criteria for

diagnosis of RA (1987) (1). These criteria have been updated in 2010 for identifying patients with a relatively short duration of symptoms who may benefit from early institution of DMARD therapy (2)(Table 1.2).

Although RA develops its pathology within the synovium many nonarticular organs become involved, particularly in patients with severe joint disease. Despite the differences between the normal form and function of joints and, for example, the bone marrow, it is becoming more clear that the same cytokines that drive synovial pathology are also responsible for generating pathology in extraarticular tissues (such as skin, eye, lungs, heart, kidney, blood vessels, salivary glands, the central and peripheral nervous systems, and bone marrow). As examples extraarticular manifestation can involve the lung with pulmonary nodules (similar to rheumatoid nodules), but also the heart with pericarditis and myocarditis. Hematological disorders such as the Felty's syndrome manifest with seropositive rheumatoid arthritis and neutropenia, often with an associated anemia or thrombocytopenia, an enlarged spleen, and (rarely), leg ulcers.

Recently, antibodies against citrullinated peptides (ACPA) were linked to RA and, indeed, ACPA have been identified in up to 90% of patients with RA and although they are not specific to RA they correlate with disease severity (3-5). Thus a serologic classification of RA is attractive. However this is not entirely clinically useful due to considerable variation in presentation even within this group. Therefore, RA patients could be classified per their responsiveness to therapies (responders vs. non-responders). For example, not all patients with RA respond to the standard dosage of anti- Tumour Necrosis Factor- α (TNF- α) agents. In large randomized trials, 28-58% of all patients with RA showed little response to these drugs (6, 7), but might respond to different targeted drugs like IL-6 inhibitors (tocilizumab) or drugs which block T cell activation (abatacept). These responses may reflect either true molecular differences in pathology or perhaps distinct phases of disease at which therapeutic resistance may be distinct. Genetic or epigenetic distinctions are also possible. With this broad clinical spectrum, distinguishing other arthropathies such as PsA from RA can be challenging.

Criteria	Comments
1. morning stiffness	stiffness of joints lasting at least 1 hr
2. arthritis of 3 or more joint areas	Soft tissue joint swelling observed by a physician
3. arthritis of hand joints	arthritis in at least one area of hand/wrist
4. symmetric arthritis	simultaneous involvement of the same joint areas on both sides of the body
5. rheumatoid nodules	subcutaneous non tender nodules in juxtaarticular regions
6. serum rheumatoid factor	presence of autoantibodies which bind Fc portion of IgG
7. radiographic changes	RA typical changes with erosions or decalcifications in hand or wrist

Table 1.1 criteria 1987 Criteria for the classification of rheumatoid arthritis (1)
4 of the 7 criteria have to be fulfilled to be classified as suffering from RA. Points 1 through 4 have to be present for at least 6 weeks. Point 2 and 3 exclude distal interphalangeal joints (DIP) (in depth details are published by the ACR, www.rheumatology.org)

Classification criteria for RA

Patients should have at least 1 joint with definite clinical synovitis (swelling) and with the synovitis not better explained by another disease	
A	Joint involvement
	points
	1 large joint
	0
	2-10 large joints
	1
	1-3 small joints
	2
	4-10 small joints
	3
	≥ 10 joints (at least 1 small joint)
	5
B	Serology
	Negative RF and negative ACPA
	0
	Low-positive RF or low-positive ACPA
	2
	High-positive RF or high-positive ACPA
	3
C	Acute-phase reactants
	Normal CRP and normal ESR
	0
	Abnormal CRP or abnormal ESR
	1
D	Duration of symptoms
	< 6 weeks
	0
	≥ 6 weeks
	1

Table 1.2 The 2010 American College of Rheumatology/European League Against Rheumatism classification criteria for rheumatoid arthritis (adapted from (2)).
Score-based algorithm: add score of categories A–D; a score of ≥6/10 is needed for classification of a patient as having definite RA.

Inflammatory articular disease (joint, spine or enthesal) with >3 points from the following five categories:

1. Definite psoriasis (2 points) or a personal history of psoriasis (1 point) or a family history of psoriasis (1 point)*
2. Typical psoriatic nail dystrophy including onycholysis, pitting and hyperkeratosis on current physical examination or documented by a rheumatologist or dermatologist (1 point).
3. A negative test result for the presence of rheumatoid factor (1 point).
4. Either current dactylitis, defined as swelling of an entire digit, or a history of dactylitis recorded by a rheumatologist (1 point).
5. Radiographic evidence of juxta-articular new bone formation, appearing as ill-defined ossification near joint margins (but excluding osteophyte formation) on plain radiographs of the hand or foot (1 point).

Table 1.3 CASPAR criteria for classification of PsA (adapted from (8)).

***A personal history of psoriasis is only included in the score if definite psoriasis is not documented. A family history of psoriasis is only included in the score if neither definite psoriasis nor a personal history of psoriasis is present**

Approximately 6-20% of patients with psoriasis develop a chronic inflammatory arthritis or enthesitis. PsA affects approximately 0.1 - 0.5% of the general population presenting as peripheral arthritis, axial disease or a combination of both (9). In comparison to RA, peripheral PsA evolves with a distinct joint pattern, typically asymmetric and potentially involving the distal interphalangeal joints. Enthesitis is a characteristic feature of the spondyloarthropathies with inflammation at tendon or ligament attachment sites. The MRI appearance of enthesitis is quite distinctive characterised by marked inflammation in adjacent bone marrow and soft tissues (10). In PsA, MRI has detected enthesitis in clinically uninvolved joints suggesting that enthesitis may be the primary lesion in PsA. This is supported by the observation that enthesial inflammation may extend as far as the synovial cavity. Dactylitis with enthesitis involving the complete digit is a characteristic feature which is quite distinct from symptoms or signs seen in RA. The peak incidence occurs between the age of 20 and 40 years with a slight male bias except in the subset of patients with symmetrical polyarthritis in which patients are predominantly female (11). For the diagnosis of PsA, several groups have proposed different criteria. The criteria defined by Moll and Wright in 1973 were used over the last three decades (12). Five groups were defined in regard to the clinical pattern in asymmetric oligoarticular, symmetric RA-like, distal interphalangeal (DIP) predominant, arthritis mutilans and spondylitis. However, considerable overlap between groups is now recognized. The definition of "true PsA" is still a topic of ongoing discussion and different groups proposed criteria including Bennett (13), Gladman et al (14), Vasey and Espinoza (15), the European Spondylarthropathy Study Group (ESSG) (16), McGonagle et al (17), and Fournie et al (18). The recently developed CASPAR criteria have a specificity of 98.7% and sensitivity of 91.4% for diagnosing PsA (Table 1.3) (8). The authors of this study suggest that due to the high specificity of their criteria they should be used for future clinical studies. CASPAR criteria involve arthropathy with the list of criteria shown in Table 1.3.

Clinical presentation of psoriasis

Psoriasis is an autoimmune, chronic inflammatory disease targeting primarily the skin and nails affecting 2-3% of the Caucasian population (19). It is characterized by hyperplasia of the epidermis (acanthosis), infiltration of leukocytes into the dermis and epidermis as well as dilatation and proliferation of blood vessels. As a common skin disease it appears in different clinical variants. Most frequently, psoriasis vulgaris presents with scaly red plaques on predilectionary areas, e.g. on scalp, the back, dorsal skin of the elbows and ventral skin of knees. However, there is considerable variation concerning the phenotype of psoriasis and the disease can present itself as various other clinical variants such as guttate psoriasis, palmar pustular psoriasis. This considerable clinical heterogeneity in the cutaneous presentation of the disorder indicates a variety of pathogenetic processes underlying the different variants which may not be common or consistent across each clinical presentation. The skin lesions may be minimal or concealed especially in areas such as the scalp, ears, buttocks or umbilicus. While severe psoriasis has been associated with a higher prevalence of PsA (20), there is no direct temporal relationship between the severity of skin and joint inflammation.

In psoriasis patients, lesions can be triggered by a large number of factors including physical trauma to the skin (Koebner's phenomenon), rapid withdrawal of immunosuppressive medication, drugs like hydroxychloroquine, beta blockers, and infections (19). Interestingly, the trigger for PsA is not clear although a "deep Koebner phenomenon" has been suggested (21). Hereby it is speculated that mechanical damage in the joint (therefore "deep" compared to skin) leads to initiation of a repair mechanism and might trigger autoimmune processes resulting in arthritis. Mechanical damage is speculated to involve accidents, physical stress such as "moving house" or sport injuries.

Cardiovascular risk and RA, PsA and psoriasis

Patients with rheumatoid arthritis have an increased risk of premature death due to cardiovascular disease (CVD). A meta-analysis of observational studies performed by Lacaille and colleagues identified 111,758 patients with 22,927 cardiovascular events. An approximate 50% increased risk of CVD-associated

death in patients with RA was reported, however, data varied due to different study characteristics (22). Further, it has been demonstrated that PsA patients are at increased risk of cardiovascular morbidities compared with the general population (23). CVD risk in psoriasis is currently debated with studies supporting psoriasis as a risk factor and a recent study by Wakke et al. disproving this (24). In this study, the majority of patients had mild psoriasis with only a small minority suffering from severe psoriasis (<5%), therefore, selecting for a mild disease group. In a cohort study using the General Practice Research Database, Gelfand and colleagues demonstrated that patients with severe psoriasis have an increased risk of cardiovascular mortality (25). Interestingly, Gladman et al. demonstrated severe psoriasis as a risk factor for CVD in patients with PsA (23). Thus, severity of psoriasis and therefore the level of inflammation might play a role in the development of CVD. Additional studies are needed to determine the mechanism of this phenomenon and what impact therapy will have on the increased risk of developing cardiovascular complications.

Bone destruction – RA vs PsA

Interestingly, pathological signs of disease can be detected at different sites in the joint in RA and PsA patients and therefore may allow the differentiation of RA from PsA at the radiographic level. As with every characteristic, a certain amount of overlap will occur. However, the site and type of bone destruction can add important information and thus help in defining the disease clinically.

Two processes contribute to tissue destruction observed in RA joints. First: active invasion of the synovium into the cartilage and second, the activation of osteoclasts and chondrocytes and maintenance of an osteoclast favourable environment. Erosions occur at juxta-articular sites, generally at the point of attachment of the synovium. In end-stage disease, large cystic erosions of bone may be seen. Without treatment to prevent progression, this joint destruction will lead to dysfunction of the joints. In hands longstanding disease can advance to mechanical dysfunction due to involvement of the wrists with volar deviation of the extensor carpi ulnaris as well as ulnar deviation of metacarpophalangeal (MCP) joints. Why MCP and wrist joints are favourably involved has not been elucidated yet, however, neuronal axis involvement is speculated to play a role. Thus, cases of RA are reported in patients previously paralysed by poliomyelitis

or stroke, in whom the paralysed limbs have been spared totally or partially by the arthritic process, as well as patients with halted progression of arthritis in the fingers due to sensory denervation following traumatic nerve dissection (26, 27) indicate that the nervous system might be involved in the inflammatory process seen in RA.

In comparison to RA, PsA has different features of bone involvement (Table 1.4). As described above some subgroups of PsA, which are comparable to RA in regard to their clinical presentation, might demonstrate a similar bone destruction pattern. However, the major difference to RA is that PsA demonstrates a mixture between bone erosion and bone repair mechanisms, ranging from periostitis to osteolysis and new bone formation. Furthermore, PsA often shows inflammation of the enthesis (tendon bone insertion site). Enthesitis can help distinguish PsA from rheumatoid arthritis and osteoarthritis. This is evident in plain radiographs and MRI as periostitis, new bone formation and erosions (28). Axial disease with sacroileitis can be found in some PsA patients and can be used to differentiate it from RA but it also demonstrates the mixed clinical pattern overlapping with ankylosing spondylitis.

	arthritis pattern	axial involvement	RF/ACPA	joint erosions	enthesitis	skin involvement
RA	symmetric	-	+	+	-	-
PsA	asymmetric	+/-	-	+	+	+
AS	-	+	-	-	+/-	-
OA	asymmetric	-	-	-	-	-

Table 1.4 Comparison of rheumatoid arthritis, psoriatic arthritis, ankylosing spondylitis and osteoarthritis.

Demonstrated are the main features of the diseases; it has to be mentioned that in all groups overlap occurs, e.g. symmetric variant of PsA, peripheral involvement of AS, etc. -: not present; +: present; +/-: present in subgroups.

Treatment of RA and PsA

In recent years, new therapies have evolved for the treatment of RA and PsA. The current treatment paradigm for RA emphasizes the sequential use of therapeutic agents driven by measurement of disease activity. Thus early start of disease-modifying anti-rheumatic drugs (DMARDs, such as methotrexate and sulfasalazine) is considered optimal with possible step up and combinations, although this needs to be individualized for each patient. Also the choice of DMARD is an individualised decision between the patient and physician. Glucocorticoids added at low to moderately high doses to DMARD therapy can provide benefit as initial short-term treatment; however, glucocorticoids should be tapered as rapidly as clinically feasible (29).

Compared to traditional DMARDs, TNF- α blockade represents the first successful treatment using cytokine targeted therapy. Infliximab, a chimeric monoclonal anti-TNF- α antibody, adalimumab, a humanized monoclonal anti-TNF- α antibody and etanercept, a soluble TNF- α receptor construct are now widely used in clinical treatment. By preventing the cytokine to bind to the specific receptor, downstream activation signals are blocked and further stimulation of the inflammatory processes is thus reduced (Figure 1.1). Interrupting the TNF- α cascade was found to have beneficial effects on disease outcome, joint damage and function, but also on tissue inflammation and cell infiltration measured at the histological level in biopsy studies. Anti-TNF- α therapy was the successful proof of concept for cytokine-based therapies and hence initiated the development of further cytokine/immune targeted drugs.

The type of cells and mediators involved in the inflammatory processes are very similar in PsA and RA joints. Thus, it is not surprising that most of the therapies which have been successful in treating RA such as DMARDs like MTX or TNF- α blockers show similar efficacy in patients with PsA (30, 31). Due to the success seen in PsA patients, TNF- α blockers were tested in patients with psoriasis and found to be effective. These drugs are now approved for patients with severe psoriasis. Recent developments of immunotherapies use specific diseases for primary proof of concept (e.g. IL-12/23 blockade with ustekinumab in psoriasis (32)); however, overlap of treatment between diseases should be expected as autoimmune phenomena have common characteristics between diseases.

Ustekinumab has also been tested in an phase II trial in PsA with promising results (33). Whether this target also works in RA, in which the role of IL-23 biology in pathogenesis is still not finally solved, needs to be determined. Further results of translational trials are awaited.

Thus more potential therapeutic targets, some of which have been proven to play a role in disease as well as others which still need to be analysed further, will be discussed below (see 1.1.5).

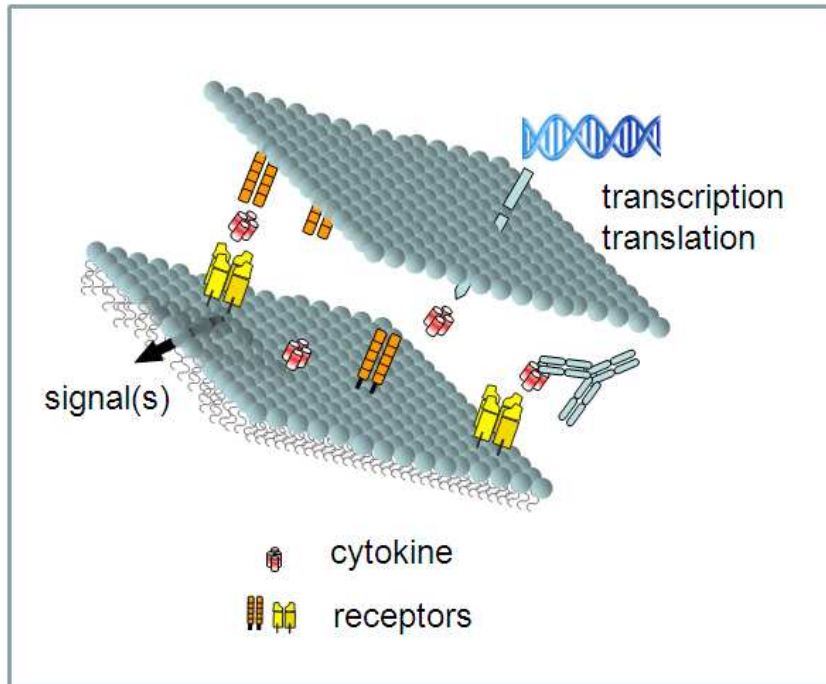


Figure 1.1 Cytokine receptor interaction

Demonstrated is a cytokine (red) binding to possible ligands. Blockade with neutralising antibodies prevents further downstream signals (adapted from Hueber, McInnes, Rheumatoid Arthritis, Mosby (34))

1.1.2 Pathogenesis of rheumatoid arthritis

Despite decades of research focused on RA, the pathogenesis of this disease is still not fully understood. So far, no single factor has been discovered that can account for the initiation of the disease; rather a conglomeration of events and factors are thought to drive RA. Recently, many new elements have been identified which link genetic associations (e.g. HLA-DRB1 and HLA-DR4 alleles within the MHC class II, polymorphisms in the genes encoding STAT4, TNF- α receptor and PTPN22) and environmental influences (e.g. smoking) to the susceptibility of RA (35, 36) (Table 1.5).

At the microscopic level, inflammation in RA seems to be maintained by various cell types. Figure 1.2 “Picture of synovial joint inflammation” shows a schematic illustration of the roles these different cell types play during inflammation in a synovial joint. Hereby recruitment of cells, cell-cell interaction via cell contact or cytokines and matrix changes such as cartilage destruction, tissue invasion by fibroblasts and bone erosion due to osteoclasts are linked with each other; all playing their parts in the initiation and maintenance of inflammation. Named are only some representative cells, however, nearly all immune cells have been at some point implicated to play a role in this complex process of autoimmune inflammation.

The trigger to synovitis is still unclear. In an arthritic joint swelling of the synovium relates to infiltration by immune cells mediated via chemokine/cytokine triggered recruitment of innate and adaptive cells. Hypervascularisation and activation of the endothelium supports migration from vessels into the tissue. Often tertiary lymphoid follicles are detected containing B and T cells and other antigen-presenting cells such as macrophages and dendritic cells. This over-compact gathering of cells provides an environment allowing the maintenance of the autoreactive immune response. Further, immune cells stimulate stromal cells such as fibroblast-like synoviocytes, which can produce proinflammatory cytokines and/or proliferate resulting in metalloproteinase/aggrecanase dependent cartilage degeneration and bone invasion. This cytokine milieu induces maturation of and thereafter, activates osteoclasts leading to an imbalance in the osteoclast/osteoblast axis thus increasing bone erosion. Therapeutic targeting of the adaptive axis or innate/stromal axis are both successful, demonstrating the close

interplay/dependence in this cellular network. A more detailed view of cytokines as mediators of inflammation will be discussed 1.1.5.

Rheumatoid arthritis	-----	Psoriatic arthritis
<i>HLA associated genes</i>		
<i>non-HLA susceptibility genes</i>		
PTPN22 (intracellular phosphatase)		IL-23 receptor
TRAF1-C5 region (TNF receptor-associated factor 1, C5 (complement))		IL-12p40
STAT4 (Signal transducer and activator of transcription 4), key molecule for interleukin (IL)-12 signalling		IL-23p19
6q23 region (e.g. TNF- α induced protein 3)		5q31 locus (IL-4, IL-5, IL-13)
PADI4 (Peptidylarginine deiminases citrullinating enzyme 4)		
4q27 region (incl. IL-2/IL-21 locus)		4q27 region (incl. IL-2/IL-21 locus)
CTLA-4 gene (cytotoxic lymphocyte antigen 4)		
KIF5A gene		
IL2RB gene		
CD40		

Table 1.5 Susceptibility genes in arthritis.
Shown are genes/gene regions associated with rheumatoid arthritis and/or psoriatic arthritis. Overview from (35, 37, 38)

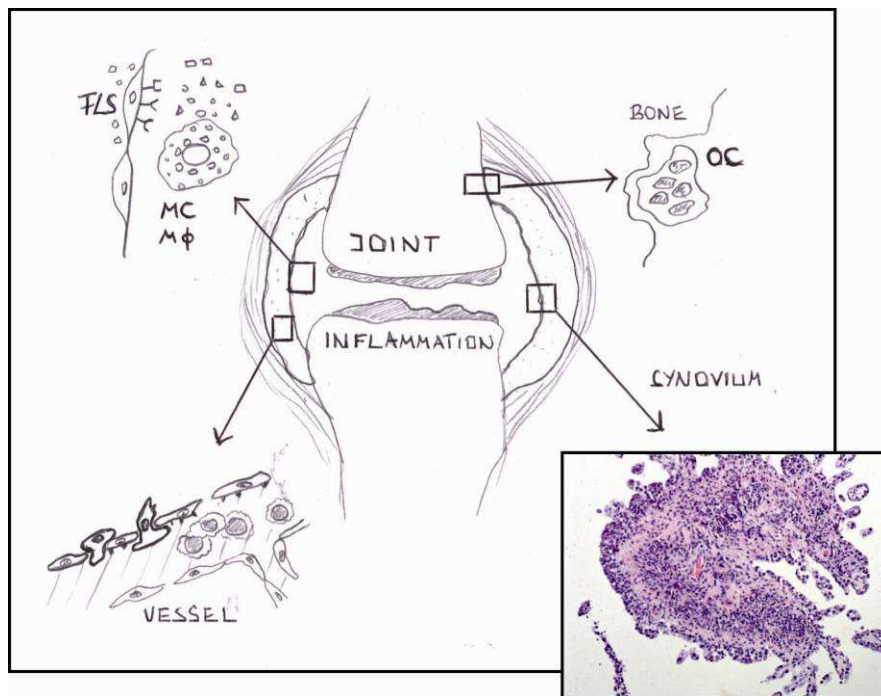


Figure 1.2 Picture of synovial joint inflammation

This schematic represents a joint which shows different aspects of inflammation. Top left corner shows synovial fluid cells (e.g. a macrophage/monocytes or mast cell (MC/M Φ), in this sketch, MC/M Φ could be replaced with mostly every immune cell) producing cytokines and chemokines. Closeby fibroblast- like synoviocytes (FLS) can respond to that signal and produce inflammatory proteins in turn. Bottom left corner shows a vessel with cells migrating from the lumen into the tissue. Top right shows a multinucleated cell (osteoclast, OC) invading the bone and leading to erosion. Bottom right is a RA synovial tissue derived from arthroplasty (stained with H&E) with infiltrates of inflammatory cells (dark purple spots).

1.1.3 Pathogenesis of psoriatic arthritis and psoriasis

Similar to RA, immune cells and the mediators they secrete influence disease initiation and progression of PsA. However, different genetic and environmental factors play a role in psoriasis and PsA. In psoriasis, micro-trauma can lead to skin lesions as is reflected by the skin pattern involved in psoriasis. Thus, areas exposed to micro-trauma or pressure such as the knees and elbows often show plaque psoriasis which is frequently most resistant to treatment. Interestingly, in PsA, DIP joints are often involved with adjacent psoriasis involvement of the nail bed. Inflammation of the nail/skin could be proposed as a possible initiator of inflammation in the closest joint causing an arthritic event or involvement of the enthesis in the process. With the extensor tendon enthesis linking the joint to the nail bed it has been suggested that involvement of the nail bed may be due to an extension of the inflammation from the joint (39). However, it is unclear if the inflammatory process is initiated in the nail bed and spreads to the DIP joint or vice versa.

Recent genetic analyses have discovered risk factors shared by psoriasis and psoriatic arthritis. Most of the genes/loci associated with PsA were initially described for psoriasis and then tested for their association with PsA. Genes and single nucleotide polymorphisms (SNPs) involved are located in the HLA class I region but also cytokine related genes such as the IL-23 pathway (IL-23 receptor, IL-12p40, IL-23p19), Th17 cell cytokines such as IL-21, the 5q31 locus (encoding for genes like IL-4, IL-5 and IL-13) and others (37).

The major difference in the pathogenesis of psoriasis as a skin disease compared to the inflammation found in the arthritic joint is the involvement of keratinocytes rather than fibroblast-like synoviocytes. Inflammation of the skin as seen in psoriasis causes keratinocytes to be stimulated by cytokines and/or inflammatory cells leading to their proliferation and production of proinflammatory cytokines (40). For many years there has been debate as to whether the onset of psoriasis is due to a fundamental disorder of tissue cells or their regulation in the skin or of the immune system *a priori*. Recently, Wagner and colleagues generated a murine model exhibiting psoriasis-like skin disease with concomitant arthritis by deleting epidermal Jun proteins (JunB and c-Jun)

normally expressed by keratinocytes. These deletions lead to upregulation of the chemotactic proteins S100A8 and S100A9 associated with recruitment of inflammatory cells. Furthermore, JunB/c-Jun deficient mice crossed on a background deficient for Rag2 still developed psoriasis-like disease suggesting a minor role of T and B cells in the aetiology of this model (41).

In contrast to this observation, recent data regarding the Th1-Th17-IL-23 axis promote the idea of an adaptive influence in psoriasis. This will be further discussed below (see subsection 1.2).

1.1.4 Pathogenic immune cells in inflammatory arthritis

Chronic inflammatory arthritis mainly targets the synovial membrane, cartilage and bone. Hereby a variety of cells play a pathogenic role of disease initiation and maintenance of chronic inflammation. The crucial triggers for the onset of articular inflammation and subsequent damage are unknown; however, mouse data, human genetic associations and targeted therapies consolidate the evidence for pathogenic immune cells in inflammatory arthritis.

T cells are implicated in the pathogenesis of rheumatoid arthritis by genetic associations with HLA-DR alleles within the MHC class II and lymphoid-specific *PTPN22*. Especially disease association with HLA-DR4 alleles which contain the shared epitope has been well described (42). Further T cells are detected in high numbers in inflamed synovial tissue. The notion that T cells take part in the pathogenesis of arthritis has been confirmed by various extensively studied mouse models of arthritis. These models such as the collagen-induced arthritis model are clearly T cell dependent. However, the question arises if these data are transferable to human disease pathogenesis. T cell modulating therapies such as cyclosporine, CD3 or CD4-specific antibodies have been disappointing (43). Interestingly, the recently approved drug abatacept, targeting the immunological synapsis by binding CD80/CD86 has shown some benefit (44). Abatacept, a CTLA-4 immunoglobulin Fc fusion protein interferes with the T cell - antigen presenting cell contact and thus prevents T cell activation. This leads to the question which T cell subsets are pathogenic. On the one hand increased numbers of regulatory T cells in synovial fluid/tissue have been described, where it is not clear if these are dysfunctional or try to keep the inflammation

at bay. On the other hand, information about subsets such as Th17 cells emerged in the literature, with some evidence for its role in arthritis (further information see in chapter 1.2).

Also B cells as part from the adaptive immune system play a pathogenic role in chronic inflammatory arthritis due to their regulation in synovitis but also their role in preclinical disease. B cell depleting therapeutics, for example rituximab, an anti CD20 antibody which is expressed on B cells, but not on plasma cells, was initially developed for B cell lymphoma therapy. Interestingly, trials in RA demonstrated significant clinical benefit (45). From a standpoint that RA is a T cell driven disease, these data demonstrated that a network of pathogenic immune cells are responsible for the chronicity of RA. More intriguingly, in autoimmunity, production of autoantibodies specific for IgG (rheumatoid factors) or recently discovered antibodies against cyclic citrullinated peptides, can occur before the onset of clinical symptoms (46). Furthermore, hits in genome wide analysis of RA patients showed a susceptibility gene called peptidylarginine deiminases citrullinating enzyme 4 (PADI4) in Asian and US cohorts, however, could not be verified in UK cohort analysis (47, 48). This gene encodes an enzyme responsible for the conversion of arginine to citrulline residues and therefore providing a potential substrate for autoantibody production. B cells not only contribute to inflammation by autoantibody synthesis but also by the production of cytokines and chemokines (e.g. IL-6). Also the data in respect to abatacept link B cells as antigen presenting cell to T cell activation and thus provide a potential crucial role for antigen specific disease initiation and maintenance. Interestingly, autoantibodies such as RF and ACPA are not detected in PsA. Nevertheless, B cells accumulate in PsA synovium and thus might also play a crucial role.

Finally potential bystander cells from the innate immune system but also stromal cells contribute to the pathogenesis of inflammatory arthritis. Macrophages for example are considered as an important source of proinflammatory cytokines in the synovium. Macrophages but also mast cells and dendritic cells monitor organ integrity and act as sentinels in the tissue. Expression of pattern-recognition receptors (PRRs) such as Toll-like receptors (TLRs) which recognize microbial products but also endogenous ligands lead to cytokine production (49). Even more, synovial monocytes can be activated by immune complexes. Also

neutrophils are present in high numbers in synovial fluid and are detected in the inflamed synovium. At last, stromal cells, such as synovial fibroblasts can contribute to inflammation. Activation of fibroblasts by TNF and IL-1 stimulate the cells to produce TNF, IL-1 and IL-6 but also MMPs. This feedback loop prepares the tissue for local migration of T and B cells which further can support synovial fibroblast activation. (50)

This demonstrates an inflammation loop with cells talking from an adaptive to innate to stromal cell system. Disruption of this interaction loop with TNF inhibitors finally demonstrated benefit in clinical settings. In the next paragraphs cytokine biology with regard to its source will be described (see also table 1.6).

1.1.5 Cytokines in synovitis and dermatitis

The molecular/cellular pathogenesis of autoimmune diseases can be described in two ways. Firstly; to describe the cell as source of pathogenic products (e.g. proinflammatory cytokines) in the context of the immune dysfunction. Or secondly; to describe the pathogenic products themselves with focus on their actions thereafter in immune dysregulation. In general, in disease pathology, cells as crucial source for cytokines may be:

- Behaving in a dysregulated manner due to some intrinsic aberration - there is little evidence for this as a causative feature of RA or PsA beyond perhaps the roles of keratinocytes and fibroblasts which exhibit semi-autonomous behaviours - the latter certainly contribute to perpetuation and chronicity.
- Operating in the wrong context
(e.g. T cell help at the wrong time and place; autoreactive)
- Attacking structures they should not attack
(e.g. macrophage/neutrophil activation)
- Reorganising tissue in an aberrant way
(e.g. osteoclast activation, fibroblast/keratinocyte proliferation).

Rather than describing the cells' actions, the following paragraphs will focus on the major soluble mediators produced by immune cells: cytokines. Thus, I have elected to discuss the important immune cells in the context of the cytokines they produce or respond to (summarized in Table 1.6 Selected cytokines implicated in pathogenesis of RA, PsA and psoriasis).

Cytokines are mediators that transmit signals between cells in an autocrine or paracrine manner acting either in soluble or membrane bound form. Initially, cytokine families were named for their origin—for example, lymphokines, monokines, and interleukins. However, as many of these molecules also act on and/or are produced by non-lymphoid cells, the term *cytokine* is more appropriate. Cytokines are divided into families reflecting either their core functional domains and/or their shared structural homology, including, for example, hematopoietins, chemokines, interferons, TNF superfamily, IL-6 superfamily, IL-10 superfamily, and the IL-12 superfamily. Cytokines may exist as monomers, homo- or heterodimers, trimers, or tetramers. Receptors mainly comprise heterodimers; cytokine receptor families often utilize common receptor subunits (e.g. common γ chain receptor, IL-1RAcP, see 1.3.1). Receptors, like cytokines, can exist as membrane-signaling molecules, or may be released as soluble entities as a result of enzymatic cleavage from the cell membrane, or through the generation of alternatively spliced mRNA species. Soluble cytokine receptors can act as inhibitors of their ligands or act to facilitate signaling. Cytokine-receptor complexes may thereafter be internalized by endocytosis, fused with a lysosome where the cytokine will be destroyed. The receptor itself may either shuttle back to the cell surface or undergo degradation.

TNF- α is a central cytokine in inflammation and blocking its actions has proven to be a successful treatment for some autoimmune diseases. This cytokine will hence be discussed in more detail in the following section. Furthermore, IL-17A biology will be introduced to prepare a rationale for one aim of this thesis. This subchapter is summarized as a table describing cytokines involved in RA, PsA or psoriasis. Noteworthy, all the cytokines mentioned in Table 1.6 have been chosen as a target for drug development and have been tested in various stages of clinical trials including drugs in phase I as well as fully approved drugs (source: clinicaltrials.gov).

The success story: Tumour Necrosis Factor- α

TNF- α (also termed cachexin or cachectin) plays a central role in inflammatory arthritis and has therefore been a perfect target for therapy making it the most successful biological innovation in rheumatology so far (51). TNF- α is detectable in synovial fluid, expressed in synovial tissue and produced by monocytes, macrophages, mast cells, fibroblasts, keratinocytes, T cells, B cells and neutrophils upon cytokine activation, TLR ligation or cell-cell interactions. TNF- α is synthesized as a 26 kDa, type II transmembrane molecule, which can be processed by a TNF- α converting enzyme (TACE or ADAM17), to generate secreted 17 kDa monomers (52). Monomeric TNF- α is a 17350 Da antiparallel β -sheet sandwich, with 'jelly roll' topology interacting with two further monomers forming the functional trimeric unit (53). This trimer binds and clusters high affinity TNF receptors (TNF-R, 55 kDa or 75 kDa) present in great numbers on most cells. TNF- α exerts its effects by activating NF- κ B leading to the secretion of multiple pro-inflammatory cytokines, e.g. IL-1 and IL-6. *In vitro*, the effects of TNF- α on synoviocytes (synovium derived fibroblasts) could be blocked by addition of anti-TNF- α antibodies (54). The importance of TNF- α in arthritis has been confirmed by multiple *in vivo* studies, such as mice expressing human TNF- α which spontaneously develop arthritis (55, 56). These studies demonstrated that TNF- α plays a pivotal role in arthritis and this knowledge was subsequently used successfully to develop antibody targeted therapies in RA patients.

TNF- α is expressed in PsA synovial lining and sublining layer as well as in psoriatic skin lesions (57). It is therefore not surprising that TNF- α was also the first successful target of cytokine mediated therapy in psoriasis and PsA. Targeting TNF- α delivers beneficial effects on joint damage and function as well as disease outcome, but also on tissue inflammation and cell infiltration measured histologically in biopsies as part of proof of concept studies. Treatment with infliximab decreases proinflammatory cytokine expression in psoriatic skin and reduces the numbers of infiltrating T cells as well as vessel formation in involved skin and synovium. Furthermore, adhesion molecules important for cell infiltration have been reported to be decreased upon treatment with infliximab and other TNFi (TNF inhibitor) agents (58-60).

In summary, the promising experience with anti-TNF- α therapy has driven the search for further potential targets in autoimmune diseases. However, TNF- α blockade is effective in only approximately 70% of patients receiving treatment, thus leaving room for improvement and rendering it necessary to explore the therapeutic potential of targeting other inflammatory pathways.

Cytokines in RA, PsA and psoriasis

Cytokine	Cellular source	Receptor	Major signalling pathway	Major function	Role in psoriasis / PsA / RA
IL-6	Macrophages, T and B cells, endothelial cells, FLS	IL-6R/gp130	NFκB	Inflammation, acute phase response	elevated in serum and synovial fluid
IL-12 (IL12p40/IL-12p35)	B cells, monocytes, macrophages, DC	IL-12Rβ1/2	STAT4	Differentiates CD4 T cells to Th1 cells. Activates NK cells	Clinical improvement of psoriasis in anti IL-12p40 treatment
IL-15	Macrophages, FLS, endothelial cells	IL-15Rα /IL-2/15Rβ, common γc subunit	JAK1/3, STAT3/5	IL-2 like function, inflammation	Expressed in Pso/PsA/RA lesions Elevated in synovial fluid.
IL-17A	T cells	IL-17R	TRAF6 MAPK (?) NFκB (?)	Inflammation, neutrophil recruitment, cytokine secretion, bone metabolism	Elevated in synovial fluid
IL-18	Macrophages, DC, FLS, OB, KC	IL-18Rα/Rβ	MyD88, IRAK, TRAF6, NFκB	Proinflammatory, induces IFN production by T cells	Expressed in PsA similar to RA
IL-23 (IL-12p40/IL-23p19)	Macrophages, DC	IL-12Rβ1/IL-23R	Jak2, STAT3	Maintain Th17 cells, Induces IL-19 and IL-24	Increased in Pso lesions Clinical improvement of psoriasis in anti IL-12p40 treatment
<i>IL-10 family</i>					
IL-10	T cells, monocytes, KC	IL-10Rα/IL-20Rβ	JAK1, STAT1/3, SOCS3	Anti-inflammatory / regulatory actions, induces proliferation of B and mast cells	Decreased in Pso/PsA lesions. IL-10 improves skin disease
IL-19	Monocytes	IL-20Rα/Rβ	STAT3	Induces IL-6 and TNF-α expression by monocytes	Expressed in Pso lesions, RA synovial cells
IL-20	Monocytes	IL-20Rα/Rβ IL-22R/IL-20Rβ	STAT3 (?)	Induces keratinocyte proliferation and proinflammatory genes	Overexpression induces psoriasis-like phenotype
IL-24	Monocytes, T cells	IL-20Rα/Rβ IL-22Rα/IL-20Rβ	STAT3	Inhibits tumour growth	Expressed in Pso lesions
IL-22	Th17 cells, activated T cells, NK cells, mast cells	IL-22Rα/IL-10Rβ	ERK, p38 MAPK	Acute phase response, proinflammatory properties	Induces Pso like inflammation, expressed in RA synovium
IL-26	memory T cells	IL-20Rα/IL-10Rβ	?	Unclear role in herpes virus saimiri transformed T cells	?

Table 1.6 Selected cytokines implicated in pathogenesis of RA, PsA and psoriasis
DC: Dendritic cell; FLS: Fibroblast-like synoviocyte; KC: Keratinocytes; NK cell: Natural killer cell; Pso: Psoriasis; OB: Osteoblasts; OC: Osteoclasts.

Table 1.6 continued: Cytokines in RA, PsA and psoriasis

Cytokine	Cellular source	Receptor	Major signalling pathway	Major function	Role in psoriasis / PsA
OPG	OB, FLS	RANKL	-	Decoy receptor, inhibits osteoclastogenesis	Expressed only in endothelial cells below the synovial lining
RANKL	T cells, OB, fibroblasts, FLS	RANK	TRAF6, NFκB	Osteoclastogenesis	Expressed in synovial tissue, esp. in synovial lining layer
IL-1	Monocytes, Macrophages, FLS, B cells, neutrophils, chondrocytes	Type-1 (CD121a) or Type-2 (CD121b) receptor	NFκB	proinflammatory, cartilage degradation,	expressed in RA synovium, limited efficacy in clinical trials
April	DC, T cells	BCMA and TACI	NFκB	B cell proliferation	Increased in RA fluid and serum.
BAFF	Macrophages, FLS, T cells	BCMA, TACI and BAFF-R	TRAF2 and NFκB2 (BAFF-R), NFκB (TACI, BMCA)	B cell proliferation	Increased in RA fluid and serum; elevated in Pso serum.
GM-CSF	T cells, macrophages	GM-CSF-R		proinflammatory, T cell modulation	expressed in RA synovium, elevated in RA plasma

1.1.6 Mouse models of inflammatory skin disease

Studying psoriasis has advantages compared to other autoimmune diseases. Access to the inflamed tissue is far easier and generally presents fewer complications when using biopsy approaches. Compared to RA or systemic lupus erythematosus (SLE) in which biopsies of joints/kidneys are expensive and invasive, punch biopsies of the skin are quick and easily performed rendering enough material for mRNA, protein analysis or histology. However, research involving human psoriasis material has its disadvantages including; diversity of individuals (phenotype and genotype), difficult culture conditions due to bacterial and fungal contamination, range in intercurrent therapies, as well as limitation in donor numbers.

To overcome these problems and to study single proteins/genes which might influence the pathogenesis of diseases, different mouse models have been created in order to study psoriasis. There are currently several different models available (reviewed in (61, 62)). Various established rodent models have been created by inducing spontaneous mutations, genetic engineering via transgenic approaches or immunological strategies. The common approach to elicit the overexpression of proteins of interest in the epidermis is to put the gene of interest under the transcriptional control of the Keratin 14 (K14) promoter in the case of basal keratinocytes or K5 or 10 promoters to express it in differentiating keratinocytes. Other approaches have used tissue-specific deletion of proteins. Expression of inflammatory mediators or keratinocytes growth factors such as BMP6, Interferon- γ , KGF, TGF- α , IL-1- α , TNF- α and IL-20 lead to the recreation of only partial features of psoriasis (62). Overexpression of TGF- β 1 or VEGF in mouse skin was shown to generate a phenotype more similar to human psoriasis with acanthosis, increased vascularization, and leukocyte infiltration (63, 64). In both models as well as in the Jun protein deletion model (see 1.1.3 (41)) the major mechanism appears to rely on recruitment of immune cells by keratinocytes. These models are consistent with the hypothesis that an initial defect in the skin environment causes the recruitment of immune cells which induce inflammation and tissue damage. Further models which reflect the human situation are xenotransplantation models, using e.g. SCID mice. Recently, reports demonstrated the growth of reconstructed human epidermis by culturing

keratinocytes on inserts with specific differentiation media. After confluency of the keratinocytes was achieved on this inert surface, an air-liquid interface with nutrition from below initiated the creation of a three dimensional structure, closely resembling the epidermis (65). This epidermal reconstruction was used in subsequent studies to examine the influence of cytokines on the epidermal response (66), with results showing that IL-22 upregulates proliferation and differentiation of keratinocytes similar to that seen in psoriasis. Other psoriasis/skin inflammation models induce psoriasis like inflammation using stimuli such as chemicals or cytokines. In this thesis the two following models have been used: a TPA skin inflammation model and an intradermal cytokine injection model.

The first model reflects broad inflammation induced by a phorbol ester (TPA) on the back of the shaved mouse. This has been used to study effects of skin inflammation in knock out mice. For example in D6 deficient mice TPA treatments lead to inflammation with hallmarks of psoriasis compared to wildtype mice. Interestingly, skin inflammation was TNF- α and IL-15 dependent (67).

An alternative model of skin inflammation is induced by intradermal injection of cytokines. This method was originally established using IL-23. Intradermal injections of IL-23 into the dorsal skin induced a psoriasis-like phenotype (68). The model was subsequently improved by injecting into the ear pinna, hence allowing measurements of ear thickness and quantification (69). This has further been utilized by other groups using IL-22 and IL-23 (70, 71). Repeated injection of IL-22 or IL-23 every alternate day for 2 weeks led to ear as well as epidermal thickening with hyperkeratosis. Although these models are not a perfect representation of human psoriasis they offer the advantage of daily readout (ear thickness) rather than endpoint readouts such as tissue sections and histology, allowing the acquisition of data over a time course. Such in vitro models can therefore be utilized to identify crucial molecules involved in the pathogenesis of psoriasis and test potential targets for future therapies.

1.2 Th17 cells and their role in rheumatoid arthritis/psoriasis

The understanding of pathology in regard to its cytokine network has led to new therapies. TNF- α has been demonstrated as the first target of many to follow. However, it is necessary to find new targets to broaden and specify the therapy portfolio and improve current standards. *Hence the next subsections focus on the cytokine axis IL-17 - IL-23 and the novel cytokine IL-33.*

Immunological host defence relies on two parts of the immune system. As a first line of defence, the innate immune system responds to danger (e.g. pathogen invasion, trauma, physiologic or metabolic dysfunction) in an antigen-non-specific way without inducing classical immunological memory. In a second phase, the adaptive antigen-specific immunity provides a fine-tuned immune response including specific antibodies and the advantage of memory for future events. As a part of the adaptive immune system, CD4+T helper (Th) cells are activated by antigen presenting cells (APC, e.g. dendritic cells, B cells) via MHCII (major histocompatibility complex)-bound antigenic peptides. This signal 1 is supported by further costimulatory signals (signal 2) to fully activate the T cells. In the presence of signal 1 and 2 naïve T cells will differentiate into Th effector cells. So far, subsets called Th1, Th2, Th9 and Th17 cells have been described, in addition to distinct regulatory T cell subsets (Treg) (Figure 1.3). Th1 cells produce IL-2 and interferon (IFN)- γ and are thought to regulate cellular immunity, whereas Th2 cells produce IL-4, IL-5 and IL-13 thus being mainly involved in the protection against parasitic helminths (72). IL-4 and IL-13 are the major mediator of IgE class switching in B cells. Th2 cells induce IgG₁ and IgE antibodies in mice and IgM, IgG₄ and IgE in humans and thus Th2 cells can regulate humoral immunity (73). Th17 cells have been recently described, defined by their production of IL-17A. These cells also produce IL-17F, IL-21 and IL-22 (72). Th17 cells were initially identified and characterized in the murine system but have been since shown to exist in humans. Studies carried out with human Th17 cells have shown that there might be some differences between murine and human Th17 cells.

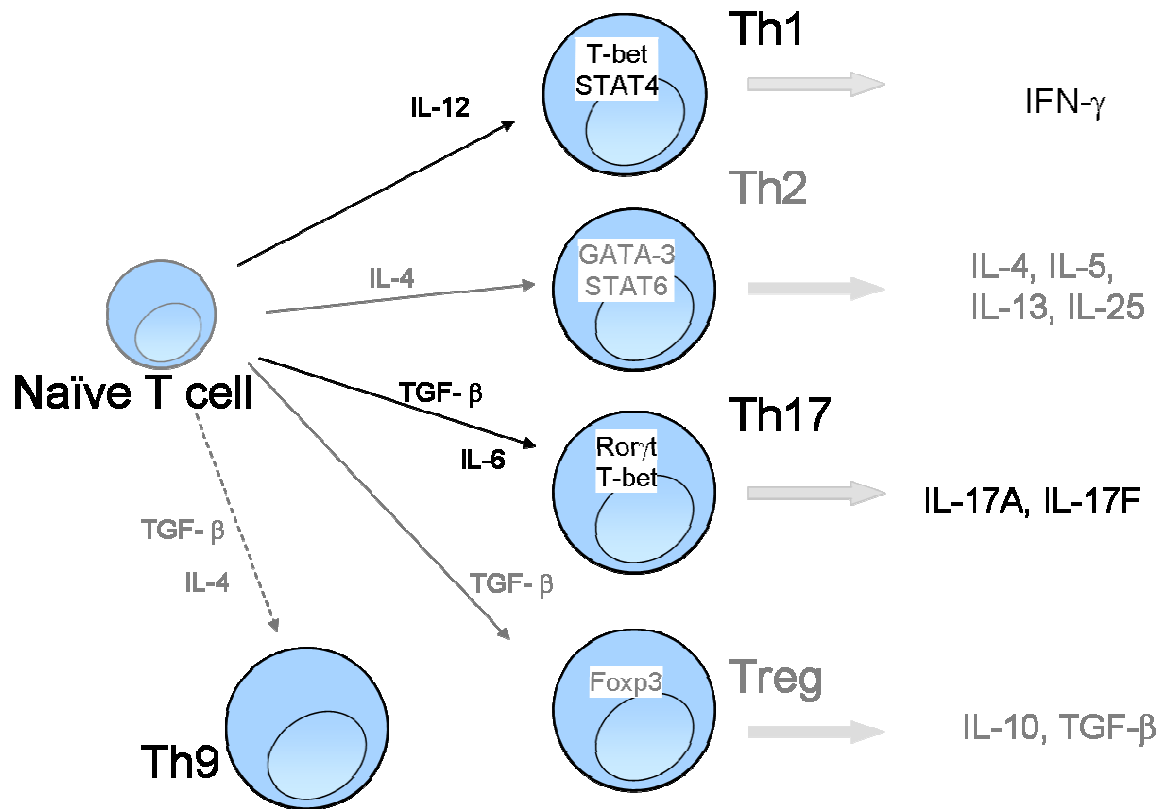


Figure 1.3 T helper cell differentiation (overview).

Differentiation driven by various cytokines to either proinflammatory cells such as Th1 and Th17 (mouse differentiation, see also Figure 1.4), but also regulatory cells (Tregs).

Points of discussions are

- Differences in Th17 differentiation between human and mice
and
Development of TH17 cells in human memory and naïve CD4⁺ cells
- Plasticity of Th17 cells in vivo
- Function(s) in disease

In mice, a series of elegant studies over the last few years have shown that IL-6 and/or IL-21 and TGF- β are in fact the key cytokines in the development of Th17 cells (74-76). The Th17 lineage defining transcription factor was found to be ROR γ t (77). Interestingly, key cytokines of Th1 and Th2 cells, namely IFN- γ and IL-4, block Th17 cell differentiation (78). The cytokine IL-23 (comprising 2 subunits IL-12p40 and IL-23p19) is essential for the maintenance and expansion of murine Th17 cells (79). Other factors have been demonstrated to support differentiation like TNF- α and IL-1 β and recently IL-21 in an autocrine manner (76) (Figure 1.4).

Similar to their mouse counterparts, human Th17 cells express RORC2, the human orthologs of ROR γ t (80). Development of human Th17 cells is less straight forward and includes more variables. First, Th17 cell development depends on the T cell type, differing between naïve T cells and memory T cells. Naïve CD45RA⁺CD161⁺ T cells have been studied derived from umbilical cord blood and differentiate to Th17 cells under the influence of IL-1 β and IL-23 (81). This process is TGF- β independent; however, TGF- β is speculated to support Th17 differentiation by inhibiting T-bet and hence Th1 development (82).

In peripheral blood, differentiation of Th17 cells from naïve T cells is not fully elucidated as yet. Specifically, the need for TGF- β is controversial as serum containing media might be contaminated with platelets and TGF- β . Serum free approaches demonstrated an essential requirement for low dose TGF- β in conjunction with IL-1 β and IL-23. However, the different approaches used in many of these studies, such as various purification techniques and culture conditions, make direct comparison of results difficult (reviewed in (83)).

Interestingly, in human blood serum concentrations are usually higher than the concentrations which were used for culturing T cell *in vitro* in any of the described studies, and therefore most likely do not represent the *in vivo* situation. However, TGF- β is not the only cytokine involved in the differentiation and maintenance of Th17 cells. Other cytokines such as IL-6, IL-21 and TNF- α have also been shown to support Th17 polarisation from naïve Th cells (Figure 1.5).

More clear is the development of Th17 cells from the memory pool. These effector cells can be identified by the combined expression of CCR4 and CCR6 (84) - another group described a CD4⁺CD45RO⁺CCR7⁻CCR6⁺ population which produce IL-17 (85). CCR6 is thought to be involved in the recruitment of Th17 cells to sites of inflammation via the ligand CCL20. IL-1 β , IL-23 and IL-6 promoted production of IL-17; however, TGF- β inhibited IL-17 (85, 86). To summarize, due to different cell culture and *ex vivo* approaches including various purification techniques ranging from cell sorting to bead purification and different cell culture conditions human Th17 biology is still elusive.

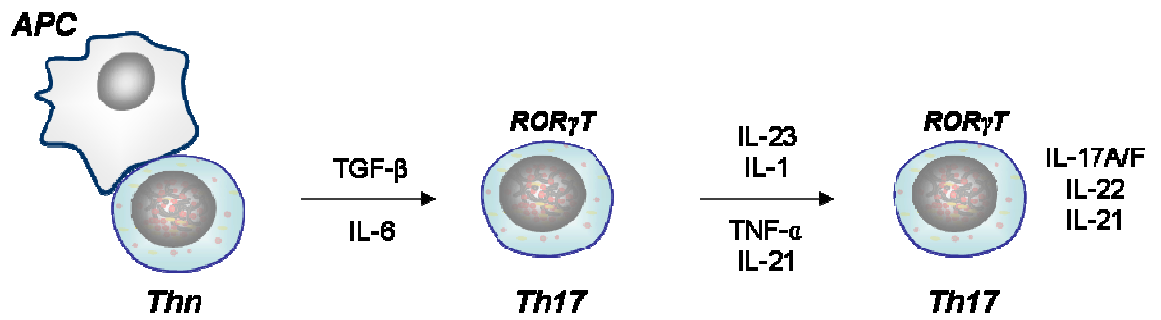


Figure 1.4 Th17 cell differentiation in mice

APC: antigen presenting cell, Thn: naïve T helper cell, Th17: Th17 cell. ROR_γT: Th17 cell specific transcription factor.

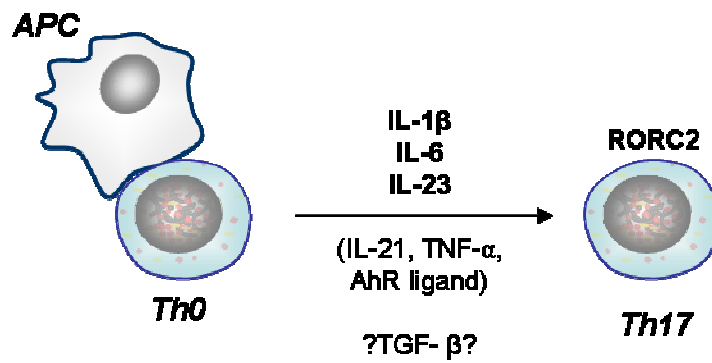


Figure 1.5 Th17 polarisation in humans.

APC: antigen presenting cell, Th0: naïve T helper cell, Th17: Th17 cell. RORC2: Th17 cell specific transcription factor in humans. AhR: Aryl hydrocarbon receptor

The classification of Th17 cells is further complicated by the plasticity of T cell subsets *in vivo*. T cells expressing both IL-17 and IFN- γ have been observed in arthritis mouse models (personal communication Dr D Asquith) and have been detected in humans (84-86). It is unclear if these cells represent a terminally differentiated subset or are precursors which are still able to commit to differentiation into Th17 or Th1 cell types. The plasticity of T cells might also play a role in the balance between differentiation of Th17 cells and regulatory T cells (Tregs) which both depend on the presence of TGF- β . Tregs can be induced by TGF- β and are defined by high expression of forkhead box P3 (FoxP3) in both the murine and human systems. These cells are strong immune-modulators which have the ability to suppress proliferation and cytokine production of effector T cells (87). In the murine system a proinflammatory environment, such as the presence of IL-6, can lead to a shift from a Treg to a Th17 biased milieu. Due to the as of yet still-defined role of TGF- β in Th17 development in the human system, it is unclear if this balance exists in humans as well. However, it has been shown in humans that Treg function is adversely affected in proinflammatory diseases such as RA and psoriasis (88, 89). Anti-TNF- α therapy reduces IL-6 levels and might therefore shift the balance away from Th17 development, thereby restoring Treg function (88, 90). There is some evidence that TNFi can reset peripheral human T cell responses towards a regulatory phenotype (88). What impact this plasticity has *in vivo* is unclear so far. It is noteworthy to particularly consider the situation during recovery from flares or periods of relative disease quiescence; eliciting the potential to re-balance the immune system and to acquire the knowledge of precise triggers that serve to initiate disease or flares will be mandatory for future understanding of the pathogenesis of autoimmune diseases in general and arthropathies in particular.

What is the effector role of IL-17? The IL-17 family comprises six cytokines termed IL-17A, B, C, D, E (or IL-25) and F. The cDNA of human IL-17 was initially cloned from a library of CD4⁺ T cells and stimulation of peripheral blood T cells was shown to induce the production of IL-17 (91). However, only IL-17A and IL-17F are produced by Th17 cells. IL-17A was found to be most homologous to IL-17F; T cells can produce three different dimeric forms of IL-17: IL-17A/A, A/F and F/F (92). The receptor biology of this family remains to be fully elucidated, but it appears that IL-17 binds to two subunits of IL17RA and one of IL17RC (93). These

receptors are ubiquitously expressed in almost all tissues thus far examined (91). Their regulatory elements remain obscure. Therefore, the ability to signal to a variety of different cells demonstrates a likely important role this cytokine plays in the immune system. IL-17 can stimulate a variety of cells including epithelial, endothelial, chondrocyte and fibroblast type cells to produce cytokines such as IL-6 and IL-8, as well as MMP molecules (94).

Further IL-17 was found to play a vital role in protection against bacterial, fungal and viral pathogens, such as *Candida albicans*, respiratory *Chlamydia* and *Klebsiella pneumoniae* (reviewed in (95)). Recent data from IL-17A receptor deficient mice suggest that IL-17 is not important for primary *Mycobacterium tuberculosis* infections - Th1 cells seem to be more important (reviewed in (96)). IL-17 serving as a mediator in the defence against pathogens, is also produced by a number of other cell types such as neutrophils, $\gamma\delta$ and CD8 T cells, macrophages and fibroblasts, although the best characterised cellular source of this cytokine is the Th17 cell (97).

Although IL-17 has evolved to facilitate protection against the infections listed above, there has been increasing evidence in the last few years that dysregulated expression of cytokines of the IL-17 family might play an important role in RA pathogenesis. In 1999, IL-17 was described in RA synovium and synovial fluid. IL-17 is expressed at relatively low levels in synovial fluid and comparatively few positive cells can be detected in tissues. Nevertheless, murine disease models showed interesting results concerning the role of IL-17 in autoimmunity (98, 99). For example, IL-17 knock-out mice showed suppressed induction and ameliorated progression of disease in an collagen induced arthritis (CIA) model (100). Studies using mice deficient for the IL-17 receptor or blocking IL-17 with anti-IL-17 antibodies further confirmed the role IL-17 plays in arthritis models (101, 102). A different chronic relapsing arthritis model showed that combined blockade of IL-17 with GM-CSF also works in a TNF-independent model (102). More interestingly, TNF- α blockade stimulates an increase in circulating Th17 and Th1 cells, likely through preventing their accumulation in the joint (103). Finally, IL-17 promotes erosions by inducing pro-erosive cytokines and by upregulation of Receptor Activator of NF κ B ligand (RANKL) on osteoblasts and promoting the creation of an osteoclast differentiating environment (99). The

broad proinflammatory effects of IL-17 in RA make it an interesting target for therapeutic blockade. So far blocking anti-IL17 antibodies has been shown to be an effective treatment of psoriasis, providing an initial proof of the feasibility of IL-17 blockade (104). Additionally, two phase I studies have been carried out in RA patients demonstrating an improvement in disease activity compared to placebo. Finally, ongoing phase II trials across a range of indications should render further information on the efficacy of IL-17-targeted therapies (105, 106). Interestingly, a recent study from Kokkonen et al. found that cytokines produced by Th1, Th2 and T_{reg} cell subtypes were upregulated in arthritis patients before the onset of disease. Levels of IL-17 did not reach significant difference to control subjects, although the concentration of IL-17 in individuals before disease onset was significantly higher than that in patients after disease onset (107). This indicates that IL-17 may play a role in the initiation rather than the maintenance phase of arthritis. However, measurements for this study were performed on peripheral blood samples and therefore might not reflect the levels of cytokines in tissues such as the joint.

As noted above, psoriasis is a model disease for cytokine targeting. Recent successes targeting TNF- α have been extended to other cytokines. Interestingly, the Th17 axis raised attention in the field with the discovery of single nucleotide polymorphisms of *IL12B* (the gene for IL-12p40 which is a subunit of IL-12 and IL-23) and *IL23R* which are associated with psoriasis (108, 109). Another potential gene locus was discovered harboring *IL2* and *IL21* (110). In preclinical studies in mouse models of psoriasis, injection of IL-23 into mouse skin induces a psoriatic-like disorder (68). Others showed that this effect is dependent on IL-22 (another Th17 cytokine) and CCR6 (a marker for Th17 cells) (69, 70). In addition, high amounts of IL-12 p40 and IL-23 p19 as well as IL-17 are detected in psoriatic skin from humans (111, 112). Trials using antibodies against IL-12p40 (IL-23p40) (ustekinumab and ABT-874) have been successful in moderate to severe chronic plaque psoriasis. Currently, trials in psoriasis are ongoing using antibodies against IL-17A (AIN457). Initial results are promising but further study results are awaited (104).

The cytokine IL-23 is a heterodimeric cytokine composed of a p40 and a p19 subunit, the former of which is shared with IL-12 (p35/p40) which drives naïve T cells into Th1 cells. IL-23 is produced by activated macrophages and dendritic

cells and seems to be important in induction and maintenance of Th17 cells as discussed above. Expression in RA synovial fluid is controversial with groups reporting low and others very high levels. Interestingly, in synovial tissue bioactive IL-23 seems to be present only in low levels despite high expression of IL-23p19 shown by histologic analysis. (113, 114)

Regarding bone homeostasis IL-23 upregulates Receptor Activator of NF κ B (RANK) on myeloid precursors and induces RANK ligand expression on CD4⁺ T cells (115, 116). This direct effect combined with an indirect effect via IL-17 strongly support osteoclast differentiation and further erosive disease. Recent genetic studies in psoriasis patients provided strong support for association with IL-23 related loci with involvement of single nucleotide polymorphism for *IL-23A*, *IL-12B* and *IL-23R* (117) (see also table 1.5). In RA so far, these variants could not be observed yet, but larger sample sets might uncover this in the future (118, 119).

Due to the shared subunits interpretation of mice deficient in p40 is difficult as it lacks IL-12 and IL-23. To test the effect of IL-23 in autoimmune disease anti-IL-23 antibodies were administered to rats with CIA which demonstrated less severity of disease (120). In a different study in mice developing spontaneous arthritis (IL1RA^{-/-} mice) showed worsening of disease after application of IL-23 (115). To understand the relationship between IL-23p19 and IL12-p40 Murphy and colleagues used mice deficient for these subunits (121). Loss of IL-23p19 protected mice against arthritis were IL-12p40 deficient mice experienced exacerbated disease.

The final proof for the importance of IL-23 in inflammatory diseases such as psoriasis was the in a phase III clinical trial with Ustekinumab, a human monoclonal antibody against IL-12p40 targeting IL-23 and IL-12. In psoriasis Ustekinumab has yielded beneficial effects in >75% of patients (32, 122). Despite not distinguishing between the two cytokines IL-12 and IL-23, targeting Th1 and Th17 cell differentiation is effective but might have future side effects due to inhibition of two T cell subsets. Thus a future more predicatively approach might be a blockade of IL-23p19. Trials are running and results are awaited.

1.3 The role of the cytokine Interleukin 33 in health and disease

The novel IL-1 family cytokine IL-33 was chosen for study for several reasons, including its striking expression pattern in the nucleus, its biology with reference to cellular release, functionality particularly its role as a novel alarmin, its divergent roles in the intracellular versus the extracellular compartment and finally activation versus neutralisation. Furthermore its role in pathogenetic processes demonstrating clear Th2 biology linked it originally to allergy and asthma; while on the other hand more recent data suggest a capacity for playing an important role in Th1/Th17 biology particularly in autoimmune arthritis. This thesis directly addresses its role as an alarmin at body barriers focussing on the autoimmune disease psoriasis which is thought to be partially regulated on the premise of damage and body defence. In this section, this novel cytokine will be introduced in the context of the IL-1/TLR cytokine family, its structure, expression and biology as well as its potential role in disease thus far elucidated.

But what is an alarmin? Pathogens can be detected via a set of receptors which detect pathogen-associated molecular patterns (PAMPs). With this ability the immune system can sense danger and respond to the signal to preserve the integrity of the body. However, another source of damage (and subsequent danger) is tissue and cell damage caused by trauma (e.g. mechanical forces, heat, cold chemical insults, radiation, etc.). The term alarmin is proposed to define endogenous molecules released during trauma, which signal tissue and cell damage. This term “alarmin” was proposed by Joost Oppenheim (EMBO Workshop on Innate Danger Signals and HMGB1, Milano, Italy 2006). The two groups, alarmins and PAMPs are subgroups of the damage-associated molecular patterns (DAMPs). (123)

1.3.1 IL-33 in the context of its IL-1 receptor / Toll like receptor family members

In the 1980s IL-1 was one of the first cytokines described, hence the number given. Prior to this, IL-1 was studied for many years under the guise of biologic activities (usually named for these e.g. endogenous pyrogen) and found to cause

fever, stimulate acute-phase proteins, induce lymphocyte responses, increase the number of bone marrow cells and cause joint damage (124). Two proteins were shown to share these activities, encoded by different genes - IL-1 α (IL1F1) and IL-1 β (IL1F2). Interestingly, despite being distinctive structural entities from TNF- α and IL-6, they share approximately 95% overlap in their effector function with the latter.

Both can bind to a heterodimeric receptor complex consisting of IL-1 receptor I (IL-1R) and IL-1 receptor accessory protein (IL-1RAcP). Binding to IL-1R leads to recruitment of IL-1RAcP with subsequent signalling via TIR (Toll/IL-1R) domains. These TIR domains are conserved intracellular receptor parts linking the IL-1 receptor family to the Toll like receptor (TLR) family and signal via MyD88. Major differences between these two receptor families are found primarily in their extracellular components: IL-1Rs consist of IgG like domains, whereas TLRs consist of leucine rich repeats. Interestingly, IL-1 α and IL-1 β share the same effector function, bind the same receptor and are structurally very similar. However, primary amino acid homology of mature human IL-1 α to mature IL-1 β is only 22% (124). IL-1R antagonist (IL-1RA), also named IL1F3, is another ligand for the IL-1R and competes for binding. This natural antagonist binds IL-1R but does not result in recruitment of IL-1RAcP and therefore prevents signalling. IL-1 belongs to the IL-1 superfamily family that includes 11 structurally related cytokines; family members had different names from Family of IL1-x (FIL1-x), IL-1 homolog x (IL1Hx) to IL-1 related protein x (IL1RPx) where x stands for different cytokine numbers. Finally, all group members have been linked together with the common name IL-1 family member x (IL-1Fx) (Table 1.7).

Interleukin (HGNC gene family nomenclature)	conventional name	receptor
IL-1F1	IL-1 α	IL-1R, IL-1RAcP
IL-1F2	IL-1 β	IL-1R, IL-1RAcP
IL-1F3	IL-1RA	IL-1 receptor (antagonist)
IL-1F4	IL-18, IGIF	IL-18R, IL-18RAcPL
IL-1F5	IL1RP3, IL1-HY1, FIL1-delta	
IL-1F6	FIL1-epsilon	IL-1Rrp2, IL-1RAcP
IL-1F7	IL1H4 (homolog 4), FIL1-zeta, IL1RP1	
IL-1F8	FIL1-eta, IL1H2	IL-1Rrp2, IL-1RAcP
IL-1F9	IL1H1, IL1RP2	IL-1Rrp2
IL-1F10	FIL1-theta, IL1HY2	
IL-1F11	IL-33, NFHEV	ST2, IL-1RAcP

Table 1.7 IL-1 family – members and nomenclature

Different names have been assigned over time to the IL-1 family members. This table shows the *HUGO Gene Nomenclature Committee* (HGNC) nomenclature (left column). Middle column shows the conventional names. According receptors are shown in the right column.

Monocytes are the main source of IL-1, however, multiple cells from hematopoietic or stromal origin can secrete IL-1 such as T cells, B cells but also epithelial cells. IL-1 α and IL-1 β are synthesized as precursors. Interestingly, IL-1 α precursor (pro-IL-1 α) is also active in its precursor form, whereas IL-1 β has to be cleaved to a mature form to become active. Pro-IL-1 α remains in the cytosol, undergoes myristoylation and translocates to the cell membrane where it can be anchored to the cell (125, 126). Calpain is required for the cleavage of pro-IL-1 α , whereas Caspase-1 and/or Caspase-8 are important for the cleavage of pro-IL-1 β (127, 128).

IL-18 (former known as IFN- γ inducing factor, IGIF) is synthesised as a 23 kDa pro-molecule that is cleaved by caspase 1 to an 18 kDa ligand which is then able to bind IL-18R (129). Pro-IL-18 is expressed in macrophages, dendritic cells, Kupffer cells, keratinocytes, chondrocytes, synovial fibroblasts, and osteoblasts (127). Upon release, IL-18 binds to IL-18R which forms a comparable complex to the IL-1R complex. IL-18R α binds IL-18, further IL-18R β is recruited which does not bind IL-18 on its own but initiates intracellular signaling in this heterotrimeric complex (Figure 1.6). IL-18R β is an accessory like protein and similar to IL-1RAcP (127).

IL-1F5 shares significant amino acid sequence similarity (52 %) with IL-1RA (receptor antagonist) and dysregulation may play a role in skin inflammation (130, 131). IL-1F5 may function as a specific receptor antagonist of the IL-1 related receptor protein 2 (IL-1Rrp2) (130). IL-1F6, F8 and F9 bind to IL-1Rrp2, requiring IL-1RAcP for signaling. IL-1Rrp2 is highly expressed on epithelial cells in the skin suggesting a possible role in host defense in these organs. IL-1F10 binds to soluble IL-1RI with an unknown effect (127).

IL-33 (IL-1F11) is the latest of IL-1 family discoveries. Initially described as nuclear factor of high endothelial venules (NF-HEV) by Girard and colleagues in 2003, Schmitz et al defined its function and role in the IL-1 family in 2005 (132, 133). This group described the *IL33* gene after searching a computational derived database of the IL-1 family members.

In the following subsections, more detail in regard to the structure, function and biological relevance of IL-33 will be given.

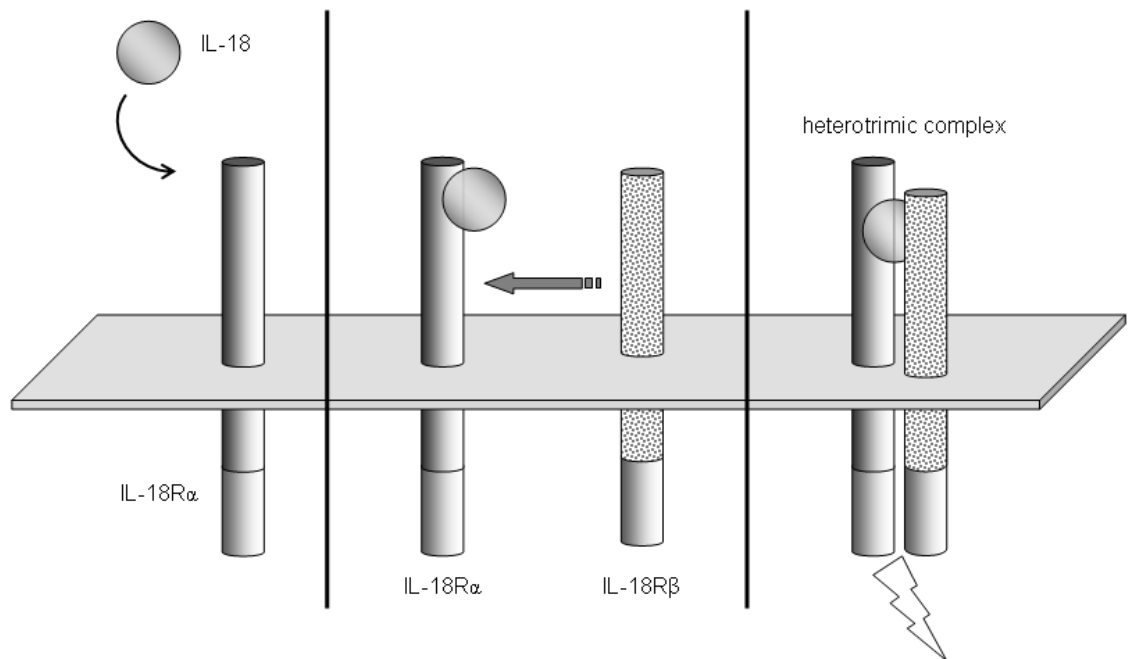


Figure 1.6 IL-18 receptor complex.

The IL-1 family cytokine binds IL-18R α (left part), however, the ligand-receptor pair can not induce signalling into the cell. This binding leads to recruitment of IL-18R β (middle part). This heterotrimeric receptor-ligand complex now signals via its TIR domains by recruitment of MyD88. Similar processes happen with IL-1 (IL-1R/IL-1RAcP) or IL-33 (ST2/IL-1RAcP). For further downstream signals see Figure 1.9.

1.3.2 Structure of IL-33

The sequence of IL-33 has been mapped to human chromosome 9 (9p24.1) and mouse chromosome 10 (19qC1). The cDNA encodes for 270 and 266 amino acids for human and mouse, respectively, and are approximately 55% identical at the amino acid level (132). Its molecular weight is ~ 30 kDa. Using sequence and secondary structure alignment, Girard and colleagues demonstrated that IL-33 consists of a homeodomain like helix turn helix motif (HTH) on the amino terminal side (133). This is followed by a nuclear localisation signal and further 12 predicted β strands comprising an IL-1 like cytokine domain with a typical β -trefoil structure. The 1-65 amino acid HTH motif of IL-33 has homology with *Drosophila* transcription factors showing the best match with *Engrailed*. These HTH motifs are known to be repressors of transcription. *Engrailed* is a *Drosophila* homeodomain protein required for proper segmentation and maintenance of the posterior compartment identity. The repressor activity of *Engrailed* lies in the sequence containing amino acids 1-298 which has been shown to confer transcriptional repression when fused to heterologous DNA binding domains. Use of dominant-negative transgenes has been successful in analysing certain pathways and using this technique to convert transcription factors into dominant repressors can be achieved by fusion to repressor domains such as *Engrailed* (134). Accordingly, translational fusions with the *Engrailed* repressor domain have efficiently converted plant transcription factors, b-catenin and c-myb, into dominant-negative proteins. Also, *in vivo*, an airway-targeted GATA6-*Engrailed* dominant-negative fusion construct was able to alter epithelial differentiation (135).

In the following figure IL-33 HTH is demonstrated (Figure 1.7, 1.6A altered from (133)). This part is built with three α -helices with the helix number 3 (H3) binding the DNA. The dark gray shaded part determines the turn in this sequence (Figure 1.7A). For illustration, figure B shows the general binding of HTH proteins into the major groove of the DNA with an example how the protein would be orientated to the DNA. Normally these proteins form a homodimer (as is IL-33) which leads to another binding of a helix most likely increasing the effect (Figure 1.7B).

Therefore, similar to *Engrailed*, IL-33 is thought to be a suppressor of transcription. Several data support this idea:

Carriere et al. demonstrated in elegant studies that IL-33, especially the HTH like part is located to heterochromatin. By truncation of IL-33 HTH like part this heterochromatin association was abolished and IL-33 expression became unrelated to the heterochromatin. More interestingly, by fusing IL-33 to the Gal4-DNA-binding domain in gene reporter assays with a GAL4-responsive luciferase reporter, transcriptional activity was reduced illustrated by decreased luciferase activity (136). This could be reestablished by mutating the DNA binding parts of IL-33 (137). More strikingly, Roussel et al. showed that the association of IL-33 to the heterochromatin is conserved in regard to this binding. Kaposi sarcoma herpesvirus (KSHV) LANA consists of a *MXLRSG* motif, which also occurs in IL-33 and is crucial for binding to histone H2A-H2B (137). Binding alters nuclear architecture and leads to chromatin compaction. KSHV LANA uses this binding for maintenance of viral genomes in latently infected tumor cells. By even mutating three amino acids in this motif chromatin binding could be prevented.

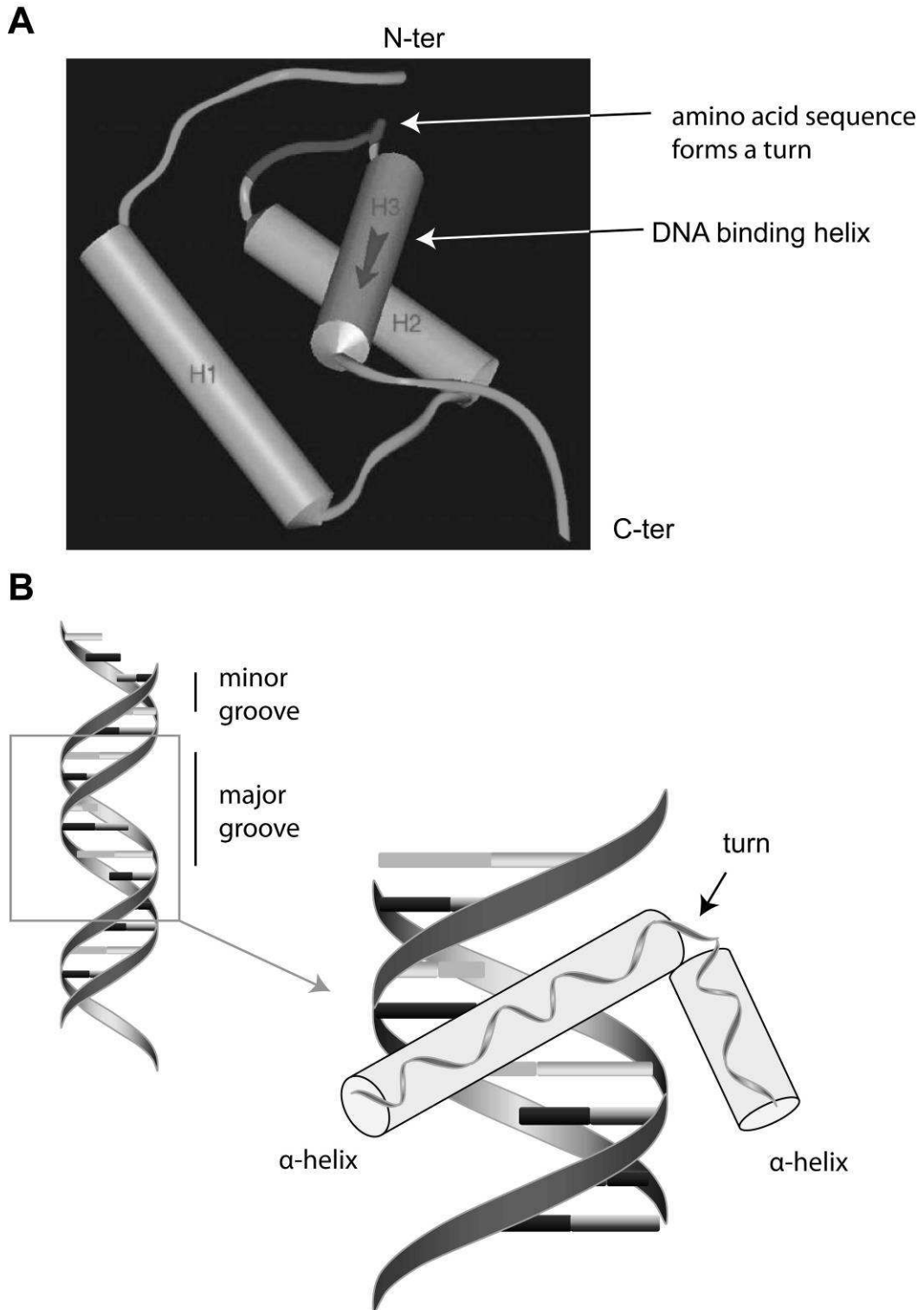


Figure 1.7 Structure of IL-33 HTH like motif

Example of HTH like motif in comparison to other HTH genes. Figure A demonstrates the structure of IL-33 HTH like part with three helices where the helix number 3 (arrow) is able to bind DNA; this figure has been altered from (133). B demonstrates a schematic picture of a HTH in which one α -helix binds DNA in the major groove. Black arrow indicates the turn.

Next to the chromatin binding domain in the HTH like motif, IL-33 possesses a nuclear localisation signal (NLS), near the N-terminal domain (Figure 1.8). Truncation of the NLS (e.g. a construct containing only IL-33₁₁₂₋₂₇₀, see Figure 1.8) leads to retention of IL-33 in the cytoplasm (136, 138). The HTH like motif and NLS (important for nuclear localisation and DNA binding) are linked to the IL-1 like cytokine domain consisting of 12 β strands. The latter part has mainly been used to study biological effects of IL-33, as it has been assumed that IL-33 is cleaved by caspase-1 leading to “mature IL-33” (the IL-1 like cytokine domain) which is thought to be released in a similar way to IL-1 or IL-18 (132). Interestingly, recent studies revealed that IL-33 is not cleaved by caspase-1, but instead cleaved by apoptosis associated caspases 3 and 7 as well as calpain and as a result is therefore inactivated rather than activated (139-141). In addition, caspase 3 treated IL-33 breakdown products are not able to bind ST2 (the IL-33 receptor), but the N terminal part still translocates to the nucleus (139). Moreover, different groups showed that full length IL-33 is bioactive and can be released by necrosis classifying IL-33 as an alarmin (140-143).

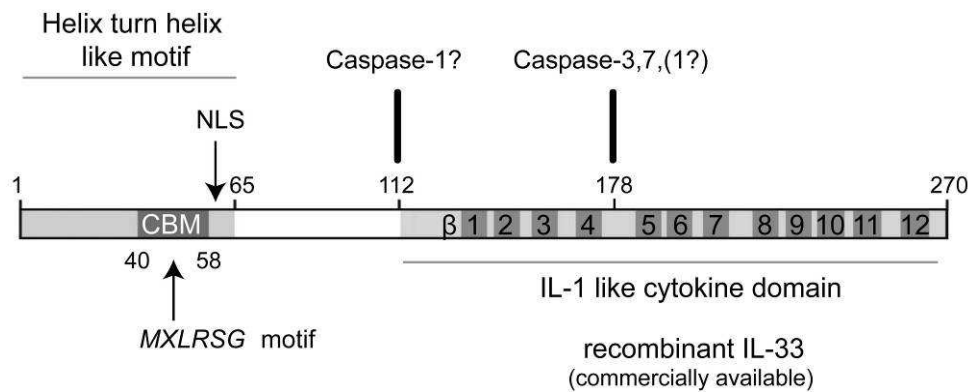


Figure 1.8 IL-33 structural components and cleavage sites.

N terminal domain shows HTH like motif including chromatin binding domain (CBM) with the specific amino acid motif and the nucleus localisation site (NLS). β 1-12 demonstrates the IL-1 like cytokine domain with 12 β strands. At localisation amino acid 112 the initial described caspase-1 cleavage site from Schmitz et al (132) is shown. Further after the residue Asp178 Cayrol et al showed a truncation by caspase 1 and 3 which deactivated IL-33 signaling through ST2 (142). One month later, Luthi et al published truncation at Asp178 by caspase 3 and 7, but did not confirm caspase 1 (143). It has to be emphasised that the structure in biological assay using recombinant IL-33 is a product reflecting the IL-1 like cytokine domain truncated at amino acid 112.

1.3.3 Tissue localisation and cellular expression of IL-33

So far, most reports visualising IL-33 expression have shown that IL-33 is exclusively expressed in the nucleus. Using antibodies against the C terminal region (e.g. Nussy-1) most analyses demonstrate in nearly every tissue nuclear expression of IL-33 (www.proteinatlas.org, IL-33 expression pattern by IHC). Few exceptions exist although cytosolic staining in LPS stimulated THP-1 cells and monocytes *in vitro* (144) and macrophages in peridontal tissue have been reported (personal communication, Dr Fukada Glasgow University). The nuclear expression pattern mainly occurs in stromal cells such as endothelial cells and epithelial cells. It is noteworthy that IL-33 has initially been described as a “nuclear factor of high endothelial venules” consistent with this reported expression pattern. Schmitz et al reported IL-33 expression in cDNA libraries. They show that IL-33 is broadly expressed in different tissues; however, on the cellular level differences occur. Mouse organs expressing high levels of IL-33 cDNA include stomach, lung, spinal cord, brain, and skin. In humans, IL-33 cDNA was detected in adherent stromal cells like epithelial/endothelial cells, smooth muscle cells, fibroblasts, and keratinocytes where the latter two upregulated IL-33 after TNF- α and IL-1 stimulation (132). Comparing cDNA reports with protein level by IHC, endothelial, keratinocyte and bronchial expression can be confirmed (www.proteinatlas.org). Staining for IL-33 in arthritic joints is reported by 2 different groups (145, 146). They concluded that these positive cells are macrophages or fibroblasts. Initial data from our lab demonstrated endothelial staining in inflamed synovium, rather than macrophages, thus uncertainties remain and this needs more investigation. Expression in lymphoid tissues has been shown to relate to endothelial cells but also fibroblastic reticular cells (147). Other expression patterns are still to be confirmed.

1.3.4 Release of IL-33

Initial studies hypothesized that IL-33 is released in a caspase-1 dependent manner. NLRP3 (NLR family, pyrin domain-containing 3) inflammasome activation by pathogen-associated molecular patterns (PAMPs) or damage-associated molecular patterns (DAMPs) leads to oligomerisation of NLRP3 and

clustering of pro-caspase-1. This results in caspase-1 auto-activation and caspase-1-dependent processing of cytoplasmic targets, including the pro-inflammatory cytokines IL-1 β and IL-18, which mediate repair/inflammation responses such as angiogenesis and neutrophil influx to remove cellular debris or fight pathogens (148). The mature cytokines are released from the cell by a secretion pathway that is currently not defined (149) but may include the P2X7 receptor. Full length IL-33 with ~30 kDa was reported initially to be cleaved to a 20-22 kDa product in a similar way to IL-1 and IL-18(132).

Until recently, IL-33 was rarely detected in serum or tissue culture supernatant mainly due to lack of good reagents however new data concerning the activation/deactivation of IL-33, has provided more clarity about its secretion. Weak secretion of full length IL-33 has been reported in a monocyte cell line (THP-1 cells) in response to LPS (142). More intriguing, cell death in particular necrosis releases IL-33. Different groups established the fact that either chemical (H₂O₂, NaN₃, Daunorubicin, TritonX100) or mechanical (scraping, scratching, freeze/thaw) necrosis of IL-33 expressing cells release full length IL-33 into the media (142, 143). Further, in diseases with a high burden of cell death serum IL-33 was detectable. Reports state IL-33 in RA synovial fluid, SLE serum and serum of sepsis patients (150-152). The mechanism/pathway as to how IL-33 is released in such disease states remains ill-defined.

IL-33 seems to play a similar role to other signals released from injured tissues that trigger the homeostatic responses that promote repair and activate the immune system. These signals, collectively referred to as damage-associated molecular patterns (DAMPs) or alarmins, possibly comprise quite heterogeneous molecules that share some functional characteristics (123). IL-33, exhibiting nuclear expression and release during cell death, reflects similar features to HMGB-1 (high mobility group box 1). In addition, HMGB1, like IL-33 is highly conserved in mammals. Furthermore HMGB1 deficient mice die shortly after birth (153) while IL-33 deficiency is embryonically lethal (personal communication, Dr D Gilchrist, University Glasgow, Dr A McKenzie, Cambridge University). In comparison, HMGB1 plays a different intracellular role as DNA chaperones influencing multiple processes in chromatin such as transcription, replication, recombination, DNA repair and genomic stability (154). Cellular release of HMGB1 can work in several ways. Stimulated cells can actively secrete

HMGB1 while cell death, particularly necrosis passively releases these proteins. During apoptosis (programmed cell death) HMGB1 binds tightly to chromatin and thereby is retained in apoptotic bodies (155). Extracellular HMGB1 delivers multiple signals: it behaves as a trigger of inflammation, attracting inflammatory cells while it promotes tissue repair by recruiting stem cells and promoting their proliferation. It activates dendritic cells and promotes their function to support antigen-specific T cells and supports their polarization towards a T-helper 1 phenotype (156). To conclude, HMGB1 and IL-33 are conserved proteins, act as alarmins, fulfill different functions in the nucleus while promote diverse signaling in inflammatory cells. Nevertheless, both proteins are unquestionably mandatory for the function of a mammalian organism.

1.3.5 IL-33 receptor signalling via ST2 and IL1RacP

ST2 receptor – discovery

The IL-33 receptor ST2 (also named T1, IL1RL1, DER4, and FIT-1) was first described in 1989 (157). Differential splicing leads to formation of 3 isoforms: transmembrane ST2, a soluble form (soluble ST2 or sST2) and a variant ST2. ST2 is a member of the IL-1 receptor family and has 38% amino acid homology to the IL-1 receptor (158). Transmembrane ST2 is membrane-bound with 3 extracellular immunoglobulin-G domains, a single transmembrane domain, and an intracellular domain homologous to toll-like receptors and other IL-1 receptors. Soluble ST2 lacks the transmembrane domain as well as the intracellular domains and is thought to act as a decoy receptor for IL-33 signaling.

ST2 receptor - deficiency

ST2 deficient mice are healthy and displayed no overt phenotypic abnormalities (159). In the initial manuscript describing ST2 deficiency, mice when challenged with a pulmonary parasite infection, had severely impaired levels of Th2 cytokine production. Subsequent studies used ST2 deficient mice for multiple IL-33 studied pathogenetic models ranging from allergy models to arthritis (more information below).

ST2 receptor - expression

ST2 is mainly expressed on mast cells and Th2 cells but not on Th1 cells (159-161). Further expression has been detected on fibroblasts, dendritic cells and other stromal cells but also on endothelial cells (146, 162, 163). Recently, basophils have been reported to respond to IL-33 (164-166). The newest subset of cells expressing ST2 has been described by 2 groups. Moro et al detected new adipose tissue-associated c-Kit⁺ Sca-1⁺ lymphoid cells which were an innate source of Th2 cytokines (167). These cells express high levels of ST2. McKenzie and colleagues defined a new innate effector leukocyte associated with the intestine. These cells were lineage marker negative, highly positive for ST2 and IL-17B receptor (IL-25 receptor). These cells produced high amounts of IL-13 and therefore McKenzie and colleagues named this new entity “*nuocytes*” owing to their high level of IL-13 expression, and nu being the 13th letter of the Greek alphabet (168). Furthermore they demonstrated that “*nuocytes*” are important in parasite defense while Moro et al showed that their cell entity is important for helminth expulsion. Due to their Th2 type role, with an innate lymphocyte signature, Moro proposed to call these cells “*natural helper cells*”. In both papers, cells responded to IL-25 and IL-33 and produced high amount of IL-5, IL-6 and IL-13. Further characterization of these cells (*nuocytes* or natural helper cells) is awaited.

ST2 receptor - signalling

Similar to IL-1 and IL-18 that require a co-receptor for intracellular signalling, Chackerian et al, and shortly thereafter Palmer et al, identified IL-1RAcP as part of the IL-33 receptor complex with ST2 (169, 170). *In vivo*, IL-1RAcP deficient mice did not respond to IL-33 treatment compared to wildtype controls (169). Interestingly, soluble IL-1RAcP enhances the ability of sST2 to inhibit IL-33 signalling (170). Signal transduction in ST2 and IL-1RAcP is mediated via the TIR domains. Binding of IL-33 to the IL-33R complex results in recruitment of the adaptor proteins myeloid differentiation factor 88 (MyD88) and other numerous activation proteins with downstream nuclear factor- κ B (NF- κ B) activation; thus IL-33 uses the same signaling components as IL-1 (Figure 1.9). Briefly, the recruitment of MyD88 leads to the recruitment of IL-1R-associated kinase (IRAK) 1 and IRAK4 and TNFR-associated factor 6 (TRAF6) (132, 171). MyD88 is essential

for IL-33 signalling as MyD88 deficient mice do not respond to IL-33 administration (169). IL-33 stimulation also leads to phosphorylation of inhibitor of NF- κ B (I κ B α) as well as the kinases Erk1/2, p38, and JNK(132). More insights in signalling cascades for MyD88 downstream pathways are summarized by Professor Luke O'Neill (172):

- MyD88 recruits IRAK1 and IRAK4; IRAK4 phosphorylates IRAK1
- IRAK1 phosphorylates Pellino-1 (E3-ligase), this leads to IRAK1 polyubiquitination
- further recruitment of NEMO¹/IKK1²/IKK2 complexes
- polyubiquitination of TRAF6 with TAK1³ recruitment to the NEMO/IKK1/IKK2 complex
- activation of IKK2 by TAK1
- TAK1 also couples to the upstream kinases for p38 and JUN N-terminal kinase-1 (JNK).

This intracellular activation cascade by IL-33 (or IL-1) is likely to be more complex, however (172). Furthermore in mast cells, IL-33 triggers Ca²⁺ influx by the activation of phospholipase D and sphingosine kinase (173).

Although ST2 receptor signaling is understood in the broad context, it is not clear, why signaling cascades through MyD88 by different receptors lead to different cellular responses. Difficulties in determination of all variables still hinder these insights.

¹ NEMO: NF- κ B essential modulator (a scaffold protein)

² IKK: inhibitor of NF- κ B (I κ B) kinase

³ TAK1: transforming growth factor β -activated protein kinase

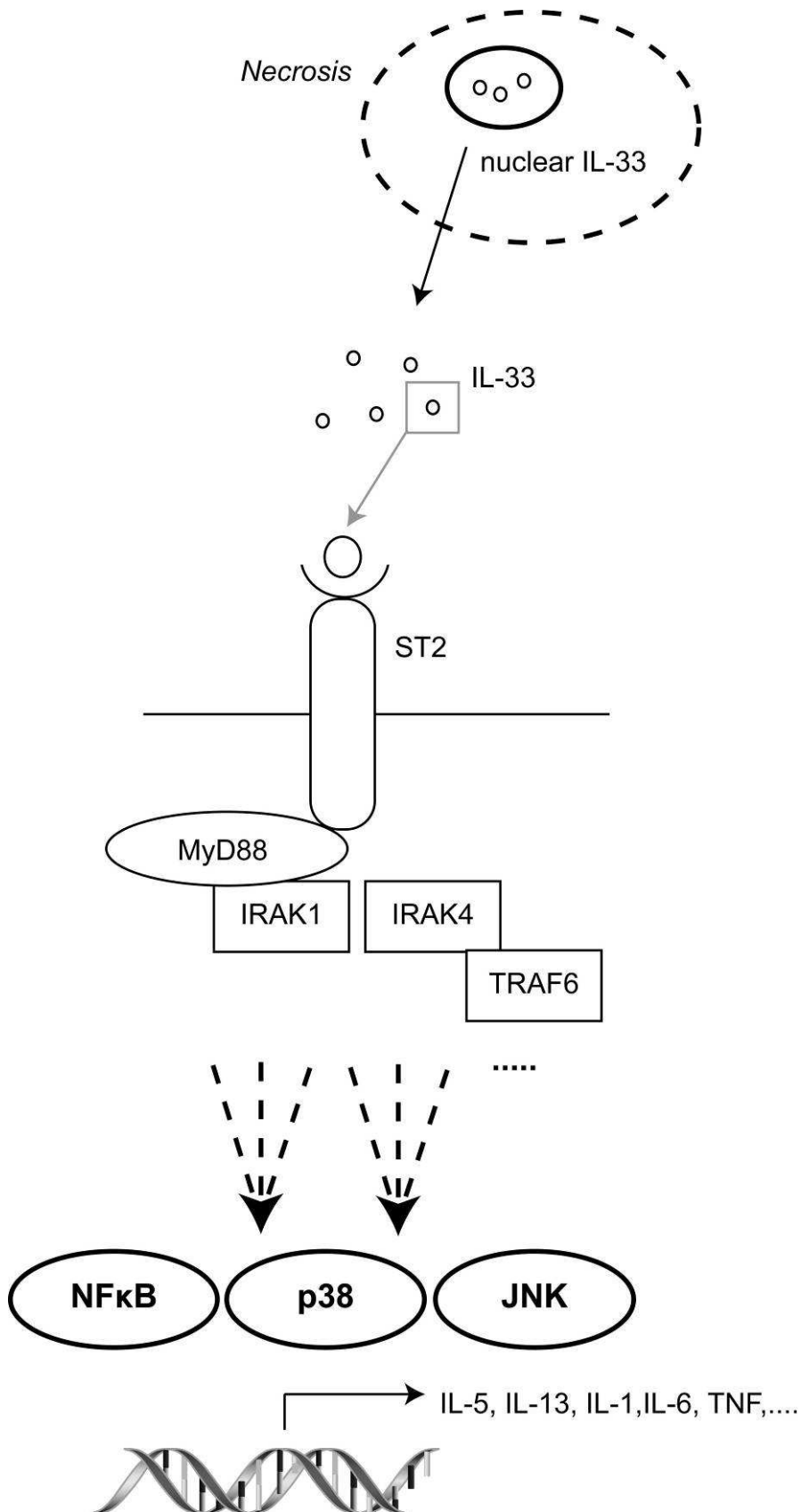


Figure 1.9 IL-33 binding to ST2 and IL1RacP signals via MyD88
 Schematic overview for binding and signalling of IL-33: nuclear IL-33 is released by necrosis and binds to ST2 which leads to recruitment of IL-1RacP, MyD88, IRAK1, IRAK4. TRAF6 is necessary for recruitment of IRAK. This signalling complex leads through further events to activation of NF-κB and p38 and JNK pathways. These pathways induce gene expression leading to cytokine and chemokine synthesis.

1.3.6 Cellular biological functions of IL-33

Initially IL-33 biology has been reported to stimulate Th2 cell and mast cells which both highly express ST2. IL-33 drives production of Th2 cytokines in *in vitro* differentiated Th2 cells but not Th1 cells with high levels of IL-5 and IL-13 expressed, but intriguingly not IL-4 (132). Further it acts as chemoattractant for human Th2 cells (174). IL-33 also stimulates NK and NKT cells to produce IFN- γ (175). DCs express low levels of ST2; however, upon stimulation with IL-33, DC can induce Th2 cytokines in CD4 T cells (163).

Mast cells are by far the most studied and responsive cell to IL-33 stimulation. Tissue and mucosa associated mast cells with high levels of ST2 expression fulfill the role of tissue guardians with the inherent capacity to respond quickly to IL-33 expression. Mast cells that are capable of producing multiple cytokines react to IL-33 stimulation with production of IL-5 and IL-13, but also IL-1, IL-6, TNF- α and other chemokines. IL-33 also induces the degranulation of IgE-primed mast cells *in vitro* and *in vivo* and enhances mast cell maturation and survival (reviewed in (176)). In co-cultures, fibroblast derived IL-33 can also regulate tryptase expression on mRNA and protein level (177). Interestingly, IL-33 also drives production of IL-17 in these cells (personal communication, Dr A Melendez, University of Glasgow).

Three reports describe basophils and their response to IL-33 (164-166). Schneider et al studied murine basophils and found that cells express ST2 and respond in an unprimed state with the production of IL-4 and IL-6 (165). *In vivo* indirect increase of GM-CSF and IL-5 promoted expansion of basophils. In humans, Smithgall et al and Suzukawa et al confirmed ST2 expression in basophils (164, 166). Stimulated with IL-33, these cells produced IL-4, IL-5, IL-6 and IL-13 and increased their adhesive function.

High endothelial venules express IL-33; however, its biology therein is unclear. An elegant study by Kuchler et al demonstrated that IL-33 is globally expressed in nuclei of vascular endothelium in normal human tissues staining vessels in human skin, small intestine, umbilical cord and lung (178). This group further shows *in vitro* that vascular IL-33 is downregulated by proinflammatory cytokines IL-1 β , TNF- α and VEGF. More surprisingly, IL-33 is strongly down-regulated in

endothelium undergoing tumor or wound healing angiogenesis. These findings stand opposite to fibroblast data, where IL-1 and TNF- α upregulated IL-33 (146). However, cell type and stromal origin could explain this difference, but also culture conditions as Kuchler et al used superconfluent cultures of human umbilical vein endothelial cells (HUVECs) and Xu et al used synovial fibroblasts with ~80% confluency.

In contrast to IL-33 expression in endothelial cells, Choi et al studied the response of HUVECs to IL-33. They reported that IL-33 has a significant effect on angiogenesis and vascular permeability by rapidly increased endothelial nitric oxide (NO) production (179). Overall, a more careful dissection of the role of IL-33 in endothelial cells is required.

1.3.7 Regulation of IL-33

Nearly all IL-1 family members are potent cytokines with powerful downstream effects. Signalling occurs through a receptor pair sequestering the primary receptor. Similar to IL-1 and IL-18 where IL-1RA or IL-18 binding protein can block signalling, the soluble form of ST2 (sST2) is thought to act as a decoy receptor. Soluble ST2 is increased in multiple inflammatory conditions (151, 180-182). On a cellular signalling basis, ST2 signalling is counter regulated by TIR8 also known as single Ig IL-1 receptor related molecule (SIGIRR). This receptor belongs to the TLR/IL-1R family, has a single extracellular Ig domain, a long cytoplasmic tail and a TIR domain (183). This receptor remains orphan. However, it inhibits TLR/IL-1R signalling and NF- κ B activation (184). SIGIRR inhibits direct IL-33 signalling *in vitro* and IL-33 responses in SIGIRR deficient mice are more severe (185). As mentioned above, depending on the context proinflammatory cytokines can downregulate IL-33 in endothelial cells, while on the contrary can also upregulate IL-33 in fibroblasts. The mode of action remains unclear.

1.3.8 IL-33 in disease

Mice treated with IL-33 exhibit splenomegaly, blood eosinophilia and increased levels of IgA and IgE. This relates to a Th2 phenotype with increased IL-4, IL-5 and IL-13 (132). Also anatomical changes of stomach and mucus- and bile-filled

duodenum as well as lung were observed with recruitment of myeloid cells and epithelial reaction with either hyperplasia (esophagus) or massive mucus production (lung). In contrast, IL-33 administration was beneficial in a model of atherosclerosis (186). In ApoE deficient mice fed on a high fat diet, injection of IL-33 significantly reduced atherosclerotic lesions in terms of size and leukocyte infiltration. Also serum levels were increased for IL-4, IL-5 (especially) and IL-13 with decrease of IFN- γ suggesting a switch from a Th1 to Th2 phenotype. This atheroprotective effect could be blocked with anti-IL-5 suggesting rather indirect effect whereby IL-33 operated via modulated IL-5 production. IL-33 also induced oxidized low-density lipoprotein (ox-LDL) antibodies which are thought to be atheroprotective. Interestingly, it has also been shown that IL-33/ST2 signaling is a crucial biomechanically activated system that controlled cardiomyocyte hypertrophy and cardiac fibrosis after pressure overload (187). Soluble ST2 levels also negatively correlate with survival and directly with cardiac injury and microvascular injury post myocardial infarction (188).

Th2 cells play an important role in allergy but also in allergic asthma. Expressing high levels of ST2, IL-33 was speculated to drive allergic airways inflammation. Indeed, IL-33 is higher expressed in asthma patients than in controls (189). In contrast to the adaptive immune response in asthma, ST2 is also highly expressed on mast cells and lead to Th2 cytokine production, which both play a crucial role in allergy. This adaptive/innate axis of IL-33/ST2 signalling may influence triggering of disease. In support to this sST2 levels are elevated in asthma patients with acute exacerbations with the assumption that the decoy receptor tries to counter regulate IL-33 pathologic signals (182). Also high levels of serum IL-33 were detected in patients with atopic dermatitis during anaphylaxis (173). Administration of IL-33 exacerbates experimental asthma and induces features of asthma in animals. Furthermore blocking ST2 or IL-33 attenuates disease in some models (176). More evidence is emerging that allergic IL-33/ST2 pathology is antigen mediated with induction of antigen specific IL-5 expressing T cells (190). Even more strikingly is the fact, that a SNP in a region flanking *IL33* is associated as risk factor for asthma in a large-scale, consortium-based genome wide association study (191).

With expression of IL-33 in the gastrointestinal mucosa Pastorelli et al studied the IL-33/ST2 axis in inflammatory bowel disease. In ulcerative colitis (UC)

patients they detected higher expression of IL-33 compared to healthy controls or patients with Crohn's disease (CD) (192). Anti-TNF therapy downregulated serum IL-33 and increased the amount of sST2. High expression in UC patients was confirmed by Kobori et al (193).

In psoriasis IL-33 has also been reported to be upregulated (194). Subcutaneous administration of IL-33, however, leads to skin fibrosis with a Th2 fingerprint infiltrate (195). Moreover, skin of atopic dermatitis patients have elevated IL-33 levels compared to controls (173). With psoriasis mainly considered as a Th1/Th17 disease, fibrosis and atopic dermatitis as Th2 disease these data have confused rather than clarified the role of IL-33 in the epithelium.

With this paradoxical switch, autoimmune arthritis supports the proinflammatory Th1/Th17 supporting role of IL-33. IL-33 and ST2 are expressed in inflamed synovium of RA patients (136, 145, 146). Synovial fibroblasts (FLS) in culture do not express IL-33, however, when stimulated with IL-1 and TNF- α , FLS upregulate IL-33 *in vitro* providing a highly responsive cell in a TNF environment like RA. Moreover, Fraser et al demonstrated that autoimmune arthritis patients (RA, PsA, gout) have high sST2 levels in the synovial fluid compared to OA (180). Also elevated levels of IL-33 have been reported (150). In a mouse model of RA, collagen induced arthritis was diminished in ST2 deficient mice (146). In addition, CIA mice treated with recombinant IL-33 led to exacerbation of disease. This had no effect in ST2 deficient mice. Furthermore, reconstituting ST2 deficient mice with mast cells (expressing normal levels of ST2) again led to exacerbation of arthritis (146). This supports the important role of mast cells in proinflammatory cytokine production. It is interesting, that despite the Th2 profile of mast cells, secretion of proinflammatory cytokines like IL-1, IL-6 and IL-17 can bias the balance to a Th1/Th17 autoimmune phenotype. It is noteworthy, that Raza et al and Kokkonen et al detected increased Th2 cytokine patterns before onset of RA disease (107, 196). The potency by which IL-33 increases severity of CIA was confirmed by Palmer et al using anti-ST2-antibodies (145). Furthermore they showed a decrease in IFN- γ as well as IL-17 production in the draining lymph nodes. Therefore IL-33 clearly drives Th1/Th17 responses in experimental arthritis. This is confirmed by higher levels of IFN- γ and IL-17 in the IL-33 treated CIA mice (146). Focussing on autoantibody induced arthritis

(AIA), IL-33 exacerbated arthritis, where AIA in ST2 deficient mice developed attenuated disease (197).

A proof of how important the IL-33 immune axis has become in terms of future therapeutics, is evidenced by the patent application from Medimmune (198). In their application, authors patent the invention of IL-33 specific binding polypeptides and compositions binding IL-33 such as antibodies. Furthermore they state possible treatment options for diseases and disorders such as asthma.

The cardiology field provides the IL-33/ST2 story from a totally different perspective. Sanada et al showed that IL-33/ST2 plays a crucial role in cardioprotection (187). With the observation that mice with myocardial infarction have increased levels of serum ST2 different groups used sST2 as a possible outcome biomarker after myocardial infarction (188, 199). Weir et al showed significant correlation with sST2 and left ventricular ejection fraction (a measurement for heart function) and also observed a relationship with infarct size using cardiac magnetic resonance imaging (MRI). IL-33 and ST2 are expressed by vascular endothelial and vascular smooth muscle cells of the heart and aorta in mice and humans (186). Therefore, cardiac infarction may lead to IL-33 release with subsequent release of sST2 to counteract possible IL-33 immune-mediated effects. In regard to this hypothesis incidences with (IL-33 containing) cell death would result in release of sST2. Indeed, when focusing on sepsis patients cell death can occur on different levels such as organ failure. In these patients serum IL-33 is increased but also sST2 (152, 200). Alves-Filho et al demonstrated that IL-33 reduces mortality in mice with experimental sepsis by restoring neutrophil migration abilities (152). Patients who did not recover from sepsis had significant higher levels of sST2. Is it possible that sST2 is unspecifically released due to severe endothelial stress? A different option would be that sST2 is released to limit the alarmin effect and thereby blocks the normal protective effect of IL-33. This would allow pathology and comorbidity to emerge in patients in whom IL-33 is involved in pathology such as asthma or RA. To conclude what role sST2 plays in these life threatening incidences such as myocardial infarction or sepsis is still unclear.

How IL-33/ST2 in epithelial cells might influence inflammation will be addressed in this thesis.

1.4 Nanoparticles in inflammation

So far, an introduction to the clinical challenge for treatment of autoimmune diseases exemplified on psoriasis, PsA and RA has been given. More insights in the immunological network underlying the aberrant functions and subsequent causes have been provided. Especially I focused in this network on two cytokines (IL-17 and IL-33) for their central role and novelty. While the clinical and scientific community focuses on more early detection of autoimmune diseases or even at a stage “pre-disease” to prevent initiation of the autoimmune response and further long term damage, techniques are lacking in its sensitivity and resolution.

Thus this section introduces how we can utilize nanoparticles as novel technical equipment to image on a cellular level to detect subclinical inflammation.

Dysregulated inflammation is a feature of a wide variety of human diseases including autoimmune, infectious, neurological, cardiovascular and metastatic conditions. Detection of such inflammation at an early, subclinical stage is critical for informing decisions relating to the necessity and intensity of therapy and to subsequent prediction of outcomes. In the above sections cytokines have been introduced and context provided how simple triggers can misbalance this sensitive system and lead to further consequences such as autoimmune disease. To image inflammation and in particular cytokines on a cellular level could be a powerful tool to diagnose diseases at early stages at which long term damage to the body not happened yet.

Although a wide range of imaging options exist including X-ray, ultrasound, magnetic resonance imaging (MRI), computer tomography (CT), positron emission tomography (PET), and single photon emission computer tomography (SPECT), all of which have led to improvements in sensitivity and specificity, these techniques are expensive and often limited in their ability to detect early subclinical inflammation (201). Recent developments in the design and application of nanoparticles could offer high resolution information-rich imaging

(possibly in real time) that can facilitate diagnosis at a pre-clinical stage previously unachievable with existing technologies.

1.4.1 What are nanoparticles?

Nanoparticles (NPs) are often defined as materials with at least one dimension of 0.1 - 100 nm (Figure 1.10). The chemical composition of nanoparticles range from coinage metals through chemical polymers such as polyethylene glycol (PEG) to inorganic nano-dyes such as quantum dots (colloidal semiconductor nanocrystals i.e. cadmium selenide, cadmium sulfide and indium phosphide) to compounds similar to liposomes (phospholipid bilayers). The important properties of NPs including surface charge, size, and solubility have varying effects on immune cells (202). Surface charge in particular can affect toxicity, binding to plasma proteins, particle clearance and immune cell stimulation. Size can play a role with divergent biologic effects mediated upon Th1/Th2 stimulation, adjuvant properties, phagocytic uptake and particle clearance based on size properties alone.

Different subjects use the term nanoparticle and the paradox between nanoparticles termed in toxicology and pharmacology needs to be addressed. In the field of toxicology mainly combustion derived nanoparticles are studied in regard to their effect on lung inflammation and toxicity (203).

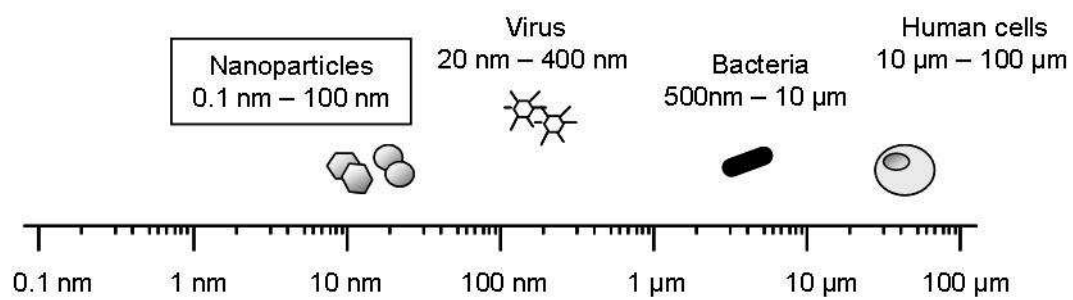


Figure 1.10 Nanoparticle - size comparison

Virtually all forms of synthetic nanoparticles are designed to have some kind of chemically modifiable surface offering potential for attachment of a wide variety of ligands. This has the effect of turning the nanoparticle into a biologic nanosensor, a nanoscale fluorescent tag, or a drug delivery vehicle. Modifying the surface chemistry of nanoparticles also plays an important role in the organ distribution and the half life of nanoparticles *in vivo*. Unmodified nanoparticles are quickly removed from the bloodstream by macrophages. Early studies with macrophages suggest that this process may have a preference for larger nanoparticles (204). The adsorption of plasma proteins to the surface, largely thought to be caused by the surface charge or hydrophobicity, is also thought to make the nanoparticles more susceptible to phagocytosis (205). The most common method of improving the *in vivo* characteristics of nanoparticles is to 'block' the surface, commonly by PEGylation. Blocking has been shown to increase the half life of nanoparticles in blood, probably by preventing plasma protein binding. Conjugation of the PEG with a drug showed in some examples increase of half-life as well a reduction in toxicity. For example, the half-life of the recombinant cytokine GCSF, which is given daily for 2 weeks to patients after chemotherapy for neutropenia, is increased by PEGylation; only a single application was needed compared to the non PEGylated GCSF (206).

The major advantage in the use of nanoparticles is the almost unlimited array of modifications possible. The breadth of NP modifications can facilitate selection of particular target cells, act as biosensors, work as drug delivery systems, guide surgical procedures and sense/signal molecular responses to therapeutic agents. The niche of "nanomedicines" has been elegantly reviewed recently (206).

Gold nanoparticles bind strongly to thiols and amines. Tsai et al. demonstrated that this binding explains observed improvement of arthritis in a rat model. In their paper they mainly focused on the binding capacities to VEGF, however, it is known that these nanoparticles also bind to other plasma proteins. Interestingly, by PEGylation of gold nanoparticles the binding is prevented and the induced arthritis not ameliorated (207, 208).

Depending on the type of nanoparticle used and surface functionalisation selection NPs can be traced by a number of different methods that include MRI, PET, fluorescent microscopy and, recently surface enhanced Raman

spectroscopy (SERS). In the last 10 years imaging in inflammation has advanced significantly by utilizing such advances in detection techniques and the next major step towards high resolution, molecular imaging is likely to involve coupling the existing techniques available with novel nanoparticles techniques under development.

1.4.2 Magnetofluorescent nanoparticles

Many of the significant advances in imaging with NPs have been achieved by the use of magnetic nanoparticles (MNP). The MNPs most commonly used in *in vivo* studies are iron oxide coated NPs whose superparamagnetic core affords the ability to easily distinguish between different tissue types using magnetic resonance imaging. Iron oxide nanoparticles have been in use as contrast agents in MRI since 1990 and are particularly useful owing to their capability for deep tissue imaging, their low toxicity and their lack of relevant immunogenic properties. A recent advance has seen MNPs linked to a fluorescent marker enabling enhanced *ex vivo* analysis. Compared to other non-nanoparticle based techniques of imaging, e.g. PET analysis with radio labelled cells or bioluminescence using luciferase, coated cells, MRI has its greatest advantage in spatial resolution and non-invasiveness. PET and bioluminescent cell imaging are both capable of sensitive *in vivo* imaging, but present substantial drawbacks. PET is not suitable for all studies owing to the opportunity cost of using a radio isotope against potential diagnosis and the high cost to produce the necessarily short-lived radionuclides. Bioluminescent cells require expensive ultrasensitive detection systems because the amount of light emitted is typically very small.

MNP have been used in two ways, namely attached to immune cells actively targeting sites of inflammation or passively untargeted by monitoring their localisation driven by vascular leakage and / or uptake by phagocytic cells. Protocols now exist to facilitate labeling of specific subsets of leukocytes e.g. circulating T cells with linked magnetofluorescent nanoparticles (209). How inflammation in autoimmune diabetes, atherosclerosis and brain inflammation could be monitored using these approaches will now be considered.

Imaging autoimmune diabetes

Type 1 diabetes is an autoimmune disease that includes lymphocytic infiltration of pancreatic islets. Autoreactive T lymphocytes target insulin producing β cells thereby leading to hyperglycemia and thereafter to diabetes. Extensive tissue damage and consequent endocrine deficiency and metabolic compromise is at this stage irreversible and therefore immune therapeutic options are distinctly limited (210). Thus a major goal is to identify patients with preclinical autoimmune diabetes for early initiation of therapy and limit further damage. At this stage it is possible that immune tolerance could be reinstated to prevent disease forthwith.

A variety of diabetes models are available including nonobese diabetic mice (NOD mice), BDC2.5/NOD mice (BDC2.5 TCR Tg, transgenic TCR which recognizes an islet β -cell antigen) to study inflammation before and at the onset of disease by various non-invasive approaches. Weissleder and colleagues injected long circulating MNP with a size of ~25nm in NOD mice and were able to show microvascular leakage in the inflamed pancreatic tissue over time. MNP leaked into the tissue and were longer detectable, most likely phagocytosed by macrophages (211). Further, by depleting T cells with anti-CD3 antibody the observed leakage was reversible in therapy responders (212). The majority of untargeted NPs are taken up by the reticulo-endothelial system (RES) of liver and spleen; unfortunately in these reports values to document uptake, quantities or time course of entry to these organs were not disclosed, or possibly measured. Nevertheless, these studies suggest that MNP detection could function as an early predictor for monitor treatment response and need of intervention.

In a further significant study, Moore *et al.* focused on tracking autoreactive diabetogenic CD8⁺ T cells *in vivo*. They used dextran superparamagnetic iron oxide nanoparticles and coated these MNP with a high-avidity peptide recognized by the TCR of diabetogenic T cells. Co-incubating T cells and MNP *in vitro* resulted in internalization of MNPs into the T cells. Further, these antigen-specific trackable T cells were injected into NOD.scid mice and over time, labeled cells accumulated in the pancreas. Interestingly, no changes were observed in the spleens or livers of the same mice (213). This method nicely

demonstrates the ability to track autoimmune cells *in vivo*. However, it is entirely dependent on the knowledge of the islet antigens recognized by autoreactive T cells - most such antigens are unknown in the context of human autoimmune diseases. Although highly specific therefore this approach can not be applied to human diseases as yet although it gives a clue as to the rich potential in the technology. Translation of this promising novel tool into humans depends on its safety in regard to immune interaction (hemolysis, thrombogenicity and complement activation) and trials are awaited.

Imaging arteriosclerosis

Artherosclerosis comprises a disease of interaction between lipid dysregulation and local inflammatory processes in the targeted blood vessel wall.

Atherosclerotic plaques are characterized by invasion of macrophages into the lesion leading to further cytokine secretion, amplification of local inflammation and subsequently to destabilisation of the plaque with plaque disruption.

Magnetofluorescent imaging in arteriosclerosis takes advantage of the property of NPs being phagocytosed by macrophages.

Nahrendorf *et al.* designed a tri-reporter NP for use in fluorescence, MRI and PET. Interestingly, these NP accumulated predominantly in the liver, followed by intestine, kidney, lung and spleen. However, the striking observation was the enhanced accumulation of NPs in atherosclerotic lesions in the apolipoprotein-E-deficient mouse model compared to normal mice. It was also possible to colocalize NPs with Mac-3 (a macrophage marker) *ex vivo* indicating uptake of NPs by macrophages (214). Despite the elegant method used in this study, broad clinical use is unlikely due to lack of PET access and the relative non-specificity of the particles employed. In other studies, in the atherosclerotic plaque, fluorescent NPs could colocalize macrophages and markers of osteogenesis (see below) (215).

Brain inflammation

Two models of brain inflammation have been studied, namely experimental autoimmune encephalomyelitis (EAE, a model for multiple sclerosis) and acute inflammation after cerebral ischemia. Brochet *et al* used non-targeted

ultrasmall-super-paramagnetic-iron-oxide particles (USPIO) (20 - 40 nm), similar to the MNP described above to study a relapsing model of EAE. With the assumption that USPIO are taken up by macrophages, lesions were monitored at the first clinical phase by MRI. Interestingly, rats with USPIO positive lesions had more severe clinical disease in the second phase (216). More specific is the approach chosen by McAteer et al (217). In a model of acute brain inflammation interleukin-1 (IL-1) was stereotactically injected into the left striatum of the brain to induce endothelial activation. After activation, endothelial cells upregulate vascular adhesion molecule 1 (VCAM-1) on their luminal cell surface. Leukocytes are then recruited via the ligand $\alpha_4\beta_1$ integrin. Microparticles of iron oxide linked to antibodies against VCAM-1 bound specifically to activated brain endothelium, compared to IgG controls (217). This concept demonstrates selective targeting of inflammatory sites within the CNS, typically a challenging region in which to define cellular or molecular expression, since relevant tissue biopsies are rarely achievable.

Recently, a new method of fluorine magnetic resonance imaging has been described employing biochemically inert nanoemulsions of perfluorocarbons (PFCs). The fluorine isotope ^{19}F is MR active and as sensitive as ^1H MRI. PFC nanoemulsions are taken up by phagocytic cells and thus inflammation in brain ischemia or cardiac infarction can be demonstrated in mouse models. Cardiac infarction was induced by ligation of a coronary artery and infiltration of PFCs was monitored 4 days after ligation. Focal brain ischemia by photothrombosis led to infiltration of PFCs examined 7 days after induction. *Ex vivo* imaging proved that rhodamine labeled PFCs showed uptake in monocytes, macrophages and B cells *in vivo*. The majority of accumulation occurred in the liver although no obvious biologic effects appeared to result (218).

In summary, MNP or MR active nanoemulsions provide feasible approaches to the detection of inflammation in humans with easy applicability to MRI. It should be noted that since current research using an untargeted approach, nonspecific accumulation of nanoparticles in organs such as the liver, kidney and spleen can occur.

1.4.3 Fluorescent nanoparticles

To date, fluorescent imaging is only of use *ex vivo* or via intravital microscopy owing to the limited and therefore superficial penetration of tissue. Using shorter wavelengths of excitation often required tends to promote background autofluorescence. In addition increased light scattering limits depth penetration making deep tissue imaging problematic. Intravital microscopy is an invasive procedure requiring high technical skills and expensive equipment. Furthermore, this method only focuses on small areas of interest; however, the sensitivity on a cellular level is outstanding compared to the other imaging techniques. An example of this method is the 3-dimensional imaging of fluorescent lymphocytes trafficking into an atherosclerotic plaque (219). A different approach combines two nanoparticles, namely an iron oxide fluorescent nanoparticle (MNP linked to a near infrared fluorescent dye), which is taken up by macrophages and a bisphosphonate-derivatized near infrared fluorescent polymer nanoparticle which detects an osteogenesis like pre-stage vascular calcification. Reports suggest that proatherogenic stimuli promote conversion of vascular myofibroblasts into osteoblastic cells which can eventually lead to calcification. Using intravital microscopy of the carotid artery in an atherosclerosis prone apolipoprotein-E-deficient mouse, it has been demonstrated that osteogenesis is associated with inflammation. Pre-stage calcification was detectable with fluorescent microscopy compared to a negative micro-CT analysis (215).

Recently, the use of nanosize semiconductor quantum dots (QD) has shown benefits compared to conventional organic dyes. QDs are superior in brightness due to good quantum yields and often exhibit greater photostability as they do not rely on organic conjugated double bond systems that are prone to photo-initiated degradation. Linked to different target specific antibodies, QD conjugates for imaging inflammation have only been tested *ex vivo* in a model of inflammatory colitis (220). However, a liposome-QD complex conjugated with a tumor detection antibody (HER2) demonstrated the feasibility in a tumor xenograft mouse model imaged with a fluorescent camera (221). Still, this method is lacking spatial resolution. Zinselmeyer *et al* report a future possibility to track inflammation with QDs. Using 2-photon imaging of a mouse footpad demonstrates the feasibility of real time imaging of fluorescent labeled

leukocytes. With the footpad being accessible for imaging, this work proves a method with excellent spatiotemporal resolution (222). Further studies are ongoing in this area to refine technologies and correlation with biologic pathways.

1.4.4 Surface-enhanced Raman spectroscopy (SERS)

Surface-enhanced Raman scattering (SERS) is a highly sensitive spectroscopic technique in which narrow vibrational signatures (~ 0.5 nm) from suitable molecules are enhanced enormously ($\sim 10^6$ to $\sim 10^{14}$) by close proximity to areas of high electric field, such as those generated at the surface of metal nanoparticles under suitable illumination. At present, this method has only been used in imaging of a cancer mouse model (223, 224). SERS active nanoparticles, in the study a gold particle linked to a Raman active dye, release a distinct signal upon excitation, which in comparison the other fluorescent dyes (e.g. QDs) is highly specific and ideally suited for multiplex analysis. In a tumor mouse model, where the tumor expressed high amount of EGF-receptor, these SERS nanoparticles functionalized with EGF-receptor antibody were measurable in the tumor tissue compared to untargeted particle controls. In common with other studies most of the particles accumulated in liver and spleen, interestingly, only the tumor targeted conjugates found their way to the tumor (223). This approach could be confirmed by Gambhir and colleagues using single-walled carbon nanotubes (SWNTs) linked with a tumor specific arginine-glycine-aspartate (RGD) peptide. This RGD peptide binds to angiogenic overexpression of $\alpha_v\beta_3$ integrin in various tumor cells. SERS signals from peptide targeted SERS active nanotubes could be detected in subcutaneous tumor cell inoculated mice compared to untargeted SWNTs (224). Thus, demonstrating feasibility of SERS nanoparticle detection in cancer this approach could represent a future application in imaging of inflammation.

In summary, using the nanoparticle delivery/imaging system provides an effective tool to target processes in inflammation, drug target and cytokine cell interaction.

1.5 Aims of this thesis

A variety of cells have been described to produce IL-17A. In tissue, the net IL-17A expression may arise from a broad array of adaptive and innate cells. This cytokine plays a vital role in protection against bacterial, fungal and viral pathogens. Opposite to this is a novel cytokine named IL-33. Nuclear expressed and associated with body barriers it is released due to cell damage and biological function composes features of an alarmin.

In this work I sought to define the role for inflammatory and regulatory cytokines in autoimmune disease with a focus on the novel entities IL-17A and IL-33. Further I sought to define their effector biology and to thereafter investigate a novel bioimaging modality to move the diagnostic and effector biology forward.

2 Material and Methods

2.1 General reagents & buffers

2.1.1 Materials and reagents

General chemicals: All chemicals were purchased from Sigma (UK) unless otherwise stated.

Plastics: All plastics used for cell culture were purchased from Corning and Gibco unless otherwise indicated.

2.1.2 Buffers and culture media

Complete media: Basic media: RPMI1640, DMEM or IMEM plus

10% heat inactivated foetal bovine calf serum, Penicillin (100 units/ml), Streptomycin (100 µg/ml) and L-Glutamine (2mM) (all at final concentration from Invitrogen).

PBS: Phosphate buffered saline was purchased from Invitrogen.

Tris-acetate-EDTA (TAE) buffer: 50x stock: 242 g of Tris base in 750 ml dH₂O. Mixed with 57.2 ml glacial acetic acid and 100 ml 0.5 M EDTA (pH 8.0). Final volume was made up to 1000 ml with dH₂O. Buffer was used at 1x concentration.

TBS Tween (TBST): 10x TBS buffer was made using: 876.6 g NaCl, 121.1 g Tris, 40 ml HCl and adjusted to pH 8.0. 10x solution was diluted 1:10 with dH₂O and 0.05% Tween added.

2.2 Patients

Glasgow Royal Infirmary Research Ethics Committee granted approval for sampling of peripheral blood, synovial fluid and synovial tissue for cytokine and inflammation analysis in June 2000. Patients with RA, PsA, AS and OA, who were

greater than 18 years of age and capable of providing informed consent, were invited to take part in the project. Such patients were identified from the Rheumatology Clinics in North Glasgow Trust, Glasgow Royal Infirmary. Further samples from consented patients undergoing arthroplasty (Orthopedic units Royal Infirmary and Southern General, Glasgow and Department for Plastic Surgery, Royal Infirmary, Glasgow) were transferred to the research unit. Tonsils were used as control tissue and were obtained by Mr Simpson, Stobhill Hospital, Glasgow. Demographic data were collected and stored in a password-protected database and samples were blinded to the researchers. Diagnosis of RA and PsA are defined by classification criteria described in the introduction.

2.3 Skin biopsy

Patients with active psoriatic plaques were identified in the Dermatology department (Dr David Burden, Western Infirmary) or Psoriatic arthritis clinic (Rheumatology, Royal Infirmary). Having identified a suitable plaque avoiding the cape area, the skin was cleansed using chlorhexidine gluconate. Thereafter 1% lidocaine with 1:200000 adrenaline was injected into the subdermis. A 5mm core punch was then made using a punch biopsy instrument in the affected skin (lesion) as well as 1 cm away in skin appearing macroscopically healthy (perilesional). A skin hook and scalpel were used to lift the skin cone from the subdermis. The skin was then sutured using 1-2x 4.0 Ethilon sutures and a dry Mepore dressing was applied. The incision site was observed for 30 minutes for bleeding. Patients were asked to attend their local GP practice nurse for suture removal at 7-10 days.

2.4 Tissue preparation

For cell harvest, explant tissue was transferred to complete medium and cultured at 37°C in 5%CO₂/95% O₂ to generate fibroblast-like synoviocytes (FLS) following prolonged incubation and passage of cells.

2.4.1 Paraffin embedded tissue

Tissue sections were prepared and stored for future analysis of tissue protein e.g. cytokine expression by immunohistochemistry (IHC). For paraffin embedded sections, tissue was stored in formalin for 24 h and transferred to 70% ethanol to retard the fixation process. Tissues were paraffin embedded and subsequently cut to thickness of 5 μm . A minimum of 2 sections were mounted on one slide to facilitate isotype staining on the same slide in IHC protocols. For back-to-back sections, single sections were mounted on a slide with the next section being used on a different slide having the same surface in common. Sections for isotypes were added subsequently. Haematoxylin and eosin (H&E) staining was performed on one of the serial sections to allow tissue morphology to be assessed.

2.4.2 Frozen tissue

Tissues (liver and spleen from mice) were snap frozen in liquid nitrogen in OCT (Tissue Tek) and 6 μm cryostat sections were cut onto silane coated slides using a microtome and stored at -70°C . Briefly, sections were rehydrated in PBS then fixed in ice cold acetone/ethanol (75%/25%) at room temperature for 10 min. The sections were air dried, then rehydrated in PBS, further washed in water and counterstained using Harris's haematoxylin (BDH Ltd. Lutterworth, Leicester, UK). After a final wash, sections were dried for 5 mins, mounted with either Cytoseal (Richard-Allan Scientific) or Vectashield (Vector) and coverslips were sealed with nail varnish. For some experiments, sections were transferred subsequently to Strathclyde University for further SERRS analysis (see nanoparticle chapter 5).

2.5 ImmunHistoChemistry (IHC) of paraffin embedded sections

2.5.1 Single staining for light microscopy

Sections were prepared as previously mentioned (see section 1.3.1). Slides containing paraffin embedded sections were heated to 65°C for 35 minutes

followed by dewaxing in xylene and rehydration through ethanol to TBS Tween (TBST). Endogenous peroxidase activity was blocked using H₂O₂/methanol (5%/95%). To expose the relevant antigen, sections were then microwaved in 0.5M citrate buffer, pH 6 for 8 min. The sections were blocked for 1 h at RT in 2.5% serum TBST of the species in which the secondary antibody was raised. The relevant primary antibody was applied overnight at 4°C 2.5% serum TBST (see working concentrations and companies in Table 2.1, page 88). The following day the sections were washed with TBST, incubated with relevant secondary antibody for 30 minutes in 5% horse serum containing TBST, washed twice with TBST then incubated with substrate Vector ABC (Vector, Peterborough, UK) for 30 minutes. Sections were washed twice with TBST before developing with 0.6mg/ml 3,3'-diaminobenzidine tetrahydrochloride (DAB) (Sigma) with 0.01% H₂O₂ for up to 5 min at RT until brown reaction product was apparent. Sections were then washed in water and counterstained using Harris's haematoxylin (BDH Ltd. Lutterworth, Leicester, UK). Finally sections were dehydrated in ethanol, cleared in xylene and finally mounted in DPX mountant (both from BDH Ltd.).

Alternatively, the second day staining protocol was altered by using the ImmPRESS kit (Vector) in which sections were incubated with a species specific polymer for 30 min replacing the secondary antibody. Sections were washed with TBST and then developed with ImmPACT DAB (Vector) for up to 2 mins. Further staining of the sections was carried out as described above.

To establish a staining procedure suitable for double-colour staining, a variety of reagents were tested. Firstly, selected peroxidase substrates Nickel-DAB, Nova-Red and VIP (all Vector) were analysed by single colour staining. IHC procedure was not altered. The Nickel-DAB staining was carried out following the DAB protocol mentioned above with the exception of adding one Nickel drop to the DAB reaction causing the usual brown DAB reaction product to appear black with the appropriate haematoxylin counterstain. Using Nova-Red as reaction product appeared with dark red colour (haematoxylin) or dark blue (methyl green counterstain). Further VIP developed a purple staining (without counterstain) or dark violet stain (methyl green counterstain).

For back-to-back sections Nickel-DAB was used as peroxidase substrate.

2.5.2 Double staining for light microscopy

Similar to single staining the 0.5% hydrogen peroxidase/methanol incubation and heat retrieval in 0.5M citrate buffer (pH 6) was followed by incubation in 2.5% species/2.5% human serum with AvidinD (4 drops/ml) (Vector Laboratories, Petersborough, U.K.). Surface expression of CCR6 was detected by staining with a rabbit anti-CCR6 antibody in the presence of Biotin (4 drops/ml, Vector) in 2.5% horse serum TBST for 1 h at RT, 2 washes with TBST, followed by a biotinylated secondary antibody for 30 min (1:200; Vector Laboratories). The reaction was developed using VIP. Following incubation for 1 h with in 2.5% species/2.5% human serum, goat anti-IL-17 in TBST was added overnight at 4°C. On the following day sections were washed with TBST, and then incubated with a biotinylated antibody for 30 min and stain developed using either DAB or Nickel-DAB. The chosen counterstain for DAB was methyl green whereas Nickel-DAB sections were left unstained. Sections were washed dH₂O, dehydrated in serial ethanol (from 70%, 90% to 100%), cleared in xylene and mounted in DPX.

2.5.3 Double staining for fluorescent microscopy

Sections were prepared as described above. To detect cell markers sections were stained for 1 h in 2.5% horse serum TBST at RT with the following antibodies: mouse anti-CD3, mouse anti-CD4, rabbit anti-CCR6, mouse anti-mast cell tryptase (MCT) or mouse anti-CD68. After 2 washes with TBST primary antibodies were detected by incubating the sections with biotinylated antibody for 30 min (1:200; Vector Laboratories) and subsequent addition of streptavidin QDot605 (1:250; Invitrogen, Paisley, U.K.) in TBST for 45 min. Goat anti-IL-17 was added overnight at 4°C, followed by 2 washes with TBST. The next day biotinylated anti-goat antibody was added for 30 min followed by 2 washes with TBST and the addition of avidin FITC (1:500; Vector Laboratories) for 45 min. Slides were mounted with Vectashield containing DAPI (Vector Laboratories) and analyzed on a fluorescent imaging microscope (BX50; Olympus, Essex, U.K.). Images were captured using Apple Open laboratory software.

Antibody	Manufacturer and clone	Source	Working Concentration
CD3	Vector	mouse monoclonal	1.25 µg/ml
CD4	Dako	mouse monoclonal	7.56 µg/ml
CCR6	Sigma-Aldrich	rabbit polyclonal	0.75 µg/ml
MCT	Dako	mouse monoclonal	0.43 µg/ml
CD68	Dako clone PG-M1	mouse monoclonal	1 µg/ml
IL-17A	R&D	goat polyclonal	5 µg/ml
IL-23p19	Sigma-Aldrich	rabbit polyclonal	1 µg/ml
IL-33	Alexis (nessy-1)	mouse monoclonal	5 µg/ml
ST2	Sigma-Aldrich	rabbit polyclonal	1 µg/ml
	R&D	mouse monoclonal	10 µg/ml
MPO	Dako	rabbit polyclonal	3.2 µg/ml
ki67	Universal Biologics	rabbit polyclonal	2 µg/ml
isotype	R&D (IL-17A) and Dako (others)	various	various

Table 2.1 Antibodies for IHC

Shown are surface marker or cytokine antibodies using in IHC. Left column shows antibody target, 2nd column manufacturer, 3rd the source and right column the working concentration. Dilutions were not mentioned as stock concentration of antibodies can vary.

Cytokine	Company
human IL-23	eBioscience
human sST2	R&D systems
human CCL3 (MIP1alpha)	R&D systems
human TNFalpha	Biosource
human IL-6	Biosource
mouse IL-5	R&D systems

Table 2.2 ELISA cytokines and companies

Shown are ELISA targets demonstrating cytokines which will be detected by an antibody pair (e.g. IL-23: capture antibody against IL-23p19 and detection against IL-23p40) Further supplier of ELISAs are shown.

2.5.4 Quantification of fluorescent IHC

Images were captured digitally and the total number of IL-17A+ cells found within duplicate tissue areas (two representative 10x fields) of 0.52 mm² was calculated. Double staining allowed the calculation of the proportion of IL-17A expressing cells per cell surface marker. Four tissues were double stained for all markers (CD3, CCR6, CD68 and MCT) with studies performed on a further 6 tissues to confirm the co-expression with MCT and CD68.

2.5.5 Mast cell staining using Toluidine blue

To stain for mast cells in tissue paraffin embedded sections were prepared as described above. Following the dewaxing and rehydrating steps the sections were stained in toluidine blue (Sigma) for 1 min, dehydrated and cleared with xylene and further mounted with DPX. Due to purple background and good visualization of the tissue architecture, counterstaining was omitted.

2.6 ELISA

Cytokine expression was tested in serum, synovial fluid and culture supernatant. ELISAs were carried out according to the manufacturers protocol. The following table summarises the cytokines tested and the manufacturer from which the kits were purchased (Table 2.1Table 2.2, page 88).

2.7 Luminex cytokine analysis

Cytokine mouse 20-plex kit (Invitrogen) to test mouse serum from IL-33 ear injection model was performed according to manufacturers' instructions.

2.8 Cell culture

2.8.1 Culture of adherent cells

Primary fibroblasts, HaCaTs (CLS cell lines service), neonatal human epidermal keratinocytes (nHEK)(Invitrogen), and HeLa cells (ATCC) were cultured in tissue

culture flasks with appropriate complete media (fibroblasts: RPMI, HaCaTs and HeLa: DMEM, nHEK: epilife from Invitrogen) and split when cells reached 80% confluence. Detachment of cells was achieved by incubation with 0.5 - 1 ml 5% trypsin in PBS for 5 min. Trypsinization was stopped by adding media containing 10 % FCS, cells were washed, counted and reseeded to a final concentration of 10^4 /ml.

2.8.2 Culture of suspension cells

The immature human mast cell line HMC-1 was cultured in complete media (IMDM, Gibco) and 64 μ l α -thioglycerole (Sigma). Cells were split once per week and were reseeded at a density of 5×10^4 /ml. For stimulation of HMC-1, 1×10^6 cells were stimulated with human rIL-33 (Biolegend) at varying concentrations for 24 h. The culture supernatant was reserved at -20°C for subsequent ELISA.

2.8.3 Purification of monocytes

Wash media was prepared from RPMI containing 2 mM L-glutamine, 100 IU penicillin, and 100- μ g/ml streptomycin (all obtained from Life Technologies, Paisley, U.K.). Culture media was prepared by the addition of 10% foetal calf serum (FCS) (Sigma) to wash medium. 25mls of heparinised peripheral blood (provided by Gartnavel Blood transfusion service) were transferred to 50ml falcon tubes and diluted with equal volumes of PBS. The blood was carefully layered onto Ficoll gradient solution (histopaque, Sigma) and samples were centrifuged at 350g for 20 min to allow separation of the blood into its component layers. Following centrifugation the interface containing PBMCs was carefully removed using a sterile pasteur pipette and placed in a fresh 15ml tube. The cells were then washed twice with RPMI (350g, 10 min). Cells were finally resuspended in PBS containing 5% Alba (human albumin). Purification of CD14-positive monocytes was performed according to the manufacturers instructions (Miltenyi). The purity of the suspension of monocytes was confirmed by FACS analysis confirming a >90% purity of CD14-positive cells. The number of PBMCs was calculated using a haemocytometer (Weber, England).

For toxicity analysis in nanoparticle experiments, monocytes were cultured 24 h in media containing 10% FCS +/- different concentration of nanoparticles.

2.8.4 Splenocyte harvest

To test biological activity of rIL-33 splenocytes were stimulated with rIL-33 and their IL-5 production measured. To isolate splenocytes, spleens of BALB/c mice and ST2^{-/-} mice were removed and washed in RPMI-1640 media and then dissociated through sterile nitex membrane. The resultant single cell suspension was centrifuged (450g, 10 min, 4°C) and the pellet resuspended in 300 µl red blood cell lysis buffer (Sigma) for 1 min to remove red blood cells. The lysis reaction was stopped by the addition of 10 ml RPMI 10% FCS. Cells were washed twice with RPMI 10% FCS (450 g, 10 min, 4°C) and then counted for further experiments.

2.9 FACS analysis

The expression of ST2 on the mast cell line HMC-1 was analysed by FACS. To this end 0.5×10^6 cells were washed and unspecific antibody binding to Fc-receptors was blocked by incubating cells with 50 µl Fc-Block (Sigma) for 15 min. 5 µl of anti-ST2 FITC were added and incubated for 15 min at RT in the dark. Cells were washed with PBS EDTA and analysed using a FACS calibur machine (BD). To test cell death of monocytes due to nanoparticle exposure cells were stained with Annexin-V and 7-AAD (apoptosis kit, BD biosciences) according to manufacturer's instructions.

For analysis of mouse cells obtained from an ear digest (see 2.11.2 Cytokine ear injection model) cells were blocked as described above and stained with antibodies against mouse CD3, CD4, CD19, CD11b, CD11c, F4/80, Gr-1 (3 µl per FACS pellet, all BD Biosciences). Cells were washed with PBS EDTA, 7-AAD (BD Biosciences) was added 5 mins before analysis for dead cell exclusion and analysed using a FACS calibur machine (BD).

FACS data were analysed using FlowJo software (TreeStar).

2.10 Animals

Mice were maintained at the Central Research Facility, University of Glasgow. All animal experimentation and husbandry was under the authority of a UK Government Home Office Project License. All protocols were approved by the Glasgow University local Ethical Review Panel. The following table gives an overview of the used mouse strains and the experiments carried out (Table 2.3, page 93). Normally, mice were used at the age of 6 or 12 weeks and were age-matched for each independent experiment. For mast cell deficient mice, the age of deficient and control mice was 5 -6 months to guarantee deficiency of mast cells in the skin. Control mice were bought from Harlan (BALB/c, C57/Bl6 and MF-1). ST2^{-/-} mice were kindly provided by Prof McKenzie (Cambridge) and kit^{W-sh/W-sh} mice by Prof Liew (Glasgow).

Experiment	Mouse strain
TPA skin inflammation model	BALB/c, ST2 ^{-/-} , C57/Bl6, kit ^{W-sh/W-sh}
cytokine ear injection model	BALB/c, ST2 ^{-/-} , C57/Bl6, kit ^{W-sh/W-sh}
wound healing model	BALB/c, ST2 ^{-/-}
splenocyte harvest	BALB/c, ST2 ^{-/-}
nanoparticle experiments	BALB/c, C57/Bl6
Embryo harvest	MF-1

Table 2.3 Mouse strains used in experiments

2.11 IL-33 related mouse experiments

2.11.1 *TPA skin inflammation model*

The dorsum of mice was shaved and 2 days later cutaneous inflammation was induced by the application of phorbol ester 12-O-tetradecanoylphorbol-13-acetate (TPA), as a 50-mM solution in acetone, to the shaved dorsal skin. Each animal received 150 μ l of this solution, which is equivalent to 7.6 nmol per mouse per application. In preliminary studies (carried out by Prof. Graham's laboratory) the following two time courses were found to be optimal), two different time courses have been chosen (67). 1) TPA was administered for 2 days or 2) for 3 days (Figure 2.1). After one day's rest, mice were culled and dorsal skin was harvested, placed on a filter paper and cut with a scalpel into squares of \sim 0.5 x 1 cm. These squares were transferred to 10% neutral buffered formalin (further stated as formalin) and fixed for 24 h followed by incubation in 70% ethanol to slow the fixation process. The skin was subsequently paraffin embedded and processed as described above. Group numbers ranged between 5-8 animals per group. To assess inflammation the following parameters were analysed: skin thickness, epidermal thickness, epidermal cell layers and staining sections for mast cells (toluidine blue) and keratinocyte proliferation (ki67).

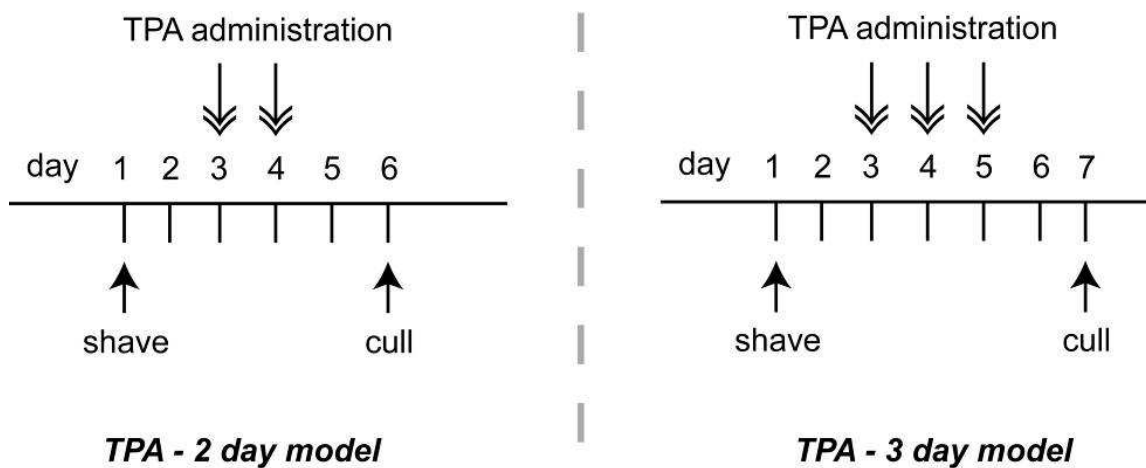


Figure 2.1 Overview of the timeline - TPA skin inflammation model

Left hand and right hand graph shows 2 different time lines for the TPA model. On day 1 the backs of mice were shaved, the one day break was given to account for irritation of the skin due to shaving. Day 3 mice were treated with 150 μ l of TPA administered onto the back in an acetone solution. This was performed under a ventilated hood. Depending on the model, mice were either treated for 2 (left side) or 3 days (right side). After 1 day rest, mice were culled and skin harvested.

2.11.2 Cytokine ear injection model

To test if IL-33 induces psoriasis-like inflammation a cytokine ear injection model was established. IL-33 was tested in a previously reported model initially described for the application of IL-23 or IL-22 (69, 70). Mouse rIL-33 (500ng in 20µl PBS) or PBS was injected intradermally into the left ear pinna of mice (300 µl insulin needle, G29, Terumo) every alternate day for 2 weeks. Before injection ear thickness was measured with a microcaliper (Keoplin (0-10mm) or Dial thickness Gauge, G-1A Peacock) (Figure 4.19). To assure proper technique intradermal injection was practised on more than 60 mouse ears of cadavers. In the week of experiments injection skill was re-practised on at least 10 cadaver ears to assure proper intradermal administration with no leakage or perforation of the ear.

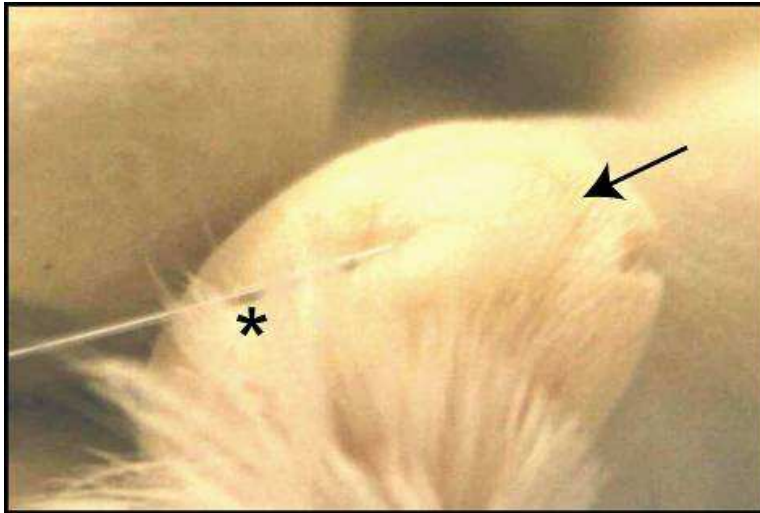


Figure 2.2 IL-33 intradermal ear injection

Mice were anaesthetized and left ear was placed on the left index finger and gently held in place with the left thumb. 20 μ l were injected using an insulin syringe with a 29 gauge needle (marked with *). Arrow demonstrates injected intradermal volume leading to a “blister like formation”.

Due to different starting ear thicknesses of $\text{kit}^{\text{W-sh/W-sh}}$ mice compared to littermate controls difference of thickness compared to the right ear was measured to standardize parameters.

On day 16, mice were culled, ears harvested, fixed in formalin and tissues processed as described above. Spleens were harvested and weighed to determine any possible systemic effects of IL-33 and also used as a surrogate marker for the bioactivity of IL-33 (systemic injection has been reported to induce splenomegaly). To determine epidermal thickness, epidermal cell layers and mast cell numbers staining of ear sections with H&E and toluidine blue was carried out. Thereafter eosinophils were counted and sections stained for MPO. Additionally, serum was harvested for cytokine analysis.

After injection, “blister like formation” was only visible for ~ 15 mins. To address immediate effects and swelling, ear thickness was measured on day 15 after injection over a time course.

To further to analyse the cellular infiltration at earlier time points, one set of mice was culled on day 10 and ears were harvested for ex vivo FACS analysis. Briefly, mice ears were transferred in PBS to the lab, split in dorsal and ventral half by pulling and splitting at the proximal side where cartilage was exposed. Tissue was incubated in eppendorff tubes containing 1 ml of HBSS including 0.4mg/ml DNase and 0.862 wüntsches units/ml eliberase3 (both Roche) to digest the tissue at 37°C for 2 h. Cells were then gently squeezed through nitex membrane with the plunger part of a 2 ml syringe. Cells were again cleared through nitex membrane, counted and further analysed (see 2.9 FACS analysis).

2.11.3 Wound healing biopsy model

For wound healing, $\text{ST2}^{-/-}$ mice or littermate controls were anaesthetized and shaved dorsal skin was pulled over a rigid plastic plate. A 5 mm punch biopsy was performed inducing 2 biopsies with a single punch (Figure 2.3). Photographs were taken with mice sitting on the cage lid with the camera fixed to a stand assuring same distance every time wounds have been assessed. Areas were captured every second day after wounding. 11 mice per group were used. On days of measurement 3 mice/ group were culled for skin harvest decreasing

numbers for subsequent measures. Images were analysed measuring the wound surface and demonstrating the average percentage of wound reduction compared to day 1.



Figure 2.3 Wound healing model

Shown is the back of a mouse after single 5 mm biopsy of the dorsal skin leading to 2 wounds. Mice sitting on a cage lid were photographed with a camera fixed to a stand to assure consistent distance.

2.11.4 Analysis of mouse embryos

A male MF-1 mouse was allowed to mate with 2 females for 2 h. Female mice were checked for vaginal plugs and positively identified mice were single caged and weight was measured daily. On day 9.5 or 10.5, pregnant mice were culled and embryos harvested using a dissection microscope. The embryos were fixed in 10% formalin for 2-3 h, embedded in paraffin and sections were cut. Right orientation of sections was checked using H&E and subsequent sections containing the dorsal aorta stained using IHC for IL-33 (see above). Placenta tissue of the same mouse was used as a positive control for staining.

2.12 Production of a K14-IL-33 construct

2.12.1 Cloning of K14-IL-33

IL-33 was amplified using primers introducing a BamHI site to the 5' and 3' end of IL-33. Primers and the template were provided by Dr Gilchrist and Pfx DNA polymerase reaction (Invitrogen) was used for this experiment. Briefly, in order to sub-clone IL-33 into the K14 vector, the IL-33 cDNA had to be amplified by PCR to introduce a convenient restriction site (BamHI). Template DNA for IL-33 was provided by Dr Gilchrist for the following PCR reaction. In short, 1 µl of the DNA were mixed with Pfx polymerase buffer (Invitrogen), 1.25 µl of the forward primer and the reverse primer (10mM), 1 µl of dNTP mix (10mM, New England Biolabs), 1.5 µl MgSO₄ (50 mM) and 0.5 µl Pfx polymerase (1.25 units) and the volume adjusted with sterile dH₂O to 50 µl.

IL-33 forward primer: AGGATCCATGAGACCTAGAATGAAGTATTC

IL-33 reverse primer: AAAGCTTTTAGATTTTCGAGAGCTTAAAC

Amplification was performed using the following conditions: 5 min at 95 °C, followed by a total of 35 three-temperature cycles (15 s at 95 °C, 30 s at 55 °C and 45 s at 72 °C) and 10 min at 72 °C. The PCR was then separated on a 1% agarose gel. Subsequently, the appropriate PCR fragments were cut out of the gel and DNA was purified according to the manufacturer's instructions using a Gel Extraction Kit (Qiagen).

To blunt ends for further ligation, adenines were added to the ends of the PCR product by incubating the product with Taq polymerase and dNTP mix at 72°C for 30 min. Of this reaction, 4 µl were incubated with 1 µl TOPO salt solution and 1 µl Topovector (PCR-2.1-TOPO, Invitrogen) for 10 min at RT. One Shot® TOP10 competent *Escherichia coli* (*E. coli*; Invitrogen) cells were transformed with DNA as per the manufacturer's instructions. Briefly, 0.1 - 0.5 µg plasmid or 5 µl ligation-reaction were added to 50 µl One Shot® cells and mixed by gentle tapping. Subsequently, the reactions were incubated on ice for 30 min. Following this incubation, the cells were heat-shocked at 42°C for 30 s before being placed on ice. Following the addition of 250 µl pre-warmed SOC media (Sigma), the vials were shaken at 3 g for 60 min at 37°C. Each transformation was then spread on separate LB agar plates containing 100 µg/ml ampicillin which were incubated at 37°C overnight.

Colonies were then picked, grown in media overnight and plasmid DNA isolated from each clone (Miniprep, Qiagen). To detect clones containing the IL-33-insert, plasmid DNA as well as a control vector containing K14 promoter (provided by Dr Gilchrist) was digested with BamHI (Roche). The digestion products were then separated on an agarose gel and inserts of the appropriate size (~750bp) identified. K14 vector and insert was cut out and gel purified. After shrimp phosphatase (Promega) incubation for 1 h at 37°C to prevent religation, enzyme was heat inactivated at 70°C for 15 min and product purified (Qiagen). Ligation was performed using Rapid ligation kit (Roche) and product transformed into competent cells. Cells were grown and colonies picked. Further BAMHI digestion and subsequently KpnI digestion performed (Figure 4.27). Clone #2 and #3 were maxiprep (Qiagen) for further transfection.

2.12.2 Transfection of K14-IL-33 in HaCaT

The right orientation of the IL-33 insert could not be shown by restriction digest. Instead HaCaT cells were transfected with both constructs to test for expression of IL-33. As HaCaTs normally express Keratin 14 (K14) the K14 promoter should be active in these cells leading to expression of IL-33, if it is present in the right orientation. For the transfection HaCaT cells were plated in a 6 well plate at 2×10^5 cells /well and incubated for 2 days to reach ~ 80 % confluency. Cells were

then transfected using Lipofectamine 2000 (Invitrogen) according to manufactures' protocol. Transfections with the following constructs were performed: mock, construct #2 and #3, and pEF6/V5-His-TOPO/LacZ (Invitrogen) allowing for β -Gal staining to assess the general transfection efficiency (Invitrogen).

24 h after transfection, cells were harvested by trypsinization, cytocentrifuged onto slides (7×10^4 cells/slide, 450 rpm, 6 min) and subsequently stained for IL-33. β -Gal staining was performed according to manufactures' instructions. Staining directly in the 6 well plate showed a transfection efficiency of 1-2%. Construct #3 was expressing IL-33 (tested by IHC) and was sent for sequencing.

2.13 Nanoparticle methods

This part of my laboratory work was done in close collaboration with Dr Ross Stevenson, senior postdoctoral fellow, Centre for Molecular Nanometrology, WestCHEM, Department of Pure and Applied Chemistry, University of Strathclyde. Dr Stevenson was responsible for chemical linkage of NP to proteins; biological assays and in vivo experiments were performed by me and ex vivo analysis with Dr Stevenson's help and supervision. Here I briefly describe the preparation of protein linked NP (2.13.1), tests to confirm linkage (2.13.2, 2.13.3), biological activity (2.13.4) and the in vivo use in regard to organ distribution and inflammation (2.13.5, 2.13.6).

2.13.1 Protein linked SERRS active nanoparticles

Citrate reduced gold nanoparticles were synthesised by the Turkevich method to ~18.6 nm diameter (size established by scanning electron microscope) (226). In certain conditions, the nanoparticle colloid was concentrated by centrifuging five 1 ml samples and resuspension of the pellets in 1ml of phosphate buffer (10mM pH 7.6). Concentrations of the colloidal solution were calculated using UV spectroscopic techniques. Colloidal nanoparticle suspensions were then labelled with the SERRS active linkers (benzotriazole or azo-dyes). Following incubation, samples were centrifuged at 5,000 rpm for 20 min to remove unbound dye, and the pellet was resuspended in phosphate buffer.

In order to link the labelled nanoparticle with the biomolecule, 980µl of nanoparticle suspension was incubated with 10 µl of 2 mg/ml solution of EDC (1-ethyl-3-(3-dimethylaminopropyl) carbodiimide hydrochloride and 10 µl of 2 mg/mL solution of NHS (N-hydroxysulpho-succinimide) for 20-40 min. This allowed conjugation of either linkers terminal carboxyl group to an amine group of proteins, by formation of a covalent amide bond. 10 µl of 1000 µg/ml etanercept (ETA), or control protein (PBS 0.1% BSA sterilised through a 0.2 µm syringe filter) was added and allowed to conjugate for 14-18hrs. Different conditions were investigated testing different concentrations of ETA as well as BSA. Further we added BSA at the end of reaction to prevent aggregation of NP (see chapter 5). Solutions were twice centrifuged and washed with phosphate buffer to remove any unbound protein.

Functionalized nanoparticles were investigated using a 632.8 nm wavelength laser (Leica DM/LM microscope, Renishaw InVia spectrometer, HeNe laser) to determine whether the nanoparticles retained SERRS activity. Raman analysis also allowed elucidation of the fingerprint spectrum from the functionalised NP.

2.13.2 Western blot of protein-linked NP

To test the concentration of etanercept (ETA) or IgG linked to nanoparticles (NP), ETA-NP probes, NP alone or IgG-NP were analysed by Western blot. Samples were incubated in reducing sample buffer (NuPage Invitrogen) at 70°C for 10 min to reduce and remove the disulfide linked protein from NP. Samples (20 µl) and marker (Seablue+2, Invitrogen) were loaded on a 4-12% Bis-Tris gel (Invitrogen) and run at 200 Volt for 1.5 h. The gel was transferred to a 0.2 micron nitrocellulose membrane using the iBlot® Gel transfer system (Invitrogen). After blocking the membrane for 1 h with 5% semi-skimmed milk in TBST, the membrane was incubated with goat anti-huIgG(Fc)-HRP 1:50000 (Sigma). Membrane was washed for 5 times and then incubated with luminol (Millipore) for 1 min. X-Ray films (Kodak) were developed at different times (10s, 30s, 1 min, 5 min).

2.13.3 *ETA-NP binding capacity*

To test the capacity for ETA NP to bind TNF, different concentrations of NP linked to ETA were incubated with 2000 pg/ml rTNF- α in 0.5% BSA RPMI 1640 in 1.5 ml eppendorff tubes at 37°C for 1 h. After centrifugation (5000 g, 5 min) supernatant was analysed for the presence of TNF- α by ELISA. Initially, NP TNF incubations were performed in RPMI only with results discussed in chapter 5 (

The use of nanoparticles to image inflammation).

2.13.4 HeLa cell activation with TNF- α and blockade with ETA-NP

HeLa cells were plated out at 2.5×10^4 cells per well in 200 μ l (96 well flat bottom plate) and rested overnight at 37°C/5%CO₂. The next day cells were stimulated with different concentrations of TNF with/without NP linked to ETA or control NP. After 6 h incubation, the culture supernatant was harvested and analysed by ELISA for IL-6 production.

This assay was used to validate activity of NP conjugated to different linkers and protein. A variation of linkages has been tested to avoid plastic binding and aggregation of NP which is discussed in the relevant chapter.

2.13.5 Nanoparticles in vivo

Initially, to test if NPs can be detected in tissue 100 μ l of NP solution was injected into the footpad or ear pinna of a euthanized mouse. After 5 min, SERRS measurements were performed (Figure 2.4B). For imaging of NP in vivo 100 μ l of a sterile NP solution was injected i.v. into the tail vein of mice. Different concentrations were assessed. Mice were culled after 4 - 6 h and laser measurements performed in an assigned room. Percutaneous measurements were performed before preparing the mouse for direct organ measurements. The setup is demonstrated in Figure 2.4A. Due to focusing problems of the initially used laser we switched to a new laser (Reporter, DeltaNu) (Figure 2.4C) with a cone head. This head touches the examined tissue achieving a fixed distance and therefore manages to standardise the laser to the right focus. Data were captured with a laptop (software: NuSpec, DeltaNu).

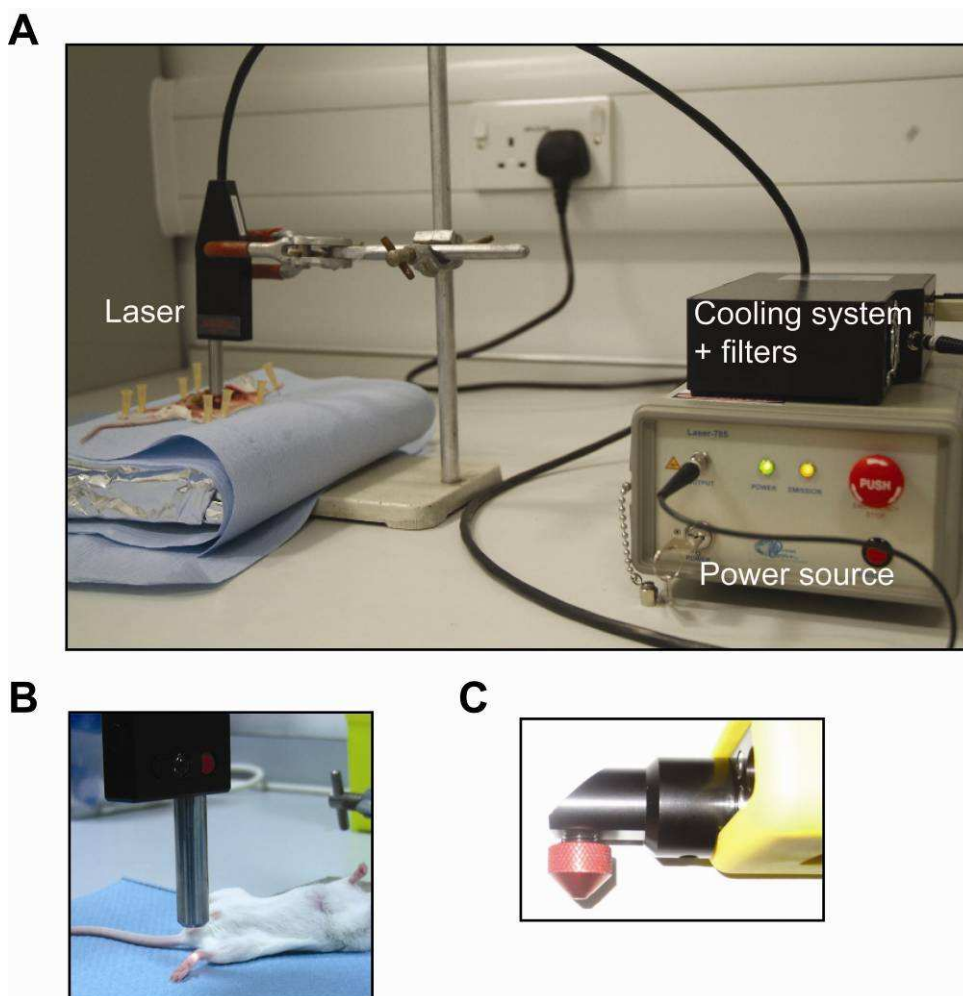


Figure 2.4 SERRS imaging ex vivo.

Setup of SERRS laser measurement (A) showing laser, cooling system and filters and power source. On the left hand a mouse cadaver was opened, specific organs prepared and SERRS signals measured. B: measurement of a footpad after local injection of NPs. C: laser system with cone head for standardized laser distance.

2.13.6 Carrageenan foot paw injection model

To test if ETA linked NP can be used to track/image inflammation a carrageenan foot paw injection model has been utilised. My aim was to detect systemically administered NP at the site of inflammation compared to control NP functionalised with IgG. To achieve this, 8 week old BALB/c mice received a 50 µl subcutaneous (subcutaneous) injection (28 G needle), into one hindpaw (the right), of PBS containing carrageenan (300 µg per paw, Sigma). The contralateral paw (left paw) received 50 µl of PBS and was used as the control. Paw edema was measured with a calliper at several time points after the injection of carrageenan.

100 µl of NP probes were intravenously injected into the tail vein using an insulin syringe and 28 G needle 68 h after carrageenan injection. 5-6 h later, mice were sacrificed and analysed for SERRS NP signals of both foot paws but also other organs. At least 3 mice per group were used.

2.14 Statistical analysis

All results are displayed as mean +/- standard error mean (SEM) and all statistical analysis was done either by students T test, ANOVA test or Mann Whitney test, as indicated in figure legends, using the Graph Pad Prism 4 software. A p value of < 0.05 was considered statistically significant.

3 Interleukin-23 and Interleukin-17 in inflammatory arthropathies

Content of this chapter has been published in the following manuscripts:

- Hueber AJ, Asquith DL, Miller AM, Reilly J, Kerr S, Leipe J, Melendez AJ, McInnes IB
Mast cells express IL-17A in rheumatoid arthritis synovium.
J. Immunol Cutting Edge 2010 Mar 3.
(selected for “Research Highlights” in *Nature Reviews Rheumatology* -2010 May 03)

- Hueber AJ, Asquith DL, Millar NL, Sturrock R and McInnes IB
“Interleukin 23 expression in inflammatory arthritis”[ABSTRACT]
ACR, Philadelphia, USA, Oct 2009

3.1 Aim and Introduction

Recently, the cytokine IL-17A (from now onwards mentioned only as IL-17) has been linked to autoimmune disease mechanisms. In rodent models, deficiency or blockade of IL-17 leads to suppression of arthritis (227). In humans, expression of IL-17 in RA synovium and synovial fluid was first described in 1999 (98). Initial phenotyping studies indicated that synovial T cells with plasmacytoid phenotypic characteristics expressed IL-17. Most subsequent reports have focused on expression in peripheral blood, and few reports have studied Th17 cell markers in situ (86, 228). Other cell types including $\gamma\delta$ T cells, NKT cells, NK cells, neutrophils, eosinophils and innate CD4⁺ lymphoid tissue inducer-like cells (LTi-like cells) have been reported to produce IL-17 (229, 230). Also recently, mast cells have been described to express IL-17A and IL-17F (231). Thus, in tissue, the net IL-17 expression may arise from a broad array of adaptive and innate cells. Such expression could confound the notion of a Th17 dominant disease state in humans despite murine data to that effect.

Interleukin (IL)-23, a heterodimeric cytokine comprising a unique p19 and shared p40 subunit (with IL-12) is implicated in expansion of Th17 cells (see chapter 1.2). Mice deficient for IL-23 receptor (IL-23R) exhibit impaired expansion and function of Th17 cells (232). Furthermore, deletion of IL-23(p19) in a murine model of arthritis ameliorated disease suggesting a pro-inflammatory role in articular inflammation (121). Genome wide analysis has identified single nucleotide polymorphisms within the genes encoding *IL-23A* and *IL-23R* that are strongly associated with psoriasis and AS (233, 234) and antibodies targeting IL-23p40 yield profound and long lasting beneficial clinical effects in psoriasis (32, 122). These studies support a pathological role for IL-23 signaling in human inflammatory diseases. Despite the foregoing, remarkably few studies have delineated IL-23 expression in relevant patient subsets, nor have the relevant conditions that could drive IL-23 expression been fully explored. IL-23p19 has also been detected in RA synovial membrane where its expression was shown to be regulated by activation of the toll-like receptor (TLR) signaling pathway (113). *This part of my work sought to determine the expression of IL-23 that could sustain Th17 biology in inflammatory arthritis. Further it sought to*

re-evaluate the dominant cellular source of IL-17A in established RA synovium.

3.2 IL-23 expression in inflammatory arthropathies

3.2.1 Synovial expression of IL-23p19

Synovial tissue samples from patients with RA (n=5), PsA (n=4) or OA (n=4) were obtained from The Centre of Rheumatic Diseases tissue bank (Glasgow Royal Infirmary) derived by arthroplasty. To explore IL-23 expression immunohistochemical analysis of paraffin sections was performed. At the time of this study, only two anti IL-23p19 antibodies were available, a product from Biolegend (mouse anti-human IL-23p19) and another from Sigma (rabbit anti-human IL-23p19). It has to be reported that the Biolegend mouse antibody has been used in the literature at 10 µg/ml, a fairly high concentration for IHC. When I explored the staining pattern for this antibody I found it was non-specific, with no cellular staining distinguishable. Titration of the antibody did not improve matters. Furthermore a closer look reveals non-specific staining of IL-23 in the company datasheet⁴ as well as the published manuscript (113). To be fair, resolution in published manuscripts may not properly reflect the true image. The Sigma rabbit anti human IL-23p19 seemed to be more convincing. It is recommended at 10 fold lower concentration and data sheet staining patterns showed specific cytosolic expression in tonsils in the DC/macrophage area of lymph follicles⁵.

I therefore elected to work up the Sigma antibody for further evaluation in synovial tissue. In the samples tested here, staining revealed consistent cytoplasmic expression for IL-23p19 in cells in RA and PsA synovial tissue primarily within and immediately adjacent to lymphocyte rich aggregates. In contrast, we detected no staining in non-inflamed OA synovial tissue (Figure 3.1). This predicts the existence of a microenvironment enriched with local IL-23 expression in inflammatory arthritis, in which in close proximity to T cells of a cytokine milieu might promote differentiation and maintenance of Th17 cells.

⁴ http://www.biolegend.com/media_assets/pro_detail/datasheets/Human_IL-23_Product_Data_Sheet.pdf

⁵ http://www.proteinatlas.org/show_image.php?image_id=598283

3.2.2 Expression of IL-23 in synovial fluid

In situ staining for IL-23p19 demonstrated the expression of one subunit of a functional heterodimeric cytokine. Next, synovial fluid expression of bioactive IL-23 by ELISA (recognizing only p19 / p40 heterodimers) was measured. Bioactive IL-23(p19/p40) was detectable in only 3 out of 15 PsA patients and was below the limit of detection in all RA and OA derived fluids (Figure 3.2). Prior studies similarly reported only low levels of IL-23 in RA SF (113, 235). This low level detection is not entirely explained – but might reflect consumption by adjacent tissues, limited specificity of the ELISA system (although it behaves well in PB assays), inhibition by a tissue specific factor e.g. bound cytokine or true low levels of IL-23 release from cytoplasm given the robust staining pattern observed above.

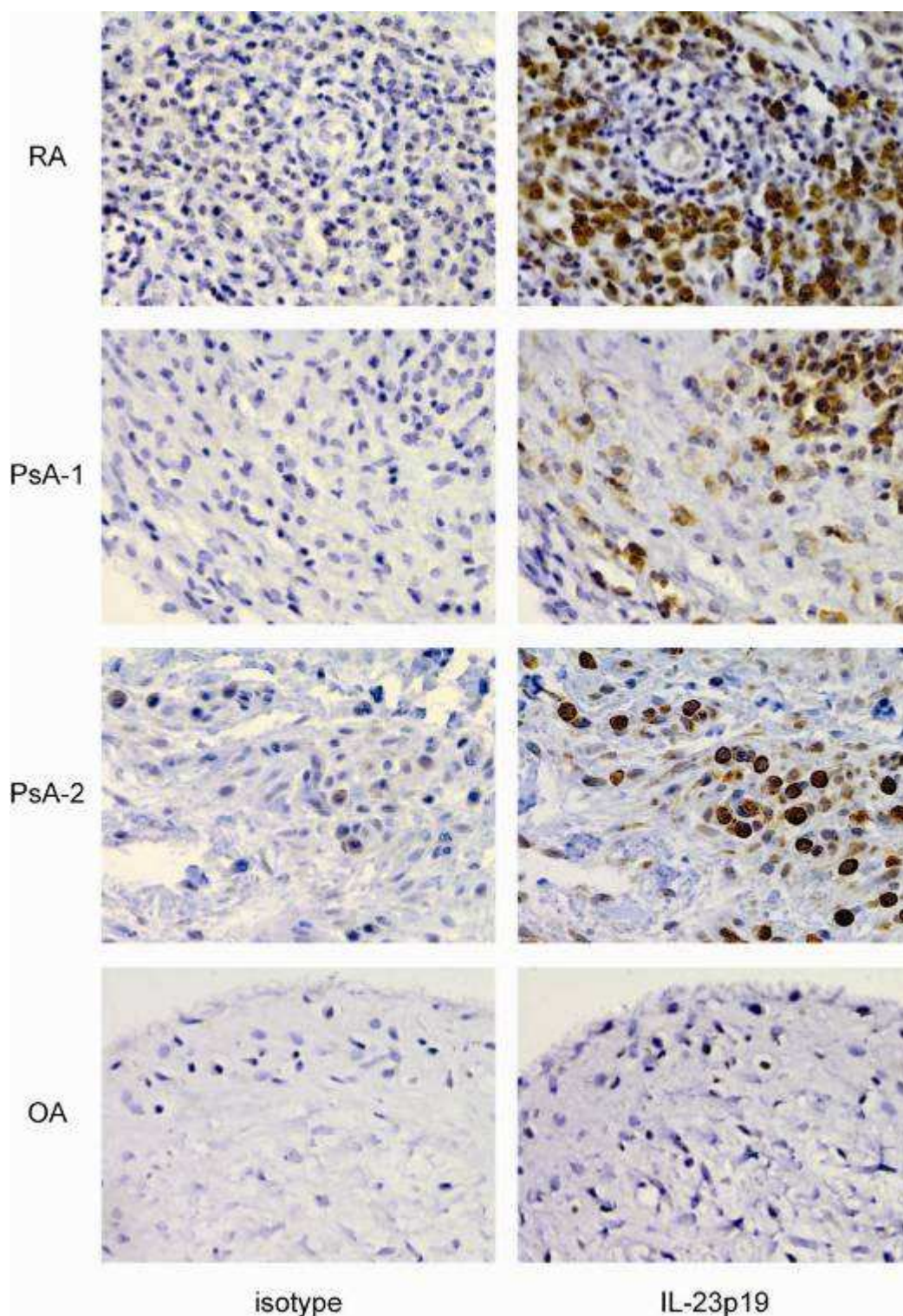


Figure 3.1 Synovial expression of IL-23 in inflammatory arthropathies. Immunohistochemistry analysis using an anti IL-23(p19) primary antibody was used to detect endogenous IL-23 in synovial tissue from RA and PsA patients (right panel). IL-23(19) was not detectable in synovial tissue from patients with osteoarthritis (OA). Representative images of RA (n = 5), PsA (n = 4) and OA (n = 4). Magnification is shown at 40X. Isotype controls are shown on the left panel.

3.3 The source of IL-17 in rheumatoid arthritis

The data above were strongly suggestive of IL-23 expression in the inflamed synovial compartment and thus this tissue provides a local environment optimized for Th17 expansion and maintenance. It is unclear if Th17 cells are recruited from the peripheral blood or if Th17 cells differentiate locally from recently recruited precursor (naïve) T cell subsets. IL-17 has been detected in synovial fluid and evidence for a role of Th17 cells in RA is growing. However, protein analysis, in particular, histological analysis of IL-17 expression is hardly reported. Further published reports show only few positive cells, provide no formal tissue analysis and conclusions about cellular source and occurrence of Th17 cells in human tissue must remain debatable. The aim of the following experiments was to characterize IL-17 expression in RA and provide formal proof of the predominant cellular source of IL-17 production.

3.3.1 IL-17 is expressed in RA synovium but only scarce in OA synovium

To investigate the expression pattern of IL-17A in rheumatoid tissue IHC was performed on tissue derived at arthroplasty. As control, tissue from OA patients was obtained and treated in an otherwise identical manner. Extensive work up of the antibody to IL-17 was performed using tonsil sections - a variety of antibodies were screened for tissue nonspecific staining and the capacity to detect cytosolic cytokine. Once a candidate antibody was selected, cytoplasmic IL-17A staining was detected in cells of ovoid / plasmacytoid phenotype, as previously described, and in cells of more irregular phenotype, both at the periphery of lymphocytic aggregates, in the sub-lining layer areas and rarely in the lining layer (nickel-DAB, black, Figure 3.3A). Interestingly, IL-17A positive cells were also detected in OA tissue, however, not consistently (DAB, brown, Figure 3.3B).

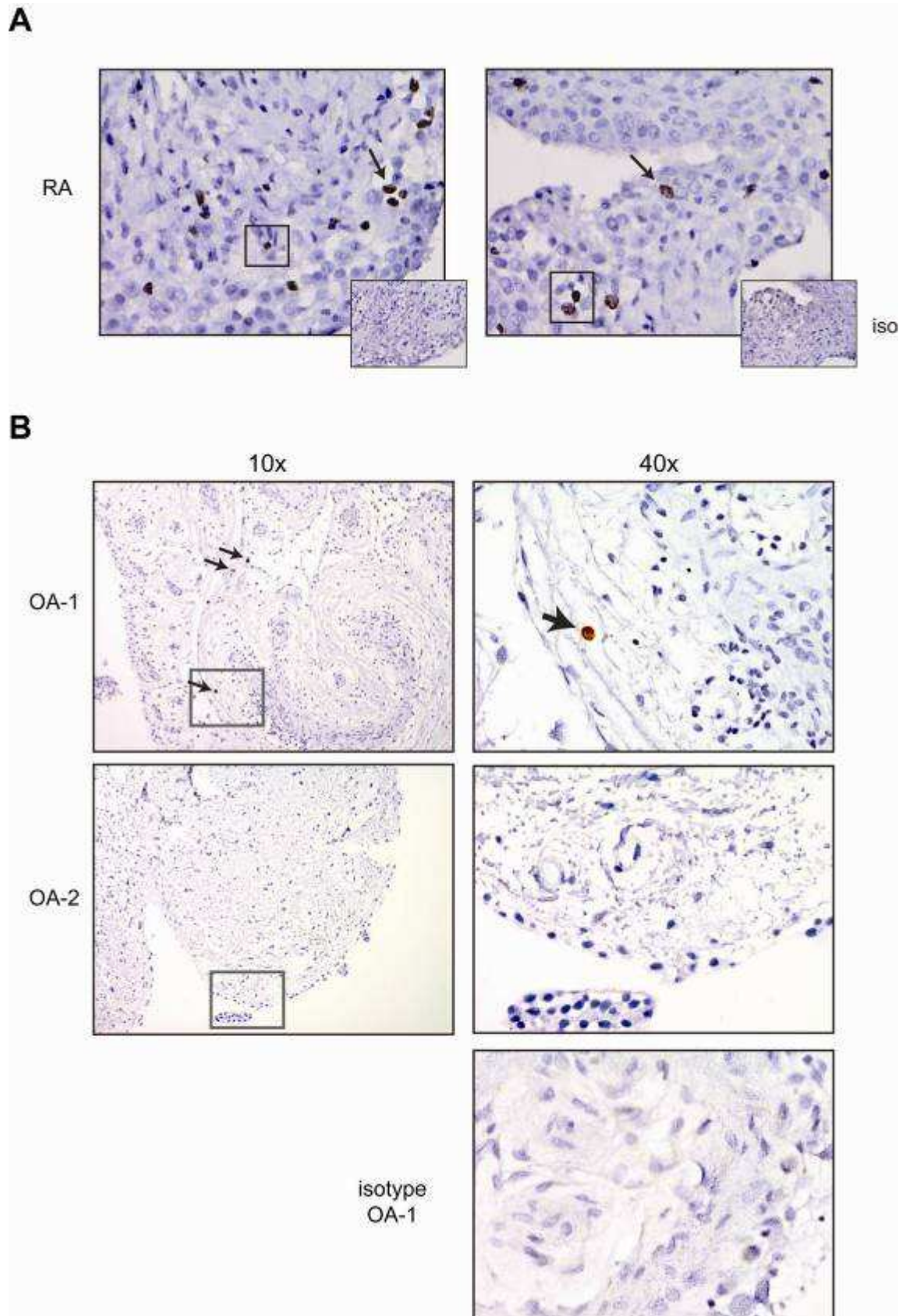


Figure 3.3 IL-17A expression in RA/OA synovium.

A: Immunostaining of IL-17A in different established RA synovial tissue. Nickel-DAB (black), counterstaining with haematoxylin. 40x magnification of two areas. Bottom right shows isotype (iso). Arrows and boxes mark differently shaped IL-17+ cells. **B:** IL-17A (DAB (brown)). OA-1 with few IL-17A+ cells; OA-2 with no IL-17A+ cells detected. 10x and 40x fields of a representative OA synovial tissue (n=4 with 2 positive and 2 negative synovial OA membranes). Arrows show positive cells. Grey box: area of magnification. Right bottom picture: Isotype control of OA-1

3.3.2 IL-17 is rarely expressed by Th17 cells in RA synovium

To formally identify these IL-17A⁺ cells in RA synovium, co-localization studies were performed. To investigate cellular markers in combination with cytokine expression double staining had to be established. For the successful staining procedures with light microscopy immunohistochemical technique was pursued. The surface marker chemokine receptor CCR6 has been reported to be expressed on Th17 cells. Staining for CCR6 was worked up, and different dyes for chemical reactions determined (Figure 3.4). CCR6 was stained with nickel-DAB counterstained with haematoxylin resulting in a black colour. Staining with Nova Red counterstained with methylgreen results in a dark blue colour. CCR6 staining pattern demonstrated membrane staining in lymphocytic aggregates but also single scattered cells were apparent. However, Nova Red which stains dark red in haematoxylin is hard to distinguish to normal DAB or nickel-DAB. Also Nova Red in methylgreen results in a dark blue stain which is difficult to differentiate to DAB. Taken together, the following combination was used for co-localization of CCR6 and IL-17 (Figure 3.5): VIP (CCR6) and nickel-DAB (IL-17) with no counterstain; Nova-Red (CCR6) and nickel-DAB (IL-17) with methylgreen counterstain.

Surprisingly, using both coloration methods distinct staining patterns were visualised. CCR6 stained lymphocytic aggregates with membrane attribution and IL-17 stained cytosolic in the periphery of these aggregates. However, it cannot be ruled out that IL-17 masks CCR6 expression, especially seen in the left panel in which black dark staining might conceal purple membrane CCR6 staining (Figure 3.5).

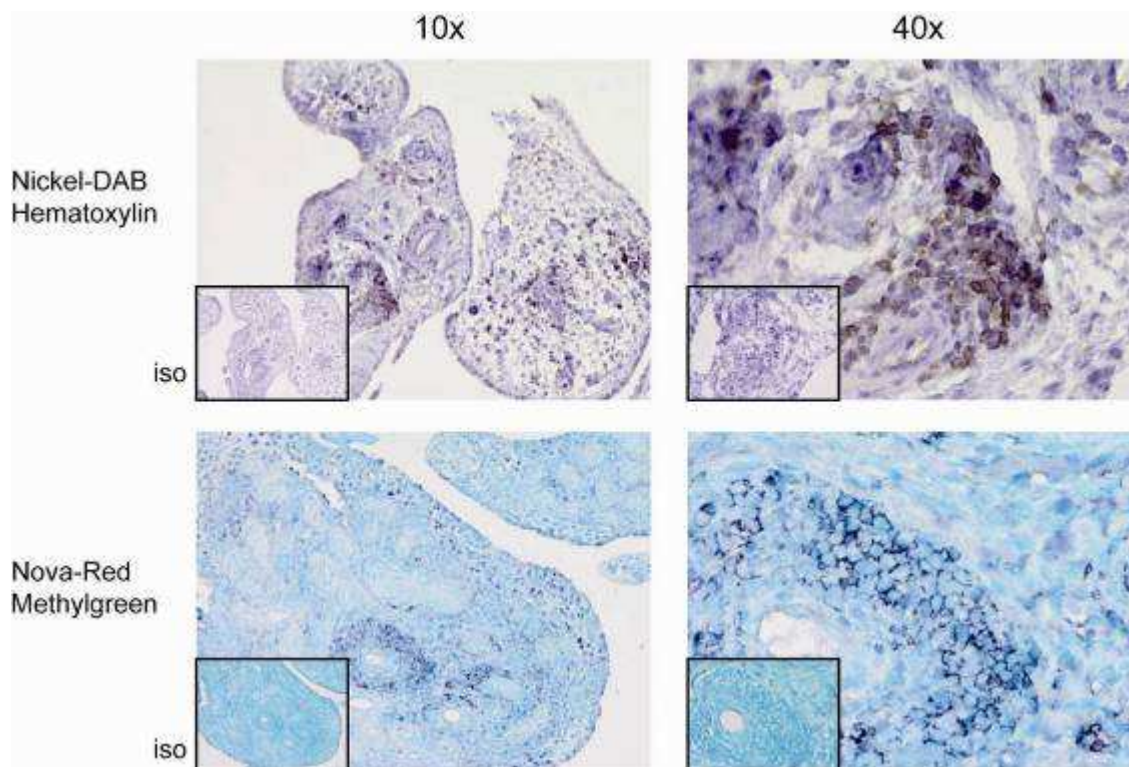


Figure 3.4 Establishing staining for CCR6 in RA
 Immunostaining for CCR6 in two different RA synovial tissues: left panel show 10x magnification and right panel 40x. Left bottom corners of pictures demonstrate the isotype. To establish counterstain 2 different dyes for the peroxidase reaction and counterstain have been used. Top row: Nickel-DAB (black) with haematoxylin. Bottom row: Nova Red (dark blue) with Methylgreen.

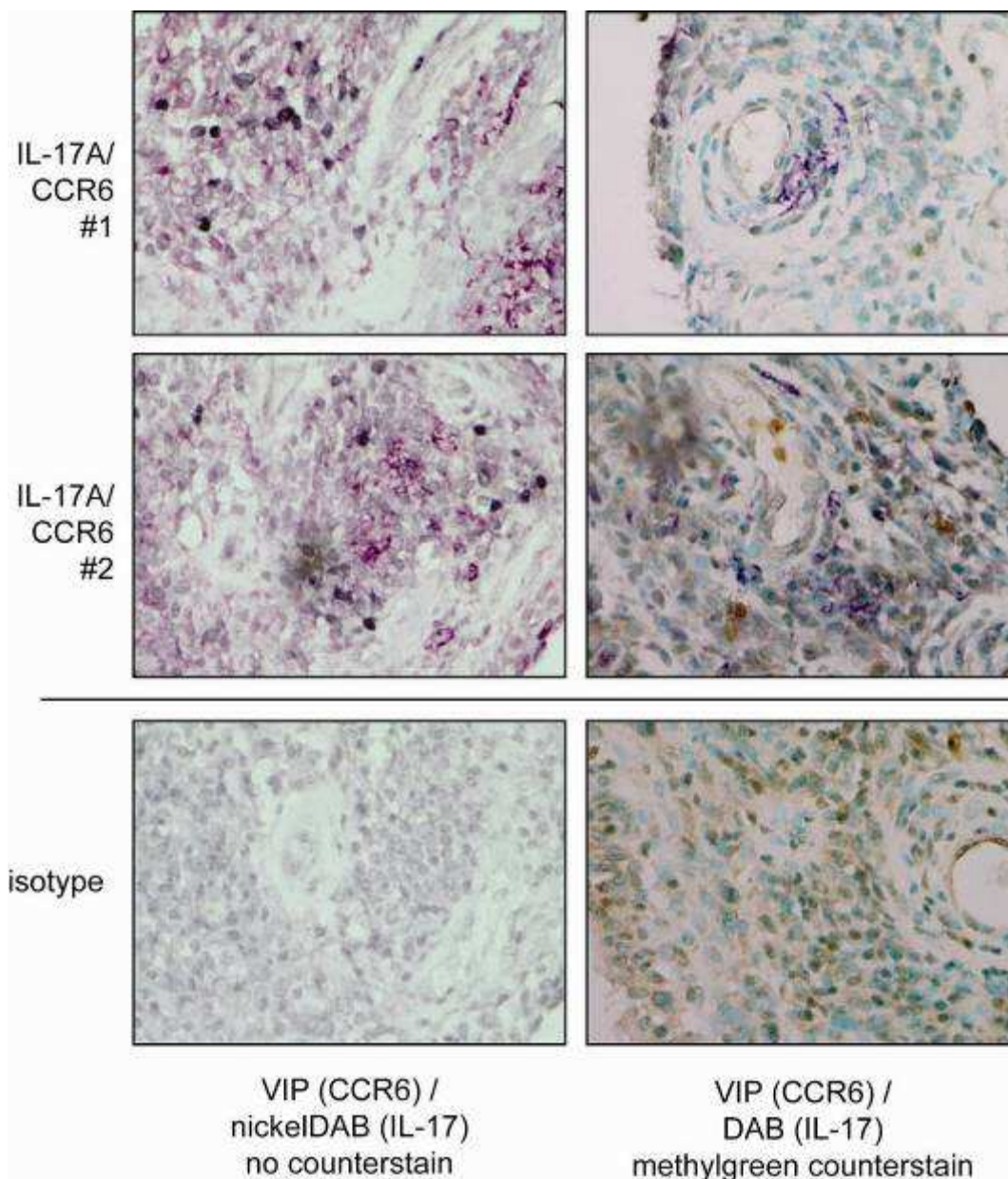


Figure 3.5 Doublestaining IL-17 and CCR6 by light IHC

Left panel demonstrates staining for CCR6 with VIP (purple) and IL-17 with nickel DAB (black). Right panel uses DAB (brown) instead of nickel-DAB and counterstains with methylgreen which leads to a blue CCR6 (VIP) stain. Cytosolic IL-17 is not co-localised with membrane expressed CCR6. Noteworthy is non-specific staining in the isotype (right panel). Shown are two examples from 2 independent RA tissues. (#1 and #2). Bottom row: isotype.

To address this problem, a back to back approach was chosen. Hereby, tissue sections were cut, turned and mounted on slides in an “open book” aspect. To visualize this, in this procedure, the same surface is apparent on two sections. If the tissue block is imaged as a book and opened in the middle, the left and right page touched each other. Back to a tissue block, when cutting one section and turning the next section, the same surface can be guaranteed and therefore a single cut through the tissue or here a cell is shown on both sides. Thus this approach can demonstrate staining of 2 targets with single staining of back to back sections.

Nickel-DAB with counterstain haematoxylin was used for staining. IL-17 and CCR6 or CD3 were targets for IHC (Figure 3.6). Due to technical difficulties, back to back sections are not absolutely identical. The IL-17 staining pattern obtained, confirmed previous staining with cytosolic detection in large cells with irregular phenotype. Comparing similar areas few cells seem to be double positive for IL-17 and CCR6 (squares, Figure 3.6A). However, other cells only express IL-17 without CCR6 (arrow marked cell as example). Similar results were obtained with IL-17 CD3 using the back to back staining method, with few cells possibly double positive (square) and others only positive for IL-17 (arrow) (Figure 3.6B). To summarize, this method presented few possible double positive cells, however, the convincing cellular source of IL-17 was still inconclusive.

To definitively define the expression pattern, double staining was established using fluorescence microscopy. With this technique exact overlay is possible and thus certainty for cellular identification should be guaranteed.

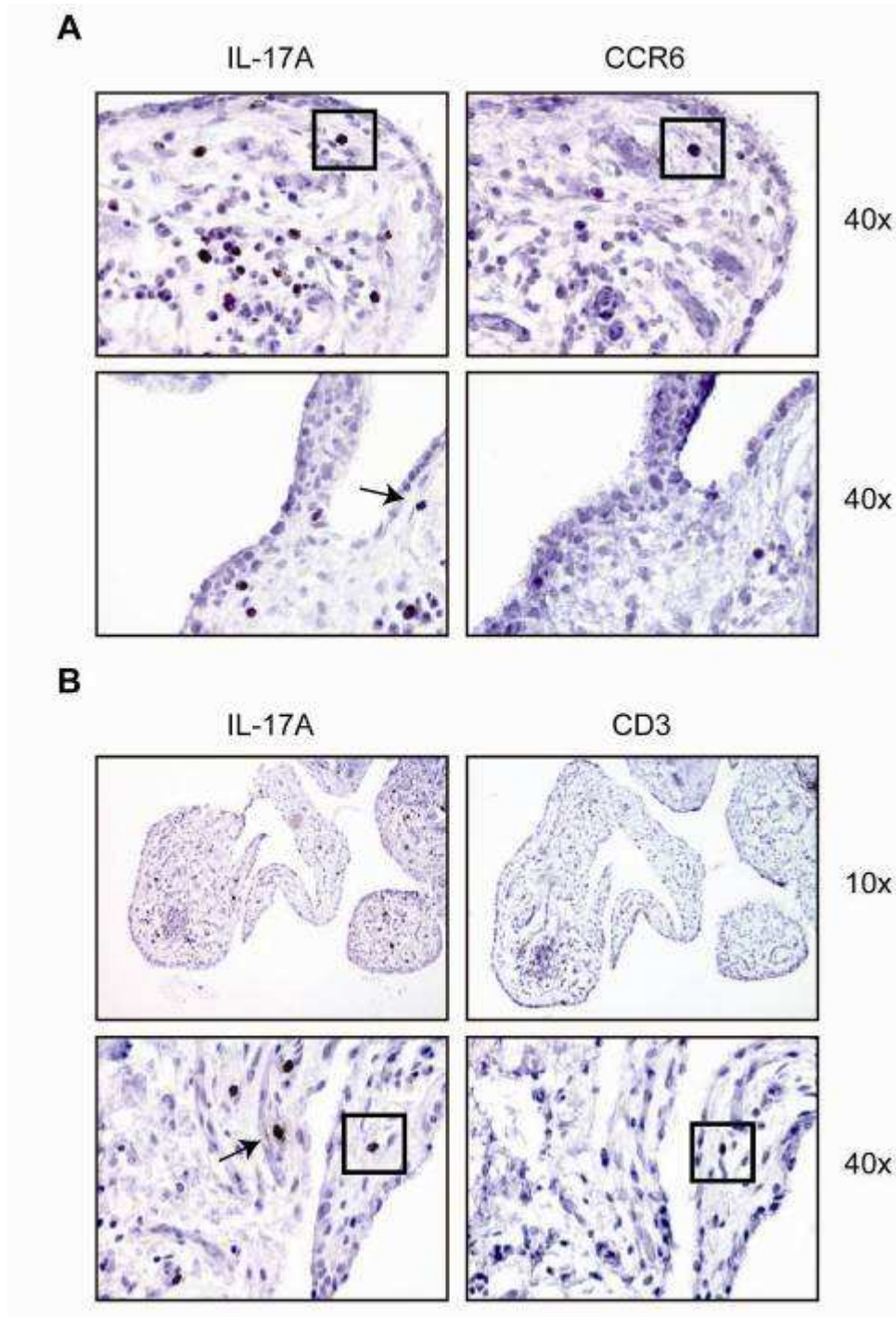


Figure 3.6 Back to back staining CD3/CCR6 and IL-17

IHC of RA synovium using back to back sections. These were stained with either IL-17 and CCR6 (A) or IL-17 and CD3 (B). Top row shows a positive cell for IL-17 in the sublining layer (square) which seems to be positive for CCR6 as well. Other cells are only single positive (arrow). Similar result was achieved with IL-17 and CD3 with few possible double positive cells (square). Also single positive cells are detectable (arrow). Nickel-DAB with haematoxylin counterstain. N=1.

(A) 40x magnification, (B, top row) 10x, (B, bottom row) 40x. No isotype shown.

Cells were stained as described in the methods chapter. Expression of IL-17 was compared initially with CD4 and CD3. IL-17 stained with FITC is shown in green where cellular markers are in red (Figure 3.7). CD4 and CD3 positive cells accumulate in lymphocytic infiltrates with membranous staining pattern (upper row). The IL-17 staining pattern observed confirmed previous IHC pictures with cytosolic accumulation in the periphery of this tertiary aggregates (middle row). To visualize cells DAPI (in blue) was used. Merged pictures clearly show distinct cells in regard to IL-17 and CD4/CD3 expression (bottom row).

Although occasional CD4 IL-17 double positive cells were identified, the majority of IL-17 positive cells were CD4 negative (<1%), consistent with the notion that CD4⁺ Th17 cells represent a minority of the IL-17 producing population in synovitis (Figure 3.7 upper left panel, Table 3.1). This also renders it unlikely that LTi-like cells are major contributors as these cells express CD4 (230). Moreover, counterstaining with CCR6 did not co-localize with IL-17 either (Figure 3.8). Strikingly, an IL-17 positive cell is in close proximity to a CCR6 positive cell. CD3/ CD8 double positive T cells have been shown to produce IL-17 (236). Of interest, only 1-8% of IL-17 expressing cells were found to express CD3 (Figure 3.7, Table 3.1).

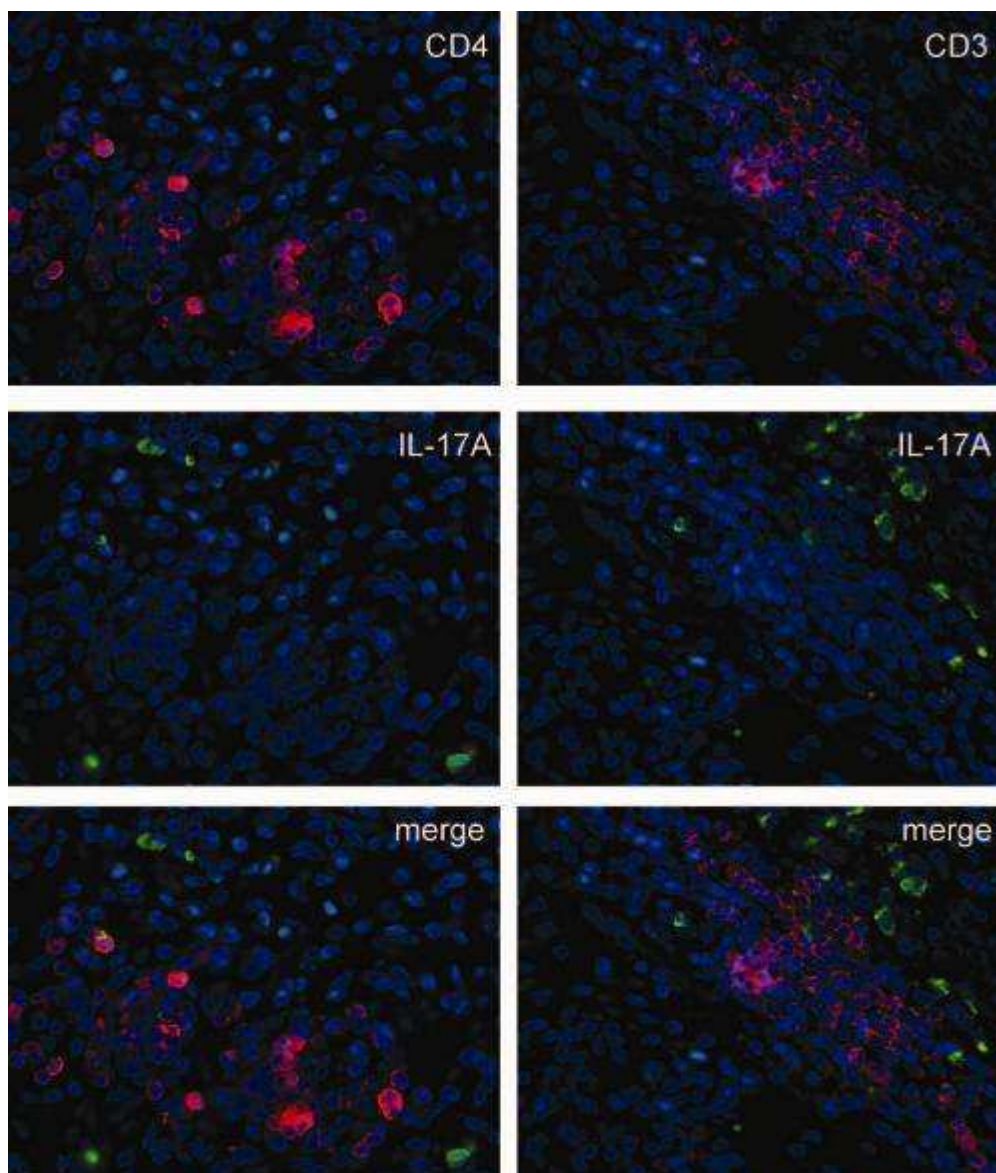


Figure 3.7 Doublestaining of Th17 cell markers and IL-17A. Th17 cells are hardly detectable in established RA synovium. Synovial tissue samples from RA patients (n = 10) were stained for IL-17 (green) and CD4 (left panel) or CD3 (right panel) (both red). Sections were counterstained with DAPI (blue). Bottom row show merged staining. Images are shown at 40x magnification.

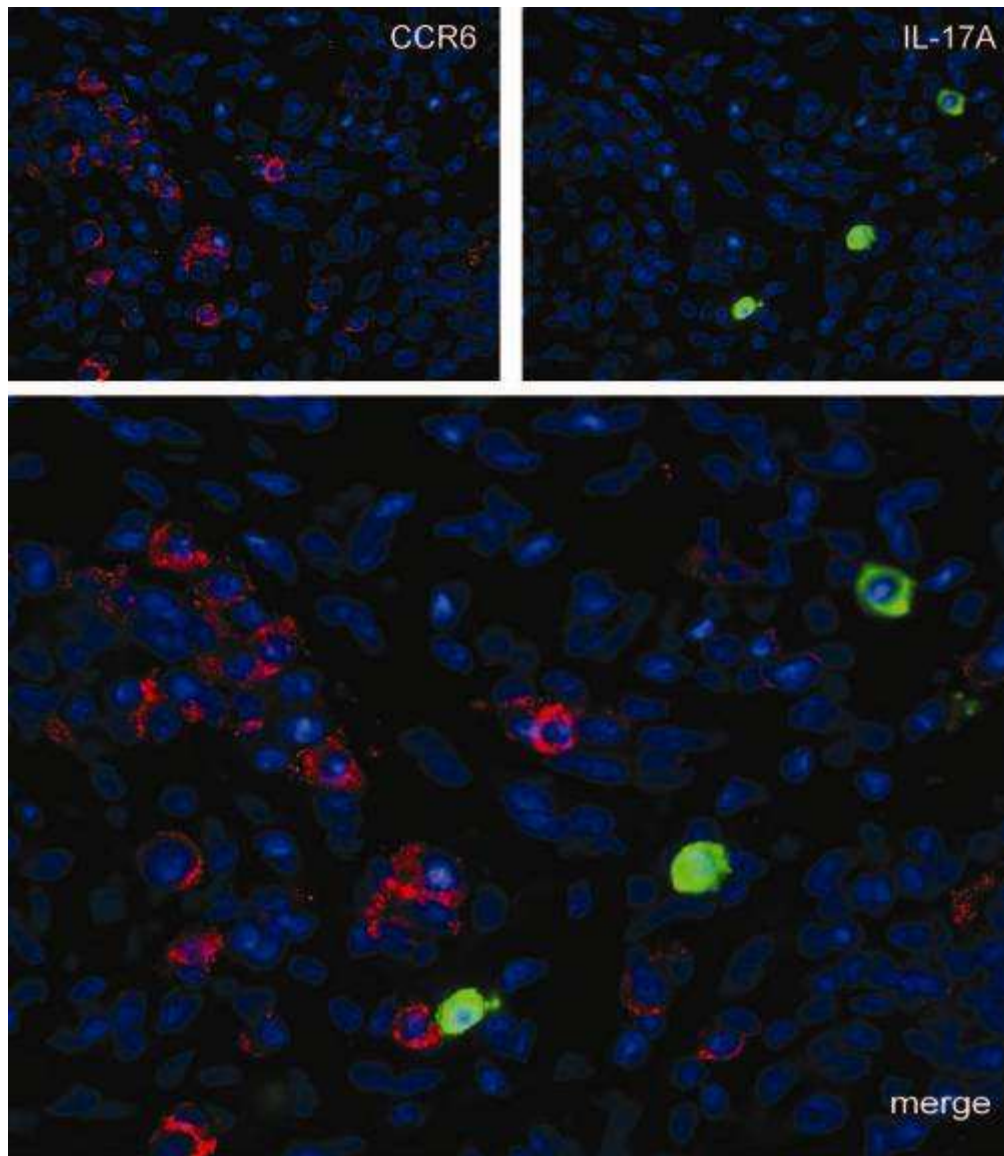


Figure 3.8 Doublestaining of Th17 marker CCR6 with IL-17A. CCR6 (red, top left) does not colocalize with IL-17 (green, top right). Sections were counterstained with DAPI (blue). Bottom image shows merged staining. Images are shown at 40x magnification with bottom picture electronically magnified.

3.3.3 IL-17 is produced by innate immune cells mainly mast cells

Results described above exclude T cells as the main source of IL-17 in established RA synovium. Therefore the question arose - which cells produce IL-17 in the synovium? IL-17 positive cells were bigger in size, some demonstrated ovoid/plasmacytoid or irregular shape and commonly these cells were detected in the periphery of lymphocytic aggregates. With the phenotypically distinct subset of IL-17⁺ cells of irregular shape and this expression pattern, macrophages were postulated as a potential lineage.

Double staining was performed therefore for IL-17 and CD68 (Figure 3.9). CD68 is a late endosomal protein primarily detected on monocytes and macrophages and is considered a pan- macrophage marker. Staining revealed that up to 35% of IL-17 positive cells were CD68 positive (Table 3.1). Figure 3.9 demonstrates double positive cells (arrow); however, still some cells expressed only IL-17 (square). Moreover, expression of CD68 in IL-17 expressing cells is weak and thus more difficult to detect (arrows).

Mast cells have been reported to produce IL-17 (231). To determine whether mast cells might be an additional source for IL-17, we co-localized mast cell tryptase (MCT) and IL-17 in 10 RA synovial tissues (Figure 3.10). Surprisingly, the majority of IL-17 cells double-stained strongly with MCT (46-100% of IL-17-expressing cells per tissue area across patients), clearly demonstrating that mast cells are key producers of IL-17A in RA synovium (Table 3.1). Interestingly, MCT stained cytosolic but also weakly scattered around the cells, a typical staining pattern for mast cells. Table 3.1 summarizes the occurrence of IL-17 positive cells in conjunction with the markers CD3, CD68 and MCT. Initially 4 patient tissues were examined and for confirmatory studies for CD68 and MCT, numbers were increased to n = 10.

Of marked importance, these studies therefore identified mast cells, a tissue resident innate immune cell population, as the predominant cellular source of IL-17 in established rheumatoid arthritis. These findings contrast with expectations regarding the cellular source of IL-17 in the inflamed joint and suggest a paradigm shift in the understanding of how the IL-17 axis operates in human inflammatory disease as opposed to murine systems.

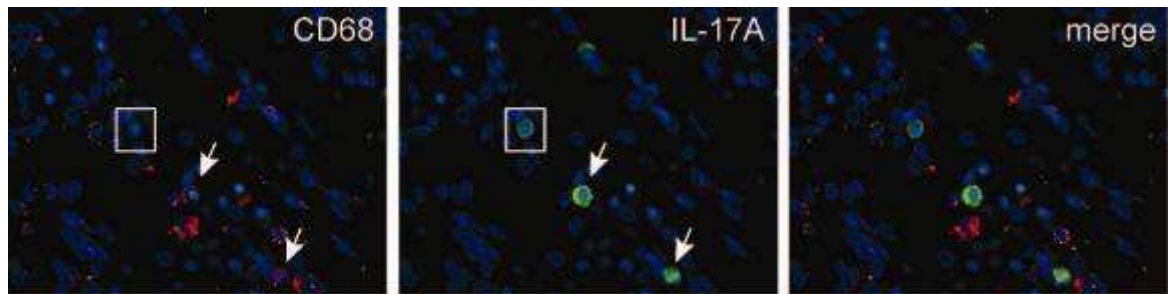


Figure 3.9 Doublestaining of IL-17 pos. cells with CD68
 RA synovium, n=10. fluorescent microscopy. CD68 (red) and IL-17 (green) are shown single stained and merged with DAPI (blue) counterstain. 40x magnification

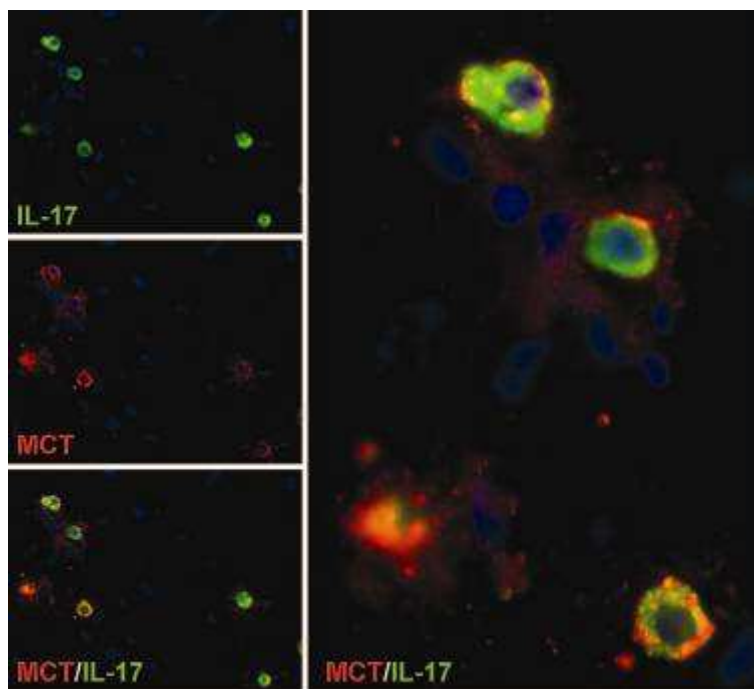


Figure 3.10 Mast cells express IL-17A in RA synovium.
 MCT (red) and IL-17A (green) are shown single-stained and merged with DAPI (blue) counterstain (left panel, 40x magnification). This is further digitally magnified to demonstrate cellular structure (right panel).

		cells per mm ²	percentage of IL-17+ cells (mean)	percentage of IL-17+ cells (min/max)
CD3 analysis (n=4)	CD3- IL-17+	64		
	CD3+ IL-17+	2	3.4%	0.88% / 7.94%
CD68 analysis (n=10)	CD68- IL-17+	57		
	CD68+ IL-17+	6	9.8%	0% / 35%
MCT analysis (n=10)	MCT- IL-17+	8		
	MCT+ IL-17+	83	91%	45.71 % / 100%

Table 3.1 Percentage of double positive cells compared to IL-17+ cells. Absolute cell numbers (3rd column) and ratios are shown for CD3+ IL-17+ (n=4), CD68+IL-17+ (n=10) and mast cell tryptase (MCT)+ IL-17+ (n=10) to total amount of IL-17+ cells (4th column). Cell numbers were assessed in 2 independent fields with each ~0.5mm².

3.4 Discussion & conclusion

Th17 cells have been proposed as causal for a variety of autoimmune diseases including multiple sclerosis, inflammatory arthritis and psoriasis. Disease related mouse models support this notion. Using gene-deficiency approaches (e.g. IL-17 receptor deficient mice) most experiments strengthen this notion. In contrast, human data are rather rare, focus mainly on peripheral blood studies and are limited to disease tissue due to limited resources. In this chapter, tissue at the site of inflammation was the focus. Thus it was investigated whether a Th17 cell favorable environment exists comprising expression of IL-23, a main player for Th17 cell biology. It is already known that IL-6, IL-1 and IL-21 are present in the RA synovium and as such the cytokine milieu is a priori attractive as a Th17 enriching environment.

The cytokine IL-23 (or at least on subunit) was detected in inflammatory arthritis with no expression in osteoarthritis. In synovial fluid only low levels were present in PsA (3 of 15 positive samples), with no detection in RA or OA. Interestingly, when focussing on peripheral blood significant higher expression was present in PsA patients compared to healthy controls. To address a potential mechanism by which IL-23 is secreted it was determined if IL-23 was secreted upon the interactions of T cells and macrophages. Utilising an in vitro model of synovitis healthy human CD3⁺ T cells were activated in the presence of IL-2, IL-6 and TNF- α for 6 days (TcKs, previously been shown to represent synovial T cells) and co-cultured with syngeneic MCSF matured CD14⁺ macrophages. Indeed, co-culture resulted in the secretion of IL-23 in addition to IL-1 β and IL-6 (personal communication Dr Asquith, University of Glasgow). To summarize, the above data show the expression of IL-23 in synovitis which appears to be specific to the pathology of a proportion of patients with PsA. Furthermore, data suggest that within the synovium IL-23 secretion is mediated through the interactions of T cells and macrophages; thereby providing an environment that is supportive of Th17 cell polarization and expansion necessary for driving disease pathology.

As a next step the cellular source of IL-17 in RA synovium was sought. Utilizing the marker CCR6 for Th17 cells, IHC double staining for IL-17 and CCR6 was performed. No convincing positivity was detectable raising a number of critical

questions concerning the prominence of the Th17 responses in RA. These include - No detection due to technical difficulties?; Downregulation of CCR6 due to migration into the tissue or due to local stimuli?; Or lastly, is IL-17 expressed by other cells? To address these points methodology was adapted to embrace fluorescent microscopy and other markers for Th17 cells such as CD3 and CD4 were added to the investigation. With high degree of plausibility, it was demonstrated that Th17 cells hardly exist in the tissue examined. IL-17 production by macrophages has been suggested in allergic lung inflammation (237). Consistent with this, up to 35% of IL-17 positive cells were macrophages (CD68 positive) in RA synovium. More surprisingly, mast cells accounted as main source in the synovium. These data were confirmed by Dr Veale and colleagues; further they demonstrated that neutrophils express IL-17 as well in RA synovium (238).

These data only provide a snapshot of the disease process. Gathering samples from arthroplasty selects patients with RA at established to late stage of the disease. Nevertheless, when comparing RA tissue sections with OA samples a total different degree in inflammation was obvious. This was reflected by the amount of IL-17 positive cells detected. In every RA tissue IL-17 positive cells were present, compared to only 2 out of 4 OA samples. Furthermore expression in positive OA samples was scarce (Figure 3.3). In contrast to this still inflamed established disease is the urge to determine what initiates the pathologic disease process. For this question tissue from early arthritis or even pre-arthritis is needed. Leipe et al focussed on peripheral blood and synovial fluid and showed that Th17 cell frequencies and IL-17 production strongly correlated with systemic disease activity at both, the onset and the progression of the diseases (personal communication, Dr Leipe, University of Munich, data in press, Arthritis & Rheumatism). Th17 cells were reduced to control levels in patients with treatment-controlled disease activity. At onset of disease, Th17 cells were enriched in the synovial fluid, and increased frequencies of synovial Th17 cells expressed CCR4 and CCR6, indicative of selective migration of Th17 cells to the joints. Unfortunately, synovial fluid as follow up was not obtainable to test for Th17 occurrence. Thus to determine Th17 cell tissue expression in early disease examination of synovial biopsies is mandatory.

What drives mast cells to produce IL-17? In collaboration with Dr Alirio Melendez he demonstrated that CD34 progenitor derived mast cells produce IL-17 in response to various stimuli which have been suggested to play a role in RA (239) (Figure 3.11) (this collaborative work was performed by Dr Melendez and is here shown for completeness). These stimuli included TNF- α , IgG complexes, the complement component C5a and lipopolysaccharide (LPS). Further mast cells express the gene encoding the transcription factor retinoic acid receptor-related orphan receptor C. (*RORC*) (a transcription factor specific for Th17 cells, see 1.2, Th17 cells and their role in rheumatoid arthritis). Expression is increased by the factors that induce IL-17 production. *RORC* could be silenced by small interfering RNA which then blocked expression of IL-17, but not IL-5 or IL-6. Thus, in human mast cells the production of IL-17 appears specifically to be *RORC*-dependent.

In conclusion, this chapter demonstrates that proportionally mast cells and not Th17 cells appear to be a major source of IL-17 in established RA synovium. Further in collaboration with Dr Melendez we showed that such production can be driven by a variety of pathways abundantly expressed therein.

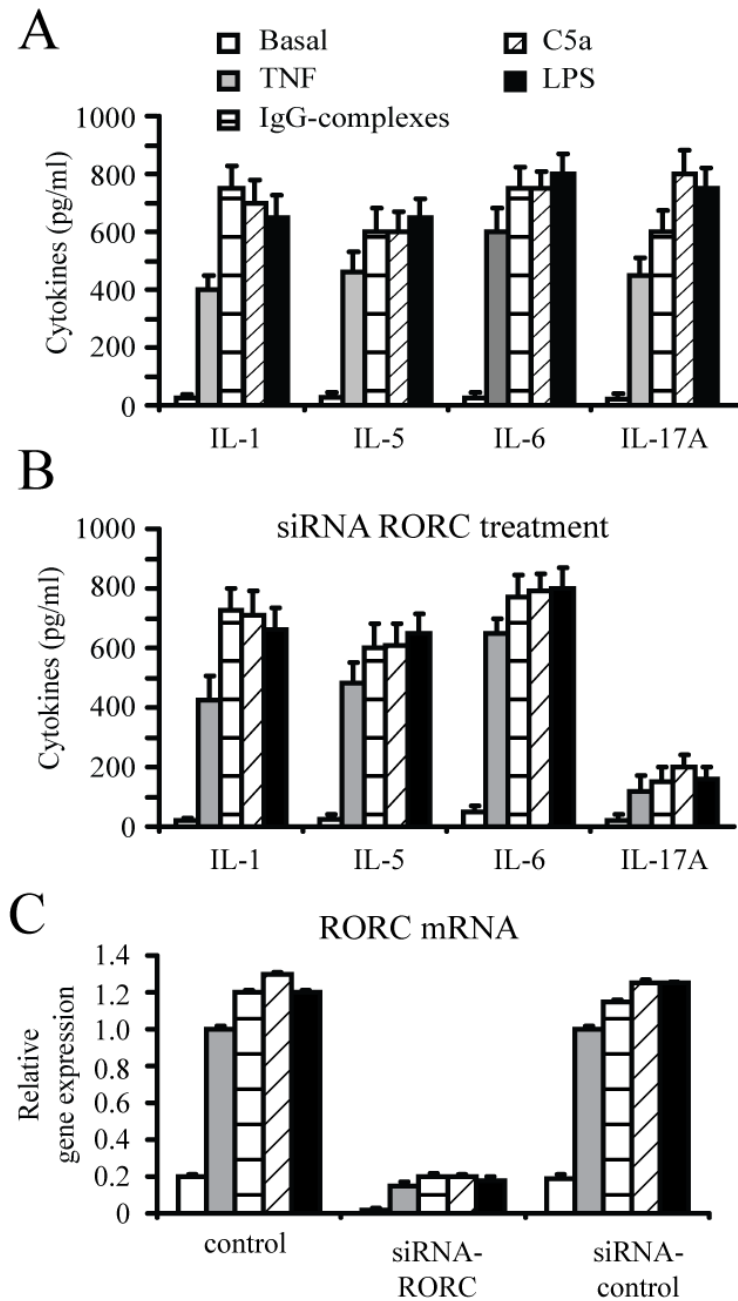


Figure 3.11 RORC dependent IL-17A production by CD34⁺ derived mast cells. Cytokine release was determined from mast cells (untransfected (A) or siRNA-RORC transfected (B)) after 24 hrs stimulation with TNF α , IgG-complexes, C5a and LPS, compared to a basal secretion (un-stimulated cells). Cell culture supernatants were analyzed for bioactive IL-1 β , IL-5, IL-6 and IL-17A by ELISA. RORC gene expression was determined by quantitative RT-PCR and silenced by siRNA targeting RORC (C). Results shown are the mean plus the standard deviation of triplicate measurements of three separate experiments.

4 Analysis of Interleukin-33 as an alarmin in psoriasis

Content of this chapter has been presented at the following meetings:

- “The alarmin IL-33 is overexpressed in psoriasis and induces ST2 dependent psoriasis like dermatitis”
EWRR Abstract Award, Oral presentation
EWRR, Bamberg, Germany, March 2010
- “The alarmin interleukin-33 and its role in psoriasis”
Invited speaker
EULAR, Rome, Italy, June 2010

4.1 Aim and Introduction

IL-33 is a novel cytokine of the IL-1 family and recently has been described to function as an alarmin. Arguments supporting this idea are expression in tissues with predominant barrier function, release upon cell death and broad biologic function with activation of several components of the immune system. The cellular expression is mainly in the nucleus in endothelial and epithelial cells but other cells have been reported to express IL-33. Initially described as “high endothelial nuclear factor” for its expression pattern in vessels, further work focused on its biology in regard to stromal organ expression and its effector function via the receptor ST2. Two recent reports focused on epithelial expression in the skin in diseases such as atopic dermatitis and psoriasis - Theoharides showed higher expression in psoriasis of epithelial IL-33 compared to healthy skin: however the biology of IL-33 in these diseases is quite unclear (173, 194).

Psoriasis is a disease which provides an ideal model choice to study IL-33: Psoriasis plaques occur at areas where constant microtrauma irritates the skin and tissue. These are commonly knees, scalp and elbows. Another feature of psoriasis is Koebners phenomenon by which physical trauma to the skin can trigger a psoriasis lesion. Whilst disruption of the body barrier “skin” and constant mechanical microtrauma can lead to inflammation, the role of IL-33 has not been studied in this context despite it potentially fulfilling as an alarmin all features necessary to trigger inflammation. Thus ***this chapter aims to understand the role of IL-33 in psoriasis*** with the specific task of exploring the following hypothesis (Figure 4.1):

‘IL-33 is expressed by human keratinocytes; an insult to the skin releases IL-33 due to cell damage of some kind. Dermal immune cells, especially mast cells which express the IL-33 receptor ST2 are stimulated by IL-33 and become activated. Mast cells produce cytokines and chemokines which recruit other immune cells and in the appropriate context (e.g. a psoriasis patient) inflammation is maintained and lesions develop.’

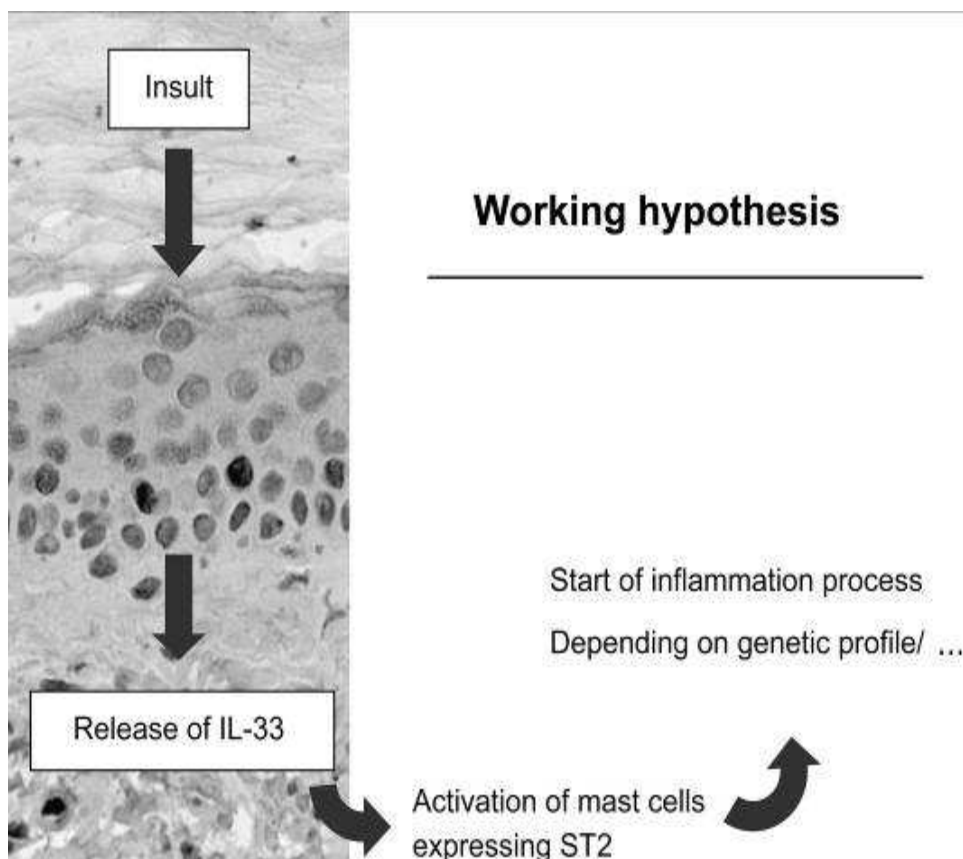


Figure 4.1 Hypothesis for the role of IL-33 in psoriasis
 Left image shows a histological section of the human skin. Aim is to examine if IL-33 release by an insult can activate immune cells and lead to skin inflammation.

Furthermore, and provoked by ideas emerging in the exploration of the potential role of IL-33 in barrier tissues, this chapter also addresses the expression of IL-33 in arthritis and provides entirely novel preliminary construct data for a transgenic mouse expressing IL-33 under a keratinocyte 14 promoter. In particular, IL-33 expression during embryogenesis has been determined.

4.2 IL-33 and ST2 is expressed in inflammatory tissue such as psoriasis

4.2.1 Expression of IL-33 and ST2 in autoimmune diseases

IL-33 has been reported to be expressed in cells of body barriers but also in associated inflammatory tissues for example tonsils. The aim of the following experiments was to investigate IL-33 expression in inflammatory diseases such as inflammatory arthritis and psoriasis. To evaluate IL-33 expression, IHC staining was performed on tonsil tissue serving as a positive control (Figure 4.2). Consistent with previous reports, IL-33 was detected in the nuclei of endothelial cell area. These cells could also be fibroblast reticular cells described by Moussion (147). After establishing the methodology for IHC of IL-33, skin from healthy individuals was investigated. Strong nuclear staining was detected in endothelial cells in the dermis (black arrows), but also weak staining of nuclear IL-33 was noted in the stratum spinosum of the epidermis (dashed arrows) (Figure 4.3).

Focusing on inflamed tissue, psoriasis skin was studied next. Hereby, two sample types were examined: Biopsies of lesions (psoriasis plaques) and perilesions. Perilesions were defined to be macroscopic healthy skin with no signs of inflammation such as redness, induration or scaling but to be in close conjunction to a psoriasis lesion (approx 1 cm distance from the leading edge of the psoriatic lesion). IHC revealed strong epidermal expression of nuclear IL-33 in the stratum spinosum of lesional skin (Figure 4.4). Compared to other body barriers such as bronchial epithelium in which local tissue stromal stem cells express IL-33, basal keratinocytes (local epidermal stem cells) did not stain for IL-33 (240). Evaluating the number of IL-33 positive cells, lesional skin appeared to express higher levels of cytokine than perilesional skin. Further epidermal expression compared to endothelial staining appeared stronger in psoriasis skin than healthy skin (Figure 4.3 compared to Figure 4.4). This subjective evaluation has been confirmed with mRNA data by Theoharides et al (194). Together these data suggest that IL-33 is upregulated in at least lesional psoriasis and when considered in conjunction with data from Theoharides et al even in perilesional skin compared to healthy skin. (We did not reproduce those data for time and

resource constraints)

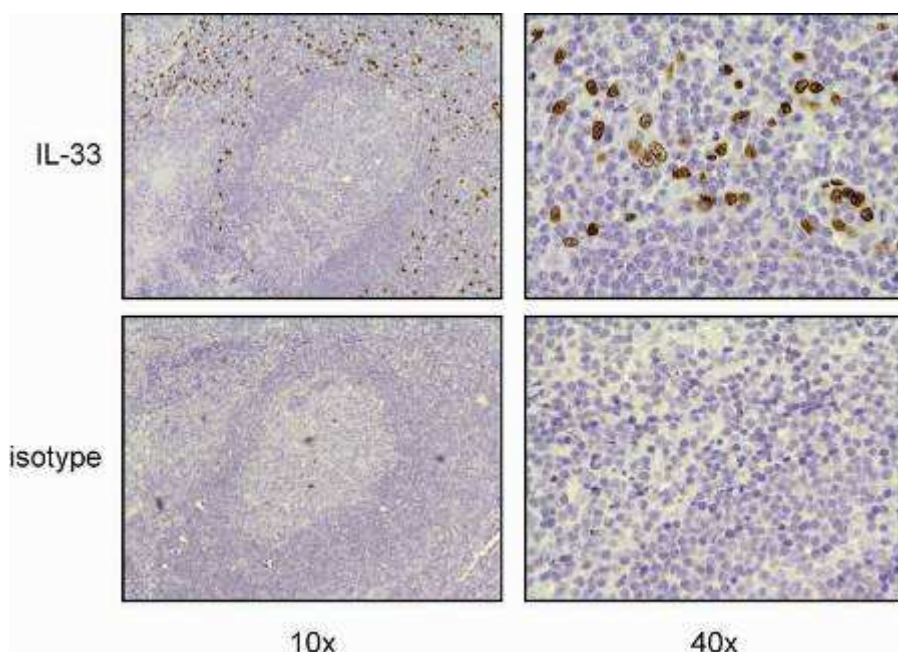


Figure 4.2 IL-33 in tonsil – work up of IHC staining
Paraffin sections of tonsils have been stained for IL-33 (brown dye) using Nesy-1 as primary antibody. Top row shows parafollicular nuclear staining pattern for IL-33. Bottom row shows the isotype staining. Left panel 10x magnification, right panel 40x. Representative pictures of at least n=3. Counterstain with haematoxylin.

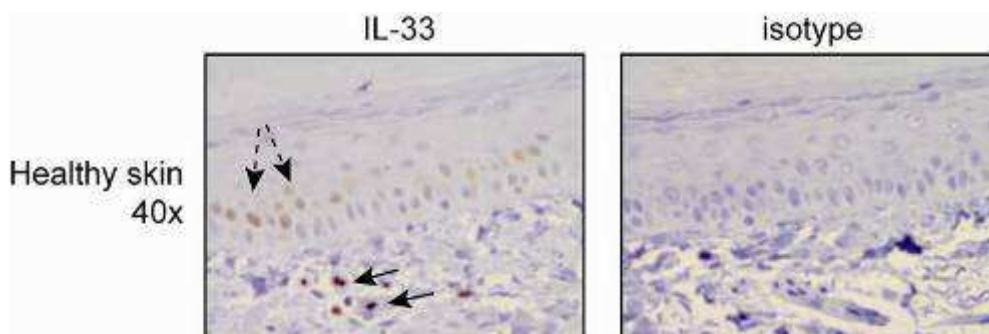


Figure 4.3 IL-33 expression in healthy skin
Immunostaining for IL-33 in healthy skin (n=2). Right image shows IL-33 (brown dye) with positivity in endothelial cells in the dermis (black arrows). Weak staining is demonstrated in the epidermis with IL-33 only expressed in the stratum spinosum (dashed arrows). 40x magnification, counterstain haematoxylin.

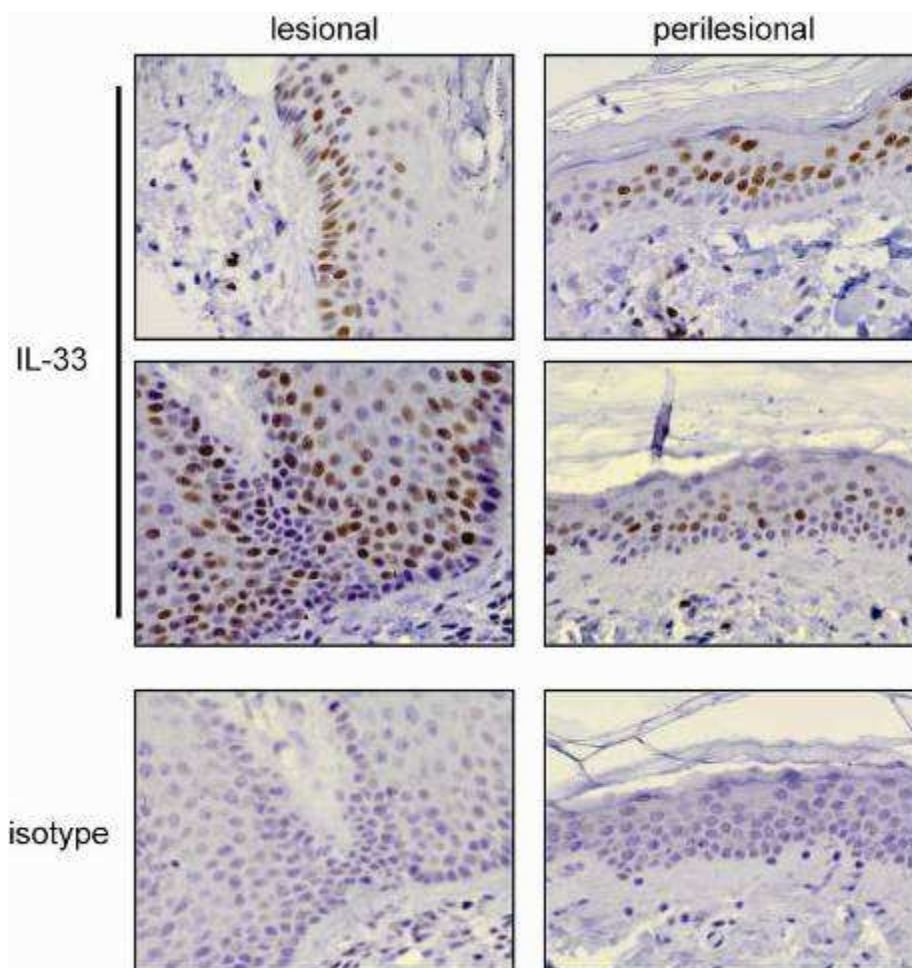


Figure 4.4 IL-33 in psoriasis

Psoriasis skin expresses IL-33 in the stratum spinosum. Lesional and perilesional skin was stained by IHC with anti IL-33 (Nessy-1) (brown dye). Left panel shows lesional plaque psoriasis sections with two donors (top and middle) and isotype control (bottom). Right panel shows perilesional skin sections (biopsy tissue 1 cm distance to a psoriatic plaque) of the same patients. Nuclear staining is detected in all samples in the dermis (endothelial staining) and epidermis restricted to the stratum spinosum. No staining is visible in the stratum basale (epidermal stem cells). Magnification 40x. Counterstain with haematoxylin. Representative histology of n=5.

In Figure 4.3 and Figure 4.4 basal stem cells are shown without expression of IL-33. To confirm this restriction, keratinocyte cell lines were examined for IL-33 expression. Two cell lines were tested: HaCaT, a human immortal non cancerous keratinocyte cell line and nHEK which are neonatal foreskin derived human epidermal keratinocytes which both reflect basal keratinocytes. Cells were cultured on chamber slides and stained for IL-33. Procedures were slightly altered compared to paraffin IHC as the fixation process was different for the cell lines. In concordance with my skin expression data, IL-33 did not stain in keratinocyte cell lines (Figure 4.5). However, in nHEK only a few positive cells were detected (less than 1%). Also stimulation with cytokines (IL-1 or TNF- α) or LPS did not upregulate IL-33 (data not shown, similar pictures like Figure 4.5). To account for the method alterations applied to cell lines, other experiments demonstrated IL-33 in cultured cells as positive control (see “Figure 4.10 IL-33 expression in synovial fibroblasts” and “Figure 4.28 Transfection of HaCaTs with K14 IL-33”). In conclusion these data confirm the lack of IL-33 expression in basal keratinocytes.

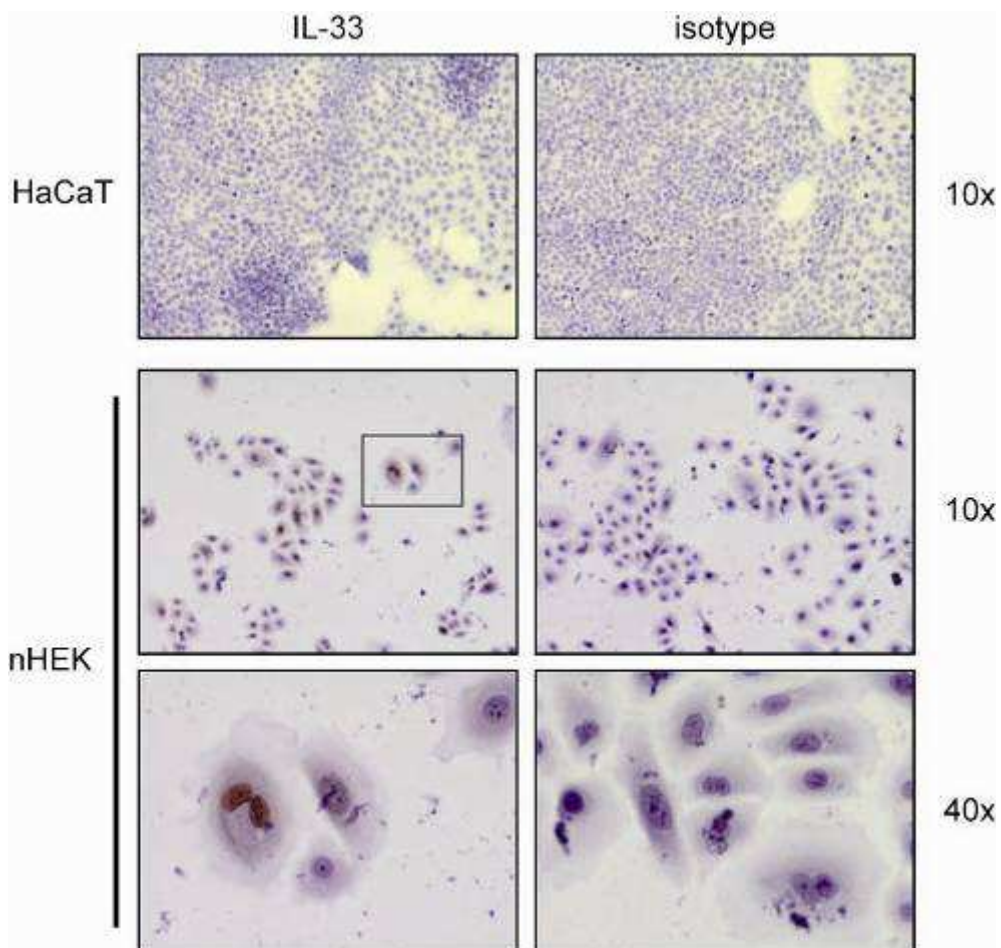


Figure 4.5 IL-33 is not expressed by basal keratinocyte stem cells
IL-33 immunostaining of HaCaTs and nHEK cells (n=2). Experiments to active/differentiate HaCaTs to express IL-33 lead to no result (see Figure 4.28 Transfection of HaCaTs with K14 IL-33).

Next, the expression of the IL-33 receptor ST2 was determined in skin. Healthy tissue from 2 donors was stained by IHC (Figure 4.6). Positive cells were detected in the dermis, most likely revealing expression in endothelial cells. Staining could also be observed in the basal keratinocyte cell layer. The cellular staining pattern was associated with membrane and cytosolic localisation, but unexpectedly, was also partly nuclear. Controls demonstrated no non-specific binding of the isotype antibody.

In contrast to healthy skin, psoriasis biopsies showed a different pattern of ST2 expression. Here, ST2 was widely expressed in the cellular dermal infiltrates, but also in vessels and basal keratinocytes (Figure 4.7). In comparison to the lesional skin, ST2 was expressed in perilesional skin at lower levels, limited to the vessels and keratinocytes and a few scattered mononuclear cells. Cellular expression ranged again from nuclear, cytosolic to membranous patterns. Thus, ST2 expression is higher expressed in lesional psoriasis skin compared to perilesional and healthy skin. This demonstrates a system in which endothelial cells can potentially react upon local release of IL-33. While ST2 in healthy skin could lead to an immune response (ie fulfilling alarmin type function), inflamed psoriasis lesions highly express ST2 and therefore could be more susceptible to local IL-33 production and lesion induction.

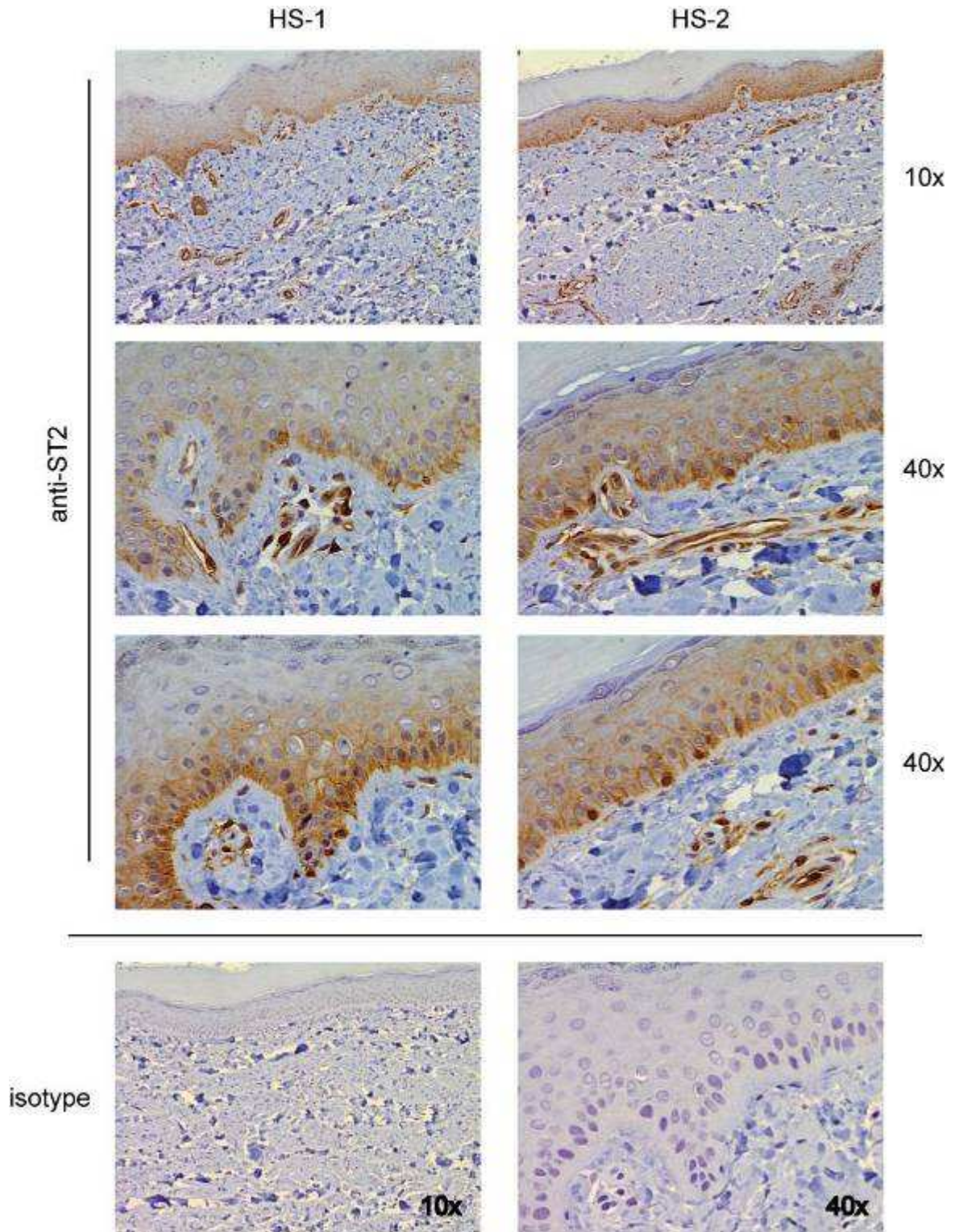


Figure 4.6 ST2 expression in healthy skin
 ST2 immunostaining in healthy skin (n=2). Staining is limited to endothelial cells and inflammatory cells guarding the epidermis. Staining of keratinocytes accumulates in the basal layer. Staining pattern ranges from membrane, cytosolic but also nuclear expression. HS-1 and HS-2: Healthy skin donor 1 and 2. Top row: 10x magnification, second and third row show different areas (40x magnification). Bottom row: Isotype control of HS-1 (10x left and 40x right).

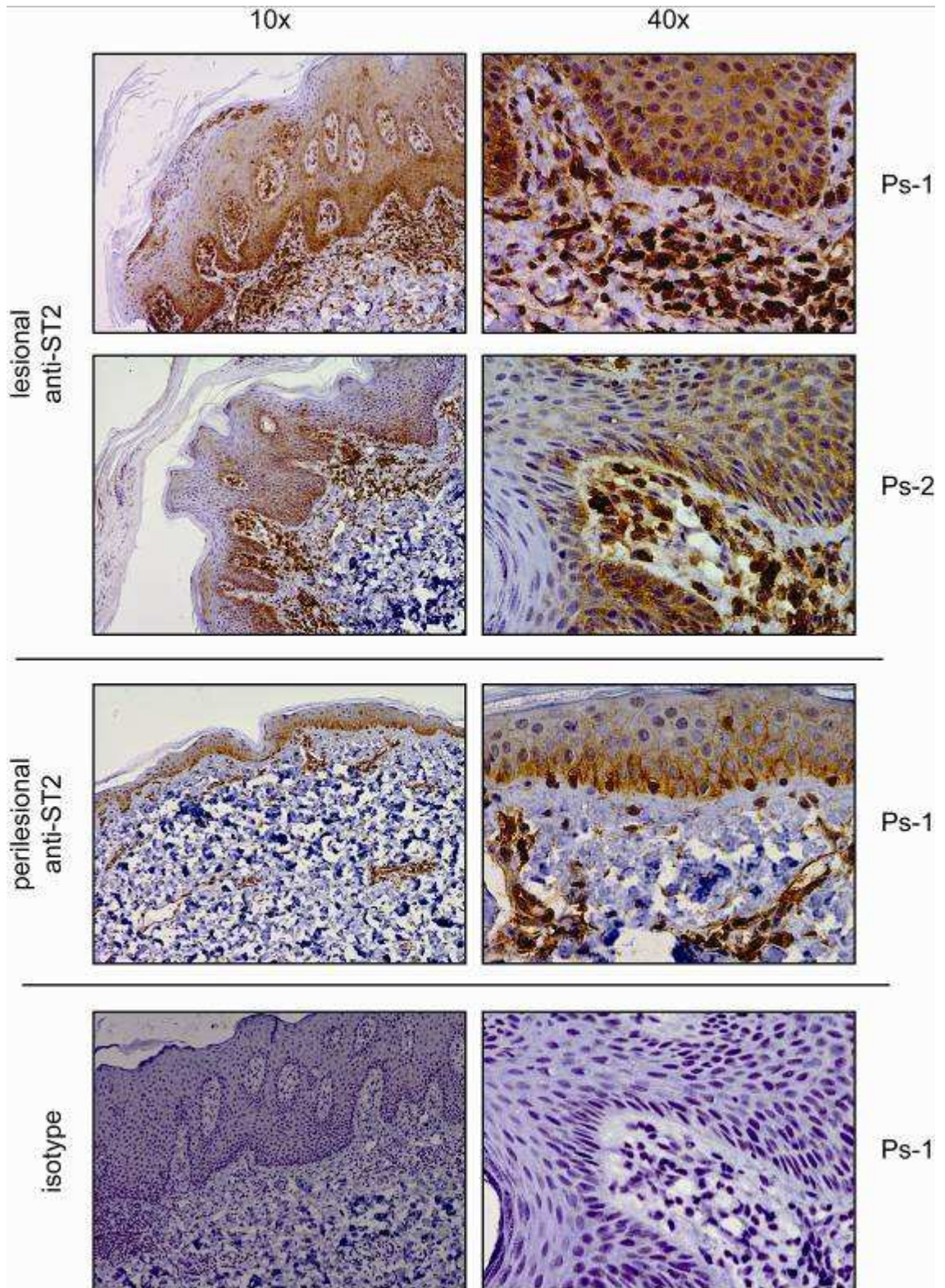


Figure 4.7 ST2 expression in psoriatic skin.

ST2 immunostaining in psoriasis (lesional and perilesional, n=5). ST2 is widely expressed in cellular infiltrates in the dermis but also in endothelial cells (1st and 2nd row). Staining of keratinocytes accumulates in the basal layer. 3rd row shows perilesional skin as comparison. Less ST2 is present due to lack of cellular infiltrates. Staining pattern ranges from membrane, cytosolic but also nuclear expression. Bottom row: isotype. Ps-1 and Ps-2: psoriasis patient donor 1 and 2. Left column 10x magnification, right column 40x.

Whereas in skin IL-33 and ST2 is present representing a potential alarmin - data about IL-33/ST2 expression in inflammatory arthritis have been thus far only sparsely reported. Girard and colleagues showed that IL-33 is expressed in endothelial cells in the RA synovium; another group however, demonstrate IL-33 in RA synovial cells, speculating expression in endothelial cells but also macrophages (136, 145). ST2 staining is reported *in vitro* derived synoviocytes, however, tissue staining had not been formally described as I set out in my thesis.

Therefore I sought to determine IL-33 and ST2 expression in inflammatory arthritis to possibly link the hypothesis of this chapter for psoriasis with inflamed joint pathogenesis. Staining was performed in 9 individual RA and 3 PsA synovial tissues. Surprisingly, expression was limited in all tissues to endothelial structures (Figure 4.8). Inflammation severity ranged between tissues, but even in highly inflamed sections no staining of inflammatory cells for IL-33 could be detected (e.g. # 1, 2, 6, 7, 8, Figure 4.8). Similar results were obtained in PsA synovia (data not shown). Further, to test whether ST2 is located with IL-33, staining for ST2 and IL-33 in the same area was examined. As with the psoriasis data, ST2 was widely expressed in cellular infiltrates of lymphocytic aggregates in the RA synovium (Figure 4.9, top left image). In contrast, IL-33 was only weakly expressed in endothelial structures surrounded by ST2 expressing cells.

Kuchler et al showed that over time, and dose dependently, TNF- α downregulated IL-33 in HUVECs (human umbilical vein-derived endothelial cells) (178). The conclusion that IL-33 is downregulated by local proinflammatory microenvironment as suggested by Kuchler et al can not be drawn due to the low numbers of samples evaluated in my study; this remains an area requiring future analysis.

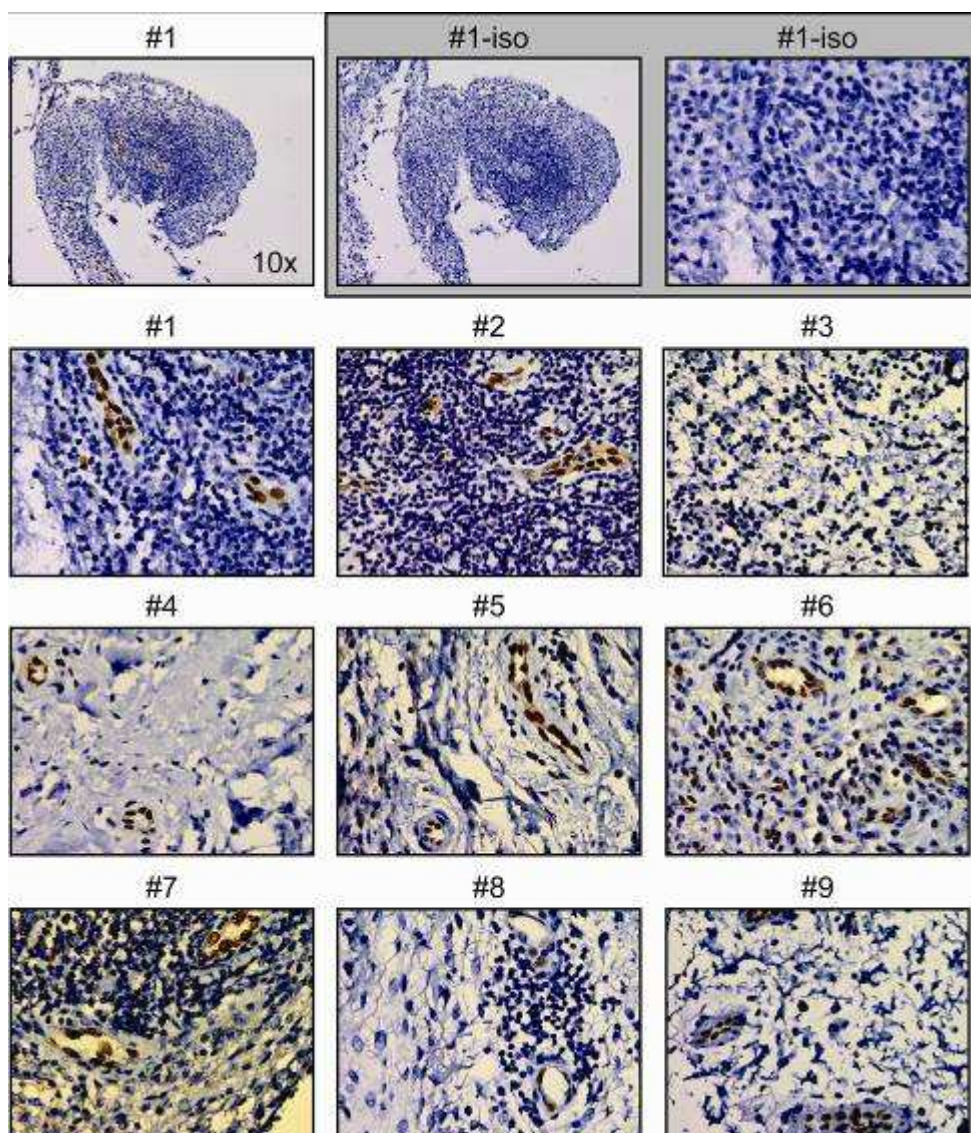


Figure 4.8 IL-33 expression in rheumatoid arthritis

IL-33 immunostaining of RA tissue derived from arthroplasty or arthroscopy (n=9). IL-33 is limited to endothelial cells (brown staining). No expression in fibroblasts or macrophages is detected. Top left and top middle image 10x magnification, all others 40x. grey box show isotype control for sample #1. #1-9 show different tissues of individual donors. Counterstain with haematoxylin.

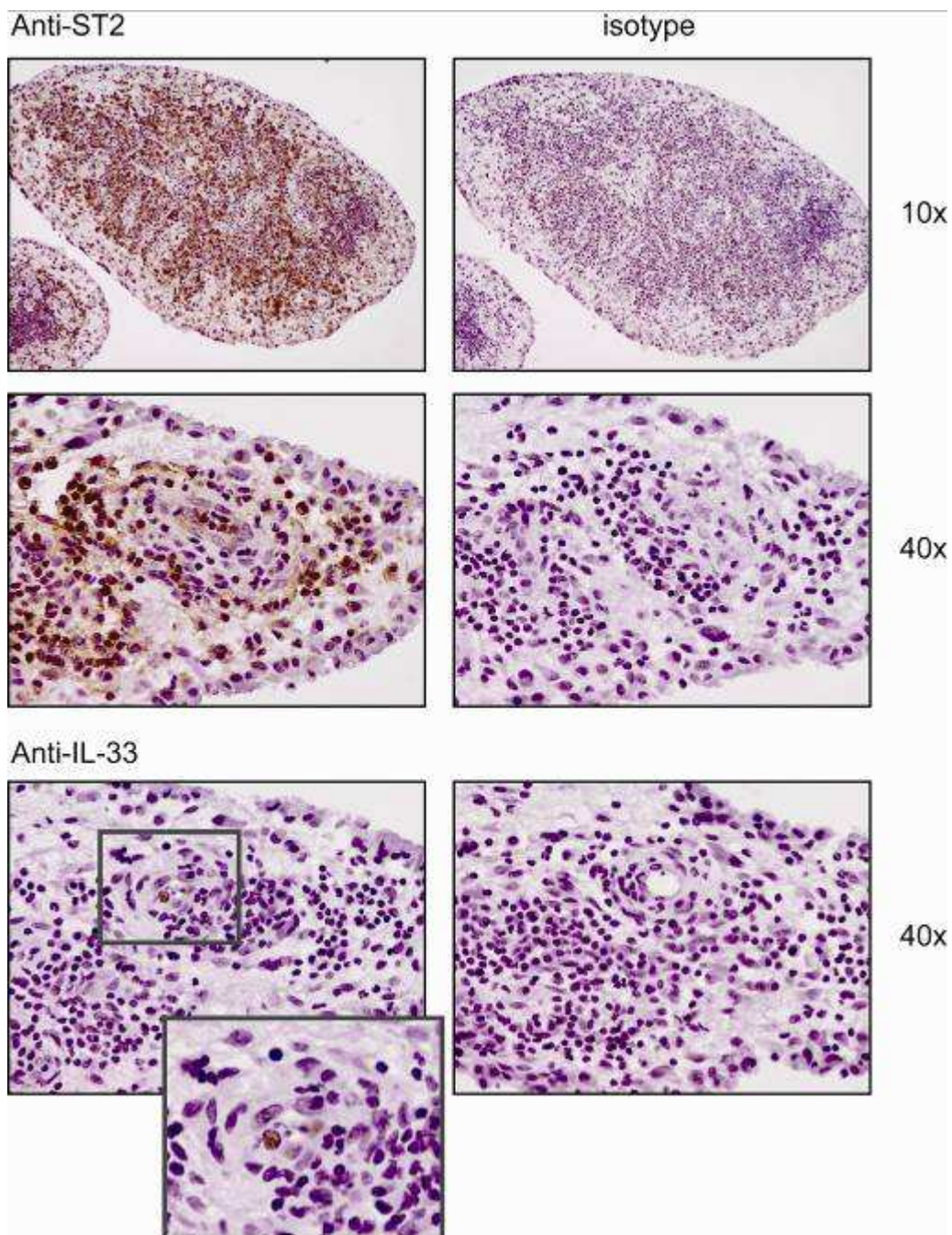


Figure 4.9 ST2 and IL-33 expression in rheumatoid arthritis
 Immunostaining for ST2 and IL-33 in one RA tissue (DAB, brown dye). ST2 is detected in multiple cells, mainly mononuclear inflammatory infiltrates. Also endothelial cells are positive. Top left (10x) and middle left (40x) image show ST2, bottom left (40x) demonstrates IL-33 staining which is further digitally magnified to show endothelial nuclear staining. Right column: isotype controls. Counterstain with haematoxylin.

IL-33 has been reported to be expressed in fibroblasts derived from synovial tissue. This supports IL-33 expression reported in other manuscripts, however, contradicts the *in situ* observations stated above (Figure 4.8 and Figure 4.9). Therefore synovial fibroblasts were examined for their expression of IL-33 by IHC. Fibroblasts were cultured until 80 % confluency and then split and plated on chamber slides, stimulated with or without TNF- α and IL-1. 18 hrs later cells were fixed and stained for IL-33 using the same protocol as for synovial staining. In confirmation with the literature, IL-33 was detected in a nuclear expression pattern in *in vitro* cultured fibroblasts and upregulated with stimulation (Figure 4.10). Interestingly, only the stimulus to re-plate fibroblasts lead to IL-33 expression in a few cells (media only control). This was not the case in longer cultured cells (personal communication, Mr J. Reilly, Mr N. Millar, University of Glasgow). At this time I am unable to reconcile the dataset herein reported and that observed elsewhere -clearly fibroblasts have the potential to express IL-33 - those from human tendinopathy and *ex vivo* lines as noted above are clearly positive. In future studies *in situ* hybridisation might usefully delineate the origin of IL-33 expression in synovial tissue *ex vivo*.

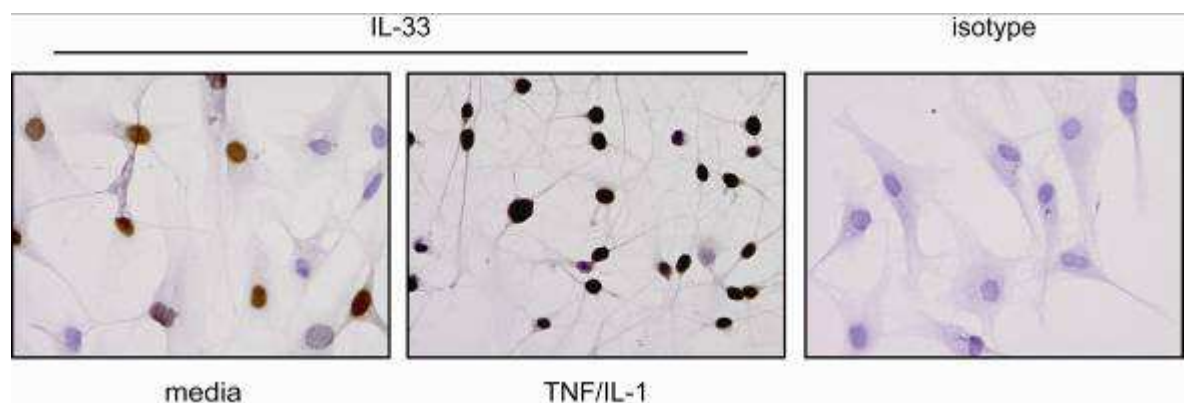


Figure 4.10 IL-33 expression in synovial fibroblasts
Cultured fibroblasts have been stimulated with TNF and IL-1 (middle image) (n=1). After fixation IL-33 has been determined by IHC (DAB, brown dye). In the media only control (left image) view cells express IL-33 which is limited to the nucleus. Stimulation upregulated nuclear IL-33 (middle image). Right image: isotype. Magnification 40x, counterstain with haematoxylin

In addition to tissue cytokine and receptor expression and given the peculiar nature of IL-1 superfamily receptor and soluble receptor components, I also wished to define the soluble receptor expression in the synovial and serum compartment. Soluble ST2 expression has been reported to be significantly higher in synovial fluid of RA patients compared to osteoarthritis fluid, but also in RA serum compared to healthy controls (180, 241). Mok et al demonstrated higher expression of sST2 in SLE patients (151). Here, I sought to determine the levels of sST2 in PsA serum and fluid compared to healthy controls or osteoarthritis as control, respectively. Similar to RA, sST2 was significantly elevated in PsA serum samples (n=36) compared to healthy controls (n=41) (unpaired t test, $p = 0.005$, Figure 4.11, left panel). These levels were lower than lowest levels reported with heart failure or acute myocardial infarction (188, 242). Focussing on synovial fluid samples, 16 PsA and 18 OA samples were analysed. Only in 5 PsA samples was sST2 detectable, all other samples levels were below the threshold of the assay (Figure 4.11, right panel). This could reflect true fluid concentrations or be due to the fact of sample storage, possible freeze thawing or age of the sample. It is also possible that consumption by tissue binding or neutralisation of the binding assay by free IL-33 could interfere with detection.

To conclude, IL-33 and ST2 is expressed in inflammatory disease tissue. The expression of IL-33 in vascular endothelial cells is undoubtedly. Evidence that IL-33 plays a role in autoimmune arthritis is strongly demonstrated by local expression of ST2 and also elevated sST2 in synovial fluid. Supporting other reports, I was able to detect IL-33 in synovial tissue, however, with only low expression in endothelial cells. This could be due to the stage of disease (in this case established arthritis) showing possible differences of IL-33 expression in early vs. established disease. These data deliver insights that IL-33/ST2 might play a role in joint inflammation or is involved in maintenance of the disease. Further work is required to address these points.

Expression in skin, especially in psoriasis is evident. Thus after showing how mast cells act on IL-33, next experiments sought out to address the influence IL-33/ST2 on skin inflammation.

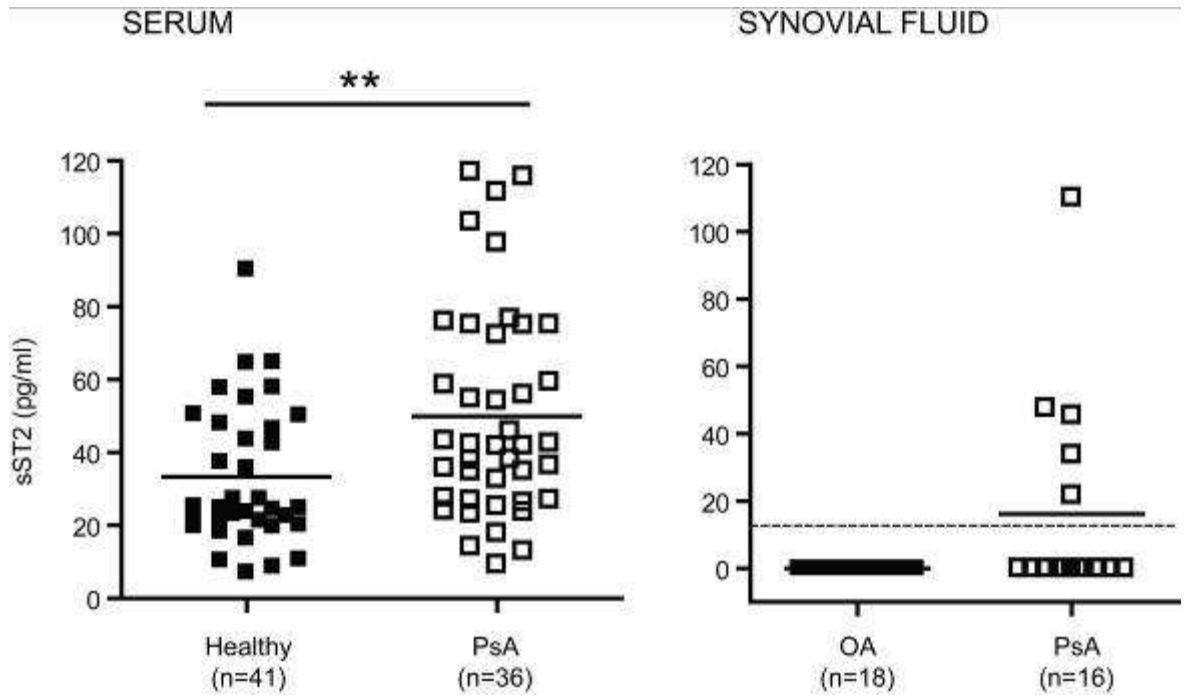


Figure 4.11 sST2 expression in PsA and healthy control serum and PsA and OA synovial fluid

Soluble ST2 serum levels show a significant increase in PsA patients compared to healthy controls measured by ELISA (left panel). Detection of sST2 levels in PsA SF compared to OA fluid. Only in 5 out of 16 PsA patients sST2 is detectable (right panel). The rest of samples are below detection threshold. Unpaired t test, $p=0.005$. Line indicates mean.

4.2.2 Interaction of IL-33 with mast cells

I next sought to define cellular subsets based upon the foregoing datasets and to move towards cellular testing systems to evaluate IL-33 effects in vitro. Mast cells and Th2 cells have been reported to express high levels of ST2 (132). Furthermore many reports have been published suggesting that mast cells respond by cytokine/chemokine production upon IL-33 stimulation. With IHC data suggesting that keratinocytes express ST2, I sought to test if the keratinocyte cell line HaCaT and the mast cell line HMC-1 (as positive control) express ST2 and can be stimulated with IL-33.

HaCaT and HMC-1 cells were stained with ST2-FITC antibody and analysed by FACS with dead cell exclusion (Viaprobe, 7-AAD). For HMC-1 cells a clear shift in expression of ST2 was detectable (Figure 4.12 A). However, very few HaCaTs expressed ST2 (less than 3%, Figure 4.12 B). In parallel, cells were tested for their capacity to respond to IL-33. HaCaTs did not respond to IL-33 (data not shown). HMC-1 demonstrated dose-dependent production of huCCL-3 (MIP1-alpha) confirming data from the literature (Figure 4.13).

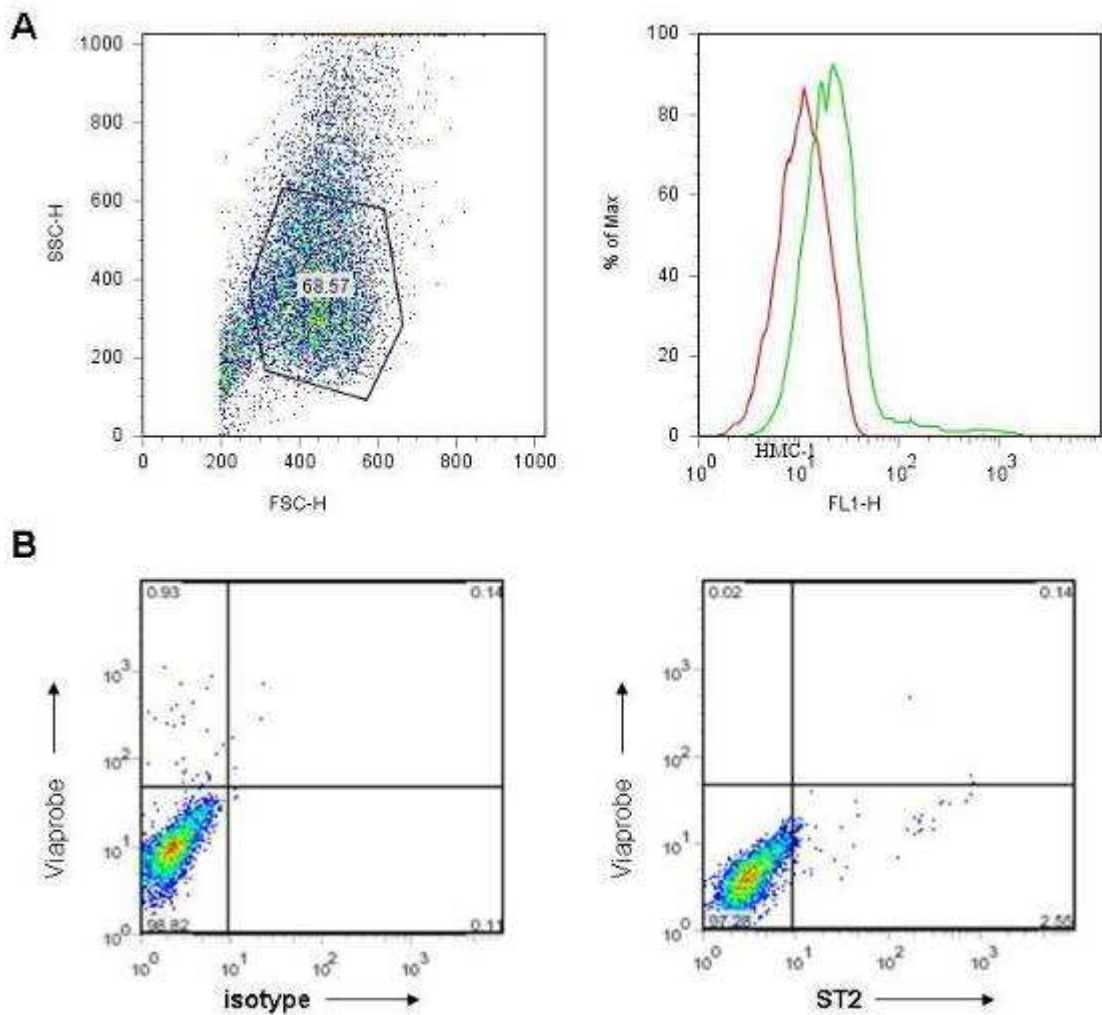


Figure 4.12 Expression of ST2 in HMC-1 and HaCaTs

FACS analysis of HMC-1 (A, n=1) and HaCaTs (B, n=2) show expression of ST2 in mast cells but only few HaCaTs express ST2. A: left dot blot shows forward side scatter plot of HMC-1, right histogram of HMC-1 expression (green line) and isotype control (red line). B: left dot blot, HaCaTs stained with isotype control and dead cell exclusion marker (viaprobe, 7-AAD). Right: ST2 in HaCaTs.

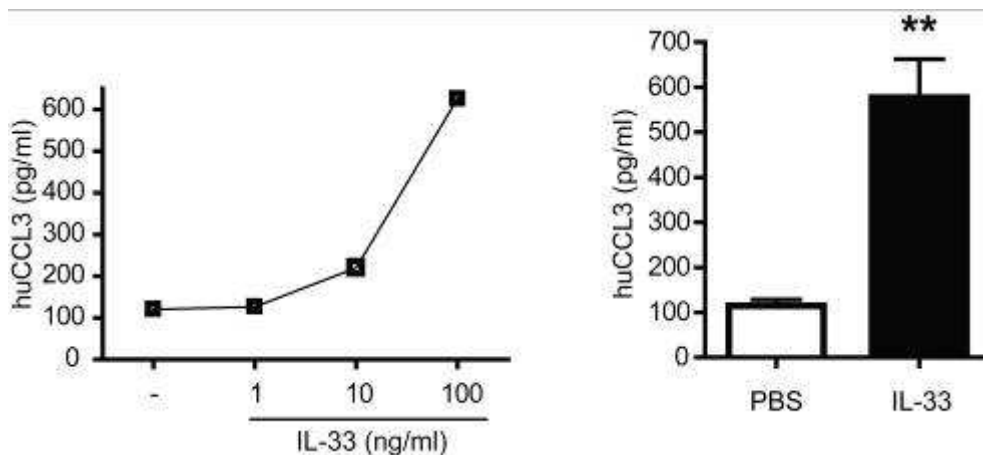


Figure 4.13 Stimulation of HMC-1 with IL-33

HMC-1 (1×10^6 /ml) stimulated with IL-33 for 24 hrs produce dose dependently huCCL-3 (left graph). Right graph shows stimulation with 100 ng/ml IL-33. Mean and SEM of 4 independent experiments done in at least triplicates. ** $p < 0.01$, paired t test. CCL3 = MIP1 α .

4.3 The role of IL-33 in skin inflammation mouse models

4.3.1 TPA induced skin inflammation

The preceding datasets clearly demonstrate IL-33 / ST2 expression in skin - however, little has been defined as to their functional significance. Phorbol esters administered on the skin can induce an inflammation process which shows in wild-type mice a transient inflammatory response (67). To test the influence of IL-33 in this model wild-type mice (BALB/c) compared to ST2 deficient mice were investigated. With the hypothesis that this inflammation process also leads to release of IL-33, subsequently inflammation processes should be reduced in the ST2 deficient mice. Jamieson et al analysed epidermal thickness as a hallmark of dermatitis/psoriasis as well as cellular infiltrates (67).

Tested in 2 independent experiments, backs of mice were shaved, rested for 1 day and then treated with TPA for 2 subsequent days. After 1 day rest, skin was harvested and processed. Epidermal thickness measured by histology showed significant differences whereby ST2 deficient mice exhibited nearly normal epidermis compared to inflamed thickened epidermis in wildtype mice ($p < 0.01$, Figure 4.14 A, C). Also cell layers were significant increased in wildtype littermates ($p < 0.001$, Figure 4.14 B, C). Furthermore, cellular infiltrates appeared to be reduced in the ST2 deficient mice; however, this was not objectively analysed. To determine if the keratinocyte proliferation was different in ST2 deficient compared to wildtype mice, IHC for ki67 (a proliferation marker) was performed. Significantly less ki67 was detected in ST2 deficient mice, demonstrating reduced levels of proliferation compared to wildtype mice ($p < 0.05$, Figure 4.15).

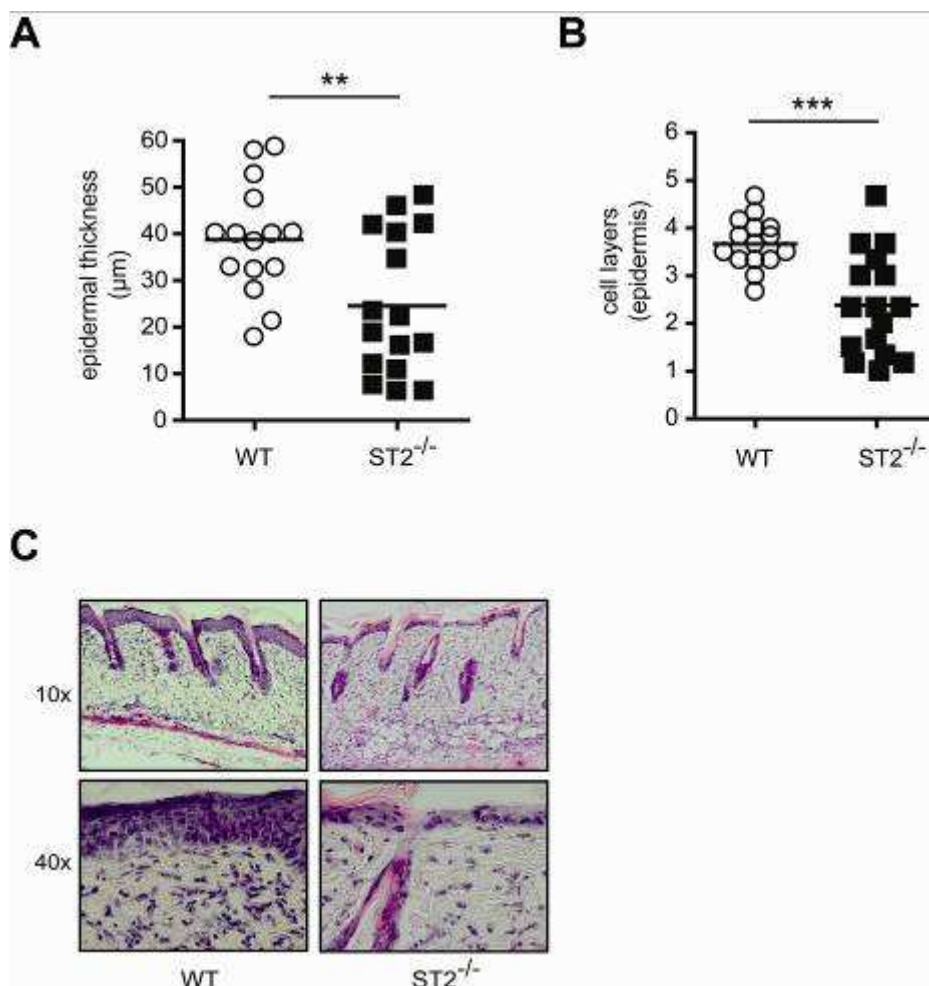


Figure 4.14 TPA induced skin inflammation – Role of IL-33/ST2
 TPA treatment of mouse skin for 2 days in WT (n=15) or ST2 deficient mice (ST2^{-/-}, n=16) of two pooled independent experiments. Histological analysis shows a significant decrease in ST2^{-/-} mice of epidermal thickness (A) and cell layers (B). C shows representative histology images, left column wildtype BALB/c mice, right ST2 deficient mice. Top row 10x magnification, bottom 40x. Staining with haematoxylin and eosin. Unpaired t test, ** p<0.01, *** p<0.001.

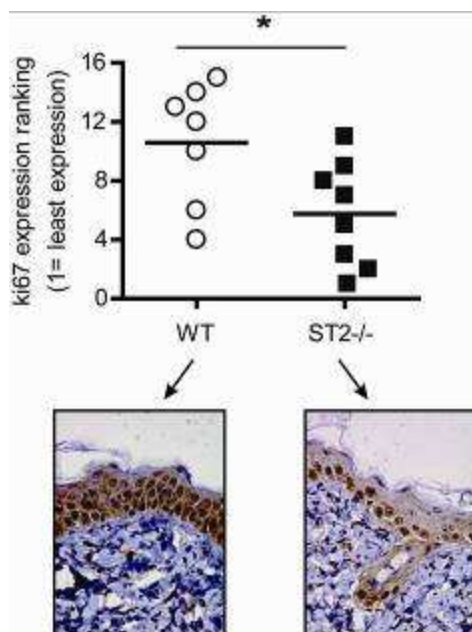


Figure 4.15 TPA induced skin inflammation – Ki67 proliferation analysis. Immunostaining for ki67 (DAB, brown dye) in TPA treated skin. Significant decrease of ki67 expression ranking in ST2 deficient mice (graph) (similar ranking method published in (130)). Bottom images show representative histology for BALB/c wildtype (n=7) and ST2^{-/-} mice (n=8). Mann Whitney test, * p<0.05.

To test if this effect was more marked in a longer time course, mice were treated with TPA 3 days instead of 2 with once again a day allowed for recovery before skin harvest. Surprisingly, in this 3 day TPA model, no differences in epidermal thickness and cell layers were observed (Figure 4.16). This suggests that the effects of IL-33 are manifest at an early time point - again consistent with alarmin type function.

In parallel, TPA painting in wildtype (C57Bl/6) and mast cell deficient mice ($\text{kit}^{\text{ws-h/ws-h}}$) showed no difference in epidermal thickness (Figure 4.17 A). Mice were used at age of 8 weeks; while a published manuscript stated that in $\text{kit}^{\text{ws-h/ws-h}}$ mice mast cells still reside in the skin up to 8 weeks, no mast cells were detectable in this experiment and hence likely reflect true mast cell deficient mice (Figure 4.17 B).

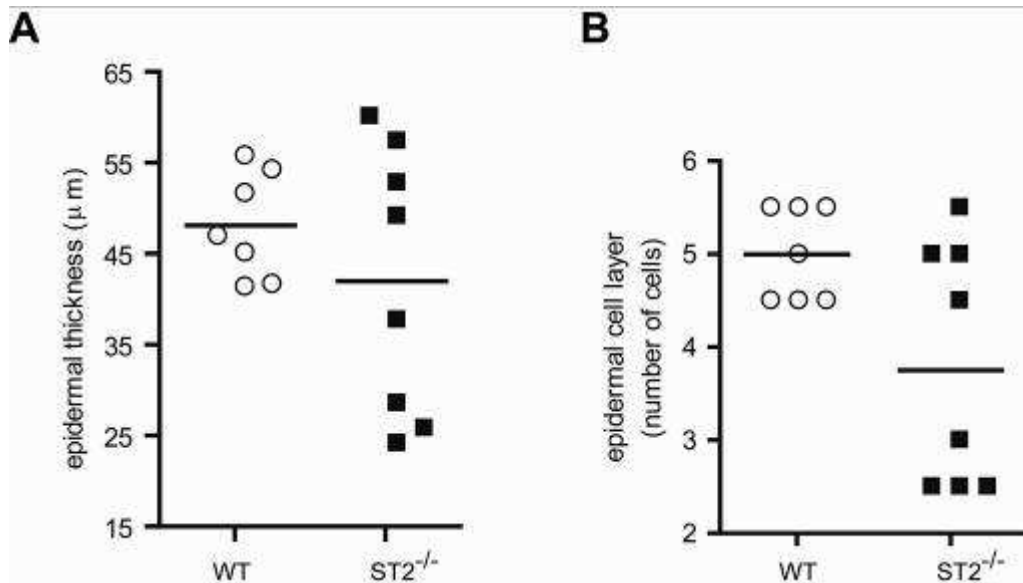


Figure 4.16 TPA induced skin inflammation ST2 dependency resolved after 3 days. TPA treatment of mouse skin for 3 days in WT (n=7) or ST2 deficient mice (ST2^{-/-}, n=8). Histological analysis show no difference in of epidermal thickness (A) or cell layers (B).

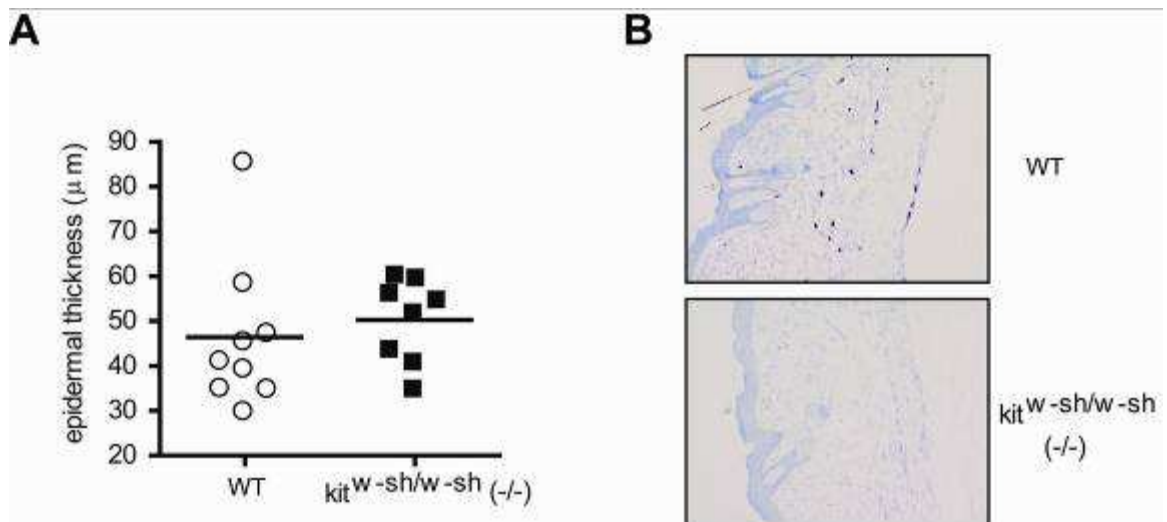


Figure 4.17 TPA induced skin inflammation in mast cell deficient mice – no difference after 3 days.

TPA treatment of mouse skin for 3 days in WT (n=9) or mast cell deficient mice (kit^{ws-h/ws-h}, n=8). Histological analysis shows no difference in epidermal thickness (A). B shows toluidine blue staining for mast cells of mouse skin (purple staining). Representative image wildtype C57/Bl6 (top) and kit^{ws-h/ws-h} (bottom) mouse skin. 10x magnification.

4.3.2 IL-33 intradermal ear injections – a model of skin inflammation

The above data demonstrate that ST2 deficiency protects skin in early phases of inflammation induced by phorbol esters. This is likely an indirect effect by preventing IL-33 signalling. As next step I sought to determine what effect IL-33 administration would have when exposed to local skin structures.

To test the bioactivity of IL-33, mouse splenocytes from ST2 deficient mice or BALB/c control mice were stimulated with IL-33 for 24 h and supernatants harvested for IL-5 analysis. Cells responded dose-dependently with IL-5 production (Figure 4.18). This effect was totally abolished in ST2 deficient splenocytes. These data confirm the bioactivity of the recombinant preparations of cytokine employed herein.

Thereafter, a psoriasis model was used in which recombinant cytokine was injected intradermally every alternate day into the ear pinna of a mouse. Similar to previously reported cytokine injections that included 500 ng of IL-22 or IL-23, injection of 500 ng IL-33 was used as described in the methods chapter. Time scale and injections of this model are shown in Figure 4.19 A. On day 16 of the model, mice were sacrificed, and ears, serum and spleen harvested. Spleen weight was determined as a surrogate for bioactivity. Interestingly, spleen size and weight increased in IL-33 injected mice compared to controls showing a possible leakage from the site of injection (Figure 4.19 B).

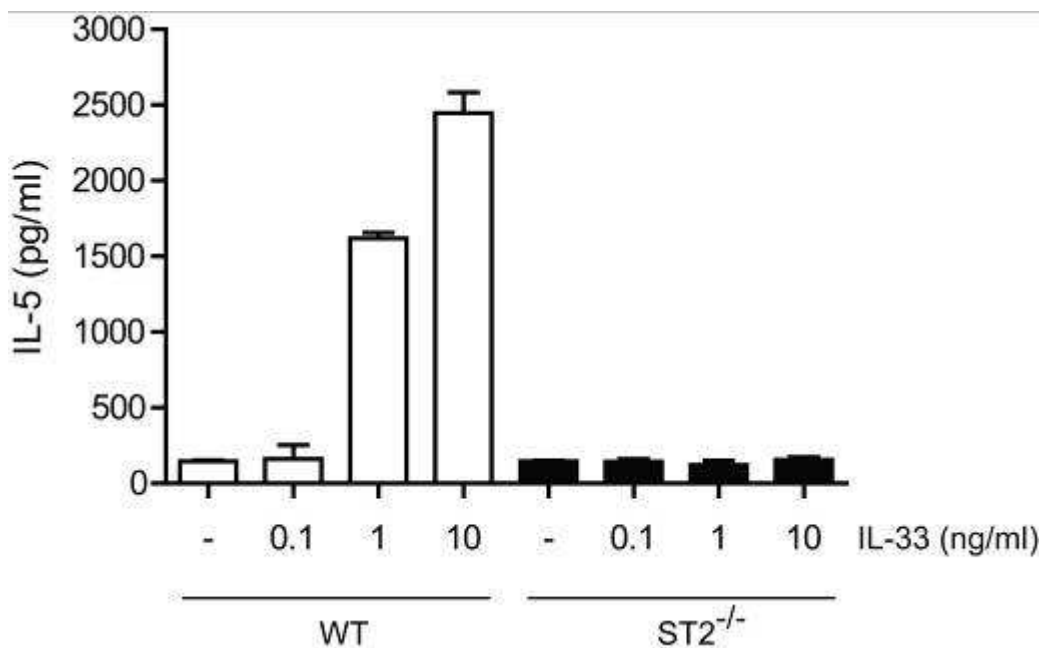


Figure 4.18 Validation of the biological function of recombinant IL-33
Splenocytes of BALB/c (WT) or ST2 deficient mice (ST2^{-/-}) were cultured 24 h with IL-33 at different doses (0, 0.1, 1 or 10 ng/ml). Supernatant was harvested and tested by ELISA for IL-5. Shown are means with SEM of triplicates (n=1).

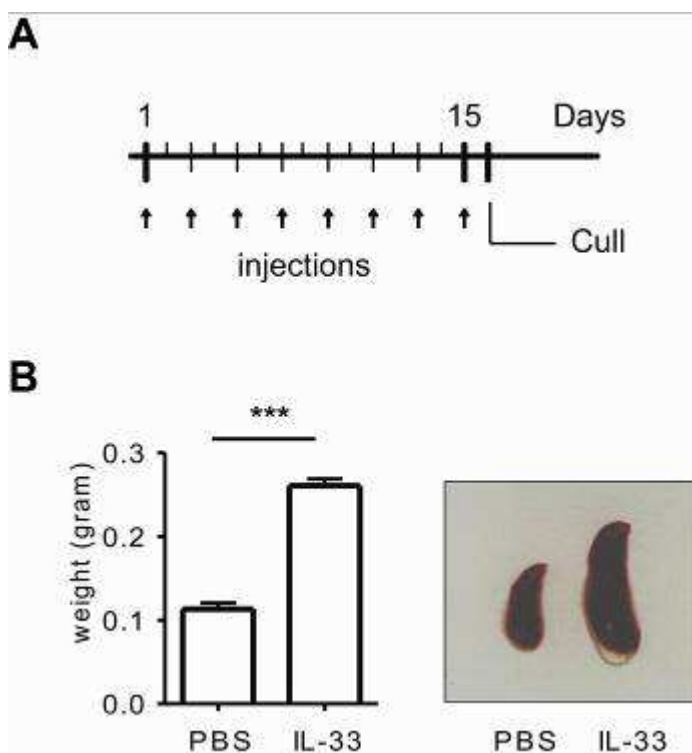


Figure 4.19 Model of injection and *in vivo* biological activity of IL-33
A. Ear injection model with injection of 20 μ l of PBS or IL-33 every alternate day (arrows). Harvest of ear, spleen and serum on day 16. B. Splenomegaly at day 16 after injection of IL-33 (right image, representative picture). Left graph mean weight of n=5/group. Results are reported as means \pm SEM, Unpaired t test, $p < 0.001$.

Mice were anaesthetised, ear thickness was measured with a calliper and then cytokine or PBS injected (20 µl volume). In the first week, no differences in ear swelling were observed. However, from day 11 onwards a differential phenotype between PBS and IL-33 injected mice was detected. On day 16 a significant difference in ear thickness was measured between groups (Figure 4.20 A). To test if IL-33 had an immediate effect on this tissue, mice were measured post injection on day 15. Measurements were performed 15, 30 and 60 min after injection; further 2 h and 24 h time points were added (Figure 4.20 B). To determine a difference, delta thickness compared to time point zero was used. Whereas the PBS group which showed initial swelling due to the injected volume, resolved swelling after ~ 60 min, the IL-33 group reached higher levels of ear thickness and sustained these over time. This significant difference of ear swelling demonstrated a higher response to the injection with IL-33 than with PBS.

To address possible methodological errors, ears were harvested on day 16, fixed and processed for histology. In haematoxylin and eosin (H&E) staining ear thickness but also epidermal thickness was determined. In agreement with the calliper measurements significant increase in ear and epidermal thickness was seen in the IL-33 administered group (Figure 4.21).

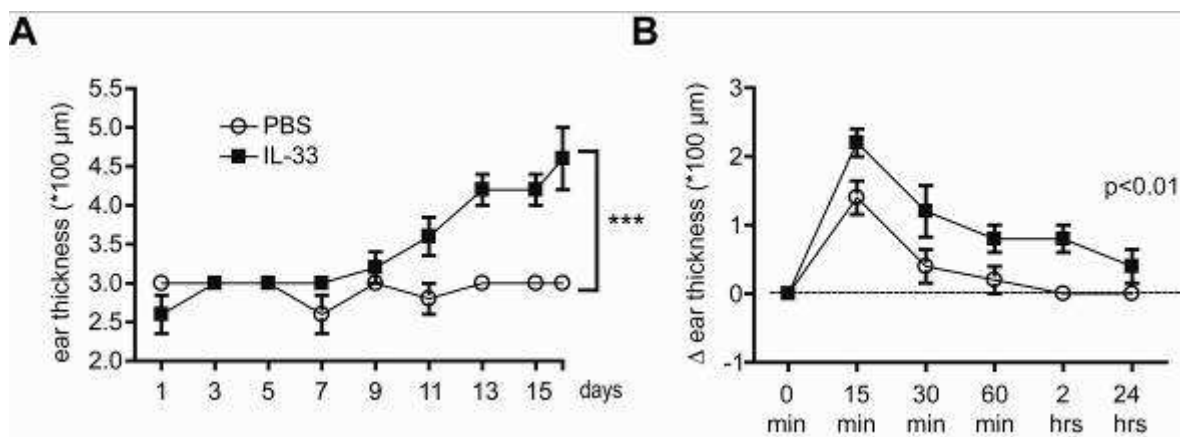


Figure 4.20 IL-33 induces ear swelling in an ear injection model

Ears from BALB/c mice ($n = 5$ for each group) were injected intradermally every other day with 500 ng IL-33 or PBS in a total volume of 20 μ l. Ear thickness was measured before each injection (A). Time course of swelling after injection was measured on day 15 showing relative thickness difference in both groups (B). Filled squares: IL-33, open circles: PBS. Results are reported as means \pm SEM and analysed by 2 way anova. *** $p < 0.0001$. Representative experiments of at least $n = 2$.

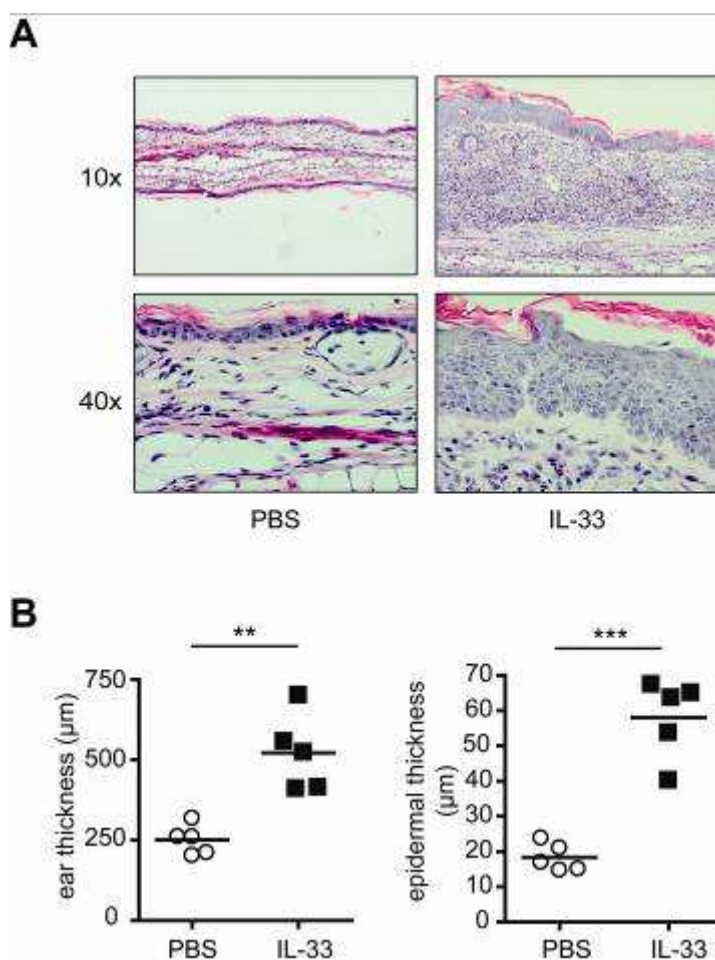


Figure 4.21 IL-33 injection- histological readout (H&E)

On day 16 ears were collected for H&E (A) and were analysed for ear and epidermal thickness (B). A shows representative images of PBS injected (left) and IL-33 injected ears (right). Magnification 10x (top) and 40x (bottom). B: Filled squares: IL-33, open circles: PBS. Results are reported as means \pm SEM and analysed by unpaired t test; *** $p < 0.0001$, ** $p < 0.01$. Representative experiments of at least $n = 2$.

To determine the cellular components subserving this increased tissue induration, H&E sections were analysed for cellularity staining, and further sections were stained with toluidine blue for mast cell determination. On day 16, a significantly higher number of mast cells were present in the IL-33 treated group compared to PBS (purple stain, Figure 4.22 A, B). Also significantly more eosinophils were visible in the IL-33 injected group (pink stain, Figure 4.22 C).

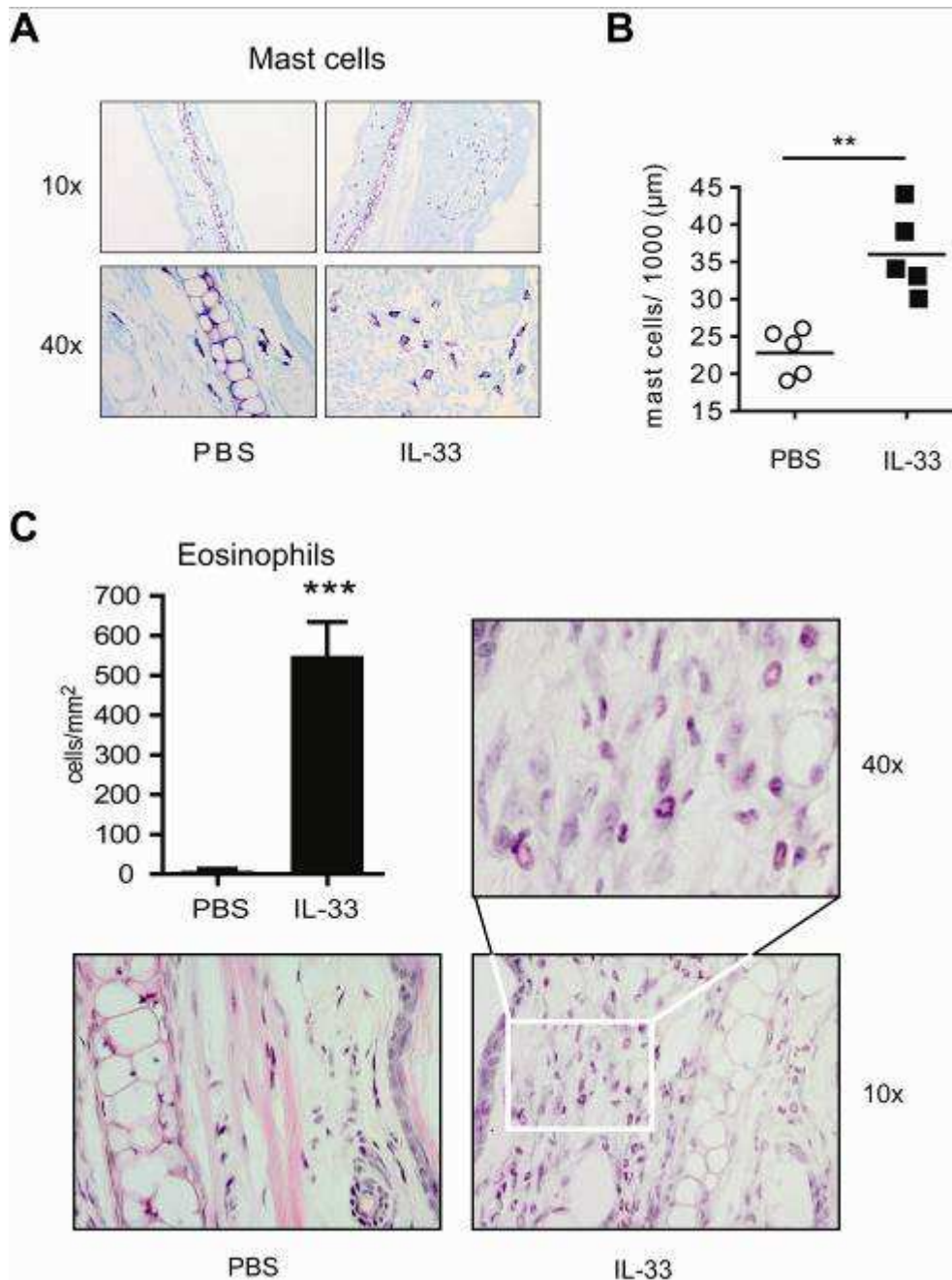


Figure 4.22 IL-33 ear injection –infiltration of mast cells and eosinophils
 On day 16 ears ($n=5/\text{group}$) were collected for toluidine blue and H&E staining (A, B) and were analysed for cellular expression. A: Mast cell staining (purple, toluidine blue) with representative image of PBS group (left) and IL-33 group (right). B: Quantification of mast cell numbers. Filled squares: IL-33, open circles: PBS. C: Eosinophil count with representative images (40x magnification): bottom right PBS, bottom left: IL-33 and top right digitally magnified to demonstrate eosinophil morphology. Results are reported as means \pm SEM and analysed by unpaired t test. *** $p<0.0001$, ** $p<0.01$. Representative experiments of $n = 2$.

Next, I investigated if the effect of IL-33 on ear inflammation, associated with thickening of the ear but also the epidermis as well as cellular infiltration, was specific or due to experimental errors such as LPS contamination or other influences. To address this question the IL-33 ear injection model was performed in wildtype (BALB/c) mice and ST2 deficient mice. This would render IL-33 signaling impossible with deficiency in its receptor. Injection into wildtype mice demonstrated again the potential for ear swelling over time compared to PBS controls (Figure 4.23 A). Injecting IL-33 in the same experiment into ST2 deficient mice led to no increase in ear thickness (Figure 4.23 B). Also histological ear analysis on day 16 demonstrated no increase in histological ear or epidermal thickness (Figure 4.23 C). Ear size rather reflects values measured with the PBS control mice (Figure 4.21 B).

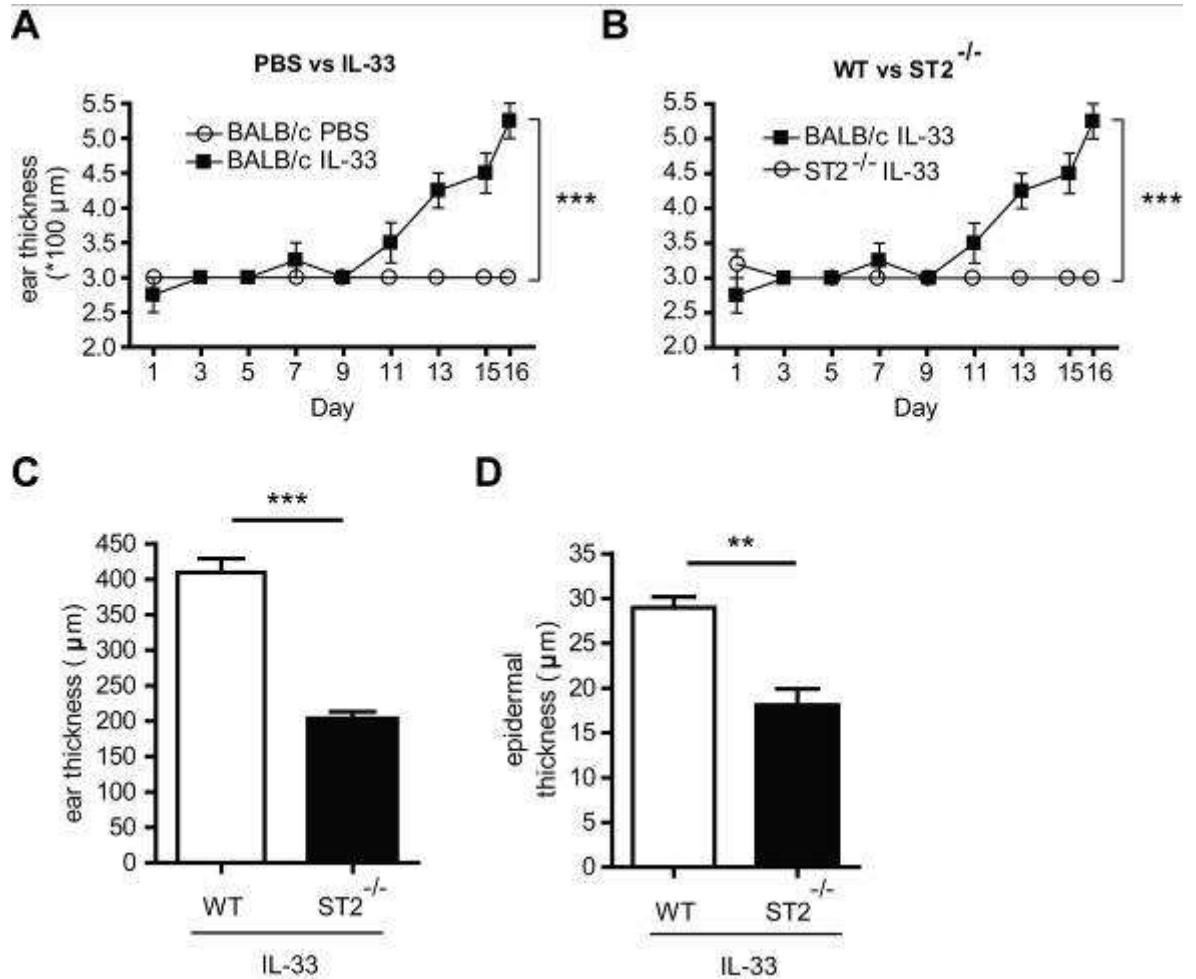


Figure 4.23 IL-33 ear inflammation is ST2 dependent
 ST2 deficient mice (ST2^{-/-}) are protected from increase in ear thickness when treated with intradermal IL-33 compared to control BALB/c mice (n=8 per group, one experiment)(B). A shows control experiment with PBS and IL-33 group (2 way Anova, *** p<0.005). Histology analysis confirms normal ear (C) and epidermal (D) thickness, unpaired t test, ** p<0.01, *** p<0.005). WT: wildtype control mice. Results are reported as means +/- SEM.

Whereas the above experiments provide proof-of-concept that IL-33 induces ST2 specific psoriasis-like dermatitis the next question I sought to address was if this effect was mast cell dependent. To test this I made use of mast cell deficient mice ($\text{kit}^{\text{ws-h}/\text{ws-h}}$ mice). Previously mast cell numbers have been examined and these experiments revealed that mice with age 8 weeks still have mast cells present in the skin despite organ deficiency (243). To ascertain that the mice were totally deficient for mast cells I used mice with age of ~ 6 months. Surprisingly, mast cell deficient mice have thinner ears than control littermates (C57BL/6 mice) (~200 μm compared to 300 μm). To account for this difference, both ears per mouse were measured and delta thickness (Δ thickness) left to right was determined.

Over the time course of IL-33 injection mast cell deficient mice reached a similar Δ thickness at day 16 compared to controls (Figure 4.24 A). However, there was significant difference over the whole experiment (2 way anova, $p < 0.05$) that was also elucidated with a reduced value of the area under the curve (AUC, Figure 4.24 B). When focussing on the first 9 days of this experiment an initial delay in response to IL-33 is evident (Figure 4.24 C, focused on the shaded part of the curve in Figure A). This could explain the significant difference; over time, however, mast cell deficient mice catch up most likely due to the influence of other ST2 expressing cells. This demonstrates a partial influence of mast cells for early responses in IL-33 exposition.

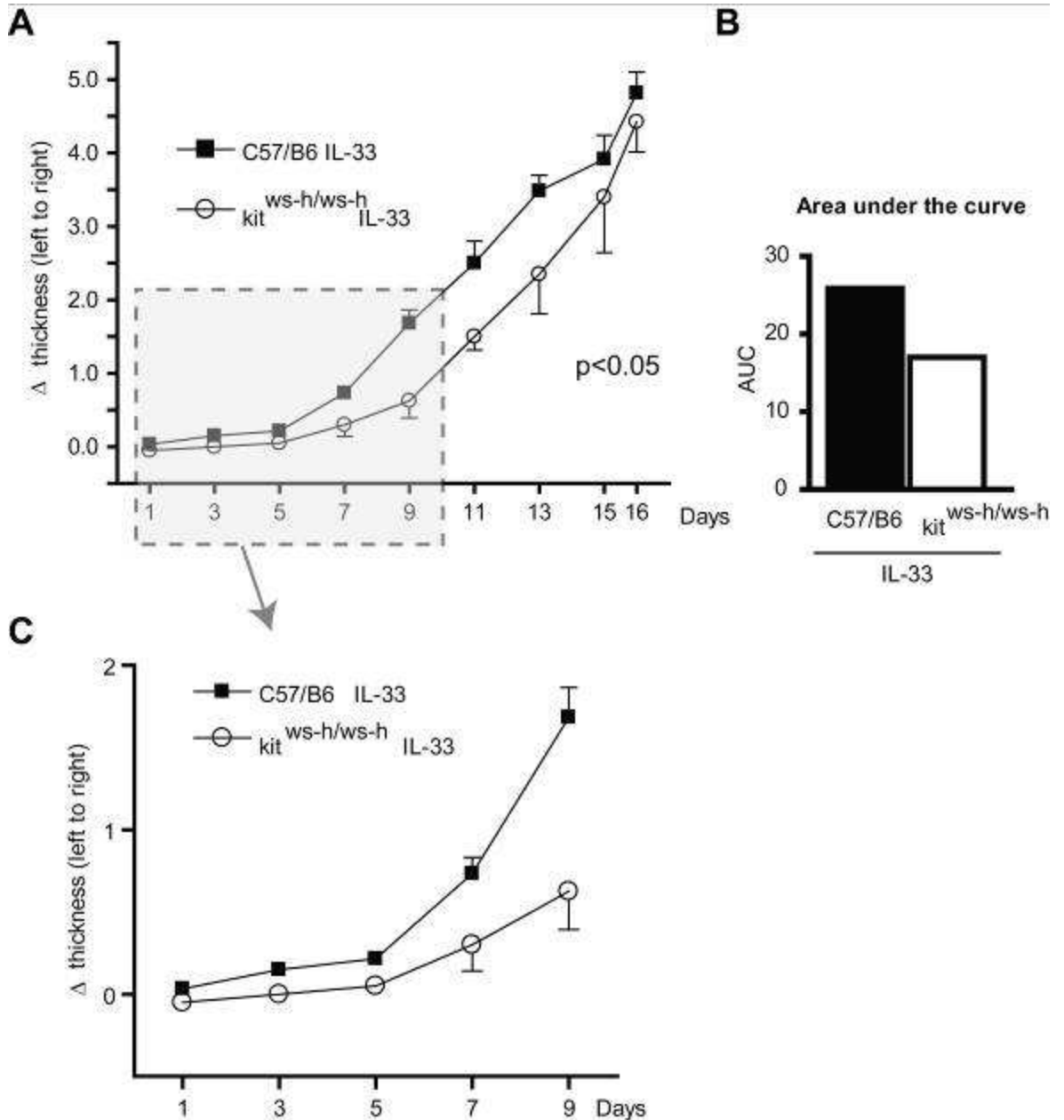


Figure 4.24 IL-33 initial effect in ear inflammation is partial dependent on mast cells
 IL-33 injection model in mast cell deficient mice ($Kit^{ws-h/ws-h}$, age of 6 months) demonstrate initial impaired response to IL-33 with reduce thickening of the ear (A, C). However, on day 16 there is no difference in thickness comparing WT to $Kit^{ws-h/ws-h}$ mice. B: area under the curve (AUC) of graph A. C: focused on gray shaded area in A to visualise early time point. Filled squares: IL-33, open circles: PBS. 2 way anova (A): $p < 0.05$. Results are reported as means \pm SEM. N=6 per group, one experiment.

Systemic responses were verified by increase in weight and size of spleens (Figure 4.18). To determine what cytokines change systemically in the serum of IL-33 treated mice, serum from the cull day (day 16) was harvested and analysed by luminex. This included the following: IL-1 β , IL-1ra, IL-2, IL-2R, IL-4, IL-5, IL-6, IL-7, IL-8, IL-10, IL-12 (p40), IL-13, IL-15, IL-17, TNF- α , IFN- α , IFN- γ , GM-CSF, MIP-1 α , MIP-1 β , IP-10, MIG, Eotaxin, RANTES, and MCP-1. Interestingly, significant differences were detected only in the signature cytokines IL-5 and IL-13 (Figure 4.25 A). Also a significant increase in KC and MCP-1 was identified. All other cytokines/chemokines were either not detectable or there were no differences in their expression patterns observed.

To determine if neutrophils are increased in IL-33 treated ears recruited by KC, IHC for myeloperoxidase (a marker for neutrophil granulocytes) was performed. MPO was only detected in IL-33 treated ears (Figure 4.25 B) thus showing an accumulation of neutrophils which could have been recruited by KC.

While end point studies revealed an increase in mast cells, eosinophils and neutrophils (Figure 4.22, Figure 4.25 B) the initial triggers of inflammation are unclear. To investigate what cells are recruited in the early phase of swelling the injection model was performed in 2 independent experiments (n = 2 per group) and at day 10 ears were harvested, cells isolated and analysed by FACS for lineage markers. At day 10, a significant change in ear thickness was already measurable (Figure 4.25 C). Harvested "ear" cells were stained for CD3, CD4, CD19, CD11b, CD11c, F4/80, Gr-1 to cover T and B cells, the myeloid lineage with monocytes, macrophages and DC and neutrophils. No difference was observed with the exception of the lineage of macrophages and neutrophils. Macrophages changed from a mean of 8.19% (PBS) to 14.33% (IL-33) (data not shown). More impressive however, was the influx of neutrophils with more than 8-fold increase from a mean of 0.73% (PBS) to 6.03% (IL-33) (Figure 4.25 D, E). This clearly demonstrates an early influx of neutrophils into the tissue mediated by IL-33.

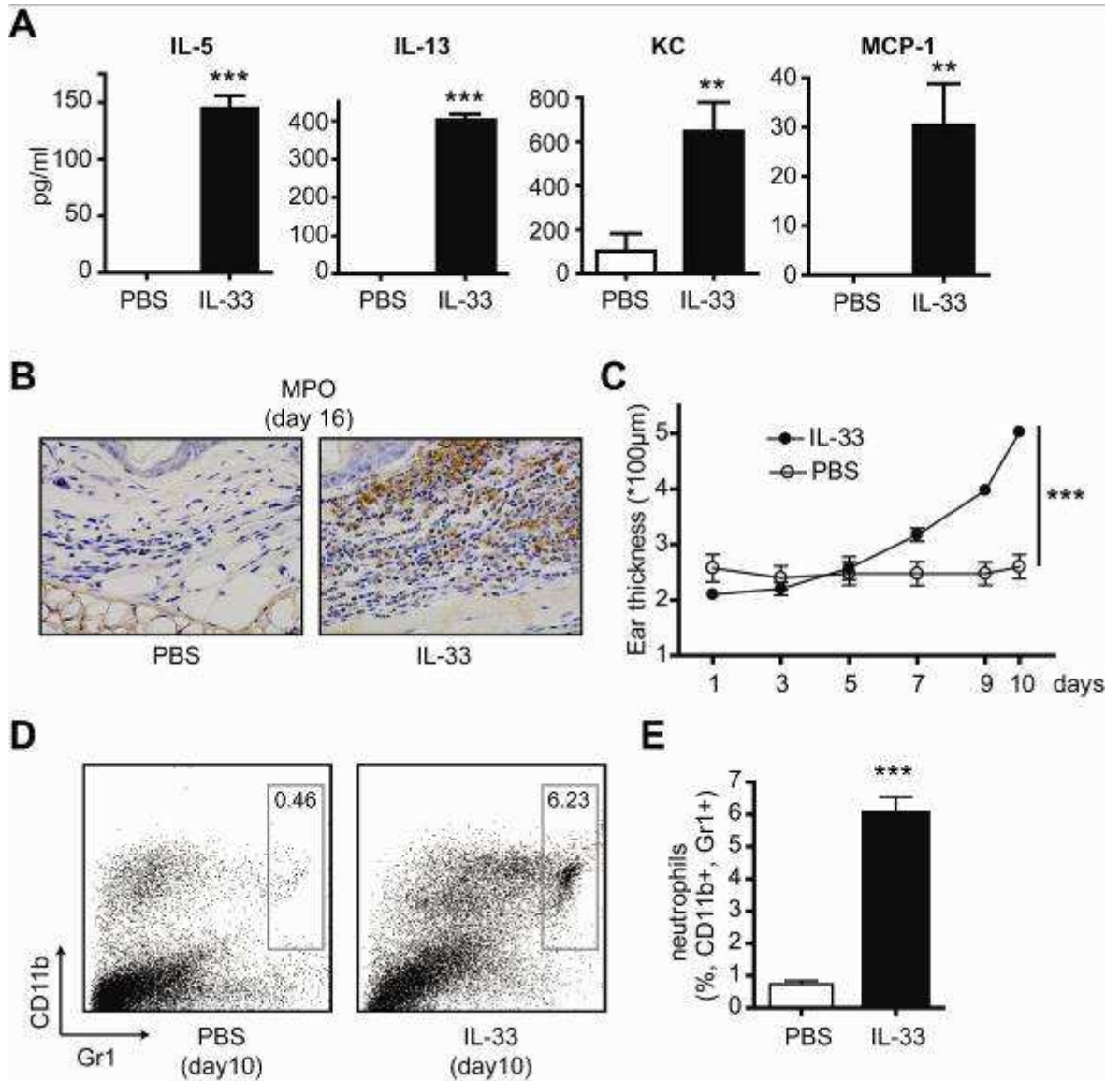


Figure 4.25 Cellular recruitment by IL-33

On day 16 of IL-33 or PBS injected mice (see Figure 4.20), serum was collected and cytokines and chemokines measured by luminex assay (all pg/ml) (A). Ears collected were immunostained for neutrophils using myeloperoxidase (B). Images shown are representative of $n = 5/\text{group}$ (one experiment). On day 10 (C), infiltrating cells were harvested and stained for lineage marker CD11b and Gr-1 (D). Shown is a representative dot blot. Neutrophils were analysed by CD11b Gr-1 positivity ($n = 4/\text{group}$ of 2 pooled independent experiments) (E). Unpaired t test, ** $p < 0.01$, *** $p < 0.0001$ (A,E), 2 way anova (C), *** $p < 0.001$. Results are reported as means \pm SEM.

4.4 Addendum - Miscellaneous biologic questions surrounding IL-33

The general biology of IL-33 remains quite intriguing. Driven by curiosity I also undertook a variety of distinct but related experimental protocols which will form the foundation for future programmes of work - they are described briefly below.

4.4.1 IL-33 in wound healing

With this robust ability to recruit inflammatory cells IL-33 fulfils its role as a danger signal or alarmin. In regard to the initial hypothesis, it was proposed that an insult (mainly mechanical damage) leads to release of IL-33. In an individual with psoriasis clinically this mechanical trauma can lead to a new lesion.

But what happens with a healthy individual? After a skin injury, wound healing starts immediately and is described in three phases that overlap in time: inflammation, tissue formation and tissue remodeling (244, 245). These phases proceed with a complicated but well organized and integrated interaction among various types of tissues and cells. During the inflammatory phase, platelet aggregation at the injury site is followed by infiltration of leukocytes, including neutrophils and macrophages, into the wound site. In the tissue formation phase, re-epithelialisation and newly formed granulation tissue begin to cover the wound area to repair tissue destruction. And further extracellular matrix reorganisation occurs with wound contraction and collagen remodelling.

To test the hypothesis that mechanical injury promotes release of IL-33 and this alarmin thereby recruit cells such as macrophages and neutrophils with the purpose of tissue repair the ST2 deficient mouse was used in a wound healing model. Five mm biopsies (2 per mouse) were induced on the shaved back of the anaesthetised mouse and photographs taken every day for analysis of the wound area (see methods chapter). Starting with n = 11 per group, every time point 3 mice were sacrificed for possible histological analysis. At day 7 the experiment was terminated. Comparing the area of decrease in wound surface no significant difference between wildtype BALB/c mice and ST2 deficient mice were observed (Figure 4.26). To conclude, IL-33 does not possess a pivotal role in tissue repair, however, local overexpression of IL-33 might unbalance the healing process by maintaining neutrophil recruitment.

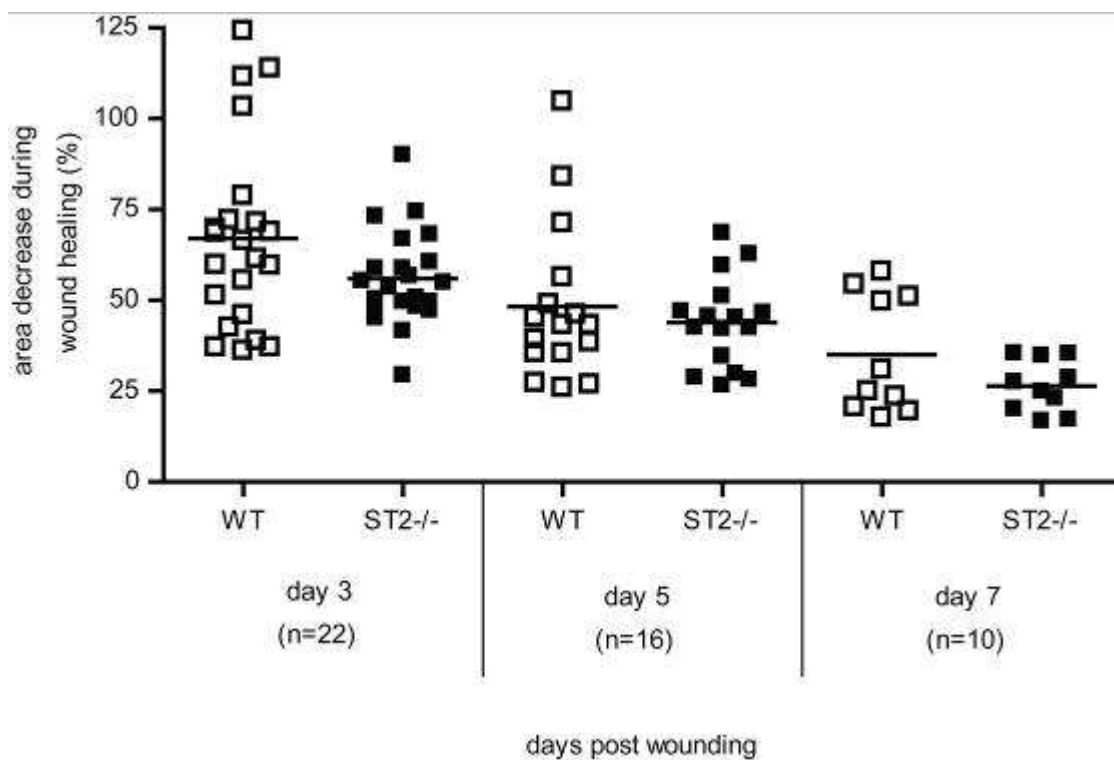


Figure 4.26 ST2 deficiency does not influence wound healing
Wound healing model with punch biopsies and measurement of healing in wildtype BALB/c (WT, open square) and ST2 deficient mice (ST2^{-/-}, black square). No significant difference between groups. Day 3 and day 5 3 mice per group were sacrificed, therefore numbers between days differ. n = number of biopsies (2 biopsies/mouse), one experiment.

4.4.2 IL-33 expressed under the K14 promotor

IL-1 family members have been shown to induce dermatitis when overexpressed in the skin under the influence of cytokeratin promoters. Recent studies from Blumberg et al demonstrated that IL-1F6 under a K14 promotor (K14) induces skin inflammation similar to psoriasis with acanthosis, hyperkeratosis, the presence of a mixed inflammatory cell infiltrate, and increased cytokine and chemokine expression (130). Here, I sought to test if IL-33 when overexpressed in the skin will lead to a skin phenotype. For this purpose a construct expressing IL-33 under K14 was designed and cloned.

Human IL-33 was amplified with BamHI sites and cloned into the K14 containing vector (DNA and vector provided by Dr Gilchrist, Glasgow University) (Figure 4.27 A, B). Figure 4.27 B shows the construct with K14, a β -globin as spacer, IL-33 and the K14 pA part. Also BamHI sites flanking IL-33 as well as KpnI restriction site is shown. After digesting the new plasmid clones #1-5 contain IL-33 (Figure 4.27 C). Due to both sides containing BamHI, the construct could be orientated in both directions. Digesting the plasmid with KpnI led to two different patterns (Figure 4.27 D, red box): a single band (#2) and two bands (#3). From this result no conclusion about the orientation of IL-33 could be drawn nor would further restriction digest answer this.

For this reason plasmid #2 and #3 were maxipreped and sent for sequencing. To test which of the plasmids translate for IL-33, HaCaT cells which express K14 were transfected using Lipofectamine (225). Cells were transfected with the constructs and 24 h later stained for IL-33 by IHC. To control for baseline levels, stained HaCaTs did not express IL-33 nor did stimulation for differentiation with Vitamin D3 induce IL-33 (Figure 4.28 A). Mock transfection was negative, as was construct #2, however, construct #3 was expressed in HaCaTs with ~ 9% transfection efficiency (Figure 4.28 B-E).

With the sequence results confirming protein data, construct #3 was ready for pronuclear injection to generate a transgenic K14 IL-33 mouse; this will be outsourced in the future.

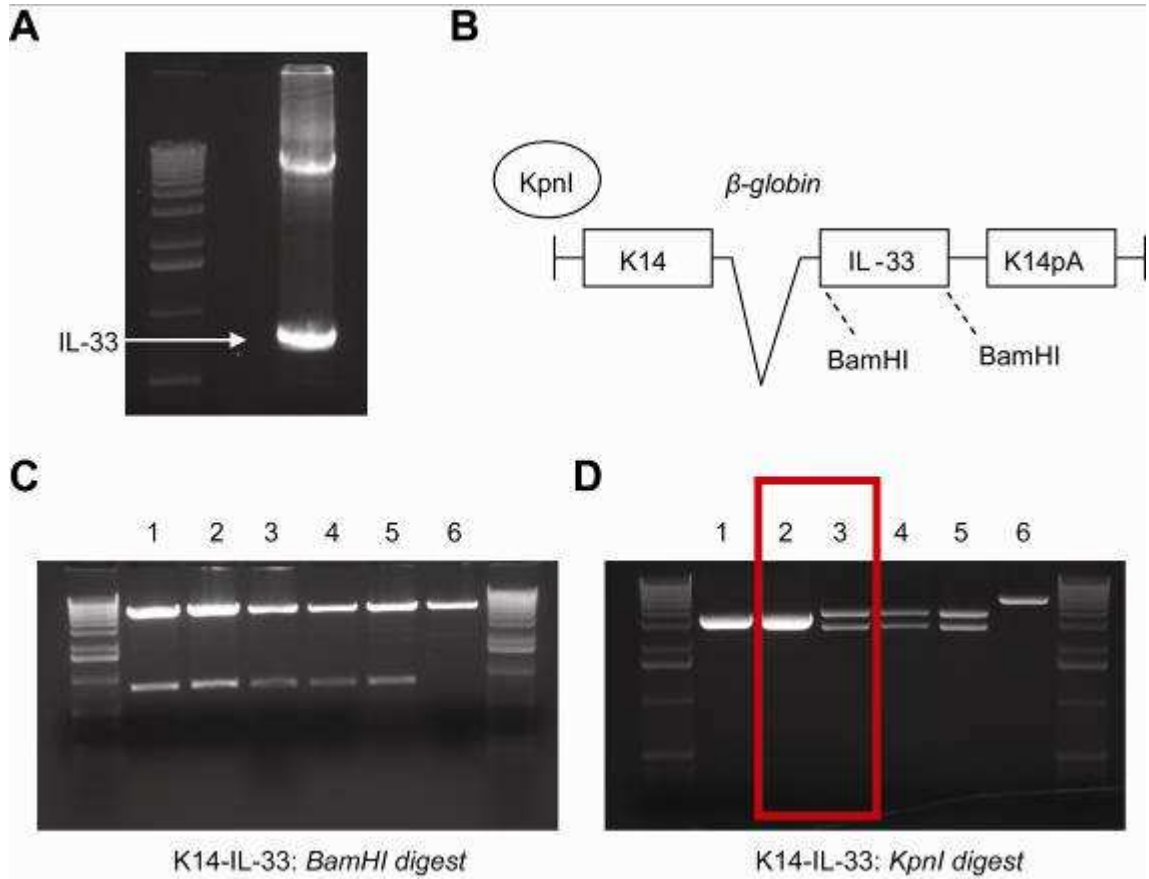


Figure 4.27 Construct and design of the K14 IL-33 plasmid.

A: Application of IL-33. **B:** Schematic of the construct with K14 promoter, β -globin and IL-33 insert, this is flanked by BamHI restriction sites, 3 prime K14 polyA tail. **C:** Restriction digest with BamHI which shows IL-33 insert in probe #1-5. **D:** Digest with KpnI; two different samples with different band pattern (#2 and 3, red box).

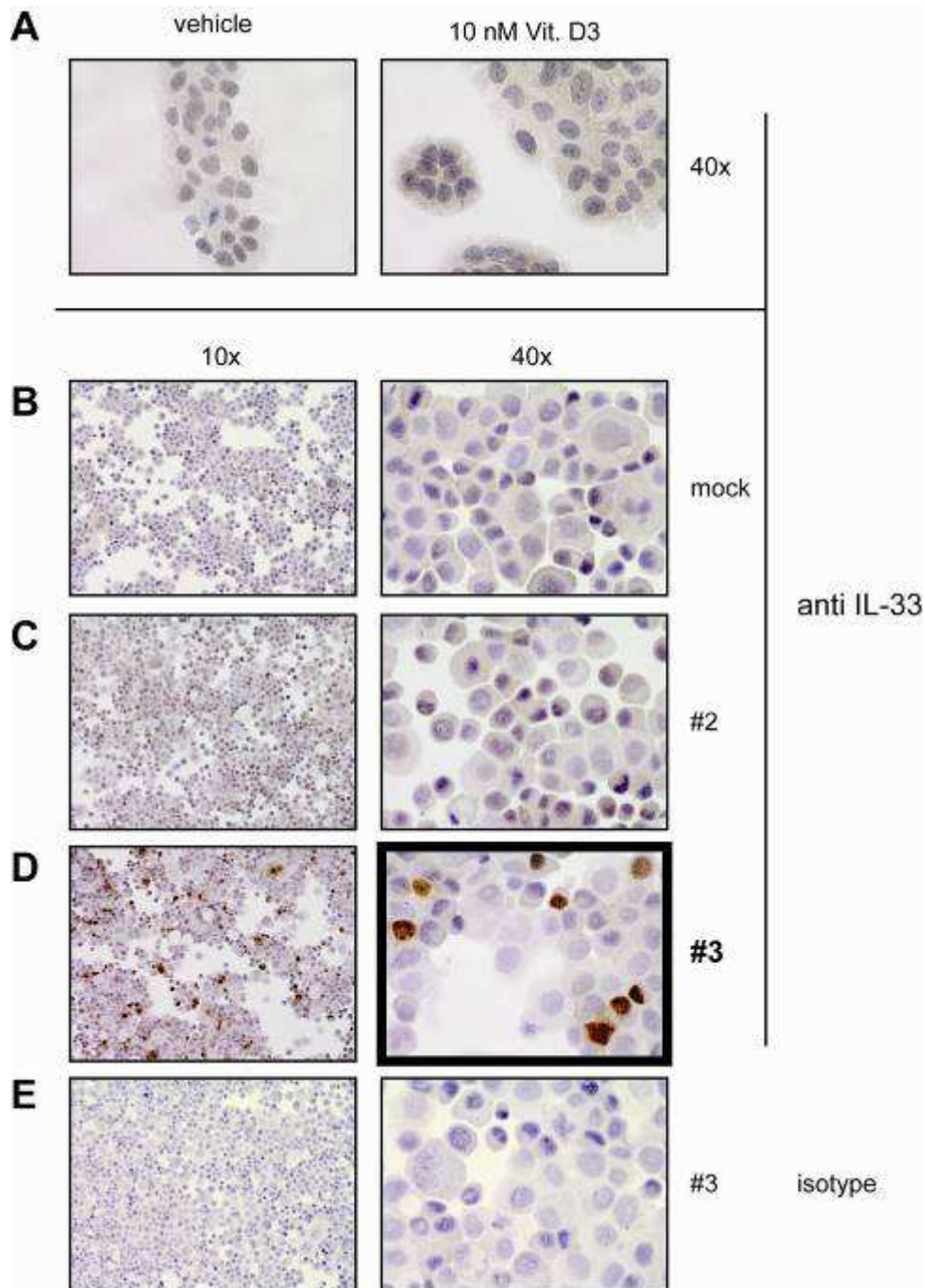


Figure 4.28 Transfection of HaCaTs with K14 IL-33

A. Control with HaCaTs treated with vehicle or Vitamin D3 to upregulate IL-33. No staining by IHC detected. 40x magnification.

B-E show transfection of HaCaTs with **B** mock, **C** #2, **D** and **E** #3. 24 h later cells were stained for IL-33 (**A-D**) or isotype (**E**). **D**: Nuclear staining in #3 (DAB, brown dye). Left column 10x, right column 40x.

Counterstain with haematoxylin. N=1.

4.4.3 Embryonic function of IL-33

As discussed in the introduction IL-33 is a cytokine with two possible functions. Nuclear localisation renders a function as a repressor of transcription with its homeodomain like helix turn helix structure. On the other hand, release of IL-33 can lead to dramatic inflammatory responses or regulation thereof. Being initially described as high endothelial nuclear factor, a marker for endothelial cells, the question arose as to how far back in development a function could be assigned for IL-33. To address this question, the Gene Expression Nervous System Atlas (GENSAT) database from the National Center for Biotechnology Information (NCBI) was search for IL-33 expression. Embryos age D10.5 were tested with an IL-33 P33-labelled RNA probe by in situ hybridisation. Staining accumulates at the dorsal aorta (GENSAT, Image 42416⁶) (Figure 4.30 C).

This result demonstrates early expression of IL-33 mRNA in embryonic dorsal aorta. To address if IL-33 is present as protein to confirm and support this result breeding pairs were set up and embryos harvested at day 9.5 and 10.5 (Figure 4.29). Embryos were fixed, processed, sections cut for histology and stained with H&E (Figure 4.29). Structures are visible with sagittal orientation and dorsal aorta. Next, embryonic sections from day 9.5 and 10.5 were examined for the protein expression of IL-33 using mouse anti human IL-33 which crossreacts with mouse IL-33. While the method worked and maternal vascular uterus tissue stained for nuclear IL-33, embryos at both age did not express IL-33 (Figure 4.30 A, B). Focussing on the dorsal aorta, at the same region GENSAT IL-33 hybridisation showed IL-33 expression, no staining by IHC could be detected (Figure 4.30 B, C). Thus embryo at day D9.5 and D10.5 do not express IL-33.

⁶ http://www.ncbi.nlm.nih.gov/sites/entrez?db=gensat&cmd=retrieve&list_uids=42416

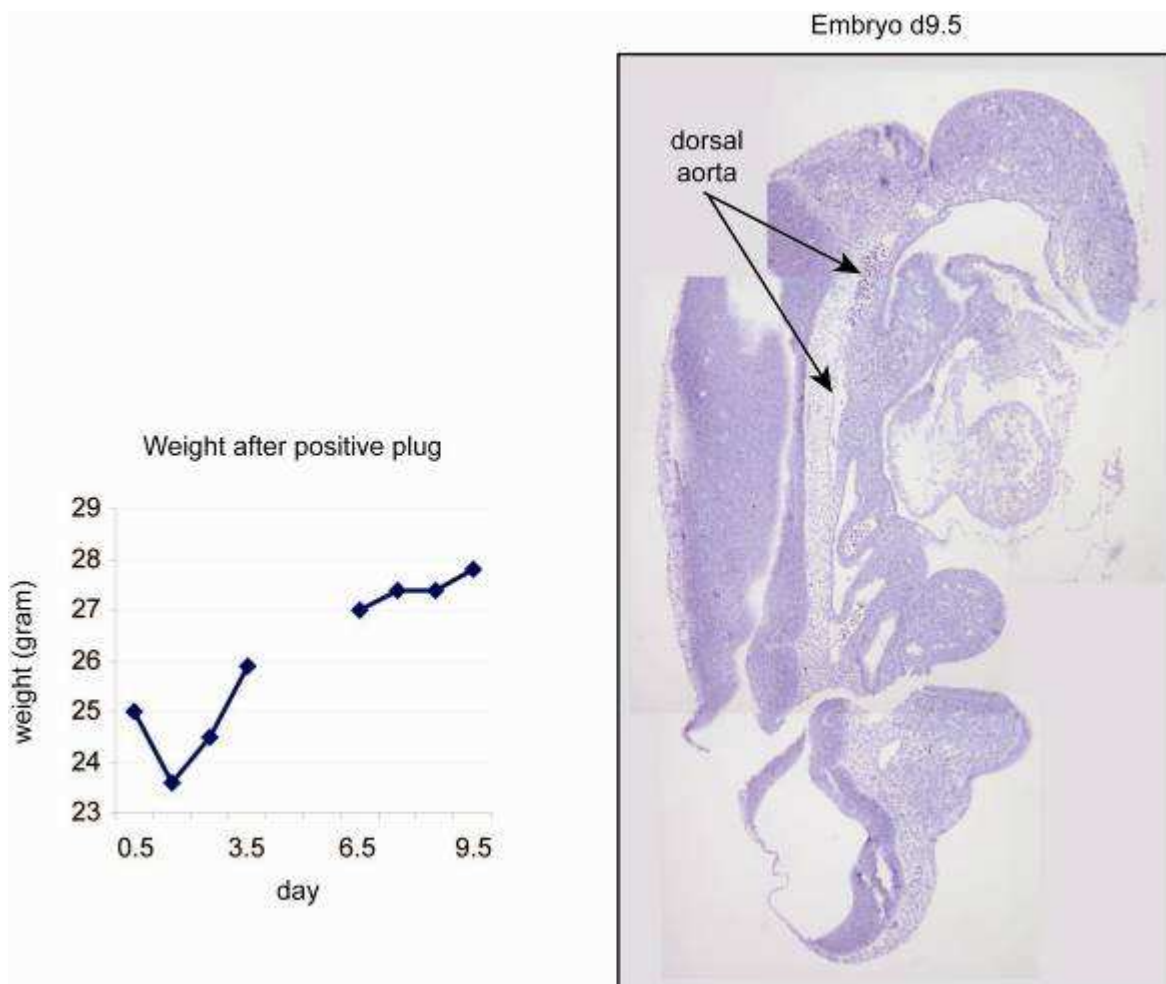


Figure 4.29 Embryo preparation day D9.5
Pregnant mouse with minimal weight increase (left graph) and harvest of embryos at day D9.5 and D10.5 (not shown). After fixation and processing, embryos orientated and sectioned to obtain a sagittal section containing the dorsal aorta for IHC (right image). Composition from multiple images from 5x magnification. Staining with H&E.

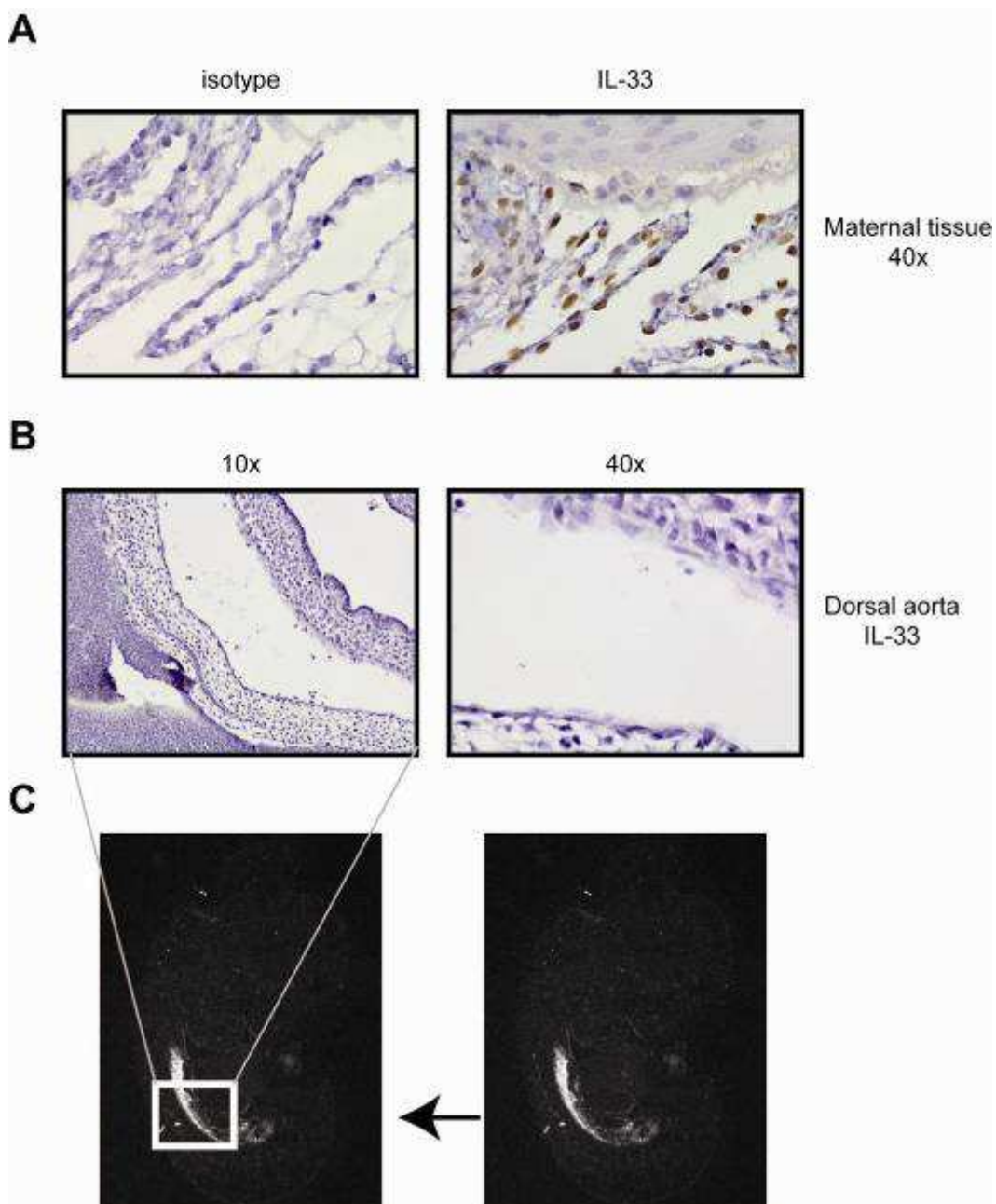


Figure 4.30 IL-33 is not expressed in the dorsal aorta day 9.5 or 10.5
 Immunostaining for IL-33 using mouse anti human IL-33 (Nessy-1) (n=1). A shows isotype control (left image) and maternal vascular uterus tissue which expresses nuclear IL-33 (right image, DAB, brown dye). B: dorsal aorta (10x, left image, 40x, right image) with no detection of IL-33. C: Pictures from GENSAT image 42416 to demonstrate area of interest.

4.5 Discussion

This chapter aimed to understand the role of IL-33 in psoriasis. Furthermore, more basic questions as to the biology of IL-33 were addressed as an adjunct component of my thesis work - this lead ultimately to embryogenesis based experimentation -in turn this sets the basis for extensive future exciting studies.

IL-33 in arthritis

Different reports have revealed the importance of IL-33 in inflammatory arthritis usually studying murine models of disease. Xu et al showed that IL-33 can exacerbate CIA and this was dependent on mast cells (146). Using an antibody induced arthritis model delivered further evidence that mast cells are crucial for IL-33 mediated inflammation in arthritis (197). On the other hand, CIA in ST2 deficient mice or treatment with ST2-Fc or anti-ST2 ameliorated severity (145, 146, 246). With this strong evidence that IL-33 is a “bad” player in arthritis translation to human disease is mandatory. However, evidence for this is not as clear as the mouse data. First, IL-33 expression in synovium has been shown by three groups (136, 145, 146). Clear nuclear staining is visible; however, double staining approaches did not convincingly identify the origin of the cell. Further 1 out of 3 groups present IL-33 only in endothelial cells (136).

My own data show IL-33 expressed in endothelial cells, but not so much in other cells which are suggested as potential sources in the literature such as fibroblasts or macrophages (Figure 4.8 and Figure 4.9). It is possible to argue that fibroblasts express IL-33 with strong *in vitro* data supporting that fact (Figure 4.10). However, all publications and my own data do not confirm that fibroblasts are expressing IL-33 *in situ*. This is interesting since *in vitro* TNF and IL-1 strongly upregulate IL-33 in fibroblasts; these two cytokines are clearly present in RA synovium. Moreover, when splitting fibroblasts or stressing them *in vitro* (for example by scratching), expression of IL-33 is observed (own data, Mr Millar, Glasgow University). Thus it has to be questioned if IL-33 expression by fibroblasts could be an *in vitro* phenomenon. Moussion reported desmin positive fibroblastic reticular cells in tonsil tissue (147). Double staining in other inflammatory tissue has to be performed to determine if these cells are also

present in RA synovium. In addition, CIA and AIA models test initiation and early phases of disease. With human biopsies studied so far, only snap shots of established diseases have been examined.

Recently, a new issue arose. By redefining the biology of IL-33, a common conclusion is that IL-33 is released by necrosis and is deactivated by apoptosis associated caspases rather than activated by caspase 1 ((142, 143). All in vivo studies with IL-33 used a so called “mature” IL-33 which reflects the IL-1 like cytokine domain initially described by Schmitz et al (132). While this potent truncated recombinant cytokine might reflect the true biology of full length necrosis released IL-33, studies still need to be performed to clarify this issue.

Focusing on the counterpart of IL-33, more and more studies report significantly elevated levels of sST2 in inflammatory diseases, raising the possibility that a decoy mechanism is in place to regulate IL-33 release and effector function. When comparing different studies a few inconsistencies merit attention. Elevated soluble ST2 has been reported in multiple myocardial infarction studies. Shimpo et al report four quartiles with the following ranges: I: 0.085-0.179 (n = 204), II: 0.180-0.235 (n = 202), III: 0.236-0.346 (n = 202) and IV: 0.347-6.88 ng/ml (n = 202) (brackets show patient numbers) (242). Weir et al reported in his cohort at baseline a median of 0.263 ng/ml (n = 100) (188). When focusing on inflammatory diseases only one, an SLE cohort serum analysis, has been reported. Mok et al show levels in their healthy controls with a mean of 0.36 ng/ml (n = 28) compared to active SLE patients with 0.51 ng/ml (n = 61) (151). Surprisingly, these levels in healthy individuals reflect quartile III to IV in Shimpo’s study and are higher than levels reported in Weir et al’s manuscript. These levels would indicate a high risk for mortality. The question is if these different results are due to technical differences or differences in patients/individual ethnicity. In comparison, the serum samples from individuals and PsA patients tested in this thesis were 0.033 ng/ml (n = 41) and 0.05 ng/ml (n = 36) respectively. This might again reflect technical differences or lack of numbers. More studies need to be performed in healthy controls to standardise the test for biomarker accreditation.

In summary, more human studies are needed to translate and verify results from mouse arthritis models, further the biology of IL-33 needs to be re-addressed in these models and sST2 as marker in inflammation more examined.

IL-33 in psoriasis – a new role for a new cytokine?

In this work, IL-33 overexpression in lesional psoriasis compared to perilesional or healthy skin was demonstrated (Figure 4.4). This has been confirmed by another group showing increased IL-33 mRNA levels from biopsies (194). When scratching a lesion of a psoriasis patient commonly this area can flare and even spread. Further mechanical damage of the skin can induce new lesions. This could concur with enhanced IL-33 mRNA levels of perilesional skin compared to healthy controls (194). To test this hypothesis two models have been used: TPA administration on the back skin and IL-33 intradermal injection. The phorbol ester TPA induces a non-specific inflammation; here, it was demonstrated that ST2 has influence in the initial phase of inflammation and an effect on epidermal reaction including proliferation measured by thickening of this skin layer and a marker for proliferation (ki67) (Figure 4.14, Figure 4.15). What is unclear is how TPA induces IL-33 release. Further it is unknown what levels of IL-33 are achieved. Already after 2 days of TPA treatment a difference in epidermal thickness is observable, which is lost in a 3 day treatment. While this points to an innate early role for IL-33 long term data in this model are not available. For example TPA in D6 deficient mice, which develop a phenotype similar to psoriasis, is used 5 to 7 days and a resolution phase of up to one week has been studied (67). Thus IL-33 biology in a TPA model still leaves open questions.

My other model, namely IL-33 intradermal injections, tackles the question from a different angle. IL-33 induces a 'psoriasis-like' dermatopathy in injected ears. This is ST2 dependent and partially mast cell dependent (4.3.2). It is unclear in what physiologic range the dose of 500 ng in 20 µl per injection lies. From its potency it is unlikely to be realistic as repeated injections of IL-33 lead to splenomegaly. This is not a common feature during even remittent trauma in humans. However, data obtained give a hint to a micro/cellular level expressed during injury and damage. That this effect is multifactorial is demonstrated by the mast cell deficient experiment. There, only an initial partial difference is seen (Figure 4.24). It makes sense as other cells than mast cells express ST2 such

as endothelial cells and maybe keratinocytes (Figure 4.7). Interestingly, KC is elevated in serum of mice treated with IL-33. This could explain recruitment and accumulation of neutrophils (Figure 4.25). Moreover, when injecting IL-33 intraperitoneal, neutrophils are recruited; this can be blocked with anti-KC antibodies (personal communication, Dr Alves-Filho, Glasgow University). Verri et al reported that IL-33 induced neutrophil migration in an arthritis model (247).

In contrast, beside KC, Th2 cytokines are also increased. While data in this chapter could explain a possible mechanism in psoriasis, Th2 related atopic dermatitis would be a similar phenotype with a totally different underlying pathogenesis. Melendez et al showed that IL-33 is upregulated in atopic dermatitis patients (173); also other IL-1 family members have been linked to atopic dermatitis, where transgenic mice expressing *IL18* from the keratin 5 promoter exhibit many features of atopic dermatitis, including infiltrates with eosinophils, mast cells and neutrophils (248). However, also an increase in tissue IL-12 and TNF- α mRNA was observed. With the assumption that IL-33 regulates a Th2 type response, upregulation in psoriasis could be interpreted as a rescue mechanism to balance against the Th1/Th17 axis. On the contrary, Melendez showed that primary mast cells can produce IL-17 upon IL-33 stimulation which rather supports a role for psoriasis than atopic dermatitis in this context (personal communication, Dr Melendez, Glasgow University). Unfortunately, in ear models performed in this thesis, mRNA was not obtainable due to technical failure.

In conclusion, IL-33 is upregulated in psoriasis. With its ability to induce an acute dermatitis and its potency as an alarmin IL-33 will most likely be a crucial player in this network of alarmin/cytokine/cell interaction.

Embryonic IL-33

The last aim of this chapter was to determine embryonic expression of IL-33. This subserves a core desire to understand the biology of nuclear IL-33 expression. With GENSAT data, this experiment seemed to be conservative. However, staining embryo tissue revealed that IL-33 is not expressed in the embryo, especially not in the dorsal aorta (Figure 4.30). However, a closer look

at IL-33 is needed before drawing early conclusions. Ensembl describes 4 variants of IL-33 (Figure 4.31). Surprisingly, the variant IL-33-003 only possesses exons for the homeodomain which is accounted as nuclear repressor. In addition, compared to full length IL-33, IL-33-003 contains a non-coding exon 2 (Figure 4.31 D). Taking this sequence of 120 bp (exon 2) of the homeodomain splice variant and using the blast machinery for mouse EST (expressed sequence tag) two hits are achieved. One cDNA hit for mouse male adult bladder and a second for cDNA of mouse embryo (day 16). This confirms the GENSAT data with IL-33 expression in the embryo. Further it can explain why anti IL-33 did not stain embryo tissue. This antibody Nussy-1 has been raised against the IL-1 like cytokine domain, which is not expressed by this variant. Using an antibody against the N terminal part could determine if this protein is also translated at that development stage. Further PCR analysis could verify expression of different splice variants in the embryo. This is ongoing work.

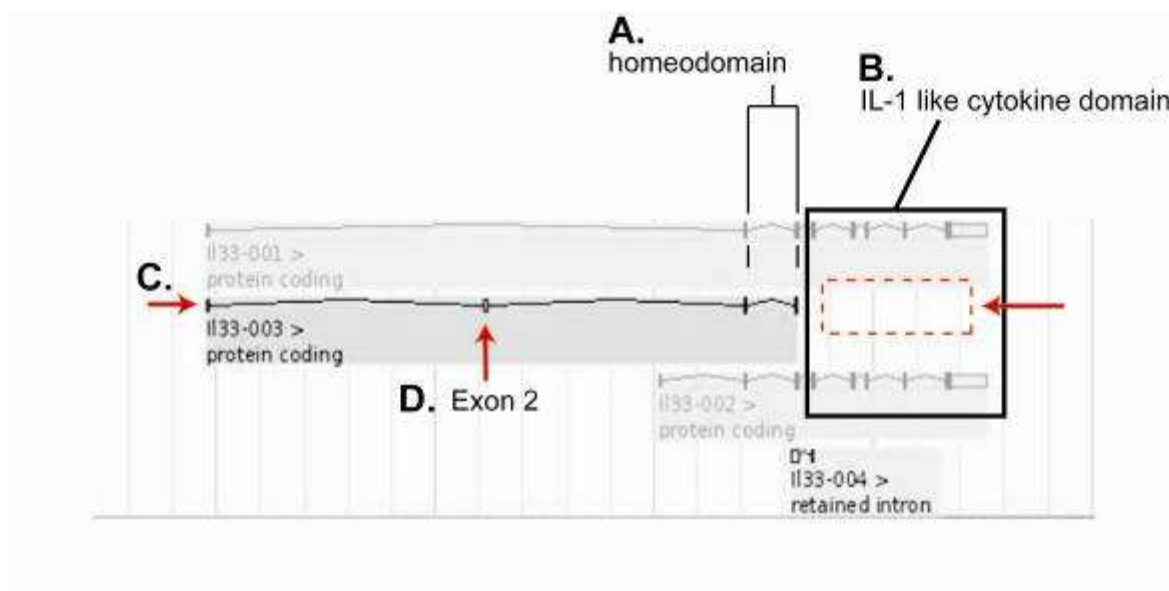


Figure 4.31 Splice variants of IL-33.

Using Ensembl.org image has been imported. 4 splice variants for IL-33 are described there. IL-33-003 contains similar to 001 and 002 the homeodomain like HTH (A, C). In contrast, 003 lacks the IL-1 like cytokine domain (B, C dashed box). A non coding exon is unique to 003 (D).

5 The use of nanoparticles to image inflammation

Content of this chapter has been published in the following manuscript:

- Graham D, Thompson DG, Mckenzie F, Faulds K, Stevenson R, Ingram A, Stokes R, McFarlane E, Alexander J, Garside P, Hueber A, McInnes IB
Functionalised nanoparticles and SERRS for bioanalysis.
Proc. SPIE. 2009 Feb, Vol. 7192, 719202; DOI:10.1117/12.810161

5.1 Aim and Introduction

Imaging of inflammation *in vivo* and in particular cytokine accumulation at the cellular/molecular resolution level is still not possible due to lack of technology which is sufficiently sensitive and specific. I set out to explore the notion that surface enhanced resonance Raman scattering (SERRS) technology could be utilized to facilitate nanoparticle imaging as a potential way to develop techniques from non-specific, descriptive imaging to specific, disease targeting detection.

Although a wide range of imaging options exists including X-ray, ultrasound, magnetic resonance imaging (MRI), computer tomography (CT), positron emission tomography (PET), and single photon emission computer tomography (SPECT), all of which have led to improvements in sensitivity and specificity, these techniques are expensive and often limited in their ability to detect early subclinical inflammation. Fluorescence imaging is far more advanced in *in vitro* and *ex vivo* analyses; however, limited tissue penetration and energy induced heat limit this methods.

Functionalised nanoparticles have been used in a number of studies and more recently as substrates for SERRS based imaging approaches. The advantages of using metallic nanoparticles are that they are very bright in terms of their optical characteristics and also can be functionalised to provide a SERRS response and hence provide a unique Raman fingerprint. Nie and co-workers have reported the use of SERRS labeled gold nanoparticles that were stabilized using PEG and subsequently functionalised with antibodies for the *in vivo* detection of EGF receptors in a cancer mouse model (223). Gambhir and colleagues demonstrated that SERRS active nanoparticles can be noninvasively multiplex imaged *in vivo* with spectral fingerprints of up to 10 different types (249).

The aim of this chapter was to establish SERRS imaging *in vivo* and to build the foundation for future noninvasive imaging of inflammation. ***Thus I sought to determine biological stability and activity of protein linked nanoparticles and their accumulation and imaging properties in vivo.***

At first it should be mentioned that this work was accompanied by different limitations and problems: Batch inconsistencies were the main problem with differences in protein concentrations but also in SERRS intensity. Also nanoparticles aggregated over time and therefore interfered with experimental setups. Thus most of the experiments are only performed once, with difficulties for inter-comparability and reproducibility due to batch differences. Further some experiments are lacking a proper control such as the HeLa bioactivity assays with lack a NP only or NP-IgG control due to lack of material. Further, during this collaborative work the detection laser was switched and NPs with a size of 10-20 nm were switched to Nanotags with a size of ~ 60 nm. Due to these multiple variables and problems during the experimental workup of nanoparticle biology the data generated here have to be interpreted very carefully. Moreover, these data bring only premature information about nanoparticle biology. Retrospectively, in vivo experiments have been conducted too early and more basic in vitro biological work up has to be established. **In summary, this chapter provides only a glance on a possible future imaging modality which still has to proof its capacity.**

5.2 Size and form of nanoparticles

Nanoparticle sizes range from 10 nm to 500 nm. The size of NP has different effects depending on the context. Smaller sizes can have larger extinction coefficients therefore offering advantages compared to bigger NPs. In contrast, larger NPs are a better target for phagocytosis and thus most likely are targeted for inflammatory tissues. However, they could also more likely accumulate in the reticulo-endothelial system (liver and spleen) or induce side effects in the lung (204, 205). In collaboration with Dr R Stokes (University of Strathclyde) transmission electron microscopy (TEM) was performed to determine the size of NPs (called nanotags) used in some of the experiments (Figure 5.1). The image demonstrates round particles with size below 100 nm (~60 nm). This shows that these particles are spherical, compared to other reported nano-rods or tubes. These nanotags have been used for imaging analysis *in vivo* due to their very bright SERRS signal ability. Other nanoparticles used had a size of 10 - 20 nm (image not shown, information provided by Dr Stevenson, University of Strathclyde). Gold nanoparticles were prepared following the Turkevich method. Briefly, HAuCl_4 was reduced using citrate to afford colloidal gold with a diameter of approximately 19 nm. Nanotags were obtained through a material transfer agreement with Oxonica Materials Inc. and their synthesis was undisclosed.

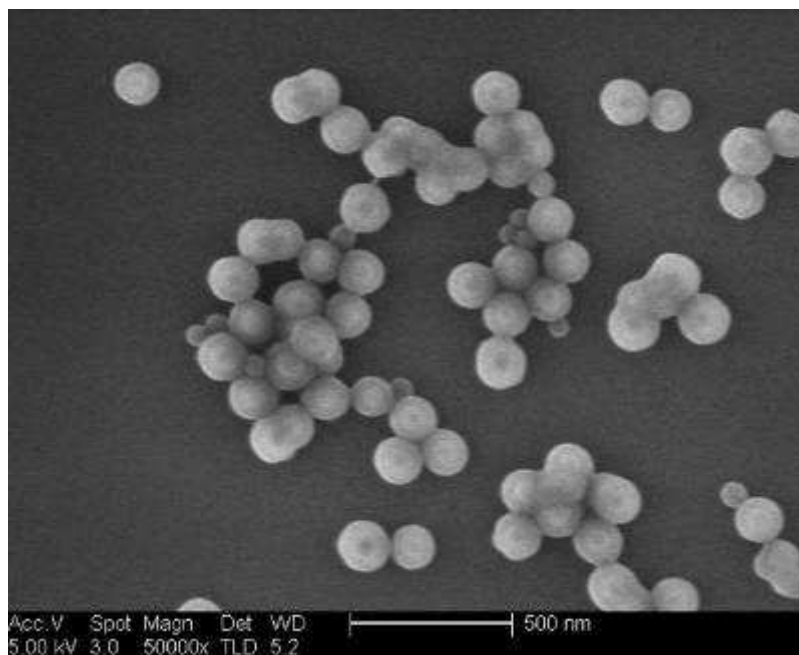


Figure 5.1 SEM on nanoparticles (nanotags)

SEM of nanotags determine their size below 100 nm, estimating ~60 nm. Nanotags are round shaped, most with the same size; only few smaller nanotags are present as well. (Picture provided by Dr R Stokes, University of Strathclyde), n=1.

5.3 Linking proteins to nanoparticles

My first task was to stably link proteins such as antibodies or cytokines to NPs. Difficulties can arise regard to stability, maintenance of SERRS signal ability, but also biological conservation of the protein itself. Linking the protein with its biologically active part to the NP would render the protein inactive (e.g. linking the antigen binding domain to the NPs instead of the Fc part). Even distant binding could modulate tertiary or quaternary structural properties of proteins to alter their precise binding properties e.g. affinities, on and off rates which may be of relevance in terms of future functional interpretation of receptor ligand binding in vivo. Figure 5.2 demonstrates the structure and process of protein linkage to the NP. Gold NPs are combined with a linker containing a surface seeking group (thiol group, which reacts with the gold surface), a SERRS active dye (SERRS tag) and a reactive acid group. This linker NP complex can then covalently bind a protein such as an antibody or, as illustrated in Figure 5.2, Etanercept (ETA, recombinant TNF receptor construct with an IgG Fc component) using EDC/NHS chemistries. Nanotags contain reactive thiol groups protruding from the silica shell. With use of a sulfo-SMCC cross-linker, its possible to conjugate antibodies and proteins to the surface. Thus functionalised NPs should retain their ability for SERRS imaging, but also should be able to bind TNF- α and block the ability of TNF- α to activate cells without being toxic to cells. Nanotags were functionalised using an alternative cross linker.

The following sections will cover these key issues:

- 5.3.1 Testing quantities of ETA on linked nanoparticles
- 5.3.2 Biological binding properties of ETA linked nanoparticles to TNF
- 5.3.3 Biological function of ETA linked nanoparticles in HeLa cells

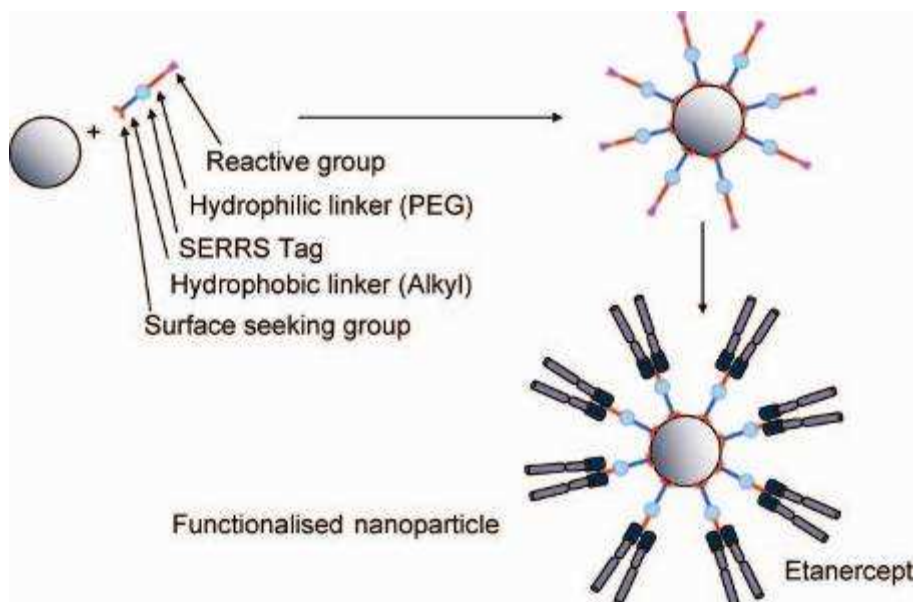


Figure 5.2 Schematic linking of proteins to NPs.

Gold nanoparticles (10 nm) bind a linker via its surface seeking group containing a SERRS tag and a reactive group. This linker can then covalently bind a protein, in this case Etanercept (ETA).

5.3.1 Testing quantities of ETA on linked nanoparticles

Before moving into activity assays, it was important to determine how much ETA actually binds to NPs. Initial experiments done by Dr Stevenson showed that an estimated 10 HRP antibodies bind to one NP (data not included). Here, a Western blot approach was used to get a rough estimate as to whether ETA binds to NPs and if so, in what concentration.

ETA was loaded with 100, 10 and 1 ng of total protein, and compared to 10 μ l solution of ETA-NP or NP alone (NP = Au (for Aurum, *latin: gold*) Figure 5.3). Solutions were incubated in reducing loading buffer, heated for 5 min at 95°C to release proteins from NPs and then run on a gel. After blotting, membrane was blocked and probed with an anti-Fc HRP which would detect the Fc region of ETA.

Figure 5.3 demonstrates that ETA (from ETA-NP) run faster than ETA protein (60 kDa vs. 75 kDa), but also depicts a ball shaped band including variable migration speed in the middle. This might arise from altered properties of NPs themselves and could alter the running speed in the gel due to differences in charge. NP alone (Au) did not result in a band. 10 μ l of ETA-NP solution contained a concentration between 1 and 10 ng of ETA (~ 0.1 - 1 μ g/ml ETA bound to NP). Similar results were obtained when using IgG bound to NP.

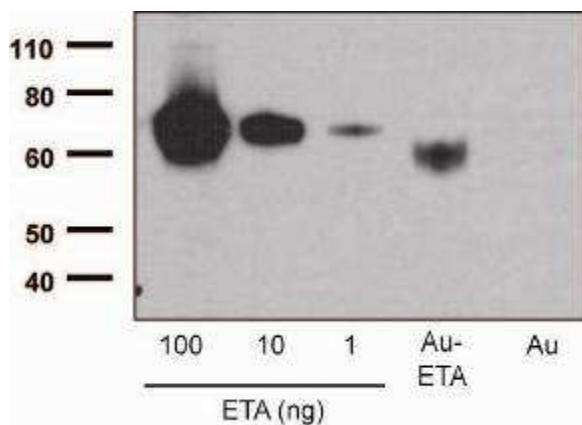


Figure 5.3 Total protein on ETA linked nanoparticles
Westernblot analysis of Au-ETA (ETA-NP) compared to different concentration of ETA (loaded 100, 10 and 1 ng of total protein). 10 μ l of Au-ETA loaded. Au = NP only with no protein linked. Y axis in kDa. Representative blot of n=2.

5.3.2 Biological binding properties of ETA linked nanoparticles to TNF- α

Next we sought to determine if ETA linked to NPs can still bind to TNF- α . Using a competition ELISA approach, a fixed concentration of recombinant TNF- α (2000 pg/ml) was incubated with different concentrations of ETA-NPs or NPs linked with IgG as control. Samples were incubated at 37°C for 1 h, centrifuged and supernatant then tested by ELISA (procedure shown in Figure 5.4). Interestingly, incubation of TNF- α only (without addition of NPs) reduced a starting concentration from 2000 to 50 pg/ml,

Figure 5.5 A, black bar. Although ETA-NP reduced levels of TNF- α , this result has to be judged cautiously, due to the loss of TNF- α in the control sample (Figure 5.5A).

To exclude possible plastic binding of TNF to the tube during the incubation period, the solution was spiked with 0.5% bovine serum albumin (BSA). Despite this, 50% of detectable TNF- α was 'lost' in the control sample (due to possible binding, or degradation),

Figure 5.5 B, black bar. Despite this, it was possible to now interpret the competitive properties of the NPs or ETA bound NPs. Thus, Au-IgG (Au = NP) or Au alone at different concentrations did not alter detectable TNF- α ,

Figure 5.5 B, white bars. In contrast, Au-ETA significantly reduced measurable TNF levels with approximately 50% reduction at 1:10 dilutions and approximately 25% reduction at 1:100 dilutions. Reduction was not possible with further dilutions,

Figure 5.5 B, grey bars.

To test if nanotags with bigger size also are able to offer appropriate linkage to ETA the above experiments were repeated using NT440. Linked with IgG no reduction in TNF recovery was detected compared to media only (Figure 5.6 white bars). In comparison, NT440 bound to ETA significantly reduced TNF- α concentrations in dilutions of 1:10 and 1:100 (Figure 5.6 grey bars).

Thus this demonstrates that ETA-NP as well as ETA-NT440 can specifically bind TNF- α compared to IgG controls.

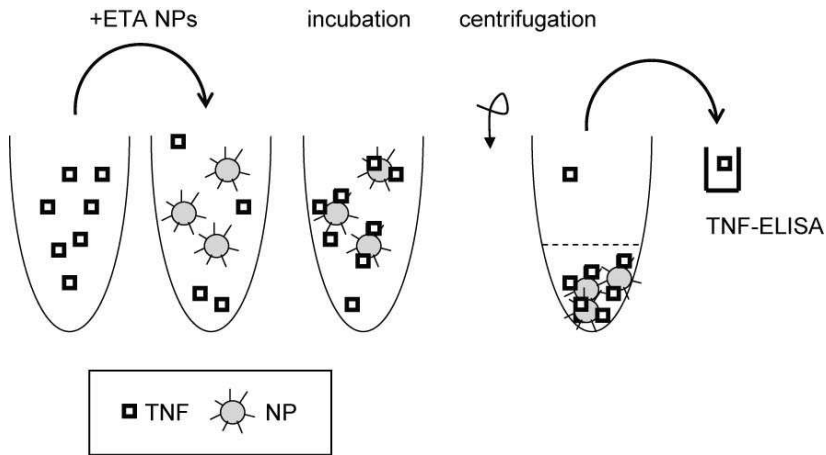


Figure 5.4 Competition ELISA to test TNF- α binding to NPs. TNF- α was incubated with NPs at 37°C for 1 h. NP pelleted by centrifugation, and supernatant tested for the remaining TNF concentration by ELISA. Incubations either with uncoated Au, Au-ETA or Au-IgG.

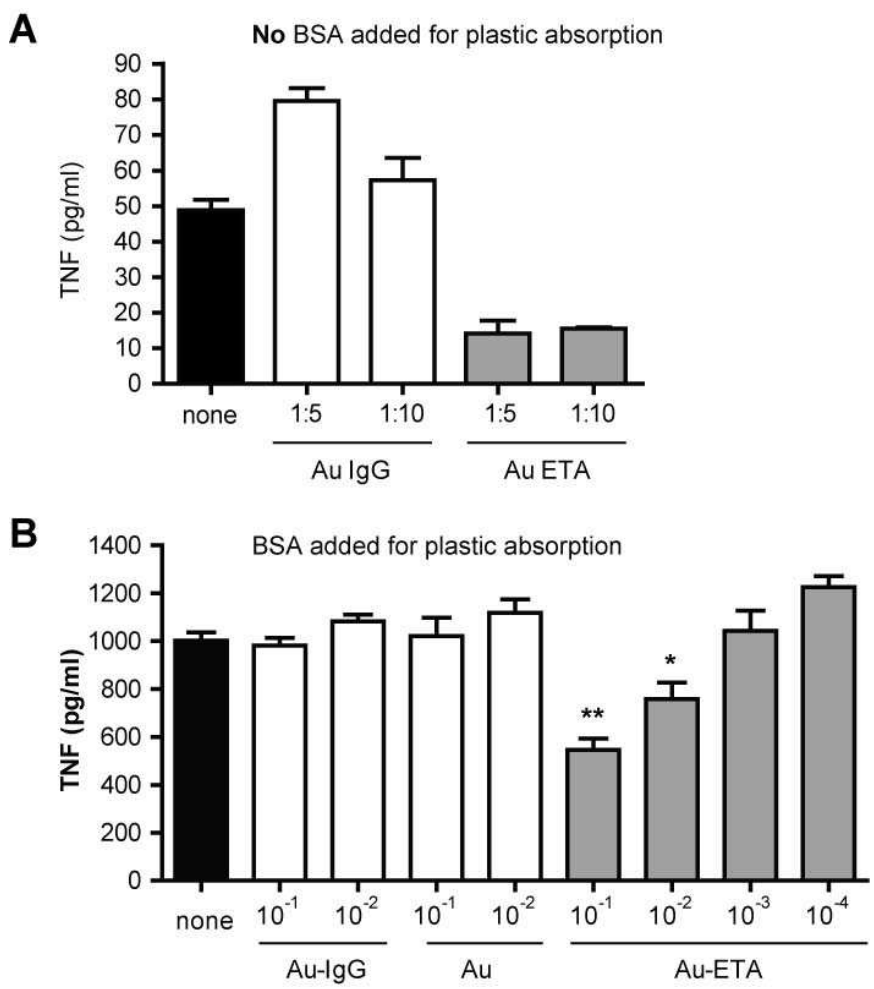


Figure 5.5 Biological binding properties of ETA-NPs. Preincubation of recombinant TNF- α with media only (none, black column), Au-IgG (Au = NP, white columns), Au only (B, 3rd and 4th white columns) or Au-ETA (grey columns) and analysis of subsequent TNF concentration by ELISA. A. TNF and NP incubated in media (without BSA). B. Incubation solution spiked with 0.5% BSA to prevent plastic adsorption. X axis show NP dilutions. Results are reported in means of triplicates +/- SEM, n=1. Unpaired t test, ** p<0.005; * p<0.05

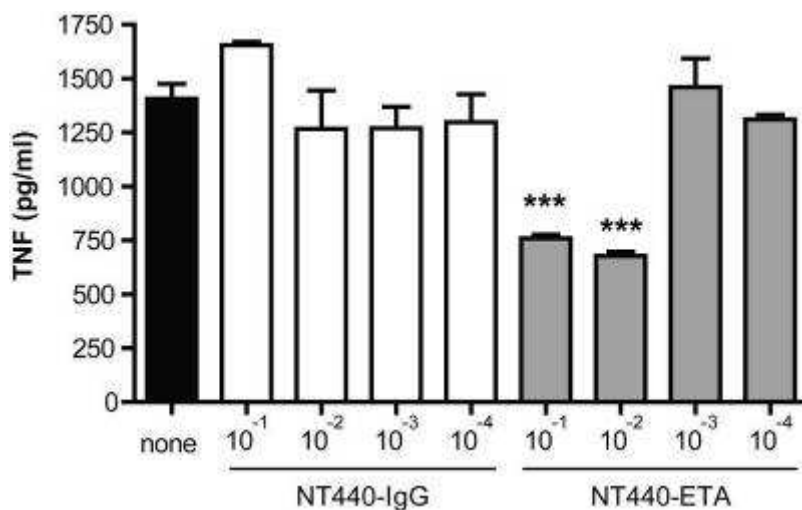


Figure 5.6 Biological binding properties of ETA-NT440.

Preincubation of 2000 pg/ml recombinant TNF- α with ETA-NT440 (NT = nanotag) particles. Solution contained 0.5% BSA to prevent plastic adsorption. Analysis done with TNF- α ELISA. Black bar: media only, white bars: NT440 linked to IgG, grey bars: NT440 linked to ETA. Results are reported in means of triplicates \pm SEM, n=1. Unpaired t test, *** $p < 0.0005$

5.3.3 Biological function of ETA linked nanoparticles in HeLa cells

After determining the biologic property of ETA linked NPs to bind TNF- α , the next issue to address was their biologic inhibitory properties in a cell dependent model system. Therefore the following assay was established. HeLa cells (an adherent immortal cell line derived from ovarian cancer) was stimulated with TNF- α and after 6 h incubation supernatant was assessed for IL-6 production by ELISA. ETA was then tested in this assay, to evaluate how it could influence IL-6 production.

HeLa cells stimulated with TNF, dose dependently released IL-6 (Figure 5.7, left graph, black bars). This was dose dependently reduced by ETA co-incubation. Culturing HeLas with media containing 10% FCS stimulated cells to produce background levels of IL-6 (~ 200 pg/ml) which was not observed when cells were grown in media alone. This was therefore considered in estimating the inhibitory effects of ETA upon subsequent TNF stimulation (Figure 5.7 left graph compared to right graph). ETA was able to block TNF- α induced IL-6 production. Thus I had generated a bio-assay in which to test the capacity of NPs linked with ETA to inhibit TNF bioactivity *in vitro*.

To test particles, a non SERRS active linker (1-mercaptoundec-11-yl) hexa (ethylene glycol) (MHA) was chosen which has the advantage of higher stability than SERRS linkers. ETA alone was again able to reduce IL-6 production induced by TNF (Figure 5.8 black bars). Similarly, Au-ETA (Au = NP) significantly reduced IL-6 production induced by TNF at dilutions of 1:10 (Figure 5.8 grey bars).

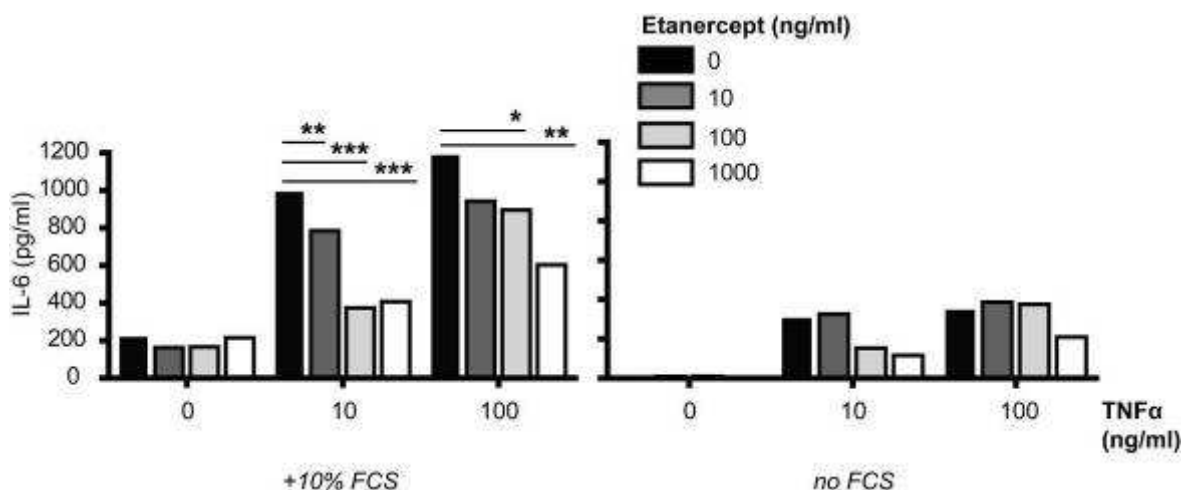


Figure 5.7 Establishing TNF stimulation of HeLa cells with ETA blockade. HeLa cells were stimulated with different doses of TNF- α (0, 10 and 100 ng/ml) incubated in media with (left panel) or without (right panel) 10% FCS for 6 h. Blockade of TNF was tested with different concentrations of Etanercept (black bar: 0, dark grey: 10, grey: 100, white: 1000 ng/ml ETA). IL-6 production in the supernatant was assessed by ELISA. Shown are mean of triplicates and analysed by unpaired t test, $n=1$. ** $p<0.005$; *** $p<0.0001$

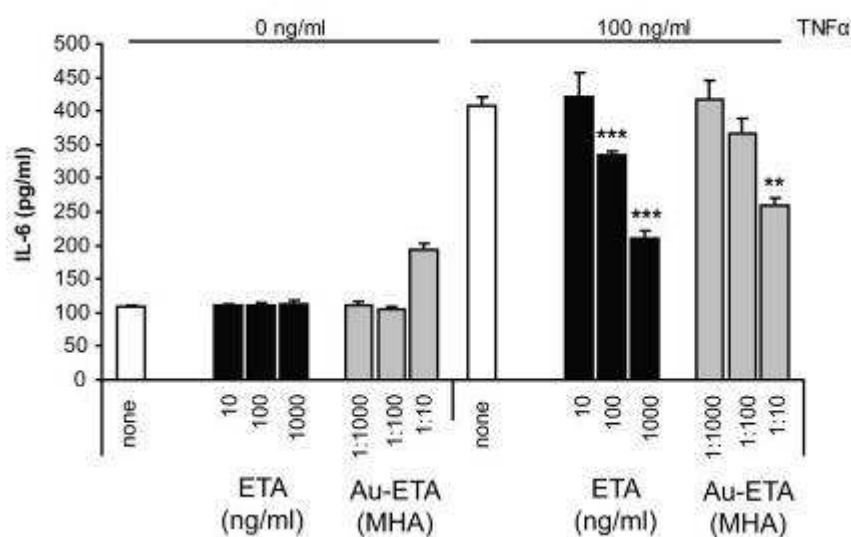


Figure 5.8 IL-6 production by TNF stimulated HeLa cells blocked with Au-ETA. Coincubation of HeLa cells with TNF (10 ng/ml) and different concentrations of Au-ETA (Etanercept (ETA) bound to nanoparticles with linker 1-(mercaptoundec-11-yl)hexa(ethylene glycol)(MHA)). Left part shows incubation without TNF, right part with TNF 100 ng/ml. White bar: media only, black bars: dose concentration with ETA in ng/ml. Grey bars: dose concentration with Au-ETA. Analysis of the supernatant for IL-6 secretion by ELISA. Shown are mean \pm SEM of triplicates, $n=1$, unpaired t test. ** $p=0.0011$, *** $p<0.0005$

Next, NPs were tested that contained a SERRS active linker bound to ETA. Surprisingly, some batches aggregated in the tube (Figure 5.9, left tube, NPs aggregated to the plastic). Because this initially seemed to be random, linkage methods were altered to guarantee batch consistencies. Thus, after linkage different concentrations of BSA was added to the solution to prevent aggregation. Different batches were then tested in the “HeLa assay” (Figure 5.10). Two types of NPs linkers were used: The SERRS active linker containing the dye Azo (Au-Azo) and the MHA linker (Au-MHA). After linker attachment to NPs these were incubated with ETA (final concentration 10 $\mu\text{g}/\text{ml}$ and for one batch with MHA 100 $\mu\text{g}/\text{ml}$). At the end of incubation two different concentrations of BSA (1 $\mu\text{g}/\text{ml}$ or 10 $\mu\text{g}/\text{ml}$) were added to prevent aggregation. The linking process was completed by multiple washes and then tested in the HeLa stimulation assay. In the absence of TNF none of the NPs stimulated HeLa cells to produce IL-6 (Figure 5.10 first eight bars). Stimulation with TNF induced IL-6 (white bar) which was inhibited by ETA (black bars). From the NPs solutions the most effective inhibitor was that containing an Azo linker (#2) which was incubated with 10 $\mu\text{g}/\text{ml}$ BSA (grey bar, #2). This was also the case for Au-MHA (dark grey bar, #4). Using a higher concentration of ETA (100 $\mu\text{g}/\text{ml}$ instead of 10 $\mu\text{g}/\text{ml}$) did not derive stronger IL-6 inhibition (compare MHA, dark grey bar #4 vs. #5). Results from this experiment were used to inform future linking processes an “anti-aggregation” step with the addition of 1 $\mu\text{g}/\text{ml}$ BSA.

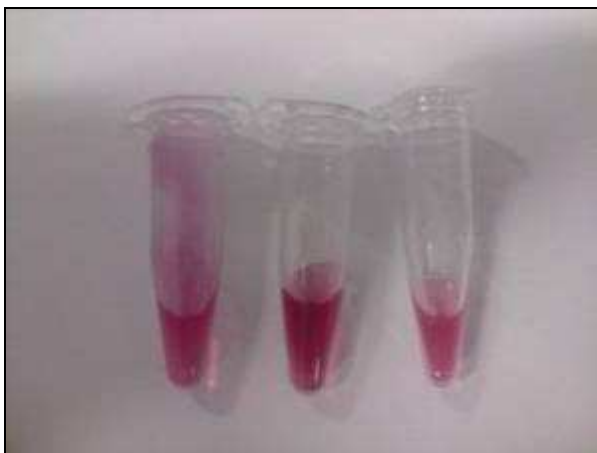


Figure 5.9 Nanoparticles aggregate over time.

Left tube shows aggregation of Au-IgG nanoparticles to the plastic wall. Middle and right tube show unlinked nanoparticles in solution with different dilutions.

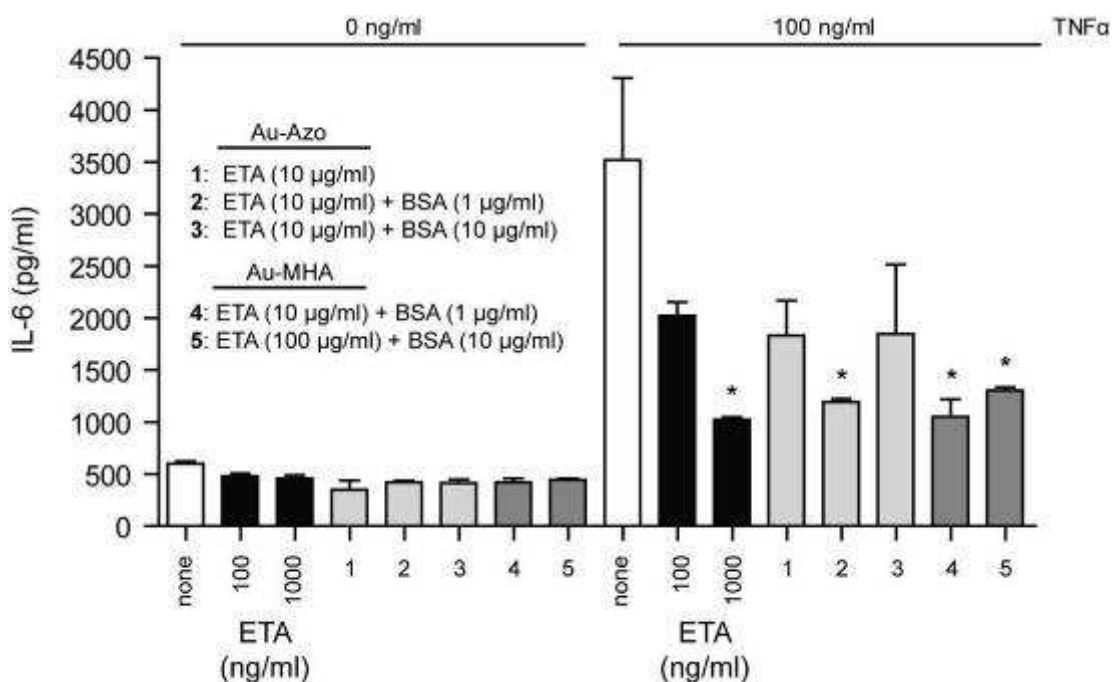


Figure 5.10 Linkage and bioactivity of ETA-NP (Au) with BSA.

HeLa cells were incubated with with or without 100ng/ml TNF- α and either ETA only or 1:10 dilution of NPs solutions (numbered #1-5). NPs were linked with Azo dye or 1-mercaptoundec-11-yl)hexa(ethylene glycol) (MHA). Then linked by incubation with ETA (different conc. #4 vs. #5) and addition of different conc. of BSA at end of incubation. Analysis of supernatant by IL-6 ELISA. white bar: media only, black bar: ETA, grey bars: #1-3, Au-Azo, dark grey bars: #4-5, Au-MHA. Results are reported in means of triplicates \pm SEM, n=1. Unpaired t test, * p<0.05

5.4 The detection of nanoparticles in vivo

Future ideas as to the use of nanoparticles range from drug delivery with specific tags to targeting of drugs specifically to the site of action, e.g. a tumor cell or immune cells. A further possibility is to utilize this approach to image the occurrence, migration and tissue concentration of these cells. This can further be used as a follow up approach to monitor disease activity or tissue responses to therapeutics or injury. So far, nanoparticles have been used in humans only to stabilize drugs e.g. PEGylation of cytokines or antibody fragments. NP constructs for other purposes, in which nanoparticles are the main delivery component linked to a drug or antibody, have not been tested in humans. NP constructs have been studied mainly *in vitro* with few reports addressing *in vivo* utilization. Imaging and cancer treatment is at the forefront for the use of NPs. In regard to imaging, common caveats have been described to their general introduction include the limit of depth penetration or lack of resolution. Using SERRS active nanoparticles with a penetration of ~ 2mm I sought to overcome the issue of depth and to try to establish SERRS active NPs in vivo. Thereafter I explored the proof of concept of imaging NPs in vivo.

5.4.1 SERRS profile of NP (Strathclyde)

Imaging of tissue with fluorescence has the major disadvantage that laser wave length induces heat and therefore can damage the tissue. Here, gold NP (Au) were linked with a near infrared linker (NIR) which may be excited at 785 nm and does not induce strong heat transfer. Inelastic scattering from the Raman dye, enhanced by the metal surface accounts for a specific pattern with distinct Raman shifts/peaks compared to a fluorescent smooth curve (NIR-Au, Figure 5.11). Different linkers result in distinct individual patterns and therefore multiplexing without problems of compensation is possible.

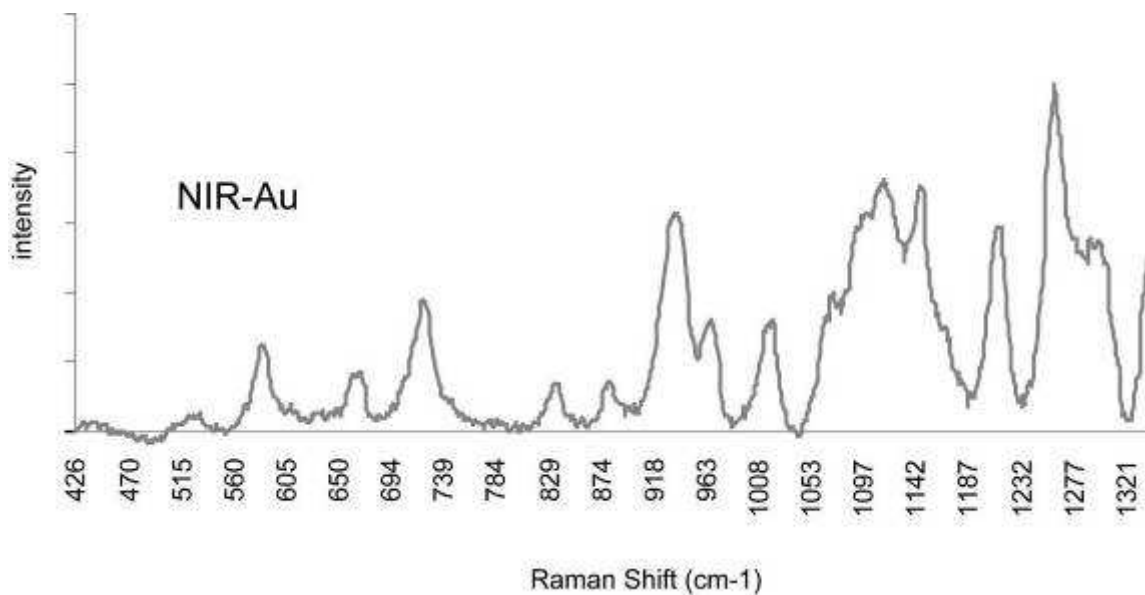


Figure 5.11 SERRS profile of NIR-Au-NP.
As example for a SERRS profile Raman shifts of a NIR-Au-NP (near infrared linked gold NP) were measured. Distinct intensity peaks (e.g. at ~ 700 or ~950) are shown.

5.4.2 Detection of NPs in tissue

To address if NPs are detectable in tissue a mouse cadaver was injected with NIR linked NPs into the footpad (100 μ l) and the ear pinna (50 μ l). Before injection background values for SERRS signals were measured. A handheld laser was fixed in a stand to guarantee a standard distance with a focal length of $\sim f = 7.5$ mm (Figure 5.12A). Measurement was performed at 800 - 930 range (200-2000 cm^{-1}) with an assumption of depth penetration of 2 mm. Signal was captured for 1 s. SERRS was detected in both tissues after injection (Figure 5.12B,C). For the footpad, ankle and popliteal areas were measured as control sites to determine leakage due to the pressure of injection. At the ankle, SERRS was also detected while the popliteal region derived only a very weak signal. Differences in intensity between footpad and ear pinna could be explained by reduced volume injected for the ear pinna. In conclusion, SERRS active NPs can be detected in tissue after injection. Thus skin and other structures do not appear to significantly interfere with this methodology.

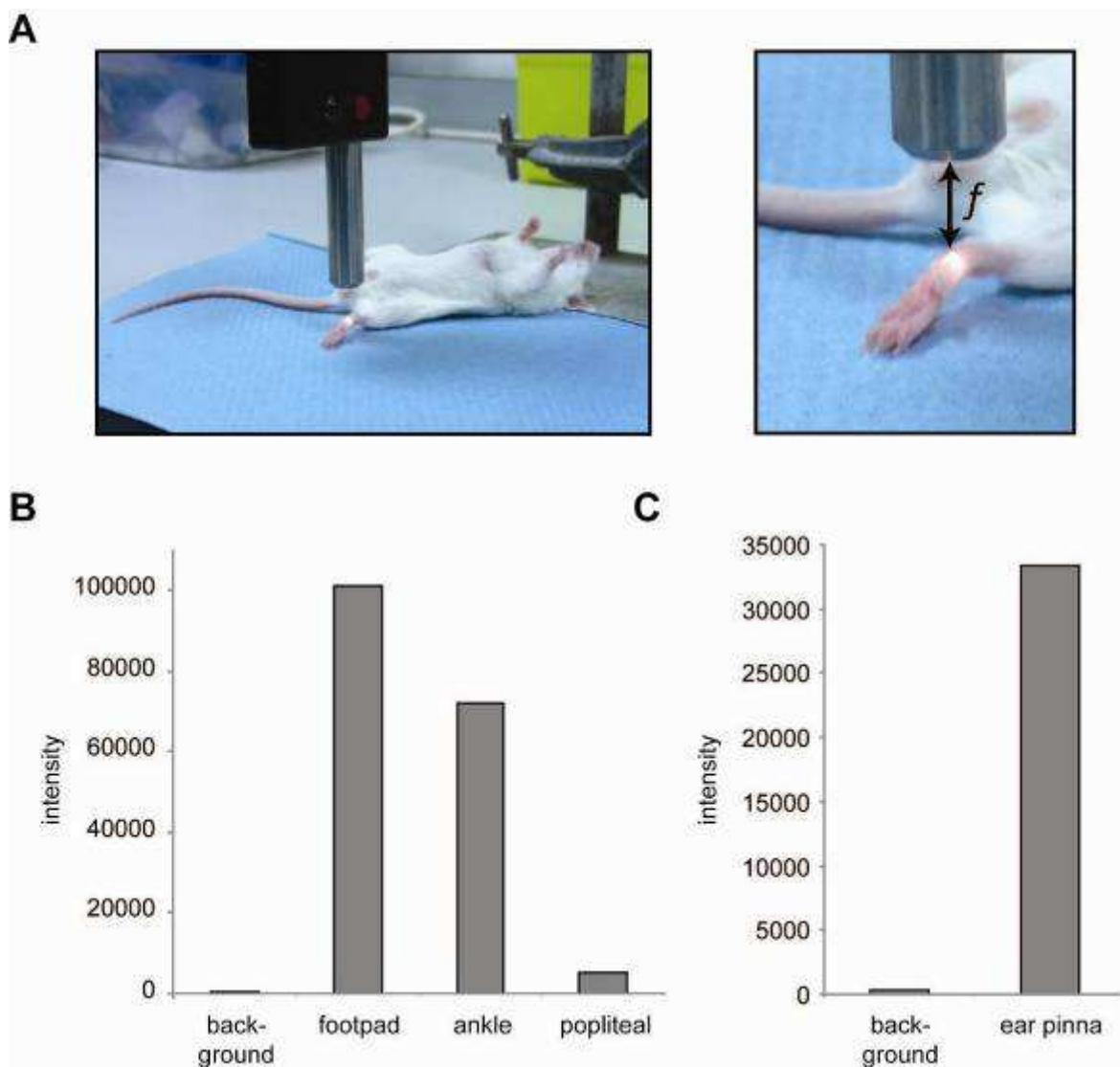


Figure 5.12 Detection of Nanoparticles in tissue

NPs were injected into the footpad or intradermally into the ear and SERRS signals were detected using a handheld laser ($n=1$). **A.** measurement procedure as an example at the ankle with distance f laser exit to tissue. **B.** intensity of fluorescence, with background intensity, measurements at footpad, ankle and popliteal area. **C.** Measurement of SERRS at the ear pinna after NP injection. Injection volume: Footpad: 100 μl , ear 50 μl . Capture time 1s.

5.4.3 The detection of NPs in inflammation

The next step involved the Raman detection of NPs in an inflammation model. Initial experiments comprised intravenous tail vein NP injection into a live mouse. Six hours later, the mouse was sacrificed and organs measured for SERRS activity. In agreement with the literature, signals were detectable in liver and spleen; however, no specific signals could be located in organs like heart, lung, muscle, kidney or lymph nodes (data not shown). This likely reflects accumulation of NPs in the reticulo-endothelial system (RES) recently described by Qian et al. (223).

To address if ETA linked NPs specifically track to the site of inflammation, the carrageenan induced arthritis model was used. With the hypothesis that high amounts of TNF are present in the arthritic joint ETA linked NP accumulate at the site of inflammation while IgG linked control NP do not. The right paw of $n=3$ /group were injected with a carrageenan solution while the left paw as control was injected with PBS. Three groups were used with the following NP solutions injected 68 h after arthritis induction: Au-IgG (1:100, control group), Au-ETA (1:100) and Au-ETA (1:1000). Paw thickness was measured before injection and at different time points after administration (Figure 5.13A). Already 4 h after administration severe swelling of the paw as well as the ankle (not shown) occurred in the right paw compared to the left demonstrating the acute model of action in this inflammation model. 68 hr after induction, NP solution was injected i.v. and 6 h later at the peak of inflammation (experiments performed with Dr Asquith, Glasgow University, who established the model in our group) mice were sacrificed and SERRS measured at both paws (Figure 5.13B). As expected significant difference in SERRS activity was measured in Au-ETA administrated paws (Figure 5.13B, black and grey (filled and shaded) bars, $p < 0.05$). Au-IgG control injection showed no significant difference between paws, however, counts achieved in the control reached similar levels as Au-ETA groups.

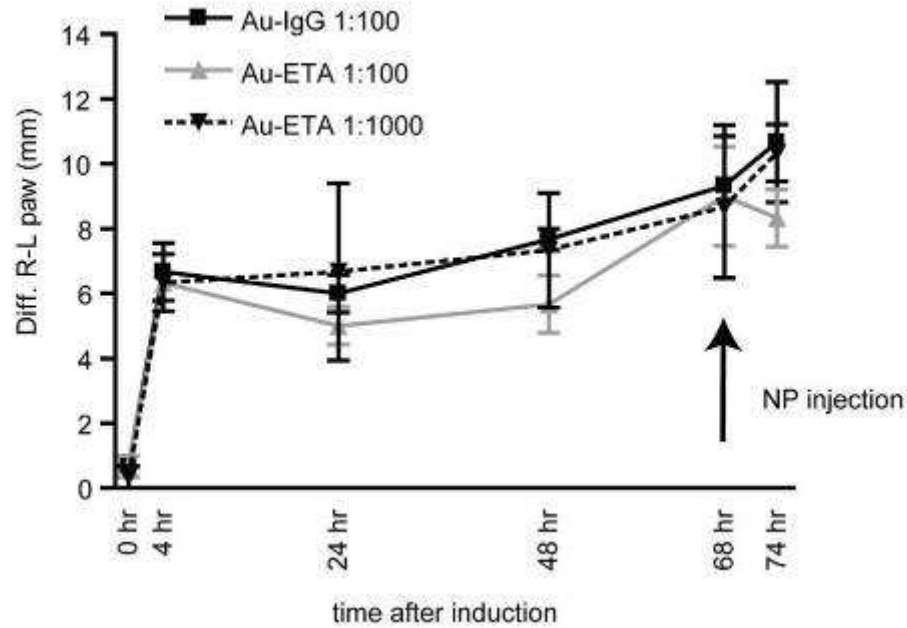
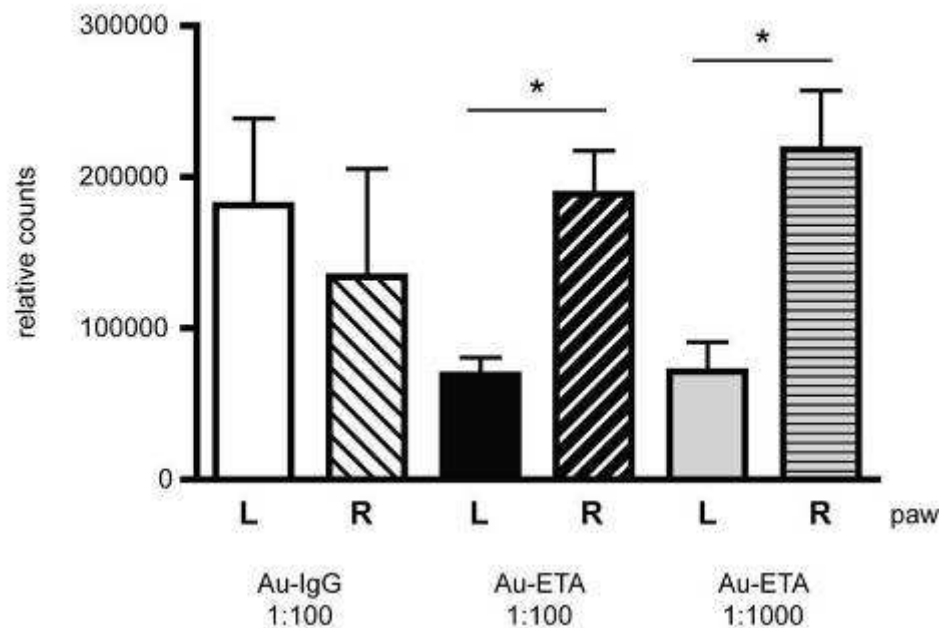
A**B**

Figure 5.13 Detection of NPs in the carrageen footpad injection model. Inflammation of the footpad was induced by injection of carrageen (100 μ l, right paw) or PBS (control, left paw). Paw swelling was monitored every day and is demonstrated in the difference of right to left paw (A). Six h before the peak of inflammation (68h post carrageen injection) NP solutions were administered i.v. by tail vein injection (100 μ l) in different concentrations (see arrow in A). Six h post NP injection, mice were sacrificed and SERRS measured in paws (B). No difference is seen between left and right paw injected with Au-IgG (1:100 concentration, open and white dashed bar). Significant difference between right (black or grey bar) and left (black or grey dashed bar) paw in Au-ETA administered mice. Shown is mean \pm SEM analysed by unpaired t test. * $p < 0.05$. $n = 3$ per group.

To further explore the effect of Au-ETA, the experiment was repeated with two groups using an NP dilution of 1:100 and higher number of mice: Au-IgG (n = 8) and Au-ETA (n = 9). Paw thickness measurements indicated similar severity compared to the foregoing experiment with rapid onset of satisfactory incidence of swelling 4 h after induction (Figure 5.14A).

Measurement of SERRS activity 6 h after injection resulted in no significant difference in both groups comparing left (PBS) and right (NP) paw (Figure 5.14B). Similar to the first carragean experiments, levels of SERRS were comparable between Au-IgG and Au-ETA. After normalising the intensity retrospectively no specific SERRS pattern was detected but an increase in tissue fluorescence enhanced by nanoparticles was observed (communication Dr Stevenson, University of Strathclyde). The gold nanoparticles used to this point could be considered a soft shell nanoparticle, i.e. the gold was encased in a soft PEG-shell with the antibody attached. As the linker is attached through the adsorption of a thiol group to the gold surface, the linker could possibly be leached from the surface by extreme salt or pH conditions. In the case that the linker detaches from the surface, SERRS signal is lost. However, the fluorophore normally quenched by the close proximity of the nanoparticle surface regains its fluorescence. This could explain the loss of SERRS detection and an increase in fluorescence. The use of nanotags, i.e. nanoparticles with a 'hard' silica surface should provide a more stable platform for in vivo SERRS.

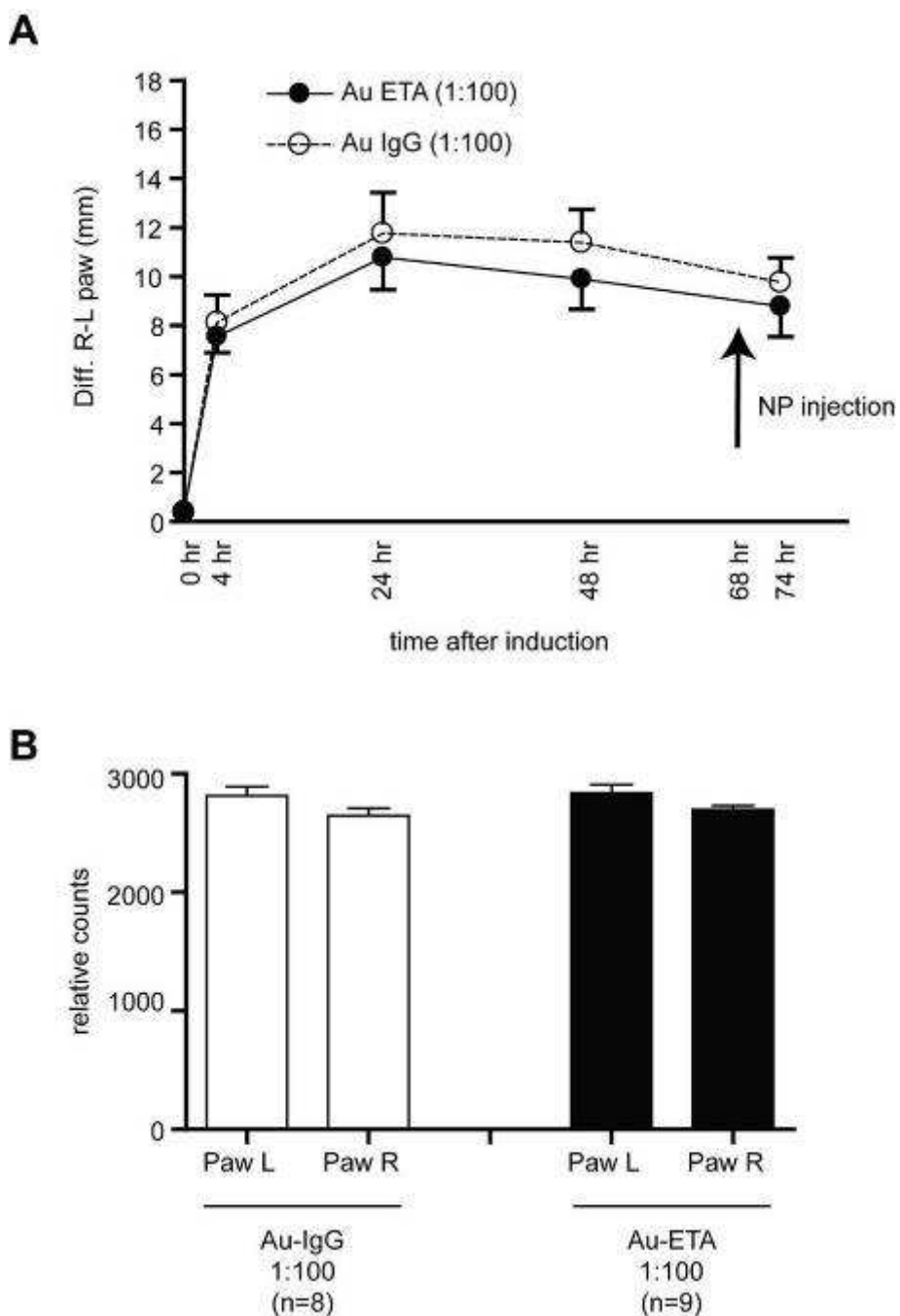


Figure 5.14 Tracking of Nanoparticles to the site of inflammation. Mice injected with carrageen into the footpad were injected i.v. with nanoparticles at the peak of inflammation. A. Same setup was used compared to Figure 5.13. Only one concentration was used (1:100) for each Au-IgG and Au-ETA (B). No difference in SERRS counts were observed between left and right paw for IgG and ETA. Shown is mean \pm SEM. n=8 for Au-IgG and n=9 for Au-ETA.

5.4.4 Switch of detection laser and Nanoparticles to Nanotags

The inconsistency of the carragean arthritis imaging could be accounted for by several issues which include technical and hypothetical biological reasons: these range from malfunction of the NP-SERRS linker, reduced brightness of NP, subjective laser data capture, but also including to rejection of the hypothesis implying preferential accumulation of ETA NPs compared to IgG NP. In discussion with Prof. Graham (University of Strathclyde, Centre for Nanometrology), NP size with 10-20 nm do not emit a strong SERRS pattern.

To address this a series of experiments were planned and performed as follows. Instead of using NP described above, silica shelled Nanotags (NT) were used. These NTs are NPs with a core gold nucleus ($d=50-60$ nm) wrapped in a SERRS active linker and further encapsulated with a silica shell (d total =90 nm). Figure 5.1 shows a TEM of Nanotags with a size of ~ 60 nm. NTs also have the advantage of the availability of multiple different SERRS pattern NTs. This opens the possibility for multiplexing in future. Further the method of SERRS detection was changed. The laser used in the experiments above had the disadvantage that the distance from laser to tissue was changeable and therefore the focus and subsequently the intensity of SERRS output is variable. To overcome this problem a different laser was used with a cone head to standardize laser-tissue distance (see methods Figure 2.4).

5.4.5 SERRS profile of nanotags (NT)

Figure 5.15 demonstrates the SERRS pattern of two different NTs. NT440 and NT420 exhibit different distinct peaks. Comparing the pattern of both NTs identifies a discrete peak for NT420 at ~1068 and ~1300 Raman shifts. On the other hand NT440 shows a discrete peak at ~1325 (Figure 5.15).

Bioactivity of NTs linked to the protein ETA has been tested as well. This has been demonstrated in “Figure 5.6 Biological binding properties of ETA-NT440.”.

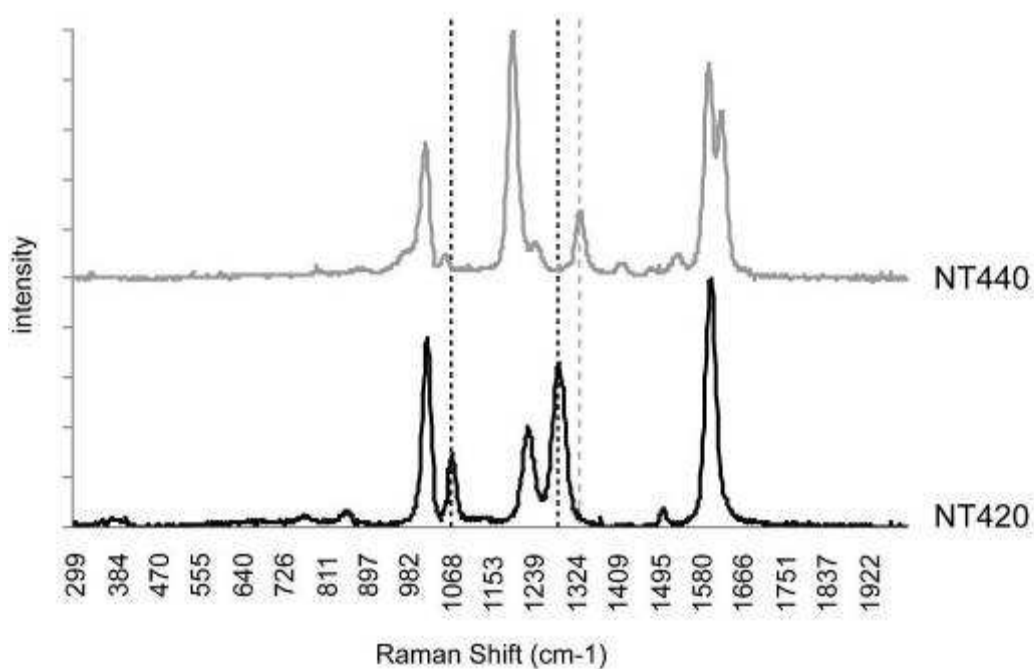


Figure 5.15 SERRS profile of NT440 and NT420

Solely the patterns for NT440 and NT420 are unique, however, for multiplexing experiments distinct peaks have been identified. SERRS profile Raman shifts of NT440 with a distinct peak at ~1325. Distinct intensity peaks for NT420 at ~ 1068 and ~1300. Representative measurement of $n=2$.

5.4.6 Detection of *i.v.* administered NT440 *in vivo*

To test if NTs were also detectable *in vivo*, a solution of PBS containing NT440 was injected *i.v.*. Six h later, mice were sacrificed and organ uptake was measured *in situ* with the cone laser head. Clear detection of SERRS output by NT440 was observed in organs of the RES (Figure 5.16A). Spleen showed highest intensity compared to liver. Control organs measured were lung, kidney, heart, muscle and lymph nodes and no signal was detected in these organs (only heart shown). Distinct peaks in liver and spleen are shown with for example the double peak at ~1600 Raman shifts. To compare intensity of NTs, Figure 5.16B demonstrates spleen, liver and heart signals in relation to NT440 (named in figure NP 1:10) measured in the tube.

In conclusion, NTs are detectable *in vivo* with a distinct SERRS output, accumulating mainly in the RES (liver and spleen).

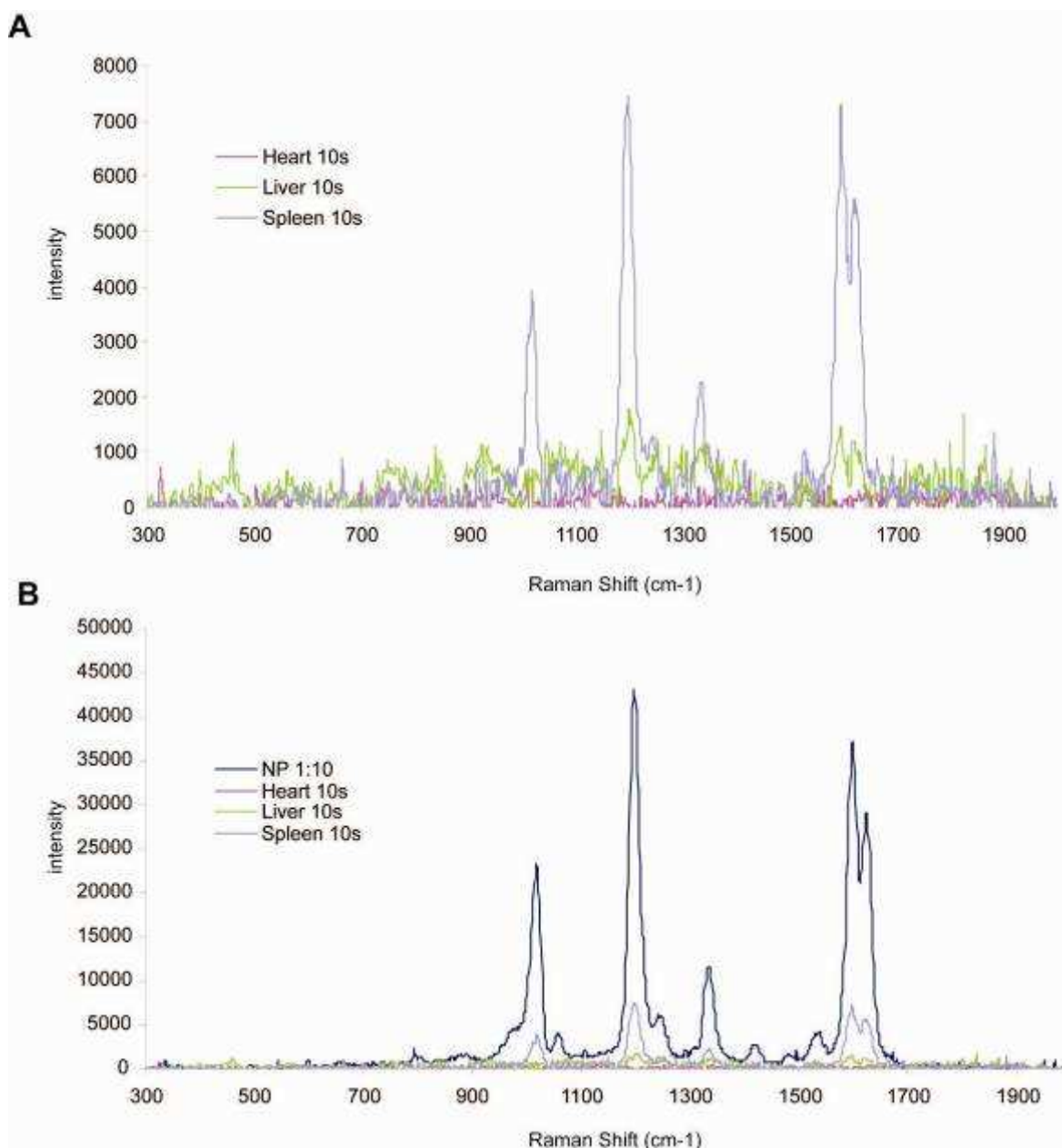


Figure 5.16 SERRS signal of NT440 in tissue.

Injection of 100 μ l NT440 (1:10 dilution) i.v. and detection 6 h later, n=2. With an accumulation time of 10 s clear NT440 Raman peaks are detectable in organs of the RES (liver and spleen) compared to no signal in the heart (A). B demonstrates the different intensity of NT440 in RES organs compared to NT440 (NP) measured directly in a tube.

5.4.7 Ex vivo SERRS mapping analysis of spleen

Figure 5.16 demonstrates the feasibility of SERRS detection in organs. However, high resolution for imaging was not achieved with a handheld laser set-up and no cellular resolution could be utilized from this approach. To overcome this problem and to determine if NTs are detectable within an organ structure or at the cellular level, spleens were harvested, snap frozen and mounted in OCT. Cryosections were cut, tissue fixed and stained with haematoxylin for visualisation. Mounted slides were analysed on a fast mapping Raman detection system (Centre for Nanometrology). NTs accumulate in the spleen with specific Raman signals in distinct regions (Figure 5.17). Shown is a spleen section; the SERRS map was colored by integrating the area under single characteristic peaks (here 1600 peak). A single point at the cross section in the picture is reflected by the Raman curve below demonstrating the distinct double peak at ~1600.

This experiment demonstrates the feasibility to use SERRS as a potential new method for imaging.

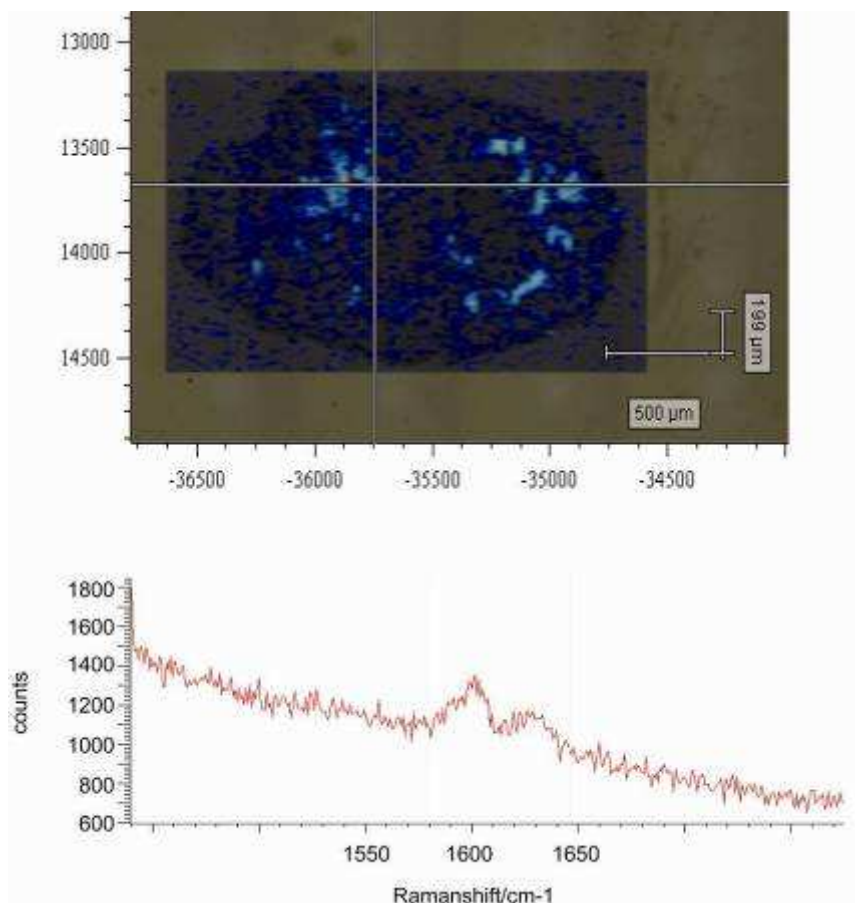


Figure 5.17 SERRS image of a spleen section.
Renshaw InVia SERRS map of frozen spleen derived section. From the experiment above (Figure 5.16) spleens were harvested, snapfrozen and mounted in OCT. 8 μm sections were cut, fixed, counterstained with haematoxylin and mounted. For analysis of the tissue the distinct NT440 Raman double peak at ~ 1600 (compare with Figure 5.16) was used (bottom panel). The tissue was scanned and Raman counts (intensity) are shown as a heat map (top panel). Raman counts of the cross-section point in the spleen section (top panel) are shown in the bottom panel.

5.4.8 Multiplexing of NT *in vivo* and *ex vivo*

To exploit the actual advantage of SERRS with distinct peak patterns to multiplex a combination of NTs were injected i.v. and examined *ex vivo*.

NT440 and NT420 were injected either alone or as a mixture. Figure 5.18A shows the different Raman pattern for both NTs. Six h after injection mice were sacrificed and spleen and liver measured. NT440 showed a distinct pattern of expression in both organs with a 1 s capture time (Figure 5.18B, dark green: liver; bright green: spleen). NT420 had a weaker signature at 1 s capture time, but still a discrete peak at 1600 was detectable (Figure 5.18C). Increasing the capture time enhanced the pattern and produced a clearer graph (data not shown). To test, if the NT SERRS signal is influenced by linking proteins to NTs, NT420 linked with ETA was examined (Figure 5.18D). Liver measurement demonstrated again a weak but distinct signal at 1 s capture times, but when increased to 5 s, peaks were sharper with higher intensity and NT420 pattern clear visible (dark grey 1 s, bright grey 5 s). Finally, injection of NT420 and NT440 mixture revealed a detectable Raman fingerprint. All of the peaks can be assigned to the NT440 in the mixture; no clear peak of NT420 is distinguishable (Figure 5.18E).

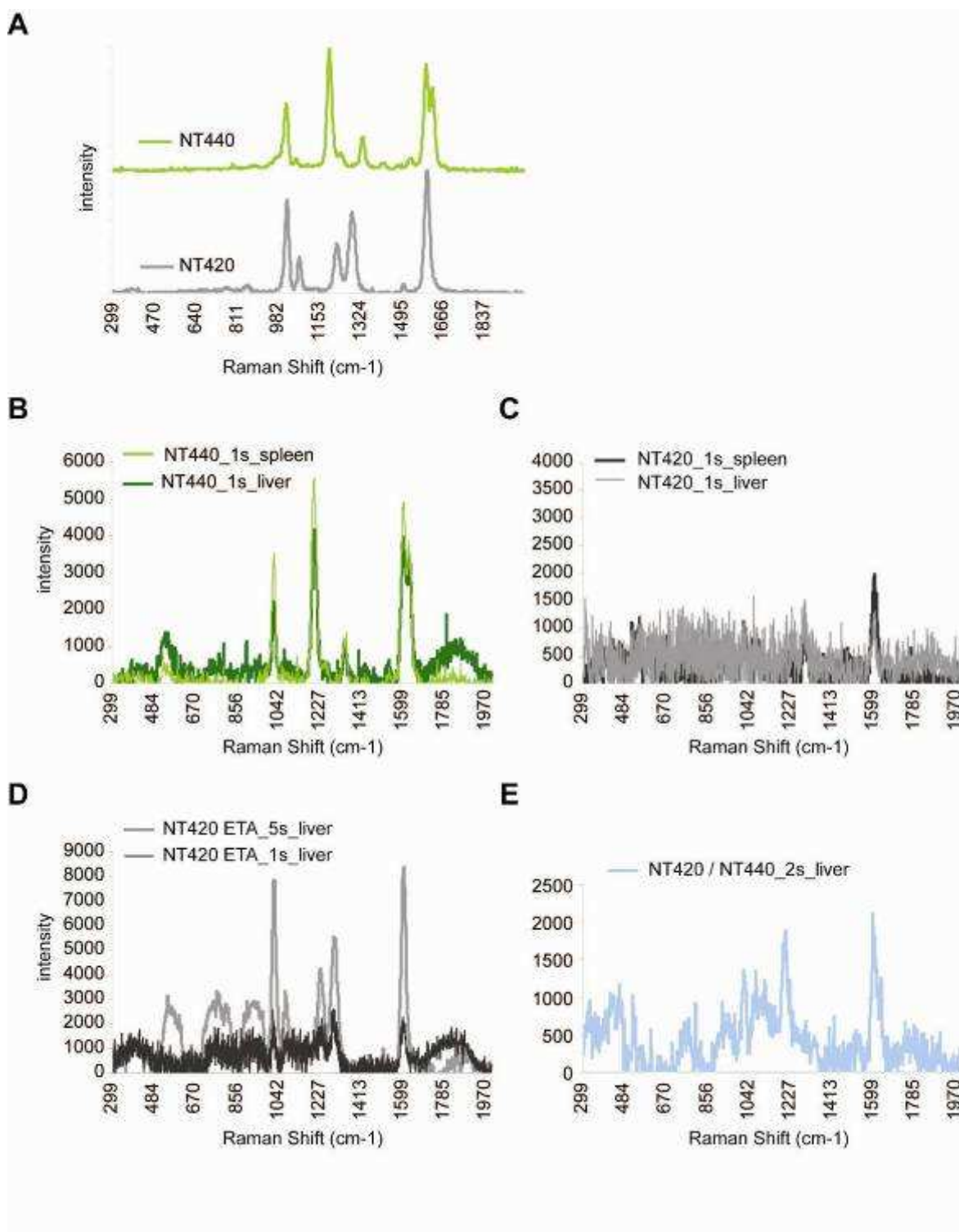


Figure 5.18 SERRS signals of liver and spleen in NT injected mice. SERRS active NTs (NT440 and NT420) were injected i.v. and 6 h later measured in liver and spleen for their expression and signal strength (1 mouse per injection, n=1). A. shows different Raman pattern of NT440 and NT420. B. Single injection of NT440 demonstrates clear detection in liver and spleen (capture time 1 s). C. Single injection of NT420 with low detection in liver (capture time 1 s). D. NT420 linked with ETA retains SERRS pattern in tissue (capture time 1 s and 5 s). E. Injection of NT440 / NT420 and measurement in liver. SERRS signal detectable, but no differentiation between NTs possible (similar result for spleen and longer capture times).

5.5 Conclusion and Discussion

The aim of this chapter was to develop nanoparticle probes as a novel tool to image inflammation with use of SERRS. SERRS active probes provide a unique detection platform capable in theory of surpassing fluorescent alternatives. Owing to the loss of signal observed through tissue dampening effects (quenching) broad wavelength fluorescence analysis is not possible *in vivo*. There exists a window between 7XX nm -8XX nm where laser analysis can be optimised and SERRS probes allow multiplexed deep tissue imaging in this region. Not only is the specificity of SERRS probes an advantage but also the spectra used offer opportunities: this does not induce heat compared to lasers normally used for fluorescence which would cause heat damage to the tissue. This chapter arises from a unique collaboration between the Centre for Molecular Nanometrology and Division of Immunology addressing a fascinating subject translating novel chemical discoveries into biological applications. Joining two expertises together is mandatory for success; however, it also identifies limitations and learning opportunities on both sides.

Two goals were addressed in this chapter: first, to determine the linking ability of SERRS active NPs with proteins, and second, to utilize SERRS active NPs to image inflammation *in vivo*. Here, I show that we can link proteins to NPs, and these constructs remain bioactive. Limitations were batch inconsistencies in protein concentrations but also in SERRS intensity. Also HeLa bioactivity assays lack a NP only or NP-IgG control. Further NPs linked with proteins aggregated over time and therefore again led to reduced concentration. The SERRS active linker was attached to the gold NP by a thiol adsorption. The protein was then covalently attached to the SERRS active linker. Although unlikely, a potential detachment could occur at the disulfide bond releasing the protein. In a cell culture system, ETA linked NPs were able to prevent TNF stimulus on HeLa cells to produce IL-6.

This indicates potential side effects of nanoparticles *in vivo*. Not only does induction of cell death in phagocytosing cells have to be considered, but also potential influences on the RES, potential accumulation in the lung, secretion by the kidneys, interaction with platelets and erythrocytes. Each factor is a

probable site for side effects ranging from a low to severe potential. Incubation in 50 % FCS at 37°C for 1 h has been tested for SERRS activity loss with no difference detected (Dr Stevenson, data not shown); however, performance in 100 % serum or equivalent incubations reflecting *in vivo* situation has not been studied in regard to accumulation, aggregation, protein loss, and changes in bioactivity and are rarely studied in other published reports. Despite these issues manufacturing of SERRS active NPs linked to ETA was possible. In conclusion, these NPs studied *in vitro* were bioactive and retained their SERRS signaling capability.

In vivo experiments performed in this thesis considerably advanced knowledge about the capability of NPs and their measurement. Thus the initial laser used was dependent on the distance and observer; a switch to a different system achieved a defined distance between tissue and laser exit which was less observer dependent. Further we could demonstrate that NPs are detectable *in vivo* with accumulation in the RES. These data are in concurrence with Qian et al. (223). Unfortunately, quantitative measurement of inflammation was not achievable. This could be due to the fact that the NPs used were too small to deliver a strong SERRS signal. Qian et al used 60 nm size NPs where NPs used here in the carragean inflammation model were ~15 nm. However, also other unknown factors could have influenced the experiment such as ETA as proper protein-target choice, concentration of NP or ETA, time of administration or the model as the right selection could be questioned. Future studies will be required to resolve these issues.

To address the capability to image NPs and to potential multiplex *in vivo* we switched to NTs which are bigger in size and provide a set of different NTs with distinct SERRS patterns available. Here, we could demonstrate that NTs are measurable *in vivo*; however, multiplexing was not feasible with the current methods used. Gambhir and colleagues published multiplexing studies in nude mice (249). In our approach, SERRS imaging of tissue slices was measured by a Renishaw InVia Raman microscope. Conversely, NPs in tissue were measured with a handheld laser with restricted detection capabilities. Thus Gambhir demonstrated the feasibility of multiplexing; however, with our resources this was not reproducible as yet.

Despite the problems addressed thus far, the method has a high potential for success. Currently, driven by nanoparticles imaged with MRI, different techniques will become accepted and the field of activity will grow addressing topics such as biodistribution, excretion and a rapid clearance from blood (250). NPs taken forward by the cancer field as therapeutics and cancer detection will lead to future knowledge and utilization in inflammation diagnostics. In summary, we demonstrated how NPs can be assembled to present bioactive molecules and how these NPs might be used for imaging of inflammation. Further we provided preliminary work which address solvable limitations in this method.

6 Discussion & conclusion

Cytokines play a pivotal role in the cellular network by sending messages with a huge variation of content. This can range from simple production orders, to signals of danger and thus activation of cells or messages with the aim to tranquilize the responder or even to initiate self destruction. This tense framework of cytokines supports the body defence against intruders and is precisely balanced between immune activation and inhibition. Thus this guarantees a fast response to matters of immune defence in which the system has to react as quickly as possible. However, as fast as the system has been activated, scavenging mechanisms such as decoy receptors, regulatory proteins and cells can rebalance the system. Combined with host defence memory it can react even faster in similar future events. Although this system seems perfect for its purpose, the balance can tip over in the wrong context. Thus, in autoimmune diseases cytokines have been shown to play a critical role as mediators of autoimmunity. Twenty years after the introduction of TNF blockade in RA, now nearly every cytokine has been addressed in this context and have been chosen as therapeutic target.

In this thesis three novel cytokines have been studied. IL-33 for its novelty being a recent described IL-1 family cytokine, IL-17 and IL-23 not for its timely novelty but its novelty in the knowledge in its crucial role of inflammation. Recent trials demonstrated that IL-17 or IL-23 blockade leads to brilliant outcome in autoimmune psoriasis. For IL-17/IL-23 aim was to address which cells are the source in RA, as data so far were scarce in regard to local tissue expression and despite clear evidence that Th17 cells are main producer of IL-17, more and more other cells have been described to add IL-17 to their cytokine portfolio. Unexpectedly, I have demonstrated that not Th17 cells but mast cells are the main source in RA synovium (239). This contradicts various publications in which Th17 cells have been described to play a pivotal role in RA synovium (98, 251). Expression of IL-17 by mast cells, but also other cells like NKT cells, NK cells, macrophages, neutrophils, eosinophils and CD4 positive lymphoid tissue inducer-like cells have been described (229, 230, 239, 252). Origin in multiple sources demonstrates the ability of adaptive but also innate parts of the immune system to produce an important cytokine for host defence. A similar cytokine with high biologic potential is TNF- α , expressed also by cells of the innate and adaptive immune system. Thus the fact that mast cells produce IL-17 strengthens the

ambivalent role of pivotal cytokines by its production of multiple possible cells. Also these data rather reinforce than weaken the hypothesis of IL-17 blockade in autoimmune diseases.

IL-33, a Th2 cytokine which induces IL-5 and IL-13 has been reported to play a role in autoimmune arthritis which is defined as Th1/Th17 disease (145, 146). This is another cytokine with multiple roles, supporting either a Th2 profile for parasite defence or Th1/Th17 profile studied in arthritis depending on the environment. In skin disease, a misbalance to Th2 can lead to atopic dermatitis, where a shift to Th1/Th17 can induce psoriasis. Interestingly, presentation of pathology is similar in regard to histological changes and cells involved; however, clinical features such as areas involved are different as is the cytokine profile. Similar to the ambivalent source of IL-17, this demonstrates production of two totally different disease associated cytokines by potentially the same cells. I studied IL-33 in psoriasis and detected high expression in human skin biopsies of psoriasis patients. Further, IL-33 epidermal injections led to psoriasis like dermatitis. Interestingly, cytokine profile in these experiments demonstrated a shift to Th2 with IL-33 signature cytokines such as IL-5 and IL-13. Pathology with epidermal thickening and infiltration of mast cells, macrophages and neutrophils could potentially account for an atopic Th2 disease. Despite this fact, the TPA model in ST2 deficient mice showed ameliorated skin inflammation allocates IL-33 more in the proinflammatory Th1/Th17 area. This cytokine with a crucial role as an alarmin seems to be able to tip the balance in the wrong context. It is surprising, how the normal protective effect of IL-33 is susceptible for these changes, although this would account for a high sensitivity in a system. Even more complex is the interplay with sST2/ST2. It could be that sST2 is released to limit the alarmin effect and thereby blocks the normal protective effect of IL-33. This would allow pathology and comorbidity to emerge in patients in whom IL-33 is involved in pathology such as asthma or RA. Evidence was shown by Dr Alves-Filho with IL-33 attenuating sepsis (152). Individuals who did not recover from sepsis had significantly more soluble ST2 those who did recover demonstrating the protective role of IL-33 countered by sST2.

Understanding the biology of the cytokine IL-33 is central to understanding its role in disease and how it can account for different types of diseases. Making it even more complex, IL-33 is expressed in the nucleus as a suppressor of

transcription, it was surprising to address the role of IL-33 in the nucleus in which Girard and colleagues showed the conserved features with binding to the heterochromatin and how a herpes virus uses this binding site for maintenance of viral genomes (137). Giving the hints, that IL-33 also is expressed in the embryo, however, most likely by a different splice variant adds another feature to IL-33's portfolio. This preliminary data and initial hypothesis needs to be further investigated.

At last, I explored how nanoparticles can be utilized to image inflammation, to translate insights of cytokine biology and relevance in pathology, to early disease diagnosis. At a glance, despite being premature, it might be feasible to drive this technology to further levels. Undoubtedly, its potential has advantages compared to common techniques such as PET, MRI and other imaging modalities. However, also downsides which have to be addressed cautiously are present: toxicity (such as haematological alterations, immune system activation, and organ accumulation), long term effects but also clearance with kidney and lung involvement. With the cancer field pushing nanomedicines (nanoparticles linked with chemotherapeutics or proteins such as antibodies) forward, most of these queries will be answered in the future. Thus more work needs to be done to find the best possible target (or combination of multiple targets), setting and optimal technological realisation for early inflammation imaging.

While medicine and especially rheumatology constantly advances in its knowledge about disease pathology, major questions still remain. This work demonstrated how complex even initial translations from mouse to human are, by discovering the source of IL-17 in synovium and thus complicating the Th1-Th2-Th17 understanding. Further the ambivalent role of IL-33 supports the immense complexity of cytokine biology. Future studies must identify which mediators are responsible for certain diseases and should elucidate in which context certain cytokines play what kind of role. Finally, understanding the ambivalent role of cytokines is now a matter of paramount importance, representing a factor of unexpected outcome and is crucial for future targeted therapies.

7 References

1. Arnett, F. C., S. M. Edworthy, D. A. Bloch, D. J. McShane, J. F. Fries, N. S. Cooper, L. A. Healey, S. R. Kaplan, M. H. Liang, H. S. Luthra, and et al. 1988. The American Rheumatism Association 1987 revised criteria for the classification of rheumatoid arthritis. *Arthritis and rheumatism* 31:315-324.
2. Aletaha, D., T. Neogi, A. J. Silman, J. Funovits, D. T. Felson, C. O. Bingham, 3rd, N. S. Birnbaum, G. R. Burmester, V. P. Bykerk, M. D. Cohen, B. Combe, K. H. Costenbader, M. Dougados, P. Emery, G. Ferraccioli, J. M. Hazes, K. Hobbs, T. W. Huizinga, A. Kavanaugh, J. Kay, T. K. Kvien, T. Laing, P. Mease, H. A. Menard, L. W. Moreland, R. L. Naden, T. Pincus, J. S. Smolen, E. Stanislawska-Biernat, D. Symmons, P. P. Tak, K. S. Upchurch, J. Vencovsky, F. Wolfe, and G. Hawker. 2010 rheumatoid arthritis classification criteria: an American College of Rheumatology/European League Against Rheumatism collaborative initiative. *Annals of the rheumatic diseases* 69:1580-1588.
3. Vossenaar, E. R., T. J. Smeets, M. C. Kraan, J. M. Raats, W. J. van Venrooij, and P. P. Tak. 2004. The presence of citrullinated proteins is not specific for rheumatoid synovial tissue. *Arthritis and rheumatism* 50:3485-3494.
4. Zendman, A. J., E. R. Vossenaar, and W. J. van Venrooij. 2004. Autoantibodies to citrullinated (poly)peptides: a key diagnostic and prognostic marker for rheumatoid arthritis. *Autoimmunity* 37:295-299.
5. Lundberg, K., S. Nijenhuis, E. R. Vossenaar, K. Palmblad, W. J. van Venrooij, L. Klareskog, A. J. Zendman, and H. E. Harris. 2005. Citrullinated proteins have increased immunogenicity and arthritogenicity and their presence in arthritic joints correlates with disease severity. *Arthritis research & therapy* 7:R458-467.
6. Redlich, K., G. Schett, G. Steiner, S. Hayer, E. F. Wagner, and J. S. Smolen. 2003. Rheumatoid arthritis therapy after tumor necrosis factor and interleukin-1 blockade. *Arthritis and rheumatism* 48:3308-3319.
7. Finckh, A., J. F. Simard, C. Gabay, and P. A. Guerne. 2006. Evidence for differential acquired drug resistance to anti-tumour necrosis factor agents in rheumatoid arthritis. *Annals of the rheumatic diseases* 65:746-752.
8. Taylor, W., D. Gladman, P. Helliwell, A. Marchesoni, P. Mease, and H. Mielants. 2006. Classification criteria for psoriatic arthritis: development of new

- criteria from a large international study. *Arthritis and rheumatism* 54:2665-2673.
9. Wilson, F. C., M. Icen, C. S. Crowson, M. T. McEvoy, S. E. Gabriel, and H. M. Kremers. 2009. Time trends in epidemiology and characteristics of psoriatic arthritis over 3 decades: a population-based study. *The Journal of rheumatology* 36:361-367.
 10. McGonagle, D., W. Gibbon, P. O'Connor, M. Green, C. Pease, and P. Emery. 1998. Characteristic magnetic resonance imaging enthesal changes of knee synovitis in spondylarthropathy. *Arthritis Rheum* 41:694-700 Order.
 11. Veale, D. J. 2000. The epidemiology of psoriatic arthritis: fact or fiction? *J Rheumatol* 27:1105-1106.
 12. Moll, J. M., and V. Wright. 1973. Psoriatic arthritis. *Seminars in arthritis and rheumatism* 3:55-78.
 13. Bennett, R. 1979. Psoriatic arthritis. *McCarty DJ, editor. Arthritis and allied conditions. 9th ed. Philadelphia: Lea & Febiger:p.* 645.
 14. Gladman, D. D., R. Shuckett, M. L. Russell, J. C. Thorne, and R. K. Schachter. 1987. Psoriatic arthritis (PSA)--an analysis of 220 patients. *The Quarterly journal of medicine* 62:127-141.
 15. Vasey, F., and L. Espinoza. 1984. Psoriatic arthropathy. . *Calin A, editor. Spondyloarthropathies. Orlando (FL): Grune & Stratton p.* 151-85.
 16. Dougados, M., S. van der Linden, R. Juhlin, B. Huitfeldt, B. Amor, A. Calin, A. Cats, B. Dijkmans, I. Olivieri, G. Pasero, and et al. 1991. The European Spondylarthropathy Study Group preliminary criteria for the classification of spondylarthropathy. *Arthritis and rheumatism* 34:1218-1227.
 17. McGonagle, D., P. G. Conaghan, and P. Emery. 1999. Psoriatic arthritis: a unified concept twenty years on. *Arthritis and rheumatism* 42:1080-1086.
 18. Fournie, B., L. Crognier, C. Arnaud, L. Zabraniecki, V. Lascaux-Lefebvre, V. Marc, E. Ginesty, V. Andrieu, C. Dromer, and A. Fournie. 1999. Proposed classification criteria of psoriatic arthritis. A preliminary study in 260 patients. *Revue du rhumatisme (English ed* 66:446-456.
 19. Griffiths, C. E., and J. N. Barker. 2007. Pathogenesis and clinical features of psoriasis. *Lancet* 370:263-271.

20. Stern, R. S. 1985. The epidemiology of joint complaints in patients with psoriasis. *The Journal of rheumatology* 12:315-320.
21. Pattison, E., B. J. Harrison, C. E. Griffiths, A. J. Silman, and I. N. Bruce. 2008. Environmental risk factors for the development of psoriatic arthritis: results from a case-control study. *Annals of the rheumatic diseases* 67:672-676.
22. Avina-Zubieta, J. A., H. K. Choi, M. Sadatsafavi, M. Etminan, J. M. Esdaile, and D. Lacaille. 2008. Risk of cardiovascular mortality in patients with rheumatoid arthritis: a meta-analysis of observational studies. *Arthritis and rheumatism* 59:1690-1697.
23. Gladman, D. D., M. Ang, L. Su, B. D. Tom, C. T. Schentag, and V. T. Farewell. 2009. Cardiovascular morbidity in psoriatic arthritis. *Annals of the rheumatic diseases* 68:1131-1135.
24. Wakkee, M., R. M. Herings, and T. Nijsten. Psoriasis may not be an independent risk factor for acute ischemic heart disease hospitalizations: results of a large population-based Dutch cohort. *The Journal of investigative dermatology* 130:962-967.
25. Mehta, N. N., R. S. Azfar, D. B. Shin, A. L. Neimann, A. B. Troxel, and J. M. Gelfand. 2009. Patients with severe psoriasis are at increased risk of cardiovascular mortality: cohort study using the General Practice Research Database. *European heart journal*.
26. Glick, E. N. 1967. Asymmetrical rheumatoid arthritis after poliomyelitis. *British medical journal* 3:26-28.
27. Kane, D., J. C. Lockhart, P. V. Balint, C. Mann, W. R. Ferrell, and I. B. McInnes. 2005. Protective effect of sensory denervation in inflammatory arthritis (evidence of regulatory neuroimmune pathways in the arthritic joint). *Annals of the rheumatic diseases* 64:325-327.
28. McGonagle, D. 2005. Imaging the joint and enthesis: insights into pathogenesis of psoriatic arthritis. *Annals of the rheumatic diseases* 64 Suppl 2:ii58-60.
29. Smolen, J. S., R. Landewe, F. C. Breedveld, M. Dougados, P. Emery, C. Gaujoux-Viala, S. Gorter, R. Knevel, J. Nam, M. Schoels, D. Aletaha, M. Buch, L. Gossec, T. Huizinga, J. W. Bijlsma, G. Burmester, B. Combe, M. Cutolo, C. Gabay, J. Gomez-Reino, M. Kouloumas, T. K. Kvien, E. Martin-Mola, I. McInnes, K. Pavelka, P. van Riel, M. Scholte, D. L. Scott, T. Sokka, G. Valesini, R. van Vollenhoven, K. L. Winthrop, J. Wong, A. Zink, and D. van der Heijde. EULAR

- recommendations for the management of rheumatoid arthritis with synthetic and biological disease-modifying antirheumatic drugs. *Annals of the rheumatic diseases* 69:964-975.
30. Mease, P. J. 2009. Psoriatic arthritis assessment and treatment update. *Current opinion in rheumatology* 21:348-355.
31. van Vollenhoven, R. F. 2009. Treatment of rheumatoid arthritis: state of the art 2009. *Nature reviews* 5:531-541.
32. Papp, K. A., R. G. Langley, M. Lebwohl, G. G. Krueger, P. Szapary, N. Yeilding, C. Guzzo, M. C. Hsu, Y. Wang, S. Li, L. T. Dooley, and K. Reich. 2008. Efficacy and safety of ustekinumab, a human interleukin-12/23 monoclonal antibody, in patients with psoriasis: 52-week results from a randomised, double-blind, placebo-controlled trial (PHOENIX 2). *Lancet* 371:1675-1684.
33. Gottlieb, A., A. Menter, A. Mendelsohn, Y. K. Shen, S. Li, C. Guzzo, S. Fretzin, R. Kunyetz, and A. Kavanaugh. 2009. Ustekinumab, a human interleukin 12/23 monoclonal antibody, for psoriatic arthritis: randomised, double-blind, placebo-controlled, crossover trial. *Lancet* 373:633-640.
34. Hueber, A. J., and I. B. McInnes. 2008. Pathogenesis in RA - Cytokines. *Rheumatoid Arthritis, Hochberg, et al. Mosby*. Book chapter.
35. Coenen, M. J., and P. K. Gregersen. 2009. Rheumatoid arthritis: a view of the current genetic landscape. *Genes and immunity* 10:101-111.
36. Stolt, P., C. Bengtsson, B. Nordmark, S. Lindblad, I. Lundberg, L. Klareskog, and L. Alfredsson. 2003. Quantification of the influence of cigarette smoking on rheumatoid arthritis: results from a population based case-control study, using incident cases. *Annals of the rheumatic diseases* 62:835-841.
37. Nograles, K. E., R. D. Brasington, and A. M. Bowcock. 2009. New insights into the pathogenesis and genetics of psoriatic arthritis. *Nature clinical practice* 5:83-91.
38. Barton, A. 2010. HLA and other susceptibility genes in rheumatoid arthritis. R. Maini, ed. UpToDate.
39. Tan, A. L., M. Benjamin, H. Toumi, A. J. Grainger, S. F. Tanner, P. Emery, and D. McGonagle. 2007. The relationship between the extensor tendon enthesis and the nail in distal interphalangeal joint disease in psoriatic arthritis--a high-resolution MRI and histological study. *Rheumatology (Oxford, England)* 46:253-256.

40. Lowes, M. A., A. M. Bowcock, and J. G. Krueger. 2007. Pathogenesis and therapy of psoriasis. *Nature* 445:866-873.
41. Zenz, R., R. Eferl, L. Kenner, L. Florin, L. Hummerich, D. Mehic, H. Scheuch, P. Angel, E. Tschachler, and E. F. Wagner. 2005. Psoriasis-like skin disease and arthritis caused by inducible epidermal deletion of Jun proteins. *Nature* 437:369-375.
42. Weyand, C. M., K. C. Hicok, D. L. Conn, and J. J. Goronzy. 1992. The influence of HLA-DRB1 genes on disease severity in rheumatoid arthritis. *Ann Intern Med* 117:801-806.
43. Keystone, E. C. 2003. Abandoned therapies and unpublished trials in rheumatoid arthritis. *Current opinion in rheumatology* 15:253-258.
44. Genovese, M. C., J. C. Becker, M. Schiff, M. Luggen, Y. Sherrer, J. Kremer, C. Birbara, J. Box, K. Natarajan, I. Nuamah, T. Li, R. Aranda, D. T. Hagerty, and M. Dougados. 2005. Abatacept for rheumatoid arthritis refractory to tumor necrosis factor alpha inhibition. *The New England journal of medicine* 353:1114-1123.
45. Edwards, J. C., L. Szczepanski, J. Szechinski, A. Filipowicz-Sosnowska, P. Emery, D. R. Close, R. M. Stevens, and T. Shaw. 2004. Efficacy of B-cell-targeted therapy with rituximab in patients with rheumatoid arthritis. *The New England journal of medicine* 350:2572-2581.
46. Firestein, G. S. 2003. Evolving concepts of rheumatoid arthritis. *Nature* 423:356-361.
47. Plenge, R. M., L. Padyukov, E. F. Remmers, S. Purcell, A. T. Lee, E. W. Karlson, F. Wolfe, D. L. Kastner, L. Alfredsson, D. Altshuler, P. K. Gregersen, L. Klareskog, and J. D. Rioux. 2005. Replication of putative candidate-gene associations with rheumatoid arthritis in >4,000 samples from North America and Sweden: association of susceptibility with PTPN22, CTLA4, and PADI4. *American journal of human genetics* 77:1044-1060.
48. Burr, M. L., H. Naseem, A. Hinks, S. Eyre, L. J. Gibbons, J. Bowes, A. G. Wilson, J. Maxwell, A. W. Morgan, P. Emery, S. Steer, L. Hocking, D. M. Reid, P. Wordsworth, P. Harrison, W. Thomson, J. Worthington, and A. Barton. 2010. PADI4 genotype is not associated with rheumatoid arthritis in a large UK Caucasian population. *Annals of the rheumatic diseases* 69:666-670.

49. Brentano, F., D. Kyburz, O. Schorr, R. Gay, and S. Gay. 2005. The role of Toll-like receptor signalling in the pathogenesis of arthritis. *Cell Immunol* 233:90-96.
50. McInnes, I. B., and G. Schett. 2007. Cytokines in the pathogenesis of rheumatoid arthritis. *Nat Rev Immunol* 7:429-442.
51. Feldmann, M., F. M. Brennan, and R. N. Maini. 1996. Rheumatoid arthritis. *Cell* 85:307-310.
52. Black, R. A., C. T. Rauch, C. J. Kozlosky, J. J. Peschon, J. L. Slack, M. F. Wolfson, B. J. Castner, K. L. Stocking, P. Reddy, S. Srinivasan, N. Nelson, N. Boiani, K. A. Schooley, M. Gerhart, R. Davis, J. N. Fitzner, R. S. Johnson, R. J. Paxton, C. J. March, and D. P. Cerretti. 1997. A metalloproteinase disintegrin that releases tumour-necrosis factor-alpha from cells. *Nature* 385:729-733.
53. Eck, M. J., and S. R. Sprang. 1989. The structure of tumor necrosis factor-alpha at 2.6 Å resolution. Implications for receptor binding. *The Journal of biological chemistry* 264:17595-17605.
54. Brennan, F. M., D. Chantry, A. Jackson, R. Maini, and M. Feldmann. 1989. Inhibitory effect of TNF alpha antibodies on synovial cell interleukin-1 production in rheumatoid arthritis. *Lancet* 2:244-247.
55. Keffer, J., L. Probert, H. Cazlaris, S. Georgopoulos, E. Kaslaris, D. Kioussis, and G. Kollias. 1991. Transgenic mice expressing human tumour necrosis factor: a predictive genetic model of arthritis. *The EMBO journal* 10:4025-4031.
56. Joosten, L. A., M. M. Helsen, T. Saxne, F. A. van De Loo, D. Heinegard, and W. B. van Den Berg. 1999. IL-1 alpha beta blockade prevents cartilage and bone destruction in murine type II collagen-induced arthritis, whereas TNF-alpha blockade only ameliorates joint inflammation. *J Immunol* 163:5049-5055.
57. Danning, C. L., G. G. Illei, C. Hitchon, M. R. Greer, D. T. Boumpas, and I. B. McInnes. 2000. Macrophage-derived cytokine and nuclear factor kappaB p65 expression in synovial membrane and skin of patients with psoriatic arthritis. *Arthritis and rheumatism* 43:1244-1256.
58. Goedkoop, A. Y., M. C. Kraan, D. I. Picavet, M. A. de Rie, M. B. Teunissen, J. D. Bos, and P. P. Tak. 2004. Deactivation of endothelium and reduction in angiogenesis in psoriatic skin and synovium by low dose infliximab therapy in combination with stable methotrexate therapy: a prospective single-centre study. *Arthritis research & therapy* 6:R326-334.

59. Ogilvie, A. L., M. Luftl, C. Antoni, G. Schuler, J. R. Kalden, and H. M. Lorenz. 2006. Leukocyte infiltration and mRNA expression of IL-20, IL-8 and TNF-R P60 in psoriatic skin is driven by TNF-alpha. *International journal of immunopathology and pharmacology* 19:271-278.
60. Goedkoop, A. Y., M. C. Kraan, M. B. Teunissen, D. I. Picavet, M. A. de Rie, J. D. Bos, and P. P. Tak. 2004. Early effects of tumour necrosis factor alpha blockade on skin and synovial tissue in patients with active psoriasis and psoriatic arthritis. *Annals of the rheumatic diseases* 63:769-773.
61. Schon, M. P. 2008. Animal models of psoriasis: a critical appraisal. *Experimental dermatology* 17:703-712.
62. Danilenko, D. M. 2008. Review paper: preclinical models of psoriasis. *Veterinary pathology* 45:563-575.
63. Li, A. G., D. Wang, X. H. Feng, and X. J. Wang. 2004. Latent TGFbeta1 overexpression in keratinocytes results in a severe psoriasis-like skin disorder. *The EMBO journal* 23:1770-1781.
64. Xia, Y. P., B. Li, D. Hylton, M. Detmar, G. D. Yancopoulos, and J. S. Rudge. 2003. Transgenic delivery of VEGF to mouse skin leads to an inflammatory condition resembling human psoriasis. *Blood* 102:161-168.
65. Poumay, Y., F. Dupont, S. Marcoux, M. Leclercq-Smekens, M. Herin, and A. Coquette. 2004. A simple reconstructed human epidermis: preparation of the culture model and utilization in in vitro studies. *Archives of dermatological research* 296:203-211.
66. Sa, S. M., P. A. Valdez, J. Wu, K. Jung, F. Zhong, L. Hall, I. Kasman, J. Winer, Z. Modrusan, D. M. Danilenko, and W. Ouyang. 2007. The effects of IL-20 subfamily cytokines on reconstituted human epidermis suggest potential roles in cutaneous innate defense and pathogenic adaptive immunity in psoriasis. *J Immunol* 178:2229-2240.
67. Jamieson, T., D. N. Cook, R. J. Nibbs, A. Rot, C. Nixon, P. McLean, A. Alcamí, S. A. Lira, M. Wiekowski, and G. J. Graham. 2005. The chemokine receptor D6 limits the inflammatory response in vivo. *Nature immunology* 6:403-411.
68. Chan, J. R., W. Blumenschein, E. Murphy, C. Diveu, M. Wiekowski, S. Abbondanzo, L. Lucian, R. Geissler, S. Brodie, A. B. Kimball, D. M. Gorman, K. Smith, R. de Waal Malefyt, R. A. Kastelein, T. K. McClanahan, and E. P. Bowman. 2006. IL-23 stimulates epidermal hyperplasia via TNF and IL-20R2-

dependent mechanisms with implications for psoriasis pathogenesis. *The Journal of experimental medicine* 203:2577-2587.

69. Zheng, Y., D. M. Danilenko, P. Valdez, I. Kasman, J. Eastham-Anderson, J. Wu, and W. Ouyang. 2007. Interleukin-22, a T(H)17 cytokine, mediates IL-23-induced dermal inflammation and acanthosis. *Nature* 445:648-651.

70. Hedrick, M. N., A. S. Lonsdorf, A. K. Shirakawa, C. C. Richard Lee, F. Liao, S. P. Singh, H. H. Zhang, A. Grinberg, P. E. Love, S. T. Hwang, and J. M. Farber. 2009. CCR6 is required for IL-23-induced psoriasis-like inflammation in mice. *The Journal of clinical investigation* 119:2317-2329.

71. Ma, H. L., S. Liang, J. Li, L. Napierata, T. Brown, S. Benoit, M. Senices, D. Gill, K. Dunussi-Joannopoulos, M. Collins, C. Nickerson-Nutter, L. A. Fouser, and D. A. Young. 2008. IL-22 is required for Th17 cell-mediated pathology in a mouse model of psoriasis-like skin inflammation. *The Journal of clinical investigation* 118:597-607.

72. Bettelli, E., T. Korn, and V. K. Kuchroo. 2007. Th17: the third member of the effector T cell trilogy. *Current opinion in immunology* 19:652-657.

73. Annunziato, F., and S. Romagnani. 2009. Heterogeneity of human effector CD4+ T cells. *Arthritis research & therapy* 11:257.

74. Mangan, P. R., L. E. Harrington, D. B. O'Quinn, W. S. Helms, D. C. Bullard, C. O. Elson, R. D. Hatton, S. M. Wahl, T. R. Schoeb, and C. T. Weaver. 2006. Transforming growth factor-beta induces development of the T(H)17 lineage. *Nature* 441:231-234.

75. Veldhoen, M., R. J. Hocking, C. J. Atkins, R. M. Locksley, and B. Stockinger. 2006. TGFbeta in the context of an inflammatory cytokine milieu supports de novo differentiation of IL-17-producing T cells. *Immunity* 24:179-189.

76. Zhou, L., Ivanov, II, R. Spolski, R. Min, K. Shenderov, T. Egawa, D. E. Levy, W. J. Leonard, and D. R. Littman. 2007. IL-6 programs T(H)-17 cell differentiation by promoting sequential engagement of the IL-21 and IL-23 pathways. *Nature immunology* 8:967-974.

77. Ivanov, II, B. S. McKenzie, L. Zhou, C. E. Tadokoro, A. Lepelley, J. J. Lafaille, D. J. Cua, and D. R. Littman. 2006. The orphan nuclear receptor RORgammat directs the differentiation program of proinflammatory IL-17+ T helper cells. *Cell* 126:1121-1133.

78. Park, H., Z. Li, X. O. Yang, S. H. Chang, R. Nurieva, Y. H. Wang, Y. Wang, L. Hood, Z. Zhu, Q. Tian, and C. Dong. 2005. A distinct lineage of CD4 T cells regulates tissue inflammation by producing interleukin 17. *Nature immunology* 6:1133-1141.
79. Stritesky, G. L., N. Yeh, and M. H. Kaplan. 2008. IL-23 promotes maintenance but not commitment to the Th17 lineage. *J Immunol* 181:5948-5955.
80. Acosta-Rodriguez, E. V., G. Napolitani, A. Lanzavecchia, and F. Sallusto. 2007. Interleukins 1beta and 6 but not transforming growth factor-beta are essential for the differentiation of interleukin 17-producing human T helper cells. *Nature immunology* 8:942-949.
81. Cosmi, L., R. De Palma, V. Santarlasci, L. Maggi, M. Capone, F. Frosali, G. Rodolico, V. Querci, G. Abbate, R. Angeli, L. Berrino, M. Fambrini, M. Caproni, F. Tonelli, E. Lazzeri, P. Parronchi, F. Liotta, E. Maggi, S. Romagnani, and F. Annunziato. 2008. Human interleukin 17-producing cells originate from a CD161+CD4+ T cell precursor. *The Journal of experimental medicine* 205:1903-1916.
82. Santarlasci, V., L. Maggi, M. Capone, F. Frosali, V. Querci, R. De Palma, F. Liotta, L. Cosmi, E. Maggi, S. Romagnani, and F. Annunziato. 2009. TGF-beta indirectly favors the development of human Th17 cells by inhibiting Th1 cells. *European journal of immunology* 39:207-215.
83. de Jong, E., T. Suddason, and G. M. Lord. Translational mini-review series on Th17 cells: development of mouse and human T helper 17 cells. *Clinical and experimental immunology* 159:148-158.
84. Acosta-Rodriguez, E. V., L. Rivino, J. Geginat, D. Jarrossay, M. Gattorno, A. Lanzavecchia, F. Sallusto, and G. Napolitani. 2007. Surface phenotype and antigenic specificity of human interleukin 17-producing T helper memory cells. *Nature immunology* 8:639-646.
85. Liu, H., and C. Rohowsky-Kochan. 2008. Regulation of IL-17 in human CCR6+ effector memory T cells. *J Immunol* 180:7948-7957.
86. Evans, H. G., T. Suddason, I. Jackson, L. S. Taams, and G. M. Lord. 2007. Optimal induction of T helper 17 cells in humans requires T cell receptor ligation in the context of Toll-like receptor-activated monocytes. *Proceedings of the National Academy of Sciences of the United States of America* 104:17034-17039.

87. Zhou, L., M. M. Chong, and D. R. Littman. 2009. Plasticity of CD4⁺ T cell lineage differentiation. *Immunity* 30:646-655.
88. Nadkarni, S., C. Mauri, and M. R. Ehrenstein. 2007. Anti-TNF-alpha therapy induces a distinct regulatory T cell population in patients with rheumatoid arthritis via TGF-beta. *The Journal of experimental medicine* 204:33-39.
89. Sugiyama, H., R. Gyulai, E. Toichi, E. Garaczi, S. Shimada, S. R. Stevens, T. S. McCormick, and K. D. Cooper. 2005. Dysfunctional blood and target tissue CD4⁺CD25^{high} regulatory T cells in psoriasis: mechanism underlying unrestrained pathogenic effector T cell proliferation. *J Immunol* 174:164-173.
90. Charles, P., M. J. Elliott, D. Davis, A. Potter, J. R. Kalden, C. Antoni, F. C. Breedveld, J. S. Smolen, G. Eberl, K. deWoody, M. Feldmann, and R. N. Maini. 1999. Regulation of cytokines, cytokine inhibitors, and acute-phase proteins following anti-TNF-alpha therapy in rheumatoid arthritis. *J Immunol* 163:1521-1528.
91. Yao, Z., W. C. Fanslow, M. F. Seldin, A. M. Rousseau, S. L. Painter, M. R. Comeau, J. I. Cohen, and M. K. Spriggs. 1995. Herpesvirus Saimiri encodes a new cytokine, IL-17, which binds to a novel cytokine receptor. *Immunity* 3:811-821.
92. Liang, S. C., A. J. Long, F. Bennett, M. J. Whitters, R. Karim, M. Collins, S. J. Goldman, K. Dunussi-Joannopoulos, C. M. Williams, J. F. Wright, and L. A. Fouser. 2007. An IL-17F/A heterodimer protein is produced by mouse Th17 cells and induces airway neutrophil recruitment. *J Immunol* 179:7791-7799.
93. Toy, D., D. Kugler, M. Wolfson, T. Vanden Bos, J. Gurgel, J. Derry, J. Tocker, and J. Peschon. 2006. Cutting edge: interleukin 17 signals through a heteromeric receptor complex. *J Immunol* 177:36-39.
94. Fossiez, F., O. Djossou, P. Chomarat, L. Flores-Romo, S. Ait-Yahia, C. Maat, J. J. Pin, P. Garrone, E. Garcia, S. Saeland, D. Blanchard, C. Gaillard, B. Das Mahapatra, E. Rouvier, P. Golstein, J. Banchereau, and S. Lebecque. 1996. T cell interleukin-17 induces stromal cells to produce proinflammatory and hematopoietic cytokines. *The Journal of experimental medicine* 183:2593-2603.
95. Crome, S. Q., A. Y. Wang, and M. K. Levings. Translational mini-review series on Th17 cells: function and regulation of human T helper 17 cells in health and disease. *Clinical and experimental immunology* 159:109-119.

96. van de Veerdonk, F. L., M. S. Gresnigt, B. J. Kullberg, J. W. van der Meer, L. A. Joosten, and M. G. Netea. 2009. Th17 responses and host defense against microorganisms: an overview. *BMB reports* 42:776-787.
97. Distler, J. H., L. C. Huber, A. J. Hueber, C. F. Reich, 3rd, S. Gay, O. Distler, and D. S. Pisetsky. 2005. The release of microparticles by apoptotic cells and their effects on macrophages. *Apoptosis* 10:731-741.
98. Chabaud, M., J. M. Durand, N. Buchs, F. Fossiez, G. Page, L. Frappart, and P. Miossec. 1999. Human interleukin-17: A T cell-derived proinflammatory cytokine produced by the rheumatoid synovium. *Arthritis and rheumatism* 42:963-970.
99. Kotake, S., N. Udagawa, N. Takahashi, K. Matsuzaki, K. Itoh, S. Ishiyama, S. Saito, K. Inoue, N. Kamatani, M. T. Gillespie, T. J. Martin, and T. Suda. 1999. IL-17 in synovial fluids from patients with rheumatoid arthritis is a potent stimulator of osteoclastogenesis. *The Journal of clinical investigation* 103:1345-1352.
100. Nakae, S., A. Nambu, K. Sudo, and Y. Iwakura. 2003. Suppression of immune induction of collagen-induced arthritis in IL-17-deficient mice. *J Immunol* 171:6173-6177.
101. Lubberts, E., M. I. Koenders, B. Oppers-Walgreen, L. van den Bersselaar, C. J. Coenen-de Roo, L. A. Joosten, and W. B. van den Berg. 2004. Treatment with a neutralizing anti-murine interleukin-17 antibody after the onset of collagen-induced arthritis reduces joint inflammation, cartilage destruction, and bone erosion. *Arthritis and rheumatism* 50:650-659.
102. Plater-Zyberk, C., L. A. Joosten, M. M. Helsen, M. I. Koenders, P. A. Baeuerle, and W. B. van den Berg. 2009. Combined blockade of granulocyte-macrophage colony stimulating factor and interleukin 17 pathways potently suppresses chronic destructive arthritis in a tumour necrosis factor alpha-independent mouse model. *Annals of the rheumatic diseases* 68:721-728.
103. Notley, C. A., J. J. Inglis, S. Alzabin, F. E. McCann, K. E. McNamee, and R. O. Williams. 2008. Blockade of tumor necrosis factor in collagen-induced arthritis reveals a novel immunoregulatory pathway for Th1 and Th17 cells. *The Journal of experimental medicine* 205:2491-2497.
104. Patel, D. D. 2008. IL-17 Blockade in Psoriasis *ACR/ARHP Scientific Meeting* 08.

105. Genovese, M., F. Van den Bosch, S. Roberson, S. Bojin, I. Biagini, P. Ryan, and J. Sloan-Lancaster. LY2439821, a Humanized anti-IL-17 monoclonal antibody, in the treatment of patients with rheumatoid arthritis. *Arthritis and rheumatism*.
106. Tak, P., P. Durez, J. Gomez-Reino, B. Wittmer, V. Chindalore, F. D. Padova, A. Wright, G. Bruin, and W. Hueber. 2009. AIN457 Shows a Good Safety Profile and Clinical Benefit in Patients with Active Rheumatoid Arthritis (RA) Despite Methotrexate Therapy: 16-Weeks Results From a Randomized Proof-of-Concept Trial. *American College of Rheumatology 1922-Abstract*.
107. Kokkonen, H., I. Soderstrom, J. Rocklov, G. Hallmans, K. Lejon, and S. Rantapaa Dahlqvist. 2010. Up-regulation of cytokines and chemokines predates the onset of rheumatoid arthritis. *Arthritis and rheumatism* 62:383-391.
108. Capon, F., P. Di Meglio, J. Szaub, N. J. Prescott, C. Dunster, L. Baumber, K. Timms, A. Gutin, V. Abkevic, A. D. Burden, J. Lanchbury, J. N. Barker, R. C. Trembath, and F. O. Nestle. 2007. Sequence variants in the genes for the interleukin-23 receptor (IL23R) and its ligand (IL12B) confer protection against psoriasis. *Human genetics* 122:201-206.
109. Cargill, M., S. J. Schrodi, M. Chang, V. E. Garcia, R. Brandon, K. P. Callis, N. Matsunami, K. G. Ardlie, D. Civello, J. J. Catanese, D. U. Leong, J. M. Panko, L. B. McAllister, C. B. Hansen, J. Papenfuss, S. M. Prescott, T. J. White, M. F. Leppert, G. G. Krueger, and A. B. Begovich. 2007. A large-scale genetic association study confirms IL12B and leads to the identification of IL23R as psoriasis-risk genes. *American journal of human genetics* 80:273-290.
110. Liu, Y., C. Helms, W. Liao, L. C. Zaba, S. Duan, J. Gardner, C. Wise, A. Miner, M. J. Malloy, C. R. Pullinger, J. P. Kane, S. Saccone, J. Worthington, I. Bruce, P. Y. Kwok, A. Menter, J. Krueger, A. Barton, N. L. Saccone, and A. M. Bowcock. 2008. A genome-wide association study of psoriasis and psoriatic arthritis identifies new disease loci. *PLoS genetics* 4:e1000041.
111. Lee, E., W. L. Trepicchio, J. L. Oestreicher, D. Pittman, F. Wang, F. Chamian, M. Dhodapkar, and J. G. Krueger. 2004. Increased expression of interleukin 23 p19 and p40 in lesional skin of patients with psoriasis vulgaris. *The Journal of experimental medicine* 199:125-130.
112. Guttman-Yassky, E., M. A. Lowes, J. Fuentes-Duculan, L. C. Zaba, I. Cardinale, K. E. Nogralas, A. Khatcherian, I. Novitskaya, J. A. Carucci, R.

Bergman, and J. G. Krueger. 2008. Low expression of the IL-23/Th17 pathway in atopic dermatitis compared to psoriasis. *J Immunol* 181:7420-7427.

113. Brentano, F., C. Ospelt, J. Stanczyk, R. E. Gay, S. Gay, and D. Kyburz. 2009. Abundant expression of the interleukin (IL)23 subunit p19, but low levels of bioactive IL23 in the rheumatoid synovium: differential expression and Toll-like receptor-(TLR) dependent regulation of the IL23 subunits, p19 and p40, in rheumatoid arthritis. *Annals of the rheumatic diseases* 68:143-150.

114. Kim, H. R., H. S. Kim, M. K. Park, M. L. Cho, S. H. Lee, and H. Y. Kim. 2007. The clinical role of IL-23p19 in patients with rheumatoid arthritis. *Scandinavian journal of rheumatology* 36:259-264.

115. Ju, J. H., M. L. Cho, Y. M. Moon, H. J. Oh, J. S. Park, J. Y. Jhun, S. Y. Min, Y. G. Cho, K. S. Park, C. H. Yoon, J. K. Min, S. H. Park, Y. C. Sung, and H. Y. Kim. 2008. IL-23 induces receptor activator of NF-kappaB ligand expression on CD4+ T cells and promotes osteoclastogenesis in an autoimmune arthritis model. *J Immunol* 181:1507-1518.

116. Chen, L., X. Q. Wei, B. Evans, W. Jiang, and D. Aeschlimann. 2008. IL-23 promotes osteoclast formation by up-regulation of receptor activator of NF-kappaB (RANK) expression in myeloid precursor cells. *European journal of immunology* 38:2845-2854.

117. Nair, R. P., K. C. Duffin, C. Helms, J. Ding, P. E. Stuart, D. Goldgar, J. E. Gudjonsson, Y. Li, T. Tejasvi, B. J. Feng, A. Ruether, S. Schreiber, M. Weichenthal, D. Gladman, P. Rahman, S. J. Schrodi, S. Prahalad, S. L. Guthery, J. Fischer, W. Liao, P. Y. Kwok, A. Menter, G. M. Lathrop, C. A. Wise, A. B. Begovich, J. J. Voorhees, J. T. Elder, G. G. Krueger, A. M. Bowcock, G. R. Abecasis, R. P. Nair, K. C. Duffin, C. Helms, J. Ding, P. E. Stuart, D. Goldgar, J. E. Gudjonsson, Y. Li, T. Tejasvi, J. Paschall, M. J. Malloy, C. R. Pullinger, J. P. Kane, J. Gardner, A. Perlmutter, A. Miner, B. J. Feng, R. Hiremagalore, R. W. Ike, H. W. Lim, E. Christophers, T. Henseler, S. Schreiber, A. Franke, A. Ruether, M. Weichenthal, D. Gladman, P. Rahman, S. J. Schrodi, S. Prahalad, S. L. Guthery, J. Fischer, W. Liao, P. Y. Kwok, A. Menter, G. M. Lathrop, C. Wise, A. B. Begovich, J. J. Voorhees, J. T. Elder, G. G. Krueger, A. M. Bowcock, and G. R. Abecasis. 2009. Genome-wide scan reveals association of psoriasis with IL-23 and NF-kappaB pathways. *Nature genetics*.

118. Chang, M., R. K. Saiki, J. J. Cantanese, D. Lew, A. H. van der Helm-van Mil, R. E. Toes, T. W. Huizinga, K. G. Ardlie, L. A. Criswell, M. F. Seldin, C. I.

- Amos, D. L. Kastner, P. K. Gregersen, S. J. Schrodi, and A. B. Begovich. 2008. The inflammatory disease-associated variants in IL12B and IL23R are not associated with rheumatoid arthritis. *Arthritis and rheumatism* 58:1877-1881.
119. Park, J. H., Y. J. Kim, B. L. Park, J. S. Bae, H. D. Shin, and S. C. Bae. 2008. Lack of association between interleukin 23 receptor gene polymorphisms and rheumatoid arthritis susceptibility. *Rheumatology international*.
120. Yago, T., Y. Nanke, M. Kawamoto, T. Furuya, T. Kobashigawa, N. Kamatani, and S. Kotake. 2007. IL-23 induces human osteoclastogenesis via IL-17 in vitro, and anti-IL-23 antibody attenuates collagen-induced arthritis in rats. *Arthritis research & therapy* 9:R96.
121. Murphy, C. A., C. L. Langrish, Y. Chen, W. Blumenschein, T. McClanahan, R. A. Kastelein, J. D. Sedgwick, and D. J. Cua. 2003. Divergent pro- and antiinflammatory roles for IL-23 and IL-12 in joint autoimmune inflammation. *J Exp Med* 198:1951-1957.
122. Leonardi, C. L., A. B. Kimball, K. A. Papp, N. Yeilding, C. Guzzo, Y. Wang, S. Li, L. T. Dooley, and K. B. Gordon. 2008. Efficacy and safety of ustekinumab, a human interleukin-12/23 monoclonal antibody, in patients with psoriasis: 76-week results from a randomised, double-blind, placebo-controlled trial (PHOENIX 1). *Lancet* 371:1665-1674.
123. Bianchi, M. E. 2007. DAMPs, PAMPs and alarmins: all we need to know about danger. *Journal of leukocyte biology* 81:1-5.
124. Dinarello, C. A. 1994. The interleukin-1 family: 10 years of discovery. *Faseb J* 8:1314-1325.
125. Stevenson, F. T., S. L. Bursten, C. Fanton, R. M. Locksley, and D. H. Lovett. 1993. The 31-kDa precursor of interleukin 1 alpha is myristoylated on specific lysines within the 16-kDa N-terminal propeptide. *Proceedings of the National Academy of Sciences of the United States of America* 90:7245-7249.
126. Dinarello, C. A. 1996. Biologic basis for interleukin-1 in disease. *Blood* 87:2095-2147.
127. Arend, W. P., G. Palmer, and C. Gabay. 2008. IL-1, IL-18, and IL-33 families of cytokines. *Immunological reviews* 223:20-38.
128. Maelfait, J., E. Vercaemmen, S. Janssens, P. Schotte, M. Haegman, S. Magez, and R. Beyaert. 2008. Stimulation of Toll-like receptor 3 and 4 induces interleukin-1beta maturation by caspase-8. *The Journal of experimental medicine* 205:1967-1973.

129. Gu, Y., K. Kuida, H. Tsutsui, G. Ku, K. Hsiao, M. A. Fleming, N. Hayashi, K. Higashino, H. Okamura, K. Nakanishi, M. Kurimoto, T. Tanimoto, R. A. Flavell, V. Sato, M. W. Harding, D. J. Livingston, and M. S. Su. 1997. Activation of interferon-gamma inducing factor mediated by interleukin-1beta converting enzyme. *Science (New York, N.Y)* 275:206-209.
130. Blumberg, H., H. Dinh, E. S. Trueblood, J. Pretorius, D. Kugler, N. Weng, S. T. Kanaly, J. E. Towne, C. R. Willis, M. K. Kuechle, J. E. Sims, and J. J. Peschon. 2007. Opposing activities of two novel members of the IL-1 ligand family regulate skin inflammation. *The Journal of experimental medicine* 204:2603-2614.
131. Mulero, J. J., A. M. Pace, S. T. Nelken, D. B. Loeb, T. R. Correa, R. Drmanac, and J. E. Ford. 1999. IL1HY1: A novel interleukin-1 receptor antagonist gene. *Biochemical and biophysical research communications* 263:702-706.
132. Schmitz, J., A. Owyang, E. Oldham, Y. Song, E. Murphy, T. K. McClanahan, G. Zurawski, M. Moshrefi, J. Qin, X. Li, D. M. Gorman, J. F. Bazan, and R. A. Kastelein. 2005. IL-33, an interleukin-1-like cytokine that signals via the IL-1 receptor-related protein ST2 and induces T helper type 2-associated cytokines. *Immunity* 23:479-490.
133. Baekkevold, E. S., M. Roussigne, T. Yamanaka, F. E. Johansen, F. L. Jahnsen, F. Amalric, P. Brandtzaeg, M. Erard, G. Haraldsen, and J. P. Girard. 2003. Molecular characterization of NF-HEV, a nuclear factor preferentially expressed in human high endothelial venules. *The American journal of pathology* 163:69-79.
134. Chandler, J. W., and W. Werr. 2003. When negative is positive in functional genomics. *Trends in plant science* 8:279-285.
135. Yang, H., M. M. Lu, L. Zhang, J. A. Whitsett, and E. E. Morrisey. 2002. GATA6 regulates differentiation of distal lung epithelium. *Development (Cambridge, England)* 129:2233-2246.
136. Carriere, V., L. Roussel, N. Ortega, D. A. Lacorre, L. Americh, L. Aguilar, G. Bouche, and J. P. Girard. 2007. IL-33, the IL-1-like cytokine ligand for ST2 receptor, is a chromatin-associated nuclear factor in vivo. *Proceedings of the National Academy of Sciences of the United States of America* 104:282-287.
137. Roussel, L., M. Erard, C. Cayrol, and J. P. Girard. 2008. Molecular mimicry between IL-33 and KSHV for attachment to chromatin through the H2A-H2B acidic pocket. *EMBO reports* 9:1006-1012.

138. Hayakawa, M., H. Hayakawa, Y. Matsuyama, H. Tamemoto, H. Okazaki, and S. Tominaga. 2009. Mature interleukin-33 is produced by calpain-mediated cleavage in vivo. *Biochemical and biophysical research communications* 387:218-222.
139. Ali, S., D. Q. Nguyen, W. Falk, and M. U. Martin. Caspase 3 inactivates biologically active full length interleukin-33 as a classical cytokine but does not prohibit nuclear translocation. *Biochemical and biophysical research communications* 391:1512-1516.
140. Talabot-Ayer, D., C. Lamacchia, C. Gabay, and G. Palmer. 2009. Interleukin-33 is biologically active independently of caspase-1 cleavage. *The Journal of biological chemistry* 284:19420-19426.
141. Ohno, T., K. Oboki, N. Kajiwara, E. Morii, K. Aozasa, R. A. Flavell, K. Okumura, H. Saito, and S. Nakae. 2009. Caspase-1, caspase-8, and calpain are dispensable for IL-33 release by macrophages. *J Immunol* 183:7890-7897.
142. Cayrol, C., and J. P. Girard. 2009. The IL-1-like cytokine IL-33 is inactivated after maturation by caspase-1. *Proceedings of the National Academy of Sciences of the United States of America* 106:9021-9026.
143. Luthi, A. U., S. P. Cullen, E. A. McNeela, P. J. Duriez, I. S. Afonina, C. Sheridan, G. Brumatti, R. C. Taylor, K. Kersse, P. Vandenabeele, E. C. Lavelle, and S. J. Martin. 2009. Suppression of interleukin-33 bioactivity through proteolysis by apoptotic caspases. *Immunity* 31:84-98.
144. Nile, C. J., E. Barksby, P. Jitprasertwong, P. M. Preshaw, and J. J. Taylor. Expression and regulation of interleukin-33 in human monocytes. *Immunology*.
145. Palmer, G., D. Talabot-Ayer, C. Lamacchia, D. Toy, C. A. Seemayer, S. Viatte, A. Finckh, D. E. Smith, and C. Gabay. 2009. Inhibition of interleukin-33 signaling attenuates the severity of experimental arthritis. *Arthritis and rheumatism* 60:738-749.
146. Xu, D., H. R. Jiang, P. Kewin, Y. Li, R. Mu, A. R. Fraser, N. Pitman, M. Kurowska-Stolarska, A. N. McKenzie, I. B. McInnes, and F. Y. Liew. 2008. IL-33 exacerbates antigen-induced arthritis by activating mast cells. *Proceedings of the National Academy of Sciences of the United States of America* 105:10913-10918.
147. Moussion, C., N. Ortega, and J. P. Girard. 2008. The IL-1-like cytokine IL-33 is constitutively expressed in the nucleus of endothelial cells and epithelial cells in vivo: a novel 'alarmin'? *PLoS one* 3:e3331.

148. Tschopp, J., and K. Schroder. NLRP3 inflammasome activation: The convergence of multiple signalling pathways on ROS production? *Nat Rev Immunol* 10:210-215.
149. Eder, C. 2009. Mechanisms of interleukin-1beta release. *Immunobiology* 214:543-553.
150. Matsuyama, Y., H. Okazaki, H. Tamemoto, H. Kimura, Y. Kamata, K. Nagatani, T. Nagashima, M. Hayakawa, M. Iwamoto, T. Yoshio, S. Tominaga, and S. Minota. Increased levels of interleukin 33 in sera and synovial fluid from patients with active rheumatoid arthritis. *The Journal of rheumatology* 37:18-25.
151. Mok, M. Y., F. P. Huang, W. K. Ip, Y. Lo, F. Y. Wong, E. Y. Chan, K. F. Lam, and D. Xu. Serum levels of IL-33 and soluble ST2 and their association with disease activity in systemic lupus erythematosus. *Rheumatology (Oxford, England)* 49:520-527.
152. Alves-Filho, J. C., F. Sonogo, F. O. Souto, A. Freitas, W. A. Verri, Jr., M. Auxiliadora-Martins, A. Basile-Filho, A. N. McKenzie, D. Xu, F. Q. Cunha, and F. Y. Liew. Interleukin-33 attenuates sepsis by enhancing neutrophil influx to the site of infection. *Nature medicine*.
153. Calogero, S., F. Grassi, A. Aguzzi, T. Voigtlander, P. Ferrier, S. Ferrari, and M. E. Bianchi. 1999. The lack of chromosomal protein Hmg1 does not disrupt cell growth but causes lethal hypoglycaemia in newborn mice. *Nature genetics* 22:276-280.
154. Stros, M. HMGB proteins: interactions with DNA and chromatin. *Biochimica et biophysica acta* 1799:101-113.
155. Scaffidi, P., T. Misteli, and M. E. Bianchi. 2002. Release of chromatin protein HMGB1 by necrotic cells triggers inflammation. *Nature* 418:191-195.
156. Bianchi, M. E., and A. A. Manfredi. 2007. High-mobility group box 1 (HMGB1) protein at the crossroads between innate and adaptive immunity. *Immunological reviews* 220:35-46.
157. Tominaga, S. 1989. A putative protein of a growth specific cDNA from BALB/c-3T3 cells is highly similar to the extracellular portion of mouse interleukin 1 receptor. *FEBS letters* 258:301-304.
158. Yanagisawa, K., T. Takagi, T. Tsukamoto, T. Tetsuka, and S. Tominaga. 1993. Presence of a novel primary response gene ST2L, encoding a product highly similar to the interleukin 1 receptor type 1. *FEBS letters* 318:83-87.

159. Townsend, M. J., P. G. Fallon, D. J. Matthews, H. E. Jolin, and A. N. McKenzie. 2000. T1/ST2-deficient mice demonstrate the importance of T1/ST2 in developing primary T helper cell type 2 responses. *The Journal of experimental medicine* 191:1069-1076.
160. Xu, D., W. L. Chan, B. P. Leung, F. Huang, R. Wheeler, D. Piedrafita, J. H. Robinson, and F. Y. Liew. 1998. Selective expression of a stable cell surface molecule on type 2 but not type 1 helper T cells. *The Journal of experimental medicine* 187:787-794.
161. Thomassen, E., G. Kothny, S. Haas, J. Danescu, L. Hultner, P. Dormer, and A. K. Werenskiold. 1995. Role of cell type-specific promoters in the developmental regulation of T1, an interleukin 1 receptor homologue. *Cell Growth Differ* 6:179-184.
162. Manetti, M., L. Ibba-Manneschi, V. Liakouli, S. Guiducci, A. F. Milia, G. Benelli, A. Marrelli, M. L. Conforti, E. Romano, R. Giacomelli, M. Matucci-Cerinic, and P. Cipriani. The IL1-like cytokine IL33 and its receptor ST2 are abnormally expressed in the affected skin and visceral organs of patients with systemic sclerosis. *Annals of the rheumatic diseases* 69:598-605.
163. Rank, M. A., T. Kobayashi, H. Kozaki, K. R. Bartemes, D. L. Squillace, and H. Kita. 2009. IL-33-activated dendritic cells induce an atypical TH2-type response. *The Journal of allergy and clinical immunology* 123:1047-1054.
164. Suzukawa, M., M. Iikura, R. Koketsu, H. Nagase, C. Tamura, A. Komiya, S. Nakae, K. Matsushima, K. Ohta, K. Yamamoto, and M. Yamaguchi. 2008. An IL-1 cytokine member, IL-33, induces human basophil activation via its ST2 receptor. *J Immunol* 181:5981-5989.
165. Schneider, E., A. F. Petit-Bertron, R. Bricard, M. Levasseur, A. Ramadan, J. P. Girard, A. Herbelin, and M. Dy. 2009. IL-33 activates unprimed murine basophils directly in vitro and induces their in vivo expansion indirectly by promoting hematopoietic growth factor production. *J Immunol* 183:3591-3597.
166. Smithgall, M. D., M. R. Comeau, B. R. Yoon, D. Kaufman, R. Armitage, and D. E. Smith. 2008. IL-33 amplifies both Th1- and Th2-type responses through its activity on human basophils, allergen-reactive Th2 cells, iNKT and NK cells. *International immunology* 20:1019-1030.
167. Moro, K., T. Yamada, M. Tanabe, T. Takeuchi, T. Ikawa, H. Kawamoto, J. Furusawa, M. Ohtani, H. Fujii, and S. Koyasu. Innate production of T(H)2

- cytokines by adipose tissue-associated c-Kit(+)/Sca-1(+) lymphoid cells. *Nature* 463:540-544.
168. Neill, D. R., S. H. Wong, A. Bellosi, R. J. Flynn, M. Daly, T. K. Langford, C. Bucks, C. M. Kane, P. G. Fallon, R. Pannell, H. E. Jolin, and A. N. McKenzie. Nuocytes represent a new innate effector leukocyte that mediates type-2 immunity. *Nature* 464:1367-1370.
169. Chackerian, A. A., E. R. Oldham, E. E. Murphy, J. Schmitz, S. Pflanz, and R. A. Kastelein. 2007. IL-1 receptor accessory protein and ST2 comprise the IL-33 receptor complex. *J Immunol* 179:2551-2555.
170. Palmer, G., B. P. Lipsky, M. D. Smithgall, D. Meininger, S. Siu, D. Talabot-Ayer, C. Gabay, and D. E. Smith. 2008. The IL-1 receptor accessory protein (AcP) is required for IL-33 signaling and soluble AcP enhances the ability of soluble ST2 to inhibit IL-33. *Cytokine* 42:358-364.
171. Funakoshi-Tago, M., K. Tago, M. Hayakawa, S. Tominaga, T. Ohshio, Y. Sonoda, and T. Kasahara. 2008. TRAF6 is a critical signal transducer in IL-33 signaling pathway. *Cellular signalling* 20:1679-1686.
172. O'Neill, L. A. 2008. The interleukin-1 receptor/Toll-like receptor superfamily: 10 years of progress. *Immunological reviews* 226:10-18.
173. Pushparaj, P. N., H. K. Tay, C. H'Ng S, N. Pitman, D. Xu, A. McKenzie, F. Y. Liew, and A. J. Melendez. 2009. The cytokine interleukin-33 mediates anaphylactic shock. *Proceedings of the National Academy of Sciences of the United States of America* 106:9773-9778.
174. Komai-Koma, M., D. Xu, Y. Li, A. N. McKenzie, I. B. McInnes, and F. Y. Liew. 2007. IL-33 is a chemoattractant for human Th2 cells. *European journal of immunology* 37:2779-2786.
175. Bourgeois, E., L. P. Van, M. Samson, S. Diem, A. Barra, S. Roga, J. M. Gombert, E. Schneider, M. Dy, P. Gourdy, J. P. Girard, and A. Herbelin. 2009. The pro-Th2 cytokine IL-33 directly interacts with invariant NKT and NK cells to induce IFN-gamma production. *European journal of immunology* 39:1046-1055.
176. Liew, F. Y., N. I. Pitman, and I. B. McInnes. Disease-associated functions of IL-33: the new kid in the IL-1 family. *Nat Rev Immunol* 10:103-110.
177. Kaieda, S., K. Shin, P. A. Nigrovic, K. Seki, R. T. Lee, R. L. Stevens, and D. M. Lee. Synovial fibroblasts promote the expression and granule accumulation of tryptase via interleukin-33 and its receptor ST-2 (IL1RL1). *The Journal of biological chemistry*.

178. Kuchler, A. M., J. Pollheimer, J. Balogh, J. Sponheim, L. Manley, D. R. Sorensen, P. M. De Angelis, H. Scott, and G. Haraldsen. 2008. Nuclear interleukin-33 is generally expressed in resting endothelium but rapidly lost upon angiogenic or proinflammatory activation. *The American journal of pathology* 173:1229-1242.
179. Choi, Y. S., H. J. Choi, J. K. Min, B. J. Pyun, Y. S. Maeng, H. Park, J. Kim, Y. M. Kim, and Y. G. Kwon. 2009. Interleukin-33 induces angiogenesis and vascular permeability through ST2/TRAF6-mediated endothelial nitric oxide production. *Blood* 114:3117-3126.
180. Fraser, A., M. Moore, S. Jongbloed, A. Gracie, and I. McInnes. 2006. Elevated soluble ST2 and cytokine levels in synovial fluids of patients with inflammatory synovitis [abstract]. *Annals of the rheumatic diseases* 65:A10.
181. Hayakawa, H., M. Hayakawa, A. Kume, and S. Tominaga. 2007. Soluble ST2 blocks interleukin-33 signaling in allergic airway inflammation. *The Journal of biological chemistry* 282:26369-26380.
182. Oshikawa, K., K. Kuroiwa, K. Tago, H. Iwahana, K. Yanagisawa, S. Ohno, S. I. Tominaga, and Y. Sugiyama. 2001. Elevated soluble ST2 protein levels in sera of patients with asthma with an acute exacerbation. *American journal of respiratory and critical care medicine* 164:277-281.
183. Garlanda, C., H. J. Anders, and A. Mantovani. 2009. TIR8/SIGIRR: an IL-1R/TLR family member with regulatory functions in inflammation and T cell polarization. *Trends in immunology* 30:439-446.
184. Wald, D., J. Qin, Z. Zhao, Y. Qian, M. Naramura, L. Tian, J. Towne, J. E. Sims, G. R. Stark, and X. Li. 2003. SIGIRR, a negative regulator of Toll-like receptor-interleukin 1 receptor signaling. *Nature immunology* 4:920-927.
185. Bulek, K., S. Swaidani, J. Qin, Y. Lu, M. F. Gulen, T. Herjan, B. Min, R. A. Kastelein, M. Aronica, M. Kosz-Vnenchak, and X. Li. 2009. The essential role of single Ig IL-1 receptor-related molecule/Toll IL-1R8 in regulation of Th2 immune response. *J Immunol* 182:2601-2609.
186. Miller, A. M., D. Xu, D. L. Asquith, L. Denby, Y. Li, N. Sattar, A. H. Baker, I. B. McInnes, and F. Y. Liew. 2008. IL-33 reduces the development of atherosclerosis. *The Journal of experimental medicine* 205:339-346.
187. Sanada, S., D. Hakuno, L. J. Higgins, E. R. Schreiter, A. N. McKenzie, and R. T. Lee. 2007. IL-33 and ST2 comprise a critical biomechanically induced and

cardioprotective signaling system. *The Journal of clinical investigation* 117:1538-1549.

188. Weir, R. A., A. M. Miller, G. E. Murphy, S. Clements, T. Steedman, J. M. Connell, I. B. McInnes, H. J. Dargie, and J. J. McMurray. Serum soluble ST2: a potential novel mediator in left ventricular and infarct remodeling after acute myocardial infarction. *Journal of the American College of Cardiology* 55:243-250.

189. Kurowska-Stolarska, M., B. Stolarski, P. Kewin, G. Murphy, C. J. Corrigan, S. Ying, N. Pitman, A. Mirchandani, B. Rana, N. van Rooijen, M. Shepherd, C. McSharry, I. B. McInnes, D. Xu, and F. Y. Liew. 2009. IL-33 amplifies the polarization of alternatively activated macrophages that contribute to airway inflammation. *J Immunol* 183:6469-6477.

190. Kurowska-Stolarska, M., P. Kewin, G. Murphy, R. C. Russo, B. Stolarski, C. C. Garcia, M. Komai-Koma, N. Pitman, Y. Li, W. Niedbala, A. N. McKenzie, M. M. Teixeira, F. Y. Liew, and D. Xu. 2008. IL-33 induces antigen-specific IL-5+ T cells and promotes allergic-induced airway inflammation independent of IL-4. *J Immunol* 181:4780-4790.

191. Moffatt, M. F., I. G. Gut, F. Demenais, D. P. Strachan, E. Bouzigon, S. Heath, E. von Mutius, M. Farrall, M. Lathrop, and W. O. Cookson. A large-scale, consortium-based genomewide association study of asthma. *The New England journal of medicine* 363:1211-1221.

192. Pastorelli, L., R. R. Garg, S. B. Hoang, L. Spina, B. Mattioli, M. Scarpa, C. Fiocchi, M. Vecchi, and T. T. Pizarro. Epithelial-derived IL-33 and its receptor ST2 are dysregulated in ulcerative colitis and in experimental Th1/Th2 driven enteritis. *Proceedings of the National Academy of Sciences of the United States of America* 107:8017-8022.

193. Kobori, A., Y. Yagi, H. Imaeda, H. Ban, S. Bamba, T. Tsujikawa, Y. Saito, Y. Fujiyama, and A. Andoh. Interleukin-33 expression is specifically enhanced in inflamed mucosa of ulcerative colitis. *Journal of gastroenterology*.

194. Theoharides, T. C., B. Zhang, D. Kempuraj, M. Tagen, M. Vasiadi, A. Angelidou, K. D. Alysandratos, D. Kalogeromitros, S. Asadi, N. Stavrianeas, E. Peterson, S. Leeman, and P. Conti. IL-33 augments substance P-induced VEGF secretion from human mast cells and is increased in psoriatic skin. *Proceedings of the National Academy of Sciences of the United States of America* 107:4448-4453.

195. Rankin, A. L., J. B. Mumm, E. Murphy, S. Turner, N. Yu, T. K. McClanahan, P. A. Bourne, R. H. Pierce, R. Kastelein, and S. Pflanz. IL-33 induces IL-13-dependent cutaneous fibrosis. *J Immunol* 184:1526-1535.
196. Raza, K., F. Falciani, S. J. Curnow, E. J. Ross, C. Y. Lee, A. N. Akbar, J. M. Lord, C. Gordon, C. D. Buckley, and M. Salmon. 2005. Early rheumatoid arthritis is characterized by a distinct and transient synovial fluid cytokine profile of T cell and stromal cell origin. *Arthritis research & therapy* 7:R784-795.
197. Xu, D., H. R. Jiang, Y. Li, P. N. Pushparaj, M. Kurowska-Stolarska, B. P. Leung, R. Mu, H. K. Tay, A. N. McKenzie, I. B. McInnes, A. J. Melendez, and F. Y. Liew. IL-33 exacerbates autoantibody-induced arthritis. *J Immunol* 184:2620-2626.
198. Medimmune. 2008. IL-33 in inflammatory disease. *World intellectual property organisation* WO 2008/144610 A1.
199. Weinberg, E. O., M. Shimpo, G. W. De Keulenaer, C. MacGillivray, S. Tominaga, S. D. Solomon, J. L. Rouleau, and R. T. Lee. 2002. Expression and regulation of ST2, an interleukin-1 receptor family member, in cardiomyocytes and myocardial infarction. *Circulation* 106:2961-2966.
200. Hoogerwerf, J. J., M. W. Tanck, M. A. van Zoelen, X. Wittebole, P. F. Laterre, and T. van der Poll. Soluble ST2 plasma concentrations predict mortality in severe sepsis. *Intensive care medicine* 36:630-637.
201. Millington, O. R., B. H. Zinselmeyer, J. M. Brewer, P. Garside, and C. M. Rush. 2007. Lymphocyte tracking and interactions in secondary lymphoid organs. *Inflamm Res* 56:391-401.
202. Dobrovolskaia, M. A., P. Aggarwal, J. B. Hall, and S. E. McNeil. 2008. Preclinical studies to understand nanoparticle interaction with the immune system and its potential effects on nanoparticle biodistribution. *Molecular pharmaceutics* 5:487-495.
203. Donaldson, K., L. Tran, L. A. Jimenez, R. Duffin, D. E. Newby, N. Mills, W. MacNee, and V. Stone. 2005. Combustion-derived nanoparticles: a review of their toxicology following inhalation exposure. *Particle and fibre toxicology* 2:10.
204. Fang, C., B. Shi, Y. Y. Pei, M. H. Hong, J. Wu, and H. Z. Chen. 2006. In vivo tumor targeting of tumor necrosis factor-alpha-loaded stealth nanoparticles: effect of MePEG molecular weight and particle size. *Eur J Pharm Sci* 27:27-36.

205. Dobrovolskaia, M. A., and S. E. McNeil. 2007. Immunological properties of engineered nanomaterials. *Nature nanotechnology* 2:469-478.
206. Duncan, R. 2006. Polymer conjugates as anticancer nanomedicines. *Nat Rev Cancer* 6:688-701.
207. Tsai, C. Y., A. L. Shiau, S. Y. Chen, Y. H. Chen, P. C. Cheng, M. Y. Chang, D. H. Chen, C. H. Chou, C. R. Wang, and C. L. Wu. 2007. Amelioration of collagen-induced arthritis in rats by nanogold. *Arthritis and rheumatism* 56:544-554.
208. Dobrovolskaia, M. A., P. Aggarwal, J. B. Hall, and S. E. McNeil. 2008. Preclinical Studies To Understand Nanoparticle Interaction with the Immune System and Its Potential Effects on Nanoparticle Biodistribution. *Molecular pharmaceuticals*.
209. Pittet, M. J., F. K. Swirski, F. Reynolds, L. Josephson, and R. Weissleder. 2006. Labeling of immune cells for in vivo imaging using magnetofluorescent nanoparticles. *Nature protocols* 1:73-79.
210. Mathis, D., L. Vence, and C. Benoist. 2001. beta-Cell death during progression to diabetes. *Nature* 414:792-798.
211. Denis, M. C., U. Mahmood, C. Benoist, D. Mathis, and R. Weissleder. 2004. Imaging inflammation of the pancreatic islets in type 1 diabetes. *Proceedings of the National Academy of Sciences of the United States of America* 101:12634-12639.
212. Turvey, S. E., E. Swart, M. C. Denis, U. Mahmood, C. Benoist, R. Weissleder, and D. Mathis. 2005. Noninvasive imaging of pancreatic inflammation and its reversal in type 1 diabetes. *The Journal of clinical investigation* 115:2454-2461.
213. Moore, A., J. Grimm, B. Han, and P. Santamaria. 2004. Tracking the recruitment of diabetogenic CD8⁺ T-cells to the pancreas in real time. *Diabetes* 53:1459-1466.
214. Nahrendorf, M., H. Zhang, S. Hembrador, P. Panizzi, D. E. Sosnovik, E. Aikawa, P. Libby, F. K. Swirski, and R. Weissleder. 2008. Nanoparticle PET-CT imaging of macrophages in inflammatory atherosclerosis. *Circulation* 117:379-387.
215. Aikawa, E., M. Nahrendorf, J. L. Figueiredo, F. K. Swirski, T. Shtatland, R. H. Kohler, F. A. Jaffer, M. Aikawa, and R. Weissleder. 2007. Osteogenesis

associates with inflammation in early-stage atherosclerosis evaluated by molecular imaging in vivo. *Circulation* 116:2841-2850.

216. Brochet, B., M. S. Deloire, T. Touil, O. Anne, J. M. Caille, V. Dousset, and K. G. Petry. 2006. Early macrophage MRI of inflammatory lesions predicts lesion severity and disease development in relapsing EAE. *NeuroImage* 32:266-274.

217. McAteer, M. A., N. R. Sibson, C. von Zur Muhlen, J. E. Schneider, A. S. Lowe, N. Warrick, K. M. Channon, D. C. Anthony, and R. P. Choudhury. 2007. In vivo magnetic resonance imaging of acute brain inflammation using microparticles of iron oxide. *Nature medicine* 13:1253-1258.

218. Flogel, U., Z. Ding, H. Hardung, S. Jander, G. Reichmann, C. Jacoby, R. Schubert, and J. Schrader. 2008. In vivo monitoring of inflammation after cardiac and cerebral ischemia by fluorine magnetic resonance imaging. *Circulation* 118:140-148.

219. Maffia, P., B. H. Zinselmeyer, A. Ialenti, S. Kennedy, A. H. Baker, I. B. McInnes, J. M. Brewer, and P. Garside. 2007. Images in cardiovascular medicine. Multiphoton microscopy for 3-dimensional imaging of lymphocyte recruitment into apolipoprotein-E-deficient mouse carotid artery. *Circulation* 115:e326-328.

220. Karwa, A., E. Papazoglou, K. Pourrezaei, S. Tyagi, and S. Murthy. 2007. Imaging biomarkers of inflammation in situ with functionalized quantum dots in the dextran sodium sulfate (DSS) model of mouse colitis. *Inflamm Res* 56:502-510.

221. Weng, K. C., C. O. Noble, B. Papahadjopoulos-Sternberg, F. F. Chen, D. C. Drummond, D. B. Kirpotin, D. Wang, Y. K. Hom, B. Hann, and J. W. Park. 2008. Targeted tumor cell internalization and imaging of multifunctional quantum dot-conjugated immunoliposomes in vitro and in vivo. *Nano letters* 8:2851-2857.

222. Zinselmeyer, B. H., J. N. Lynch, X. Zhang, T. Aoshi, and M. J. Miller. 2008. Video-rate two-photon imaging of mouse footpad - a promising model for studying leukocyte recruitment dynamics during inflammation. *Inflamm Res* 57:93-96.

223. Qian, X., X. H. Peng, D. O. Ansari, Q. Yin-Goen, G. Z. Chen, D. M. Shin, L. Yang, A. N. Young, M. D. Wang, and S. Nie. 2008. In vivo tumor targeting and spectroscopic detection with surface-enhanced Raman nanoparticle tags. *Nature biotechnology* 26:83-90.

224. Keren, S., C. Zavaleta, Z. Cheng, A. de la Zerda, O. Gheysens, and S. S. Gambhir. 2008. Noninvasive molecular imaging of small living subjects using

- Raman spectroscopy. *Proceedings of the National Academy of Sciences of the United States of America* 105:5844-5849.
225. Boukamp, P., R. T. Petrussevska, D. Breitkreutz, J. Hornung, A. Markham, and N. E. Fusenig. 1988. Normal keratinization in a spontaneously immortalized aneuploid human keratinocyte cell line. *The Journal of cell biology* 106:761-771.
226. Turkevich, J., P. C. Stevenson, and J. Hillier. 1951. A study of the nucleation and growth processes in the synthesis of colloidal gold. *Discussions of the Faraday Society* 11 pp55-75.
227. Chu, C. Q., D. Swart, D. Alcorn, J. Tocker, and K. B. Elkon. 2007. Interferon-gamma regulates susceptibility to collagen-induced arthritis through suppression of interleukin-17. *Arthritis and rheumatism* 56:1145-1151.
228. Stamp, L. K., A. Easson, L. Pettersson, J. Highton, and P. A. Hessian. 2009. Monocyte derived interleukin (IL)-23 is an important determinant of synovial IL-17A expression in rheumatoid arthritis. *The Journal of rheumatology* 36:2403-2408.
229. Miossec, P., T. Korn, and V. K. Kuchroo. 2009. Interleukin-17 and type 17 helper T cells. *The New England journal of medicine* 361:888-898.
230. Takatori, H., Y. Kanno, W. T. Watford, C. M. Tato, G. Weiss, Ivanov, II, D. R. Littman, and J. J. O'Shea. 2009. Lymphoid tissue inducer-like cells are an innate source of IL-17 and IL-22. *The Journal of experimental medicine* 206:35-41.
231. de Boer, O. J., J. J. van der Meer, P. Teeling, C. M. van der Loos, M. M. Idu, F. van Maldegem, J. Aten, and A. C. van der Wal. Differential expression of interleukin-17 family cytokines in intact and complicated human atherosclerotic plaques. *The Journal of pathology* 220:499-508.
232. McGeachy, M. J., Y. Chen, C. M. Tato, A. Laurence, B. Joyce-Shaikh, W. M. Blumenschein, T. K. McClanahan, J. J. O'Shea, and D. J. Cua. 2009. The interleukin 23 receptor is essential for the terminal differentiation of interleukin 17-producing effector T helper cells in vivo. *Nature immunology* 10:314-324.
233. Nair, R. P., K. C. Duffin, C. Helms, J. Ding, P. E. Stuart, D. Goldgar, J. E. Gudjonsson, Y. Li, T. Tejasvi, B. J. Feng, A. Ruether, S. Schreiber, M. Weichenthal, D. Gladman, P. Rahman, S. J. Schrodi, S. Prahalad, S. L. Guthery, J. Fischer, W. Liao, P. Y. Kwok, A. Menter, G. M. Lathrop, C. A. Wise, A. B. Begovich, J. J. Voorhees, J. T. Elder, G. G. Krueger, A. M. Bowcock, and G. R.

Abecasis. 2009. Genome-wide scan reveals association of psoriasis with IL-23 and NF-kappaB pathways. *Nat Genet* 41:199-204.

234. Karaderi, T., D. Harvey, C. Farrar, L. H. Appleton, M. A. Stone, R. D. Sturrock, M. A. Brown, P. Wordsworth, and J. J. Pointon. 2009. Association between the interleukin 23 receptor and ankylosing spondylitis is confirmed by a new UK case-control study and meta-analysis of published series. *Rheumatology (Oxford)* 48:386-389.

235. Melis, L., B. Vandooren, E. Kruithof, P. Jacques, M. De Vos, H. Mielants, G. Verbruggen, F. De Keyser, and D. Elewaut. 2009. Systemic levels of IL-23 are strongly associated with disease activity in rheumatoid arthritis but not spondyloarthritis. *Ann Rheum Dis*.

236. Ciric, B., M. El-behi, R. Cabrera, G. X. Zhang, and A. Rostami. 2009. IL-23 drives pathogenic IL-17-producing CD8+ T cells. *J Immunol* 182:5296-5305.

237. Song, C., L. Luo, Z. Lei, B. Li, Z. Liang, G. Liu, D. Li, G. Zhang, B. Huang, and Z. H. Feng. 2008. IL-17-producing alveolar macrophages mediate allergic lung inflammation related to asthma. *J Immunol* 181:6117-6124.

238. Moran, E. M., C. T. Ng, J. McCormick, R. Heydrich, H. Appel, U. Fearon, and D. Veale. 2009. IL-17A Expression Is Upregulated in the Hypoxic Joint and Correlates with IL-6 Production, Inflammatory Cell Infiltrate and Oxidative Damage [abstract]. *Arthritis and rheumatism* 60 Suppl 10:1343.

239. Hueber, A. J., D. L. Asquith, A. M. Miller, J. Reilly, S. Kerr, J. Leipe, A. J. Melendez, and I. B. McInnes. Mast cells express IL-17A in rheumatoid arthritis synovium. *J Immunol* 184:3336-3340.

240. Proteinatlas.

http://www.proteinatlas.org/show_image.php?image_id=6315093.

241. Kuroiwa, K., T. Arai, H. Okazaki, S. Minota, and S. Tominaga. 2001. Identification of human ST2 protein in the sera of patients with autoimmune diseases. *Biochemical and biophysical research communications* 284:1104-1108.

242. Shimpo, M., D. A. Morrow, E. O. Weinberg, M. S. Sabatine, S. A. Murphy, E. M. Antman, and R. T. Lee. 2004. Serum levels of the interleukin-1 receptor family member ST2 predict mortality and clinical outcome in acute myocardial infarction. *Circulation* 109:2186-2190.

243. Grimbaldston, M. A., C. C. Chen, A. M. Piliponsky, M. Tsai, S. Y. Tam, and S. J. Galli. 2005. Mast cell-deficient W-sash c-kit mutant Kit W-sh/W-sh mice

- as a model for investigating mast cell biology in vivo. *The American journal of pathology* 167:835-848.
244. Singer, A. J., and R. A. Clark. 1999. Cutaneous wound healing. *The New England journal of medicine* 341:738-746.
245. Martin, P. 1997. Wound healing--aiming for perfect skin regeneration. *Science (New York, N.Y)* 276:75-81.
246. Leung, B. P., D. Xu, S. Culshaw, I. B. McInnes, and F. Y. Liew. 2004. A novel therapy of murine collagen-induced arthritis with soluble T1/ST2. *J Immunol* 173:145-150.
247. Verri, W. A., Jr., F. O. Souto, S. M. Vieira, S. C. Almeida, S. Y. Fukada, D. Xu, J. C. Alves-Filho, T. M. Cunha, A. T. Guerrero, R. B. Mattos-Guimaraes, F. R. Oliveira, M. M. Teixeira, J. S. Silva, I. B. McInnes, S. H. Ferreira, P. Louzada-Junior, F. Y. Liew, and F. Q. Cunha. IL-33 induces neutrophil migration in rheumatoid arthritis and is a target of anti-TNF therapy. *Annals of the rheumatic diseases*.
248. Kawase, Y., T. Hoshino, K. Yokota, A. Kuzuhara, Y. Kirii, E. Nishiwaki, Y. Maeda, J. Takeda, M. Okamoto, S. Kato, T. Imaizumi, H. Aizawa, and K. Yoshino. 2003. Exacerbated and prolonged allergic and non-allergic inflammatory cutaneous reaction in mice with targeted interleukin-18 expression in the skin. *The Journal of investigative dermatology* 121:502-509.
249. Zavaleta, C. L., B. R. Smith, I. Walton, W. Doering, G. Davis, B. Shojaei, M. J. Natan, and S. S. Gambhir. 2009. Multiplexed imaging of surface enhanced Raman scattering nanotags in living mice using noninvasive Raman spectroscopy. *Proceedings of the National Academy of Sciences of the United States of America* 106:13511-13516.
250. Skotland, T., T. G. Iversen, and K. Sandvig. New metal-based nanoparticles for intravenous use: requirements for clinical success with focus on medical imaging. *Nanomedicine*.
251. Evans, H. G., N. J. Gullick, S. Kelly, C. Pitzalis, G. M. Lord, B. W. Kirkham, and L. S. Taams. 2009. In vivo activated monocytes from the site of inflammation in humans specifically promote Th17 responses. *Proceedings of the National Academy of Sciences of the United States of America* 106:6232-6237.
252. Korn, T., E. Bettelli, M. Oukka, and V. K. Kuchroo. 2009. IL-17 and Th17 Cells. *Annual review of immunology* 27:485-517.

8 Publications